THE UNIVERSITY OF ALBERTA

RELEASE FORM

NAME OF AUTHOR SERGIO A.B. da FONTOURA

TITLE OF THESIS TIME-DEPENDENT RESPONSE OF ROCK MASSES DURING TUNNELLING

DEGREE FOR WHICH THESIS WAS PRESENTED DOCTOR OF PHILOSOPHY

YEAR THIS DEGREE GRANTED Spring, 1980

Permission is hereby granted to THE UNIVERSITY OF ALBERTA LIBRARY to reproduce single copies of this thesis and to lend or sell such copies for private, scholarly or scientific research purposes only.

The author reserves other publication rights, and neither the thesis nor extensive extracts from it may be printed or otherwise reproduced without the author's written permission.

(SIGNED) S. Fontoura

PERMANENT ADDRESS:

Rua das Palmeiras, 32/302

Botafogo - Rio de Janeiro

RJ - Brazil

DATED March 11 1980

THE UNIVERSITY OF ALBERTA

TIME-DEPENDENT RESPONSE OF ROCK MASSES DURING TUNNELLING

by

SERGIO A.B. da FONTOURA

A THESIS

SUBMITTED TO THE FACULTY OF GRADUATE STUDIES AND RESEARCH

IN PARTIAL FULFILMENT OF THE REQUIREMENTS FOR THE DEGREE

OF DOCTOR OF PHILOSOPHY

IN

CIVIL ENGINEERING

DEPARTMENT OF CIVIL ENGINEERING

EDMONTON, ALBERTA

Spring, 1980

THE UNIVERSITY OF ALBERTA

FACULTY OF GRADUATE STUDIES AND RESEARCH

The undersigned certify that they have read, and recommend to the Faculty of Graduate Studies and Research, for acceptance, a thesis entitled TIME-DEPENDENT RESPONSE OF ROCK MASSES DURING TUNNELLING submitted by SERGIO A.B. da FONTOURA in partial fulfilment of the requirements for the degree of DOCTOR OF PHILOSOPHY in CIVIL ENGINEERING.

Prof. N.R. Morgenstern ....
Supervisor

Prof. T. Hrudey ....

Prof. D.M. Cruden ....

Prof. B. Stimpson ....

Dr. E. Hoek ....
External Examiner

Date..... March 4, 1980 ....

To my parents

Abstract

The aim of this thesis is the investigation of the time-dependent nature of the behavior of rock tunnels. This investigation was divided into three parts. The first part consisted of a qualitative analysis of the behavior of a number of examples of rock tunnels reported in the literature. The aim of this review was to identify the role of time in the behavior of these tunnels. In order to organize the case histories, modes of ground behavior were defined. The second part consisted of an experimental study of the time-dependent behavior of a jointed coal under a constant state of stress. Conventional triaxial tests were carried out. The results of these tests lead to a simple creep relationship which shows the importance of the stress level in describing creep behavior. In the third part, an analytical study of the stress redistribution and time-dependent deformations around an opening due to creep was carried out. This study consisted initially in three stages: (a) the elaboration of a 3-dimensional stress-strain-time relationship; (b) the development of a governing differential equation and its solution by numerical technique. Based on this solution procedure, the time-dependent closure of an opening in coal was compared with the predicted results and a good agreement was observed. This method was also used to evaluate the effects of factors such as size of opening and creep parameters on

the time-dependent behavior of openings.

Acknowledgements

During the past almost 5 years, many hours were spent in upgrading my background in geotechnical engineering and carrying out this research. My wife, Helena, made this long way less painful with her love and understanding. Her unselfished dedication even when she had to stop her career to join me in Canada will never be forgotten. To her my deepest gratitude and I owe her this degree.

I wish to thank my research supervisor, Prof. N.R. Morgenstern, for his guidance and moral support during the course of this research. It has been a honour for me to be associated with him in this project and of being exposed to his overwhelming enthusiasm for the teaching, research and practice of geotechnical engineering. I have profited very much from such an association.

Many people have given me their friendship and warmth during these years and although several will not be mentioned their role was outstanding. To the members of the academic staff my many thanks specially Profs. Z. Eisenstein, S. Thomsom and D. Murray. Prof. D.Cruden spent some hours sharing with me his ideas on creep of rocks.

I have also gained very much from discussions with former graduate students P. Kaiser and A. Guenot on time-dependent behavior of coal; D. Sego and W.Savigny on creep of ice and permafrost; F. El-Nahhas and O. Hungr on tunnelling behavior. Many thanks to all the other graduate students who without exception made me feel part of this big family.

I owe a great deal to my good friend John Simmons who kindly agreed in editing this thesis and with whom I share many views on the role of research in geotechnical engineering. John must be credited with whatever looks like proper english in this thesis and I must bear full responsibilities for the rest.

Many thanks to the members of the non-academic staff especially former head of the laboratory O.Wood for the tireless help during the experimental program and Head machinist, A.Muir, who not only did an excellent job on my creep rig but also provided us with the best coffee on Campus.

During the course of this research I was granted a scholarship by the Conselho Nacional de Pesquisas, a research funding agency of the Brazilian Government. My employer, the Universidade Catolica do Rio de Janeiro, provided some assistance and the Civil Engineering Department of The University of Alberta awarded me periodical teaching assistantship. Without these contributions I would have not been able to pay all the bills.

To my daughter, Daniela, product of our Canadian experience, all my love. Now I hope we can spend more time together.

Table of Contents

List of Figures

List of Tables

Chapter 1

INTRODUCTION

1.1 Background

The use of underground space has increased considerably in recent years. Over $300 billion dollars were estimated by the National Science Foundation of the U.S. to be spent in the period of 1970-1990 (about $16 billion dollars/yr) in the United States alone in underground excavations (Bieniawski(1979)). This figure will at least triple if the needs of other leading western countries as well as developing countries for works such as mining resources, railroad and highway tunnels, water and sewer tunnels, subways and underground power stations are added to this estimate. At the same time, underground openings are being used more and more for non-conventional purposes such as storage installations for water, food and oil, waste disposal, recreation and military engineering. This fairly high level of construction activities has made clear the need for heavy investments of time and money in research leading towards an improvement of the current knowledge of the behavior of underground openings.

Research in tunnelling constitutes a very active area even though many practicing engineers still regard rock tunnelling as an art. Active research areas cover subjects such as developments of empirical tunnel design, analytical modelling of underground openings and rock supporting structural interaction. At the same time, many investigations are also being carried out with regard to excavation methods and contracting practice.

Although the demand is quite high, the design of underground openings is still plagued with a high degree of empiricism that has its source in the sometimes unavoidable lack of information previous to the excavation or simply by continuation of old practice. A recent trend has been to establish guidelines for tunnel support requirements on the basis of previous experience which have been conveniently codified and translated into some parameters such as Bieniawski's and Barton's rock mass classification systems for tunnelling purposes (e.g, Bieniawski(1974) and Barton et al(1974)). These methods, even though appealing and handy, have the serious drawback of perpetuating old tunnelling practice and of giving a false sense of understanding about the main factors which control the final performance of an opening.

Also new concepts have been introduced which consist in a mixture of tunnelling practice and rational design and the best example is the NATM (New Austrian Tunnelling Method). These methods are based on the accumulated experience of the personnal involved and have not yet attained general acceptance, the reason being basically due to the fact that the principles are not easily codified and also because of the skill required by the work force. However, a large number of agencies are increasing their experience with this procedure especially through instrumentation which is expected to describe in better terms the results of tunnel behavior.

In the search for sound tunnel design or tunnel excavation procedures it is of fundamental importance that a good understanding of the many factors which are known to control the behavior of underground openings be achieved. In particular, the processes which describe the transition from a pre-excavation to a post excavation state of equilibrium of the rock mass and their time-dependent nature are of special interest.

1.2 Scope and Organization of this thesis

The design of underground openings involves decisions associated with rate and size of excavation as well as lining strategy. The aim of this thesis is to provide a contribution towards understanding the time-dependent processes associated with the excavation of tunnels in rocks. This is achieved in three ways:

1. investigations of the processes leading to time-dependent behavior of underground openings;
2. experimental data describing the time-dependent response of rock masses;
3. analytical modelling of excavations in creeping rock.

In Chapter 2, the main factors which control the behavior of underground openings are evaluated as well as the causes leading to time-dependent behavior. A critical study of published case-records in the literature is presented where the aim is to identify the role of the time-factor in the overall performance of these openings. It was considered essential for such a study to define the characteristic modes of ground behavior and then to organize the concepts leading to an assessment of the role of time-factor. Section 2.1 describes the main factors which control the underground behavior whereas section 2.2 considers the causes leading to time-dependent behavior. In section 2.3 each mode is described and illustrative case-histories are presented showing the importance of the lining strategy associated with each mode. Also a general set of guidelines is presented for the selection of a particular mode based on rock mass parameters and stresses around openings.

In Chapter 3 a comprehensive review of the time-dependent properties of rock masses is presented. The aim of this review is to assess the present capabilities of predicting the time-dependent deformations of a rock mass with especial emphasis on the empirical formulation of creep laws. In this Chapter the properties such as creep deformations, time-dependent failure and relaxation properties of rocks are reviewed.

Chapter 4 consists of a description of creep tests carried out on a jointed coal with the aim of describing the time-dependent deformations of a jointed and fractured rock. This experimental program describe both single-stage and multiple-stage creep tests.

Chapter 5 reviews some relevant theoretical solutions describing the time-dependent behaviour of an underground opening.

Chapter 6 presents the development of a solution for the time-dependent behavior of an underground opening. Initially, a governing differential equation is developed which is presented in Appendix A. This is followed by an analysis of the results obtained which concentrate on the zones of stress distribution and rate of tunnel closure. The results of a model test carried out by Guenot(1979) are predicted and the results showed encouraging similarities.

Finally in Chapter 7 the conclusions are presented and suggestions for further research are put forward.

Chapter 2

DIFFERENT MODES OF ROCK TUNNEL BEHAVIOR

2.1 Introduction

The driving of an underground excavation through stressed ground disturbs its equilibrium. In responding to this disturbance, the ground will deform and there will be an associated stress redistribution around the opening. Both deformations and stress redistribution reflect the search by the rock mass for a new equilibrium position. Evidence produced by case-records reported in the literature indicates that such a new equilibrium position may be reached without any help from external sources but, as a general rule, artificial supports have to be provided in order to maintain the opened excavation.

Experience also indicates that the passage from the pre-excavation to the post-excavation equilibrium position is a time-dependent process. This post-excavation or final equilibrium position corresponds to the situation where all the deformations as well as any stress transfer have essentially stopped. To achieve progress in both designing and constructing underground openings, it is essential that the mechanisms involved in such a transition in equilibrium position be investigated. This investigation is the aim of the present Chapter.

In the following the Author considers:

a. the mechanisms leading to time-dependent passage from a pre-excavation to a post-excavation equilibrium and,

b. the circumstances under which time plays an important role when making decisions in both design and construction stages.

In section 2.2 the probable causes for time-dependent behavior of underground openings are discussed briefly in a qualitative form. In section 2.3 the circumstances under which the time-factor plays an important role on the behavior of openings in rocks are considered. This is done by defining modes of ground behavior which are assumed to be fairly representative of the possible spectrum. The establishment of such modes constitutes an attempt by the Author to provide a suitable framework to analyze the available case-records of tunnelling in rocks. This framework serves as a basis to collect, in an orderly manner, the lessons learned from the performance of rock tunnels.

2.2 Factors controlling the behavior of underground openings

Several factors have been identified as controlling the behavior of an underground opening. They are:

1. primary factors: this designates all the factors which are a characteristic of the site in consideration, e.g., rock type and rock properties, geological discontinuities and their mechanical properties, in-situ

state of stress, ground-water regime, etc.

2. secondary factors: this indicates all the factors which are a characteristic of the opening (geometrical characteristics), e.g., size and shape of the opening, depth of the opening, relative orientation of opening axis with respect to geological discontinuities, etc.
3. tertiary factors: this indicates all the factors which are a characteristic of the constructional procedures, e.g., method of excavation and lining strategy (type, sequence and time of installation of supporting structures).

At the present stage, it is reasonable to assume that a combination of these factors controls the mechanisms or processes describing the passage from a pre- to a post-excavation equilibrium position. Of particular interest in this thesis is the investigation of the particular combination which leads to a time-dependent transition in equilibrium.

2.2.1 Causes of time-dependent behavior of underground openings

The time-dependent nature of the behavior of underground openings is normally evidenced by observations such as the increase in deformations of the excavation walls with time, increase in load or damage of tunnel linings, and delayed failure of parts or whole sections of an excavation. Constant maintainance works around openings due to heaving floors, sagging roofs, delayed roof failures, and breaking pillars are normal occurrences in deep mines.

The concern with time-dependent behavior of tunnels can be traced back to Terzaghi(1946) who introduced the concepts of bridge-action and load-increase periods. The bridge-action period, t_b, has been defined as '... the time which elapses between firing the round and the beginning of the breakdown of the unsupported part of the roof'. The load-increase period was defined by Terzaghi as '... the time which elapses until the pressure (on the support system) becomes fairly constant'. Some of the factors which control these 'periods' were identified by Terzaghi; for instance, the length of the unsupported roof as influencing the bridge-action period and the empty-spaces between support and rock as well as the presence of squeezing and swelling rock are likely to increase the load-increase period.

At present, the technical literature seems to indicate an agreement on two basic causes of time-dependent behavior of an underground opening in rocks, namely:

a. advance of the excavation face and,

b. time-dependent behavior of the rock mass.

Figure 2.1 sub-divides these two basic causes into an extensive list of possible causes which, individually or combined, may lead towards a time-dependent response of an underground opening.

The high number of possible causes displayed in Figure

2.1 as well as their nature indicates the complexity of the study of the time-dependent response of an underground opening in both qualitative and quantitative forms.

2.3 Modes of Ground Behavior

The final performance of a rock tunnel is the product of a combination of the factors discussed in the previous section. Attempts to describe the important factors and their effects in the overall performance of tunnels have been made by means of model tests (Heuer and Hendron(1971) , Myer *et al*(1977) , Kaiser(1979)) and analytical techniques(Ladanyi(1974) , Gioda and Ghaboussi(1977) , Lombardi(1977) and Guenot(1979)). The results of those studies (particularly with respect to the time-dependent behavior of openings) based on analytical models will be discussed in Chapter 5.

Another means of investigating the ground response, in particular its time-dependent nature, is by analyzing the performance of actual excavations. To proceed systematically with an overview of selected case records, it is necessary to establish a convenient framework which will provide guidelines for such an analysis.

In the following, broad classes of behavior are established which can be identified in a practical situation. The selection of the classes or modes of ground behavior follows approximately the tunnelman's terminology currently in use. However, it should be noted that this is

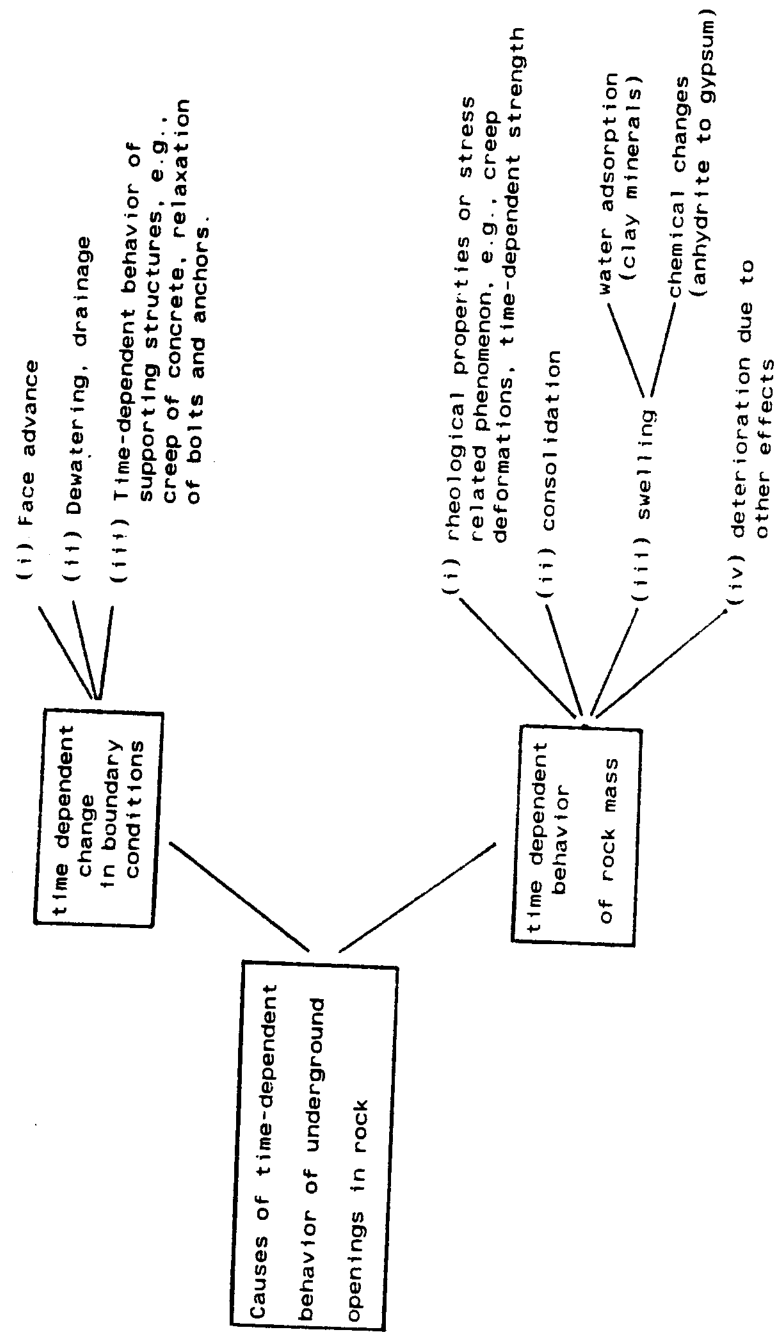

Figure 2.1 Causes leading to time-dependent behavior of underground openings

an attempt to cover the whole spectrum of the behavior of rock tunnels and one must be prepared to accept that in some cases there will be overlaps.

The grouping of case histories into broad classes allows not only the assessment of the role of the time-factor on the performance of rock tunnels but it can also be used for the evaluation of other aspects such as current design procedures, analytical methods, tunnel lining strategies, etc.

Figure 2.2 constitutes a schematic representation of the four groups which have been considered initially. For the sake of completeness, two other modes of ground behavior could have been included in this figure. They represent the class of self-supporting openings and the cases when the excavated material 'flows' and 'runs' into the opening such as saturated loose sandy gouge materials. These two classes of modes will not be discussed in this thesis.

Each mode is described by a discussion of the mechanisms or particular combination of factors leading to such behavior in order to identify the processes involved in the passage from pre to post tunnelling equilibrium. Particular attention is paid to the time-dependent nature of this passage and, whenever relevant, typical examples of deformation versus time curves, and progressive damage of roofs are given.

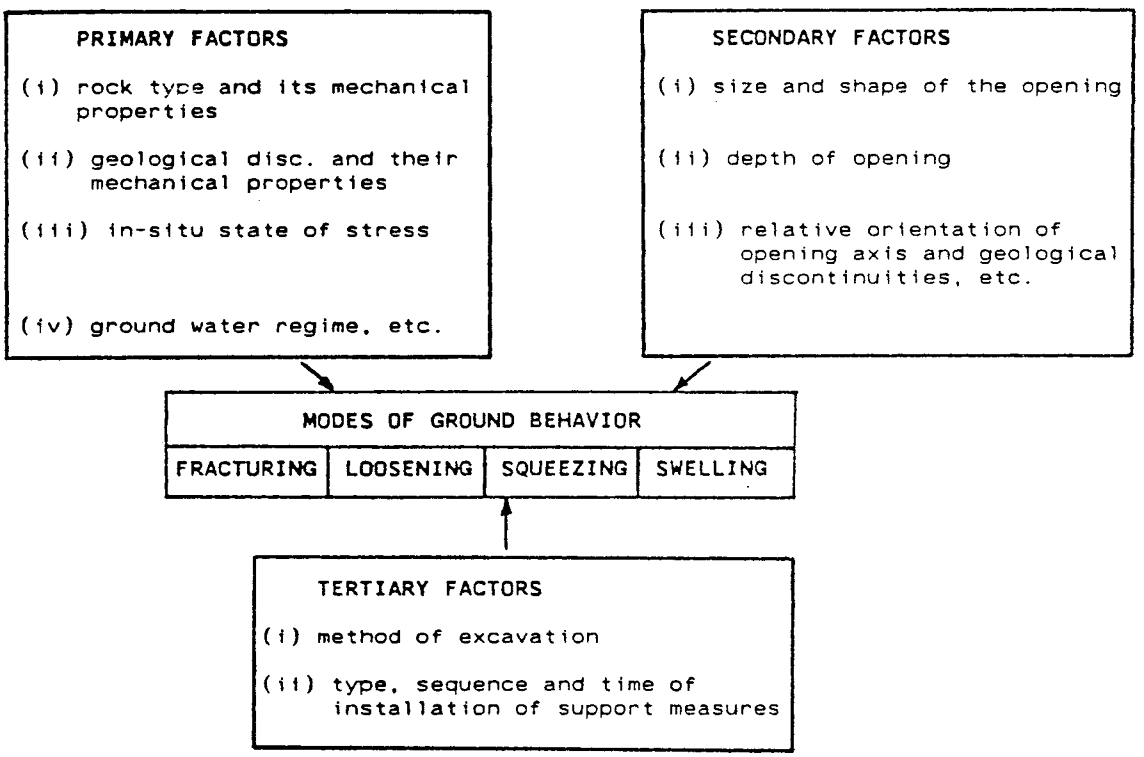

Figure 2.2 Modes of ground behavior

2.3.1 Fracturing

This mode of behavior comprises a large number of situations which have been described in the literature as rockbursts, 'popping rock', rock slabbing or spalling and corresponds to the formation and/or propagation of new fractures around the opening. A comprehensive discussion of the mechanisms leading to this mode as well as a survey of illustrative case-records follows.

2.3.1.1 Mechanisms leading to fracturing

The development of new fractures or the extension of existing ones is believed to be caused by large stress concentrations around openings in brittle rocks which may cause either tensile or shear failure. These stress concentrations can be caused by either one or any combination of the following:

a. large in situ state of stress,
b. size and shape of the opening,
c. proximity of faults, dykes or geologic structure convenientely oriented with respect to the opening,
d. developments of new workings in the vicinity of the opening.

To evaluate the possibility of fracturing, several investigators have suggested that it is useful to consider the ratio between the maximum principal stress and the unconfined compressive strength, i.e, σ_1 / σ_c, e.g., Cording et al(1971) and Cook(1973) . A ratio greater than 0.1 is generally accepted as leading to failure. Hoek and Brown(1978) suggested the ratio between the boundary stress, σ_s , and the unconfined compressive strength, σ_c , as a guideline for the assessment of overstressed zones around large underground openings. The boundary stress, σ_s , has been defined as the actual tangential stress in the immediate vicinity of the opening wall. The advantage of using the value of 'boundary stress' is that it takes into account factors such as stress field, size and shape of openings. A ratio σ_s/σ_c greater than 0.5 can be assumed as the first sign of overstressing.

Of particular significance with respect to the overall stability of the excavation is how fast and how far fractures propagate around an underground opening. To describe this failure process and the consequent stress redistribution, two similar hypotheses have been proposed, Sperry and Heuer(1972) , Rabcewicz and Golser(1974) .

Figure 2.3 illustrates the model proposed by Sperry and Heuer(1972) in which curves a to d show how the stress distribution changes with time in the case of fracturing around the opening. This process is described by Sperry and Heuer as follows:

> '....instantaneously, the circumferential stress tends to go to the theoretical elastic distribution, but in doing so the material at the perimeter is overstressed and the stress distribution is approximately as shown by curve a. With increasing time, fractures begin to form about the tunnel and the stress distribution first becomes as shown by curve b, then as shown by c as the fractures propagate and the load carried by material at the perimeter drops to zero. After fractures are

completely formed, wedges loosen and fall, moving the perimeter to its final position, and the stress distribution is shown in d. At this time, the ground in the plastic zone has yielded, but fractures have not formed completely through the plastic zone, and the yielded ground is contributing to support the opening... '

For the sake of simplicity this model has been formulated based on the behavior of a circular hole on a homogeneous and isotropic material subjected to a hydrostatic stress field. However, one should not overlook the effects of non-homogeneities on both strength and compressibility in concentrating stresses around an opening.

Both the depth to which the 'fractured zone' extends before equilibrium is reached and the rate of development of the failure about the tunnel will depend on the relative magnitude of in situ stress and strength, and the support system installed. The assessment of these conditions can only be made with some confidence by observation of actual excavations. These questions will be addressed in the next section.

Implicit in the hypothesis just described is the fact that the 'failure process' is quite stable. However, of very important practical consequence is the situation where very high strength, massive rocks fail when excavated. This situation corresponds to the so-called rockbursts which have been described as '...damage to underground openings caused by uncontrolled disruption of rock associated with a violent release of energy...', Cook et al(1966) . The mechanisms of rockbursts as well as methods for monitoring, predicting and

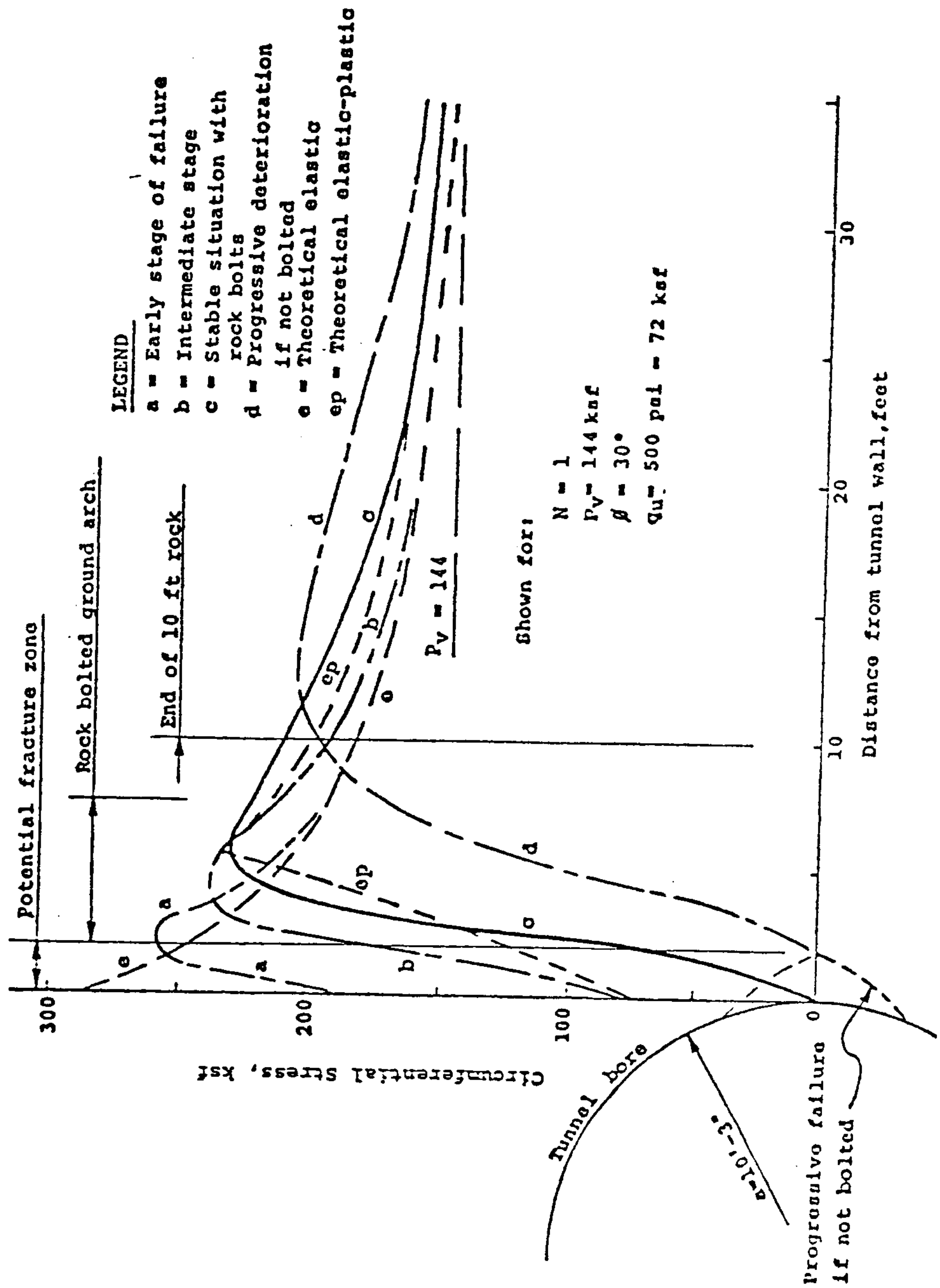

Figure 2.3 Model for the progressive change in tangential stress around a circular opening, Sperry and Heuer, 1972

controlling rockbursts have been the subject of many investigations among miners since the phenomenon was first observed in 1898 in the Kolar Gold Fields in India, e.g., Cook et al(1966) and Blake(1972) . Even though these questions are important for the ground control specialist only the aspects of 'fracturing' which are relevant for the civil engineer will be considered herein.

The evaluation of the potential for fracturing of certain rock formations constitutes an important question. This question can only be answered completely after the excavation is complete but some guidelines for preliminary estimates are necessary. Table 2.1 constitutes an attempt in using a well established rock mass parameters such as the ones defined by Barton et al(1974) to describe the possible range of rock types which lead to fracturing provided other factors such as the ratio σ_s/σ_c would assume appropriate values. Unfortunately, no cases could be obtained from the literature where enough data necessary to complete Table 2.1 could be gathered.

2.3.1.2 Survey of case records

This section presents a small collection of illustrative case-records in which 'fracturing' of rock has been observed around the opening.

Table 2.1 Rock mass parameters vs Modes of ground behavior

	Self (*) supporting	Fracturing	Loosening	Squeezing	Swelling(**)
RQD(%)	75 - 100	75 - 100	0 - 75	0 - 25	10 - 50
Joint set number(Jn)	< 9	0.5 - 3.0	2 - 15	20	10 - 20
Joint roughness number(Jr)	> 1	4 - 3	0.5 - 2.0	1.0	0.5 - 1(***)
Joint alteration number(Ja)	< 1	0.75 - 1.0	1.0 - 12	8	4 - 20
Joint water reduction(Jw)	1.0	1.0	1.0 - 0.05	1.0	1.0
Stress reduction factor(SRF)	< 2.5	2.0 - 20	1.0 - 2.5	5 - 20	10 - 15
Rock quality index(Q)	> 4	> 1.0	0.001 - 10	0.003 - 0.03	0.002 - 0.02

$$Q = \frac{RQD}{Jn} \times \frac{Jr}{Ja} \times \frac{Jw}{SRF}$$

(*) conditional requirements

if RQD < 40	Jn < 2
Jn = 9	Jr > 5and RQD>90
Jr = 1	Jn < 4
SRF > 1	Jr > 1.5
span>10m	Jn < 9
span>20m	Jn < 4 SRF<1

(**) should be complemented by classification such as Brekke and Howard(1972)

(***) nominal value

- Navajo Tunnel No.3

This is a machine-bored circular tunnel of about 6.3 meters in diameter under a variable rock cover (maximum of 321 meters). The tunnel was built as part of the Navajo Indian Irrigation Project, New Mexico by the U.S. Bureau of Reclamation. Details relevant to the geology, excavation method and equipment are given by Sperry and Heuer(1972) and Austin and Fabry(1974) .

During construction, fracturing developed in several sections. These failures were condensed into three classes, which are described in detail in Sperry and Heuer(1972). Of immediate interest is Class I which describes failure in massive, homogeneous and dry material. In this case, fracturing occurred in the roof, side walls and floor. The average rock cover at the sections considered was about 300 meters and the rock type consisted of sandstone with unconfined compressive strength varying from 2.07 to 67 MPa with the weakest 60% of the samples averaging 6.3 MPa. The ratio σ_1 / σ_c averaged about 0.66.

These fractures developed immediately after excavation, i.e.,between the face and the supported sections behind the excavation machine. In the roof, these fractures isolated slabs of rocks of about '... 8 inches thick and two to three feet in lateral dimension ...'. Under the maximum rock cover, similar fracturing occurred in both springline and invert. These fractures took from a few hours to several days to appear behind the face and were followed by ravelling of spalls and loosening of slabs.

Results of tunnel closure given by Austin and Fabry(1974) suggest that in the roof, the deformations stabilized very quickly after the installation of rockbolts. However, both field observations and displacement measurements were not enough to evaluate the time-dependent behavior of the opening as evidenced by the propagation of the fractured zone and its final thickness. The evidences were certainly erased due to the lining strategy followed which included a prompt installation of rockbolts after the excavation. Sperry and Heuer(1972) suggested the use of 1/3 of the excavated diameter as the depth of such fracturing and potential loosening as a guideline for design of anchoring depth of rockbolts.

- <u>Large underground caverns</u>

The phenomenon of 'fracturing' has also been observed in large underground powerhouses especially associated with the large stress concentration on the high walls of these caverns. Cording <u>et al</u>(1971) show the formation of shallow slabs within 5 ft of the wall surface for the case of Cavity I and II, Nevada Test site. These caverns were excavated in tuff with an average unconfined compressive strength, σ_c, of

10.5 MPa. The height of the walls amounted to about 36m and the ratio σ_1/σ_c was estimated as being 0.7. No indication is given about the propagation of those fractures but, for the final support, Cording et al(1971) recommended an anchor length of 1/3 of the height of the wall, i.e., about 12 meters long.

2.3.2 Loosening

The term 'loosening' has been used to describe the cases where '...rock fragments, blocks, and wedges tend to separate from the surrounding rock mass and move under gravity into the opening', (Cording and Mahar(1978)). This process includes the 'overbreak' which may occur in certain rock formation immediately or shortly after blasting when some rock blocks may fall out the roof and shoulders of the excavation.

2.3.2.1 Mechanisms leading to loosening

Rocks are generally discontinuous masses. These discontinuities may consist of several joint systems, bedding planes, faults and associated shear zones . They define a three dimensional array which dissects the rock mass and, depending upon relative orientation and spacing, define blocks of different sizes.

Other properties of these discontinuities such as degree of separation, aperture, infilling of joints, gouge material, and strength of 'intact' material are necessary to describe the system. Depending upon the combination of these properties, different states of interlocking are reached. As would be expected, the creation of an opening in such rocks may trigger modes of deformations which can vary within a wide spectrum depending basically on the combined properties of the geological discontinuities and size, shape and relative orientation of the opening.

The response of rock masses described as unweathered stratified , jointed massive rocks, crushed but chemically intact rocks and 'blocky and seamy' to tunnelling was first described by Terzaghi(1946) in his classical work on rock loads on steel supports. Figure 2.4 shows schematically the process of deterioration of the self-supporting ability of some jointed rock masses which occurs near the the face of an unlined opening due to the progression of deformations. Associated with this deterioration process, Terzaghi introduced the concept of bridge-action period[1] as being the period of time a certain length of excavation could remain unsupported before failure occurred. With the aim of defining loads for support design, Terzaghi considered the existence of a zone around the opening which would be the final product of the deterioration or 'loosening' process. The size of this zone and consequently the load magnitude varied with the rock type. In Terzaghi's work, no attempt was made in quantifying parameters describing the rock mass

----

[1]The same concept was reintroduced in the tunnelling literature by Lauffer(1958) as stand-up time, a term which is preferred nowadays.

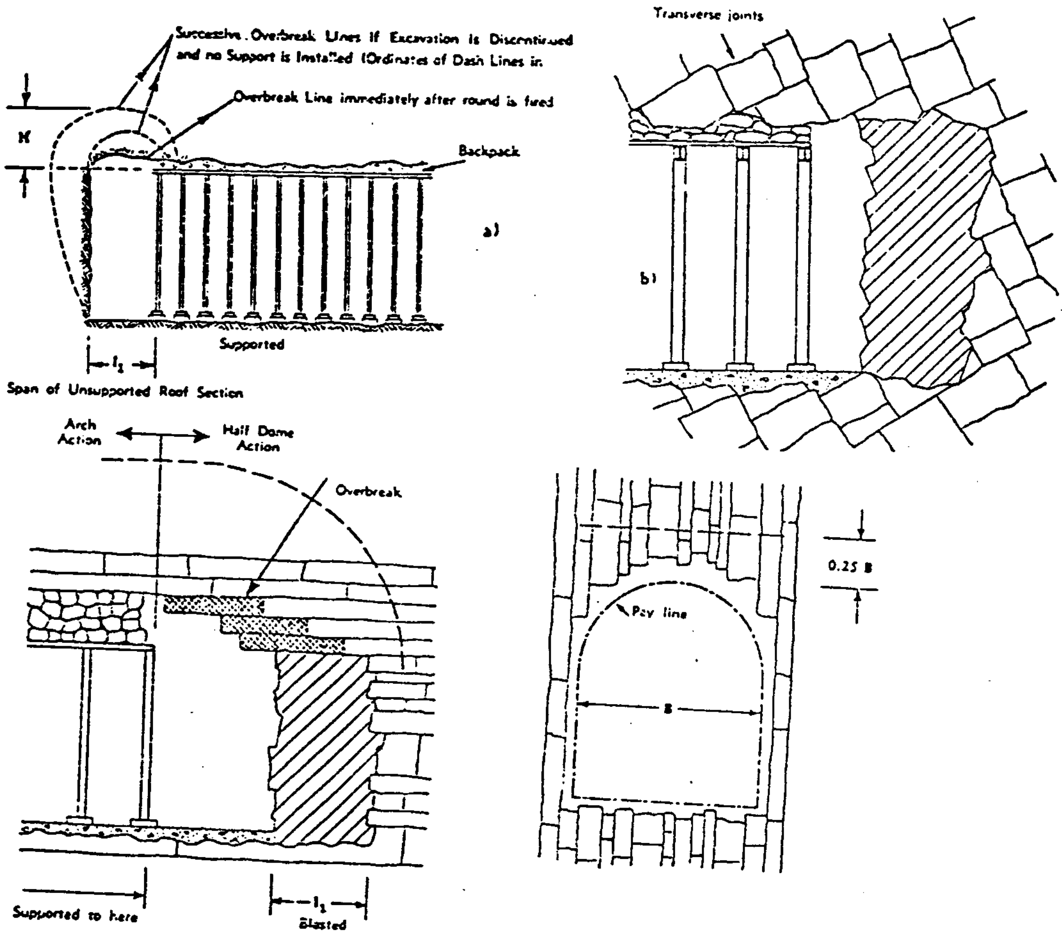

Figure 2.4 Schematic representation of the loss on self-support ability in jointed rocks (Terzaghi(1946))

and the assessment of the rock condition was based on experience. In Table 2.1, Barton's rock mass parameters are used to describe the possible range of rock types which could lead to 'loosening ground' provided other factors would assume appropriate values.

Terzaghi's concepts have been codified by other investigators who have considered the term 'loosening' to describe the loss of strength or self-supporting capability of the ground due to 'excessive' deformations. This concept can be readily appreciated by consideration of the ground reaction curve [2] or characteristic line, e.g., Deere *et al*(1969) , Lombardi(1970) . Figure 2.5 illustrates this concept.

In order to understand the concepts illustrated in this figure one should, initially, consider the type of experiment involved. It is assumed that an internal pressure, p_i , decreases monotonically and p_o , the external pressure, remains constant. The deformations are measured after each change in internal pressure. The curve obtained by plotting internal pressure, p_i , versus the accumulated displacement can be considered in three stages.

In stage (I), corresponding to AB, the rock mass responds essentially in a linear elastic manner. This is reasonable since the deviatoric stresses introduced around the opening are still very small. In stage (II),

----

[2]The ground reaction curve (GRC) describes the general response of an opening and can be applied to any type of ground. The Author, however, decided to explore the GRC only when referring to 'loosening'.

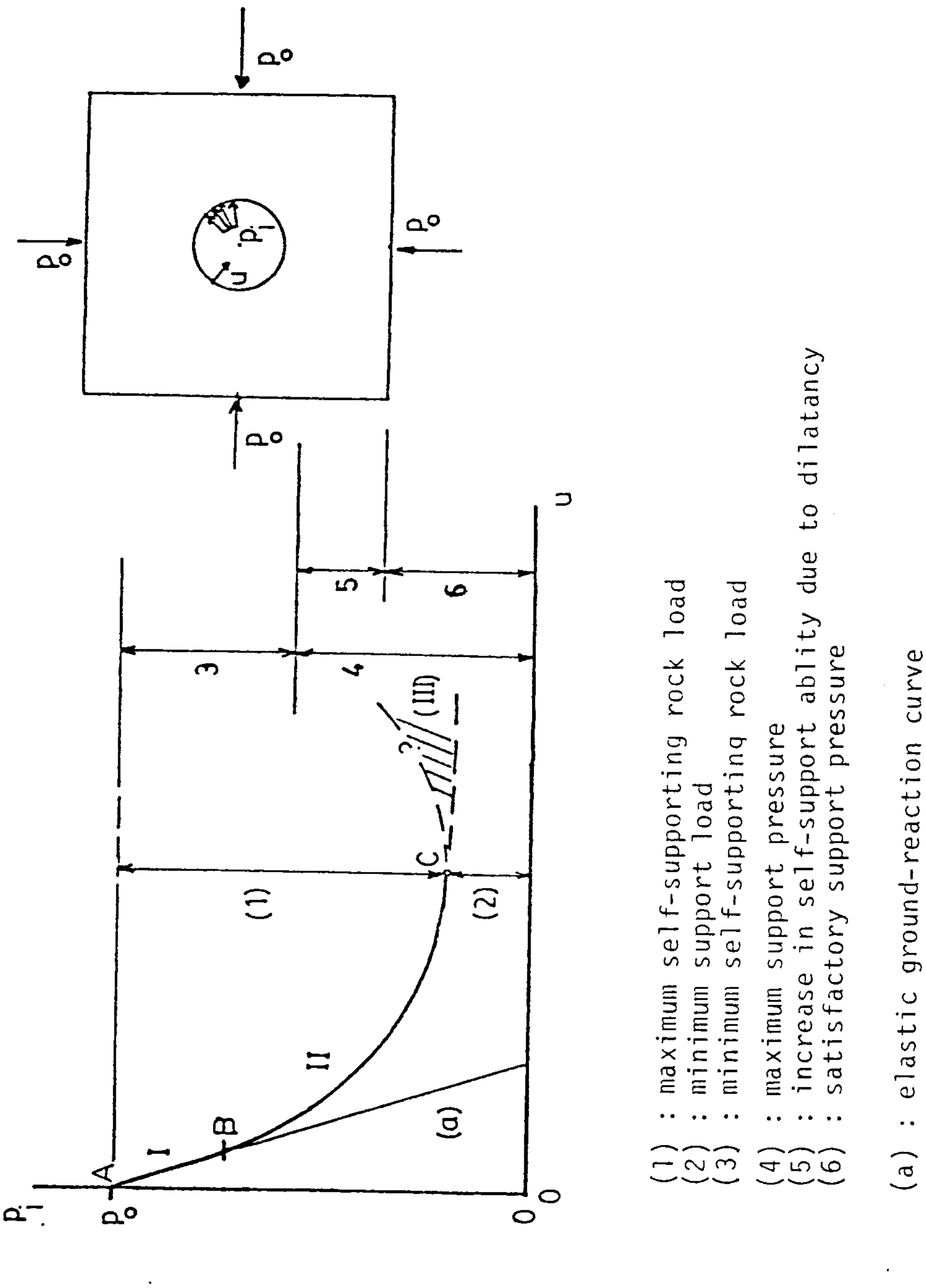

Figure 2.5 Schematic representation of Ground reaction curve

corresponding to BC , the rock mass response is controlled by non-linear behavior which is indicated by the departure from the elastic ground reaction curve, see Figure 2.5. This departure is caused by the reduction in stiffness and strength of the material around the tunnel wall which, in turn, is caused by weakening processes such as fracturing during blasting or excavation procedures, and opening of discontinuities.

Finally at point C, the rock mass has reached its maximum load-bearing capacity under the applied pressures p_i and p_o . For deformations beyond point C, equilibrium of stresses cannot be maintained unless the supporting pressure is increased over (p)min. At that stage, gravity forces may become relevant and should be added to the equilibrium equations. The process of loosening has been associated with the stage (III), as indicated in Figure 2.5 and corresponds to the deformations beyond point C.

The actual shape of the ground reaction curve for deformations beyond point C is debatable, the reason being due to all the unknowns relative to the progress of stress redistribution associated with the shear strains past peak coupled with time effects on the shear strength. In Figure 2.5 bounds to support pressures which can ultimately be used in design procedures have been indicated in a qualitative manner. Not indicated in present discussion are the effects of gravity especially on the material immediately around the opening.

A recent contribution towards the understanding of 'loosening' has been presented by Ward(1978) in his Rankine lecture. Ward shows, via a wooden block model, the influence of a common pattern of discontinuities in a sedimentary rock on the instability and yielding of a circular bored tunnel. Even though Ward's model only considers geometrical parameters, i.e,relative spacing of joints, size of opening and relative orientation with respect to tunnel axis, his results have allowed the identification of three important stages of collapse, which have compared surprisingly well with results observed in the field.

These stages of collapse indicate that increasing deformations and the eventual release of key blocks or crushing of others serve the purpose of weakening more and more the material around the opening. This process is bound to continue until the opening reaches a configuration which corresponds to a stable stress distribution around the medium.

The process just described reflects the progressive instability of an unlined opening. Next, case records will be shown which indicate such block release mechanisms and its time dependence and also illustrate the lining strategy associated with this ground behavior.

2.3.2.2 Survey of case records

- Kielder Water Scheme Experiment

This is a circular tunnel of about 3.3m in diameter excavated in strongly bedded mudstone with a very low RQD(0-8%) under a rock cover of 100m. Details of geology of the site and the project itself are given by Ward _et al_(1976) .

The experimental tunnel is about 100m long and was advanced initially using a drill and blast technique and the last sections were advanced using a roadcutter. Altogether, 8 sections of about 10m long each were provided with different types of supports. A fairly comprehensive instrumentation program was carried out in order to obtain data for the evaluation of the feasibility of each support system used in this particular site.

Deformations of the tunnel section as well as the eventual failures along the unlined section were reported by Ward _et al_(1976) and Ward(1978) . Some of these results are reproduced in Figures 2.6 and 2.7. Figure 2.6 shows the vertical displacements in both roof and invert of the unlined part of the tunnel obtained from a multiple-point extensometer installed from the surface. The deformations displayed in these curves constitute the overall deformations due to face advance and the deformations due to time-dependent behavior of the rock mass.

These observations constitute an excellent illustration of the processes involved in the development of deformations with time for the case of loosening ground. This case record

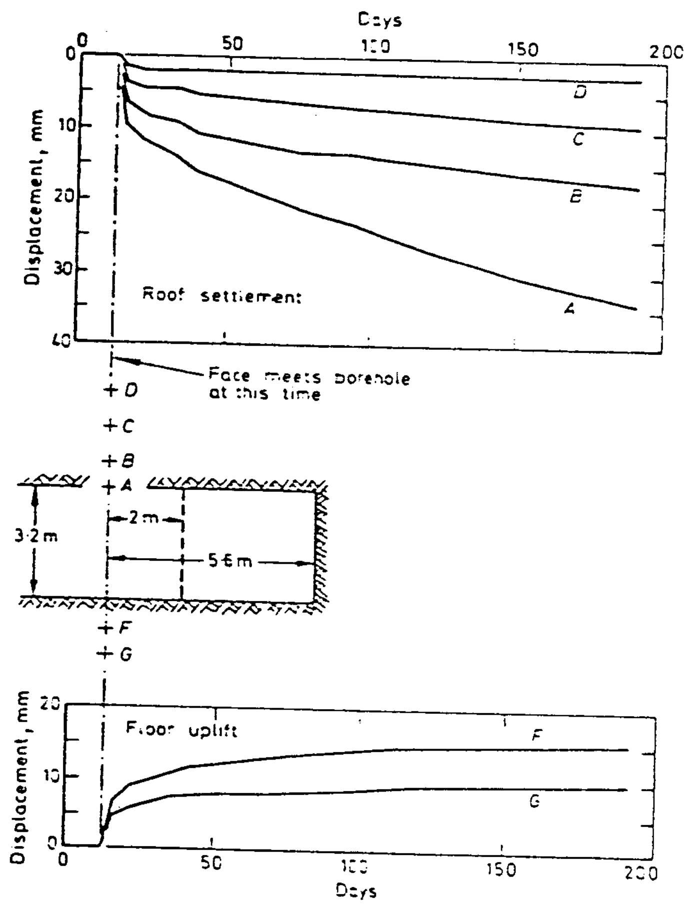

Figure 2.6 Vertical displacement of rock in crown and invert as face passes. Unlined section (Ward <u>et al</u>(1976))

corresponds to a low stress level situation (σ_1/σ_c is about 1/20) but still the initial deformations were about one order of magnitude larger than the predicted elastic deformations. This suggests that the material around the tunnel is expanding by opening of discontinuities, movements along joints and eventual crushing of block corners.

After excavation, inspection of the tunnel indicated a progressive release of blocks from shoulders and sidewalls and ultimately the failure of a large part of the roof, see Figure 2.7. This sequence of events indicates the following aspects relative to unsupported 'loosening' ground, namely:

a. The increasing deformations cause failures and subsequent stress redistribution which in turn causes more deformations;

b. failure or release of blocks can happen in a short time;

c. size of failure zone can vary very much and is difficult to predict.

Ward <u>et al</u>(1976) also presented the results of instrumentation on lined sections. Altogether, 7 different combinations of excavation methods and lining types and time of installation were used. Figure 2.8 reproduces the typical displacement curves for all the different lining strategies. It is very clear from these curves that different combinations of excavation method and lining type differ in leading the rock mass around the opening to reach an equilibrium position.

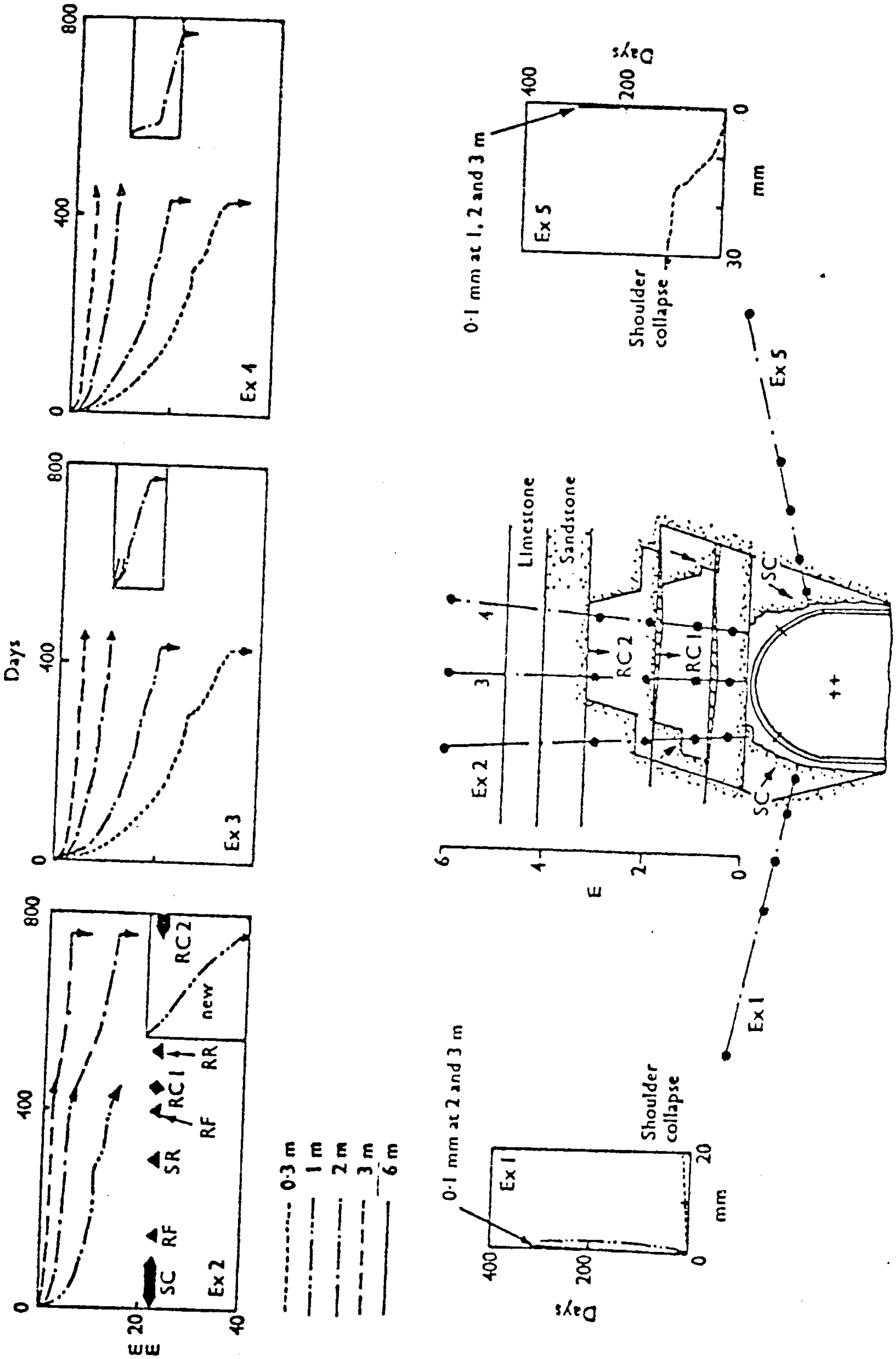

Figure 2.7 Layout of extensometers and progression of shoulder and roof collapses. Unlined section (Ward(1978))

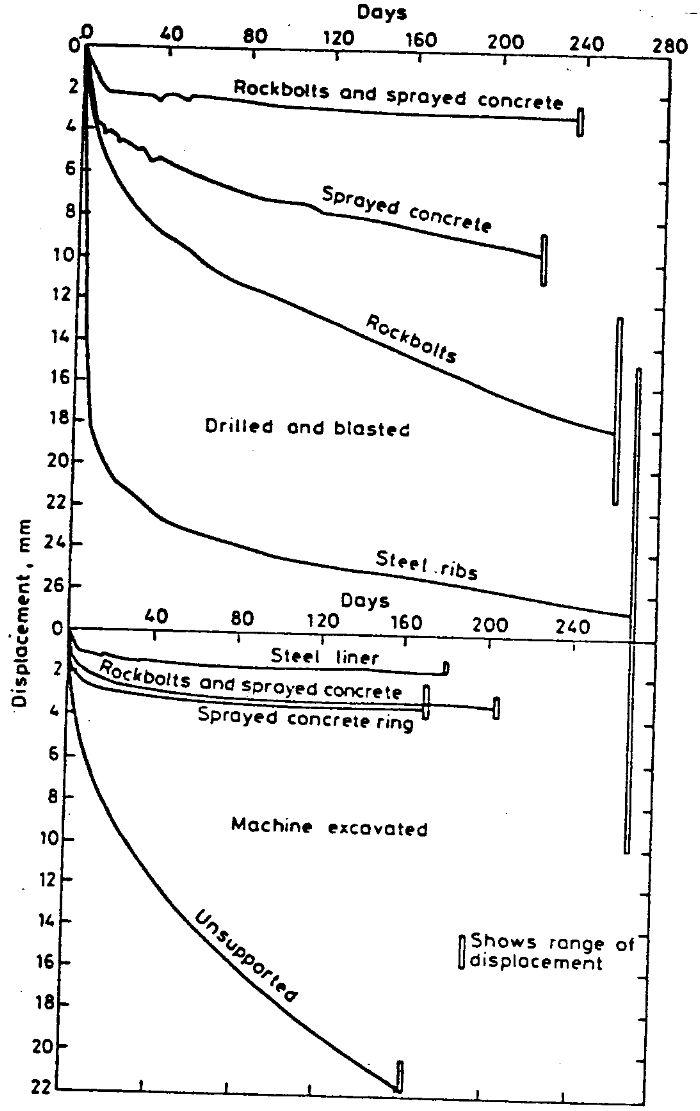

Figure 2.8 Typical displacements of rock 0.3m above crown in all support systems (Ward et al(1976))

Unfortunately, two important questions related to the time-dependent behavior could not be assessed directly from the data. The first one refers to the amount of load to be mobilized in the support as a function of its time of installation and secondly, the amount of deformations allowed to occur in a lined section before reinforcement is required.

- <u>Large underground excavations</u>

Problems associated with the design of support systems for the roof of both shallow and deep large underground chambers in jointed rock constitute another good example of 'loosening' ground. The features of particular concern are associated mainly with the large size of the span of these caverns with respect to the spacing of discontinuities.

The observation of the performance of those roofs as well as current engineering solutions can reveal certain aspects of the time-dependent character of loosening ground. One well documented case is the Washington D.C. Metro Dupont Station, a shallow depth opening of about 23m span excavated in a heavily sheared and blocky schistose gneiss under an overburden of 30m and rock cover of 10m.

A description of the geology, details about the structure of the rock and both design and performance of support system have been presented by Cording *et al*(1977) and Bawa and Bumanis(1972) .

The selection of this case history serves the purpose of illustrating the role of time in the special classes of problems associated with roofing of such large spans, namely:

a. stability of large individual blocks (wedges) and
b. the effect of excavation by stages and presupport techniques.

Figure 2.9 shows the geometry of the station, the general sequence of excavation and the lining strategy associated with each stage. A pilot tunnel was first excavated to assess the rock condition along the crown which revealed the presence of steeply-dipping shear zones closely spaced and planar, discontinuous and often slickensided joints causing the rock to be of a blocky and seamy nature. This rock mass would present, at this low stress level, the tendency for large blocks to loosen and either slide or separate from the walls and arch of the opening.

Figure 2.10 shows the excavation and deformations associated with the stage no. 1. Initially, excavation was advanced at a 6.1m wide and 8.2m high opening supported at the roof by rockbolts 7.3m long and 1.5m apart. The sidewalls were protected by a shotcrete layer of 5 cm immediately following the excavation. Figure 2.10b shows the progression of the deformations measured at three locations with time. With increasing deformations occurring in the sidewalls, the rock above the roof moved and deep deformations followed.

Figure 2.10c shows the time-dependent behavior of the rock mass after excavation with some extensometers indicating a large increase in the rate of deformation. Also displayed in this figure is the change in displacement pattern after rockbolts were installed. Even though the deformations were still not very large, within 10mm, there was a concern that the integrity of the rock arch above the crown would be in danger if these deformations were allowed to continue. For the later sections, the excavation of stage no.1 was followed immediately by the installation of support at the walls and a reduction in the height of this stage from 8.2m to 7.0m which contributed to reduce considerably both the amount and rate of deformations at the rock arch above the crown.

The movements in the roof during the widening of the span (stage no.3) were carefully monitored. The decrease in rate of deformations with time in addition to a small total deformation (3mm) were considered as indications that no worsening of the roof condition occurred during this stage. This demonstrated the effectiveness of the presupport of the roof in preventing further loosening.

2.3.3 Squeezing

The term squeezing ground has been applied in the literature to describe situations where the '...ground moved slowly into the opening' and/or linings were damaged by the ground which squeezed towards the opening. Typical examples

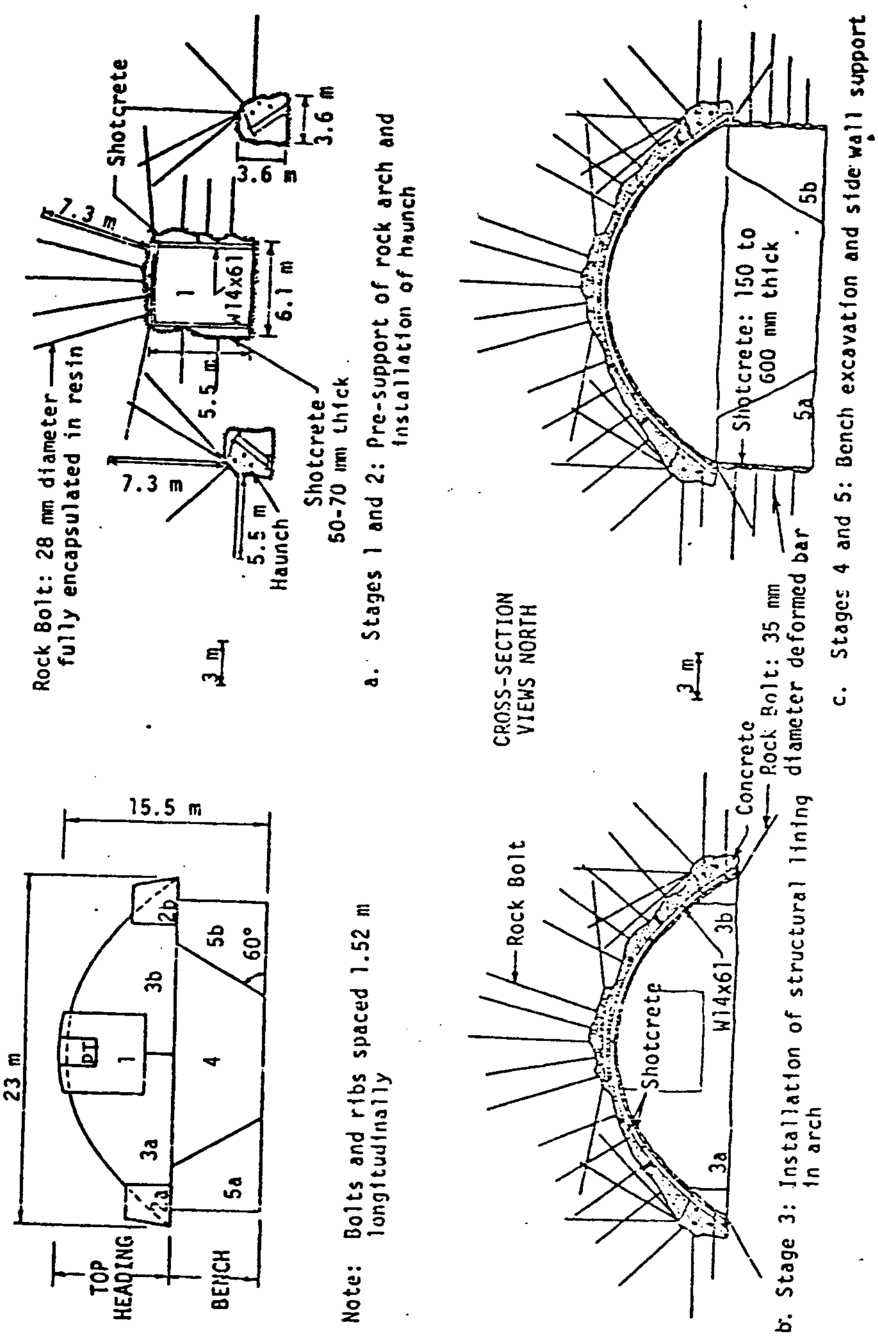

Figure 2.9 Excavation and support sequence at Dupont Circle Station (Cording *et al*(1977))

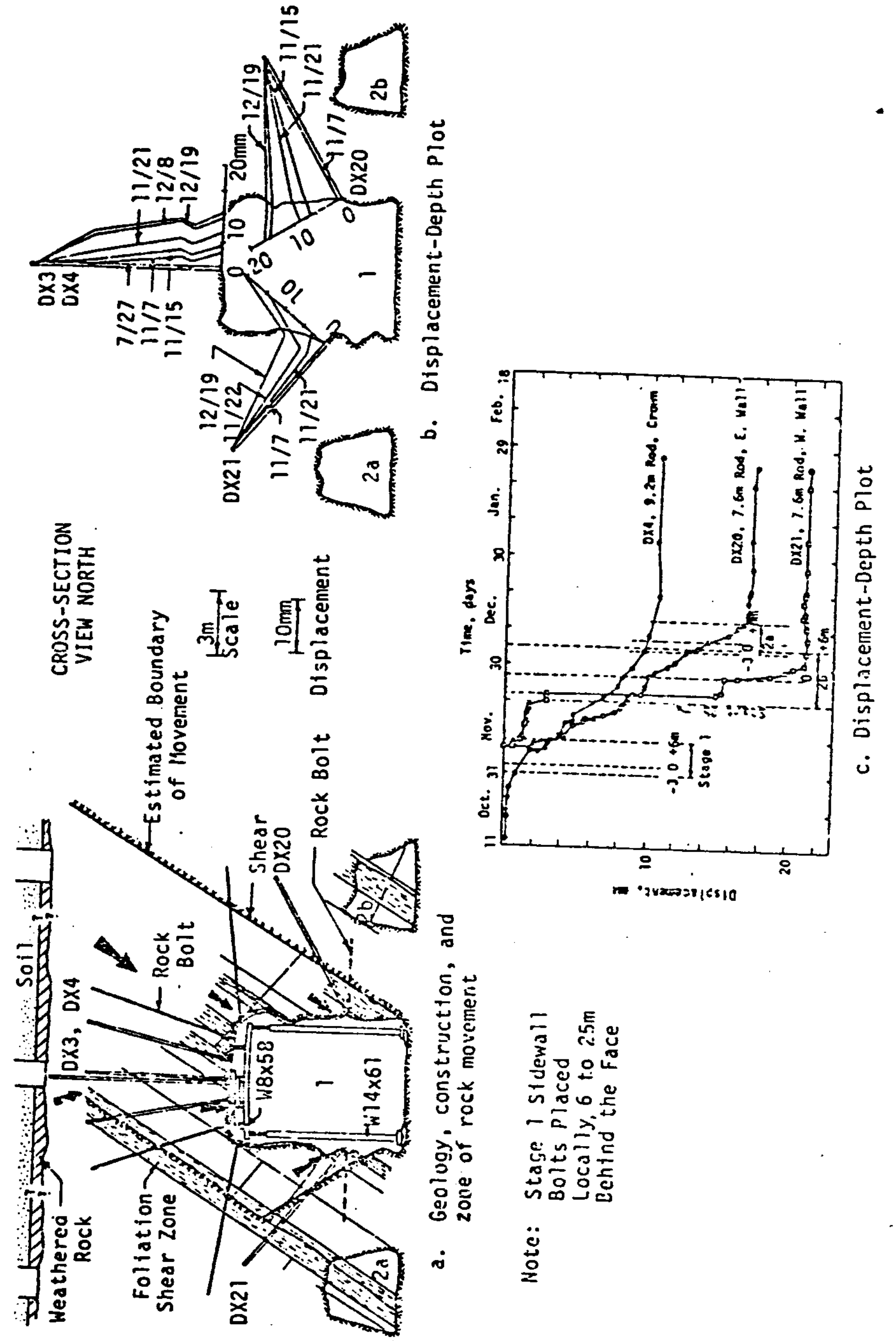

Figure 2.10 Displacement measurements associated with stages 1 and 2 - Dupont Circle Station - (Cording et al(1977))

of rock masses described as squeezing ground have been considered by Wahlstrom(1973) , namely:

a. incompetent sheared granite and gneiss (Roberts Tunnel, Colorado) ,

b. altered schist and gneiss (Vasquez Tunnel,Colorado),

c. soft to medium clays at moderate depth and clay shale at greater depths ,

d. fault gauges,

e. poorly consolidated soft mudstones and claystones, etc.

The phenomenon of squeezing ground in this thesis is associated with the delayed response of the rock mass when subjected to shear stresses which develop around the opening during excavation, i.e., this behavior is essentially due to rheological behavior of the rock mass. In order to investigate the conditions under which the ground behaves in a squeezing manner, the mechanisms leading to creep of rock mass around the opening have to be considered.

2.3.3.1 Mechanisms leading to squeezing

Two basic hypotheses have been considered in the literature to describe the stress conditions causing creep behavior of the rock mass around an opening. The most common one has been to assume that, immediately after excavation, the stresses developed around the opening do not cause failure, i.e., they are smaller than the short-term strength. It is considered then, that the new state of stress at any point around the opening causes the ground to deform with time. The analytical model associated with this hypothesis as well as some applications will be discussed in detail in Chapter 6. Figure 2.11 illustrates the process of stress transfer for the case of a hydrostatic stress field and a circular opening.

A second hypothesis, which is an extension of the previous one, considers that the state of stress immediately after the excavation will cause overstress of the material around the opening. The overstress or failure of the material described by this hypothesis is different from the one indicated in section 2.3.1 where the rock mass is more brittle. The rock mass in this situation responds in a more ductile manner. The process of stress transfer is conceptually equivalent to the one described previously, i.e, creep deformations tend to minimize stress concentration. In addition to the requirement of rheological response of the rock mass, the concept of squeezing ground also reflects the presence of soft to very weak rocks, especially highly weathered rocks and clayey fault gouge.

Unlike for the previous cases of fracturing and loosening, the use of Barton's classification system does not seem satisfactory for the purpose of providing guidelines to indicate the spectrum of rocks leading to squeezing since some parameters lose their meaning when associated with heavily weathered rocks. However, a range of values based on this classification system has been

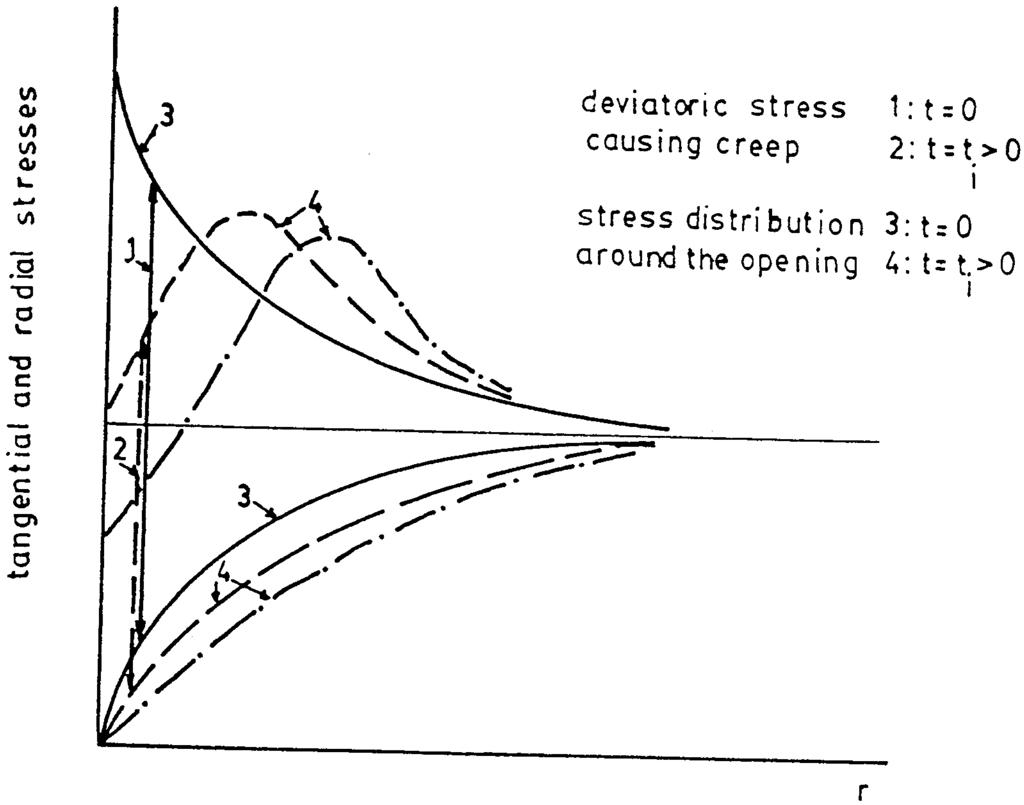

Figure 2.11 Schematic stress transfer during creep around circular opening

suggested in Table 2.1 which provides some consideration about the potential for squeezing.

2.3.3.2 Survey of case records

Semple *et al*(1973) presented a number of examples of tunnelling in ground conditions described as squeezing. Most of the reported case-records, some listed in Table 2.2, reflect tunnelling methods consisting in lining the opening with sets of steel ribs and wooden lagging. An important characteristic of these case-records is that the rock types consist mainly of highly weathered rocks, clayey fault gouges and very soft rocks presenting, in all cases, almost soft-ground tunnelling conditions at large depths. These cases cannot be described as being typical rock tunnelling situations. Therefore, the large deformations or the large number of stability problems associated with these projects are essentially due to a very low strength of the material as compared to the shear stresses mobilized during excavation.

The main purpose of Semple's survey was to collect information relative to the final thickness of sets of steel ribs as well as its spacing, i.e., the final lining necessary to control tunnel closure and reduce deformations to acceptable values in order to continue with the excavation. This summary revealed a progressive increase in the ratio h/a, where h=thickness of steel lining and a=radius of the opening, with the 'worsening' of the ground

Table 2.2 Survey of case-records in squeezing ground

Tunnel/ Project	Size and shape of exc.	Rock type description	Tunnel depth	Sources and Further comments
Berkeley Hills tunnel (California)	6.3m horseshoe	Faulted sheared shale and gouge	150m	- Ayres(1969) - steel sets as support
Straigth Creek Pilot tunnel	2.4x2.7m rectangular	Fault zone in gneiss and schist having the consistency of stiff clay	300m	- Hooper et al(1972) - squeezing movements of 12" in the sides and 24" in the invert. - steel sets as support
Tecolote Tunnel	2.7x2.7m horseshoe	Fault zone, sandstone and shale	240m	- Crooker(1955) and Trefzger(1966) - steel sets as support
Carley V. Porter Tunnel	7.2m circular	Fault zone, crushed granite	?	- Varello(1970) - steel sets as support
Mono Craters Tunnel	3.6x3.6m horseshoe	Fault zone at metamorphic and granite contact	300m	- Proctor and White(1946) and Sandborn(1950) - Wilson and Mayeda(1969) - steel sets as support
BART Fairmont Hill tunnel (California)	6.1m circular	Fault zone, decomposed serpentine, saturated	53m	- Myer et al.(1977)
Henderson Haulage Tunnel	4.6x5.2m horseshoe	Fault zone, dark clay and coarse to fine sand	400m	- Brekke and Howard(1969) - steel sets
Alpine Highway Tunnel(Alberg)	10m circular	weak phyllites	960m	- Rabcewicz(1975) - excavation procedures: top-heading and two benches. - shotcrete reinforced with rockbolts immediately after excavation. - large deformations occurred initially.

conditions. Values of the ratio h/a obtained in typical cases in soft ground tunnelling were found to be greater than the ones associated with 'heavy' squeezing conditions at much greater depths. This result, however, simply reflects the concern in shallow soft-ground tunnelling for reducing the surface settlements to a minimum which is accomplished by the use of a much heavier lining. No measurements of deformations associated with the excavation of these tunnels were reported.

Another survey of case-records in squeezing ground was presented by Myer et al(1977) . The aim of this survey was to attempt to identify in practice the factors which influence the stand-up time of tunnels in squeezing ground and some relevant solutions to increase this time. In Table 2.2 some of the case-records compiled by Myer are listed. Two features associated with these case-records deserve special attention: initially, one should notice the large spectrum of depths which can be associated with squeezing conditions and secondly, the material types identified in this selection of case-records fall into the same group of rock types as the one observed in Semple's survey.

It is important to recognize, however, that these two surveys collect basically the situations where the rock types consist essentially of very weak materials and can be considered as extreme cases in the wide spectrum of possible types of rock mass leading to squeezing. Also some of these cases are associated with a somewhat outdated excavation procedures which may have added to some of the stability problems encountered.

- Yarbo No.1 Shaft at Esterhazy, Saskatchewan

This 5.4m diameter shaft was sunk to reach potash deposits at depths over 900m. Barron and Toews(1963) describe the results of displacement measurements carried out at a depth of about 925m at an unlined section of the shaft located on a salt bed above the potash deposits. Borehole anchors were installed at depths of 0.15, 1.2, 2.8 and 3.0 meters from the shaft surface to measure the radial convergence of the rock mass surrounding the shaft. The location of these anchors is shown in Figure 2.12.

Figure 2.13 shows the displacements relative to the shaft axis versus time for each depth. The creep-like nature of the deformation versus time curves is clearly evidenced in this figure. The data indicate a change in the rate of deformations from an average of 3.8mm/day in the first day of measurements to a 0.17mm/day after about 40 days which represents a twenty-fold drop in the rate of deformations. The data displayed in Figure 2.13 have been plotted as shown in Figure 2.14 which indicates the distribution of radial displacement with time. At the end of a 40-day period, the size of the zone affected by the creep deformations can be estimated as about 7.5m or about 1.5 times the diameter of the shaft. This zone corresponds approximately to the region

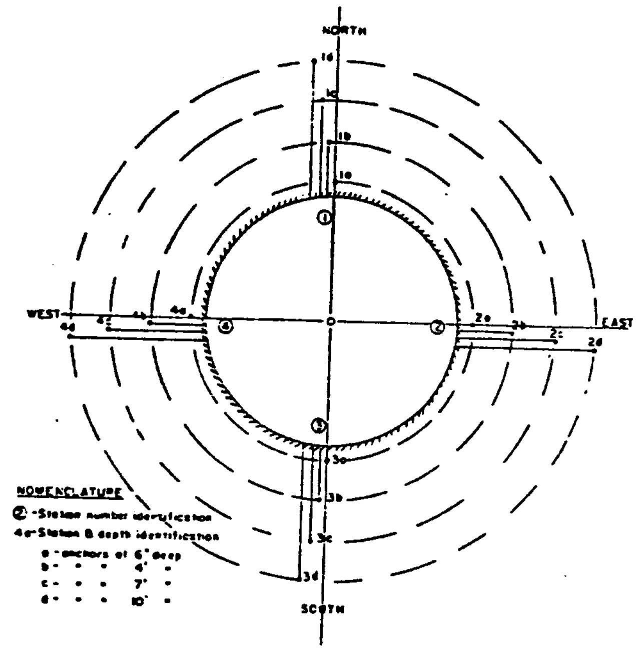

Figure 2.12 Yarbo shaft No.1 - Layout of measuring points
(Barron and Toews(1963))

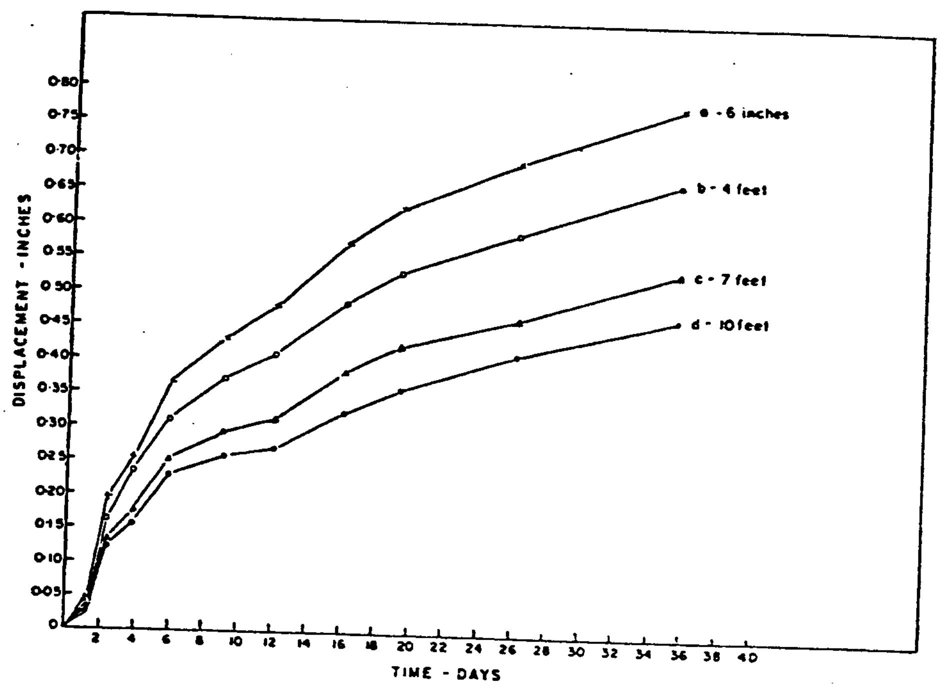

Figure 2.13 Mean radial displacement relative to shaft axis with time for each depth - Yarbo shaft No.1 (Barron and Toews(1963))

around the opening where stress redistribution occurs, i.e, the load-bearing zone.

- <u>Giri Tunnel, India</u>

This tunnel, described by Ward(1978), constitutes one of the many examples associated with Indian hydro-electric projects in the Himalayas. It consisted of a 5.5 meter diameter circular tunnel excavated in highly slickensided and fragmented phyllites at a depth varying between 200 and 300 m. The tunnel was excavated full-face and lined simultaneously with circular and strutted horseshoe steel ribs of 150 x 150 mm section at 0.5 m centers with pre-cast concrete lagging. Figure 2.15 presents some of the measured tunnel closure versus time. A very large diametrical deformation of 0.8-1.0 m(about 17%) occurred up to about 100 days when a noticeable decrease in the rate of deformations was observed.

A sudden increase in deformation rate was observed after about 220 days which could be correlated with blasting operations at the approaching face 100m away from the measuring station. This large increase in deformation rate stopped after 20 days when again a remarkable reduction in the rate of closure was observed. Although the Author was not able to check other data relevant to this case-record, it seems logical to raise the possibility that most of the initially high rate of deformations observed was in fact due

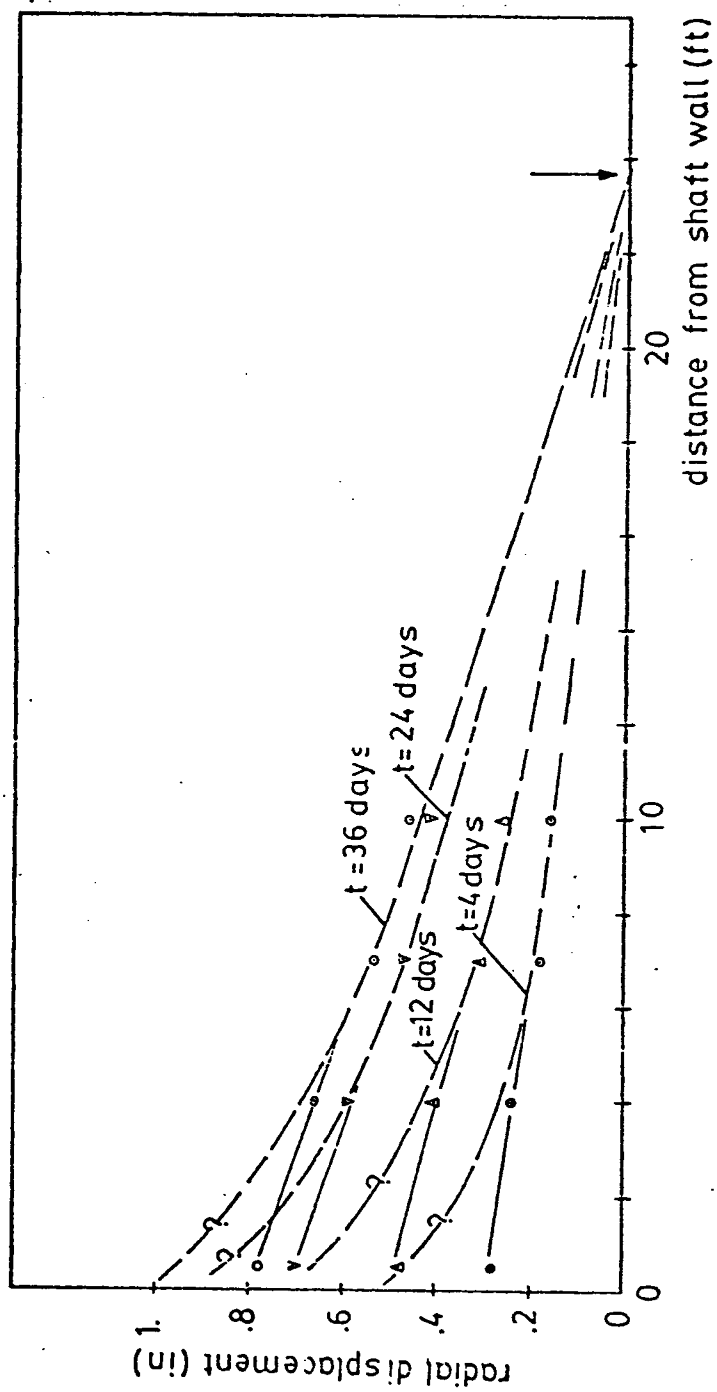

Figure 2.14 Yarbo shaft No.1 - Distribution of radial displacement versus time

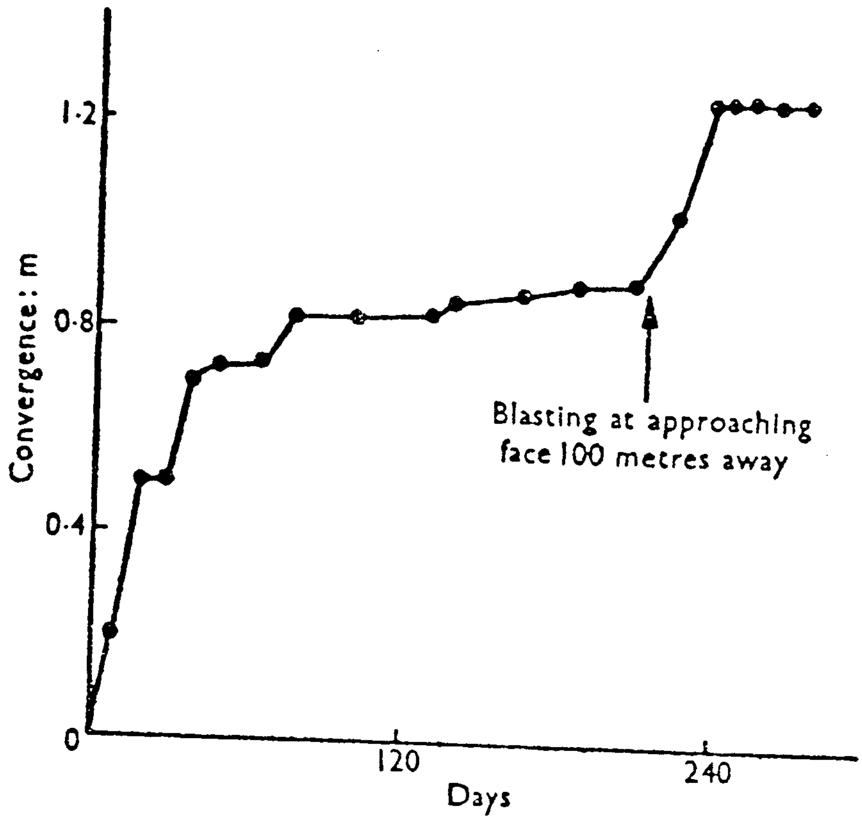

Figure 2.15 Convergence time curve for partially concreted sections of Giri Tunnel, India (Ward(1978))

to the face advancing operations. In that case, the deformations due to time-dependent behavior of the rock mass would be small compared with the deformations triggered during excavation. Ward(1978) uses this case-history to point out correctly the need and the importance of yielding supports with the capability of yielding of up to 20%.

2.3.4 Swelling

Swelling is a term normally reserved to describe the time-dependent volumetric increase evidenced by some earthen materials. A complete description of the mechanisms causing swelling in rocks as well as experimental data supporting them has been discussed extensively by Einstein and Bischoff(1975) and Lindner(1976) and include the following:

a. change in the state of stress, specially unloading,

b. water adsorption by some clay minerals, and

c. volumetric change associated with chemical changes (anhydrite into gypsum, etc).

Of particular interest to the ground control specialist is the set of conditions leading to swelling around an underground opening and its particular features.

2.3.4.1 Mechanisms leading to swelling

The following set of events causes this mode of ground behavior.

Stage no.1 : a stress relief zone is created around the opening. Wittke and Rissler(1976) considered this stress relief zone as represented by regions around the opening which presented a reduction of the first stress invariant. By simple elastic calculations, Wittke and Rissler(1976) showed that zones of stress relief can be created at roofs and floors and depend on both shape of the opening and ratio between principal stresses. Figure 2.16 illustrates the zone of stress relief around a circular opening and a ratio of principal stresses less than 1.0.

Other factors can also contribute to the creation of such a stress relief zone. They are: failure of the material around the opening, damage created during excavation, loosening of blocks and opening of joints. Also the sequence of excavation and support installation, especially for cases which cannot be advanced full-face play an important role on the size and location of the stress relief zones. As a general rule, the invert will be the region where the maximum stress relief will occur.

Stage no.2: water is needed to start the swelling process in the zone of stress relief indicated by zones (I) and (II) at Figure 2.16. This water can be provided by either one of: air humidity, ground water or any water used during excavation. Terzaghi(1946) has suggested an internal migration of water from zones of stress concentration to zones of stress relief. Terzaghi observed in some tunnels a considerable increase in the water content near the walls and which could not be explained by water provided by air moisture. Nakano(1979) suggested a similar process but with

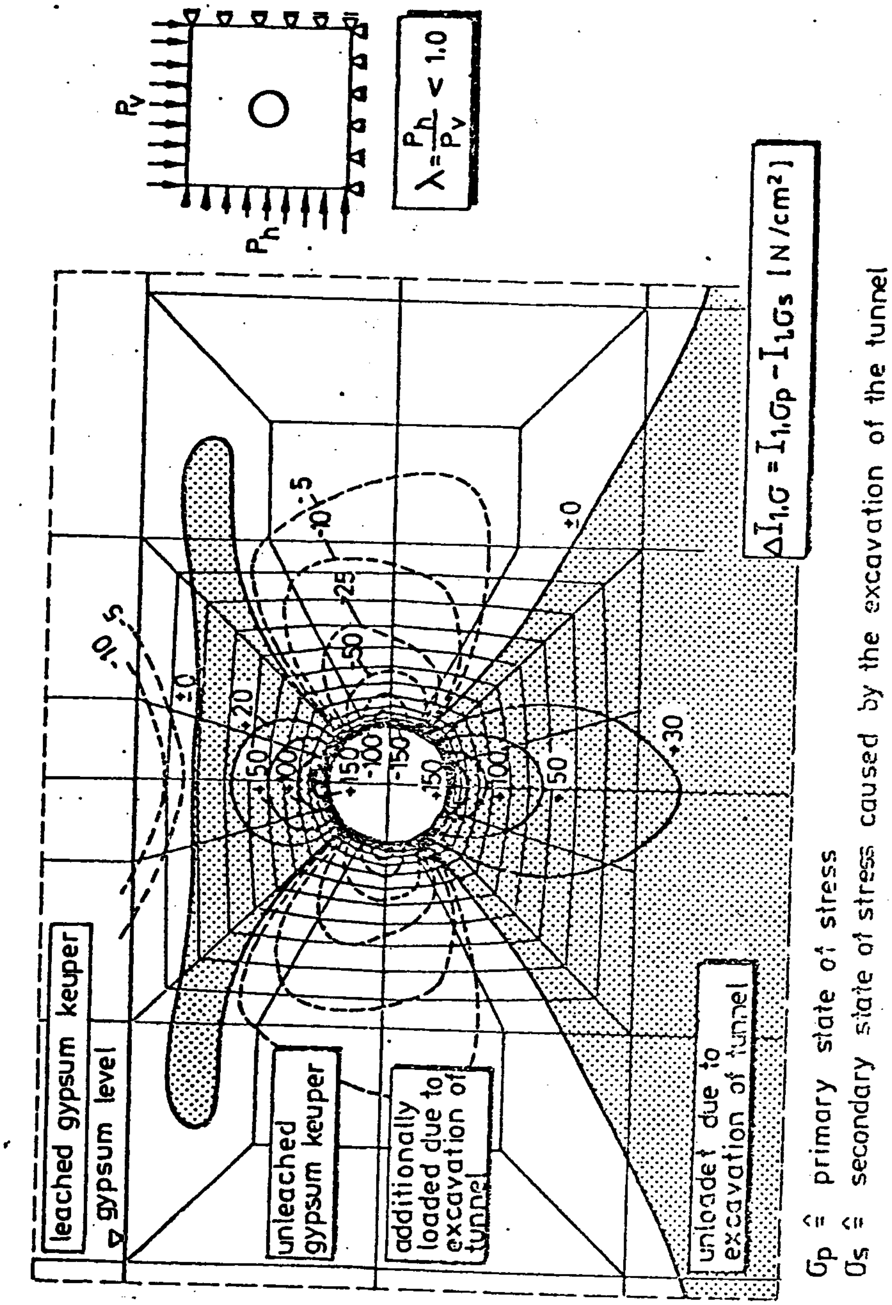

Figure 2.16 Schematic variation of the 1st. stress invariant due to tunnel excavation (Wittke and Rissler(1976))

the increase in water content being quite localized along shear planes created during excavation.

In this context large quantities of water are not necessary to initiate a swelling process. Nakano considered this process for rocks such as the ones common in sedimentary (mudstones and shale) and metamorphic (schist, phyllites, etc) formations in Japan.

Stage no.3: the material around the opening may lose strength due to either an increase in water content or some deterioration due to air exposure. This loss in strength causes further stress relief around the opening which will accelerate the stage no.2 discussed earlier. Some creep deformations are probable to occur at this stage which are difficult to distinguish in the overall process.

2.3.4.2 Survey of case records

The frequent occurrence of cases reporting swelling conditions during tunnelling has made this mode of ground behavior of great importance in certain areas, e.g., Central Europe, Japan and North America. As a recognition of this importance, the International Society for Rock Mechanics organized a commission to study the behavior of tunnels in swelling ground. In a report to this commission, Lo(1979) presented a list of case records described in the literature as being examples of swelling. This list covers no less than 11 cases in Southern Ontario, Canada, 6 cases in Norway, 6 cases in Switzerland, 2 cases in USA and 4 cases in Japan (see Tables 2.3 and 2.4). Most of the case-records constitute excellent examples of the current state-of-the-art associated with excavating and supporting these tunnels as well as the type of tests which have been proposed to evaluate the swelling potential associated with a certain formation. Next, a brief summary of these case-records is presented.

- <u>Case-records in Southern Ontario, Canada</u>

A number of case-records have been registered in Southern Ontario clearly indicating the effect of the stress relief zone and the time-dependent volumetric increase in underground structures in rocks. Table 2.3 lists some of the reported case-records summarizing briefly the rock formation, construction procedures and the performance for each one of them.

The results of measurements of the deformations at the Wheelpit of the Canadian Niagara Power Co., a 5.5 wide and 50m unsupported trench, since 1902 indicate that these deformations can occur for a long period of time without actually coming to a hault. The potential for swelling of these rocks has been studied by Lee and Klym(1978) who suggested the free-swell test as a good way to assess the time-dependent properties of these rock formations. As the deformations were found to relate in a linear manner with the logarithm of time the deformations per log cycle was

Table 2.3 Selected case-records of time-dependent deformations of underground opening in Southern Ontario - (after Lo(1979))

Location	Type of Construction	Rock Formation	Regional Stresses in Rock	Description of Performance	Reference
Wheelpit of the Canadian Niagara Power Co. (1902)	5.5 m wide by 50 m deep open excavation - unsupported	a. 36 m in Lockport limestone and dolomite; 15 m in Rochester shale b. Deformation potential of Gasport limestone and Rochester shale ≈0.1% strain per log cycle of time	6.9 MPa	a. Time-dependent deformations in the wheelpit wall was monitored since 1902. b. Time-dependent movements in the rock occurred mainly at the lower guide, turbine deck and rack deck levels located in the Gasport limestone and the Rochester shale. c. Up to the present 100 mm of deformation has been recorded at the turbine deck. d. The continuous rock movements have severely affected the operation of the turbines.	Smith(1905) Lee and Lo (1976)
Wheelpit of the Toronto Power Plant (1904)	5.5 m wide by 50 m deep open excavation partially supported with massive concrete arches (5.8 m wide 3 m deep at abutment and 1.5 m deep at midspan) at ≈1/3 points along the depth of excavation. Excavation lined with 0.6 m brick lining.	a. Approximately 45 m in Lockport limestone and dolomite; 5 m in Rochester shale b. Deformation potential of Gasport limestone and Rochester shale ≈0.1% strain per log cycle of time	6.9 MPa	a. Rock movement monitored between 1951 and 1956; magnitudes of movements in Rochester shale comparable to that in the wheelpit of Canadian Niagara Power Co. within same time period. b. Approximately 36 years after construction, buckling of the I beams across turbine deck located in Gasport limestone occurred. c. 52 years after construction, failure appeared in the massive concrete arch built into the Gasport limestone.	Lee and Lo (1976)
Thorold Tunnel (1963-1968)	26 m wide by 15 m deep excavation. Space between tunnel and rock filled with compacted rock fill except a. at west service building, 60 mm bentonite layer placed between 0.9 m bulkhead and the 1.83 m thick south wall of the tunnel. b. An additional 25 mm fibre board was placed to protect the bentonite in the north wall.	a. Lockport formation - 6 m in Goat Island dolomite and 8.5 m in Gasport limestone b. deformation potential of Gasport limestone ≈0.1% strain per log cycle of time	8.3 MPa to 14.5 MPa Stress measurement performed	a. One year after construction, minor horizontal cracks occurred in south wall of west service building. b. 3 years after construction, extensive cracking of south wall (1.83 m thick) occurred with major cracks penetrating to depths in the order of 1 m from the face of the wall. c. Remedial measure comprised of cutting 150 mm slots behind the south wall of the west service building in order to relieve pressure from the rock. d. Performance in north wall generally satisfactory.	Lo et al. (1975) Bowen et al. (1976)
Queenston Chippawa Canal (1920)	15 m wide by 25 m excavation, 150 mm thick concrete floor slab with no expansion joint.	a. 6 m overburden, 15 m of Lockport dolomite and 3 m of Gasport limestone b. Deformation potential of Gasport limestone ≈0.1% strain per log cycle of time	6.9 MPa	a. Buckling of concrete floor occurred during construction. Compressional cracks and bulges occurred at two sections of the canal and some of the bulges were as high as 1 m. b. Heaving of the concrete slab was observed over a length of 915 m when the canal was dewatered 44 years after construction.	Lo et al. (1975) Int. Report Ontario Hydro (1951) Lo (1978)

Location	Type of Construction	Rock Formation	Regional Stresses in Rock	Description of Performance	Reference
Lakeview Treatment Plant Outfall Tunnel, Mississauga (1974-1975)	4.3 m diameter circular tunnel excavated by an Alpine miner	Meaford-Dundas shale, rock cover to tunnel ≈6.7 m	6.2 MPa stress measurement performed	a. Instability of the roof developed in section supported solely with shotcrete after the tunnel was advanced by about 152 m. b. Before installation of permanent lining the rate of free deformation (closure) at the springline was 0.13 mm/day. c. The deformations in the rock were deep-seated.	Lo and Morton (1976)
Easterly Intake Tunnel, Scarborough (1974-77)	4 m diameter circular tunnel excavated by drill-and-blast technique for the first 200 m and by tunnel boring machine for the remaining 2700 m.	Collingwood shale; 33 m of overburden and 30 m of rock cover	6.9 MPa	a. Roof instability occurred in the form of slabbing and coning after the initial advance of the tunnel. b. Progressive slabbing of the roof occurred at many locations. Depth of coning reached 1 to 1.5 m. c. Rock movements of up to 13 mm were measured at the springline in 300 days.	Lo and Morton (1976)
Sir Adam Beck Niagara G.S. Twin tunnels (1951-53)	15.5 m diameter circular twin tunnels at 76 m centres, excavated with drill-and-blast technique with staged heading and benching. Minimum rock cover 30 m	Cataract group of Lower Silurian Tunnel crown in sound hard Irondequoit limestone and Reynales shale. Invert in Grimsby sandstone with frequent shale interbeds	8.3 MPa to 14.5 MPa	a. Crown apparently stable but some buckling and heaving of invert during construction. b. Progressive inward movements at springline and inward. At 300 days after construction ≈5 mm (after elastic response) inward deformations measured at springline.	Hogg (1959) Lo and Morton (1976)
Redhill Creek Sewer Tunnel Hamilton Mountain (1975)	Rectangular tunnel poured against rock in an open cut	Lockport-Anabel formation, horizontally bedded dolomites and limestones with some shaly partings	8.3 MPa to 14.5 MPa	a. Approximately 50 mm of movements (inward) have been observed on each side of trench wall. b. Shearing of borehole and inclinometer casings, and cracking of concrete lining.	Franklin (1976) Lee (1978) Quigley et al. (1978)
South Peel Trunk Sewer, Mississauga (1972-73)	3 m diameter circular tunnel excavated with full face tunnel boring machine (Robbins)	Meaford-Dundas shale, rock cover ≈ 12 m	1.4 MPa to 6.9 MPa	a. 0.45 m thick concrete lining installed several days after excavation. Horizontal cracking at springline occurred within weeks of casting. b. 2.5 mm of inward horizontal movement recorded after 4 months. Approximately 46 m of tunnel affected.	Czurda and Quigley(1973)
South Peel East Trunk Sewer, Mississauga (1974-75)	3.2 m diameter circular tunnel excavated with drill-and-blast technique	Meaford-Dundas shale, minimum rock cover 3 m	1.4 MPa to 6.9 MPa	0.38 m cast-in-place concrete lining installed one to two days after excavation. Horizontal cracks at springline noticed two to three weeks after casting, opening up to a maximum of 6.4 mm.	Morton et al. (1975) Dubnie and Geller(1975)
Heart Lake Trunk Sewer Tunnel (1973-75)	Tunnel in 3 sections: a. 2.74 m I.D. 1050 m long excavated by TBM b. 3.05 m I.D. 183 m long excavated by drill-and-blast technique c. 3.05 m I.D. precast concrete pipe laid in open cut 232 m long d. 0.3 m thick concrete lining cast-in-place for sections (a) and (b)	Meaford-Dundas shale	1.4-6.9 MPa stresses measured around tunnel in TBM and drill-and blast section	a. Concrete lining installed generally within 10 days in drill-and-blast section and between 10 days and 160 days in TBM section. b. Cracking occurred in entire drill-and-blast section at springline within 3 years after completion. c. Cracking occurred in TBM section 2 1/2 years after completion for a length of 100 m. d. Severe instability of roof occurred during construction in drill-and-blast section. e. No instability condition reported in TBM section during construction.	Lo and Yuen (1978) Lo et al. (1979)

Table 2.4 Selected case-records of tunnels in swelling ground around the world - (after Lo(1979))

Tunnel/ Project	Size and shape of exc.	Rock type description	Tunnel depth	Sources and Further comments
Noshiro Tunnel Japan	3.6m horseshoe	mudstone, LL=96% PL=48%	25-30m	- Nakano(1979) - drill and blast
Bozberg (Switzerland)	7.5m horseshoe	Anhydrite Marl	?	- Einstein and Bischoff(1975) - considerable damage to the invert in anhydrite section (30cm/30 yrs.)
Richen tunnel (Switzerland)	?	Marl	?	- Einstein and Bischoff(1975) - deformed 30-40 cm immediately after construction; destruction of invert slab.
Belchen Tunnel (Switzerland)	5.2m circular	Opalines clay shale	500m exc. stages	- Einstein and Bischoff(1975) - shortly after exc., heaving destroyed drainage pipes
Kamui	10 m		30-100 m	- Widerhofer(1972)
Kubiki	10 m	Serpentine	150 m	- Large plastic deformations thought to
Shin-Noborikawa	6.5 m	rock	300-400 m	be due to low strength of the rock.
Onitoga	7 m		300 m	- Construction difficulties improved by
(All Japanese cases)				using high flexibility tunnel supports.

selected to differentiate between rocks of different swell potential.

- <u>Wagenburg Tunnel : experimental section</u>

Wittke(1978) described the main characteristics and geological profile of this tunnel located in Stuttgart, Germany. Associated with the excavation of this tunnel, a large scale experiment involved the excavation of two adits with the aim of studying the swelling behavior of the invert. Both adits have a horse-shoe shape with a height of 2.7m and a width of 3.0m and were excavated in unleached gypsum rock at a depth of between 40 and 50m.

The invert of test adit I since its completion in 1971 was exposed only to air humidity. Five 10-m long 5-point extensometer recorded the displacements below the invert. During the first two years heaving along the axis reached about 27mm and extensometers indicated an area of 1.0m below the tunnel floor beyond which no displacements were measured. After 2 years the deformations ceased and no further displacements were measured.

In test adit II the invert was constantly irrigated since its completion in 1973. Four 10-m long 5-point extensometers were installed to record the displacements; two extensometers were installed along the axis and two others along the sides of the adit. Two zones were considered: one anchored zone consisting of a 1.4 x 1.4m rigid plate anchored by eigth 10m-long prestressed anchors and one unanchored zone. Three years after the beginning of irrigation heave up to 460mm occurred in the unanchored zone. In its turn, the anchored zone heaved, during three years, just about 23mm and as a result of this heaving pressures of up to 2.2MPa were measured along the contact plate-rock.

- <u>Storage Tunnel in Marl</u>

Einstein and Bischoff(1975) presented a summary of the discussions related to the investigations associated with this opening. Figure 2.18 presents a cross-section view of the instrumented section which shows the invert completely excavated in Marl. Also indicated in Figure 2.18 is a plan view of the instrumented section illustrating the layout of the rockbolts installed in the invert. Such a field testing program was carried out in order to assess the efficiency of rockbolts in reducing heaving of the invert.

Deformations were measured at the surface as well as at depth by means of multiple-point extensometers. Figure 2.19 shows the results of the measurements at one extensometer (E10) located at the unbolted section and their variation with time. These results clearly suggest the existence of a boundary at about 3.0m below the center of the invert defining two distinct regions as far as swelling response is concerned. Region (I) immediately below the invert is the region where most of the heave is concentrated. The maximum heave of the unbolted section observed during a period of 3 years amounted to 76 mm.

Rockbolts were installed at the invert at depths of 2.5,4.0 and 6.0m respectively. Comparisons of the effectiveness showed that only the bolts 4.0 and 6.0m long provided a reasonable reduction in total heave (about 60% reduction over a period of 3 years) which is in full agreement with the results obtained in the unbolted section.

2.4 Final remarks

In the previous sections classes of ground behavior were suggested and their main characteristics were pointed out. For each one of these classes the engineering problems associated with the time-dependent behavior were discussed. As a first approximation, the following observations can be made.

- Fracturing

1. No consistent set of field data relative to both depth of fractured zone and its eventual propagation with time could be gathered. Available data consists in measurements of the thickness of the overall damaged zone which also includes the effects of blasting, e.g., Hayashi and Hibino(1968) . The depth of anchoring is a function of the thickness of this zone and guidelines

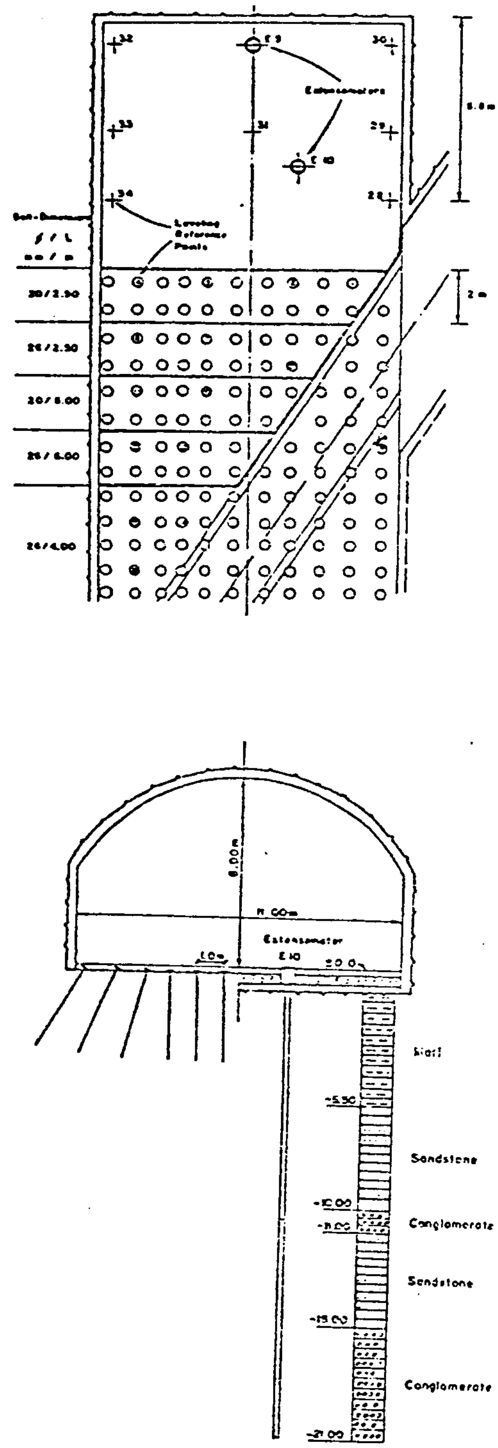

Figure 2.17 Storage Tunnel in Marl - Test section (Einstein and Bischoff(1975))

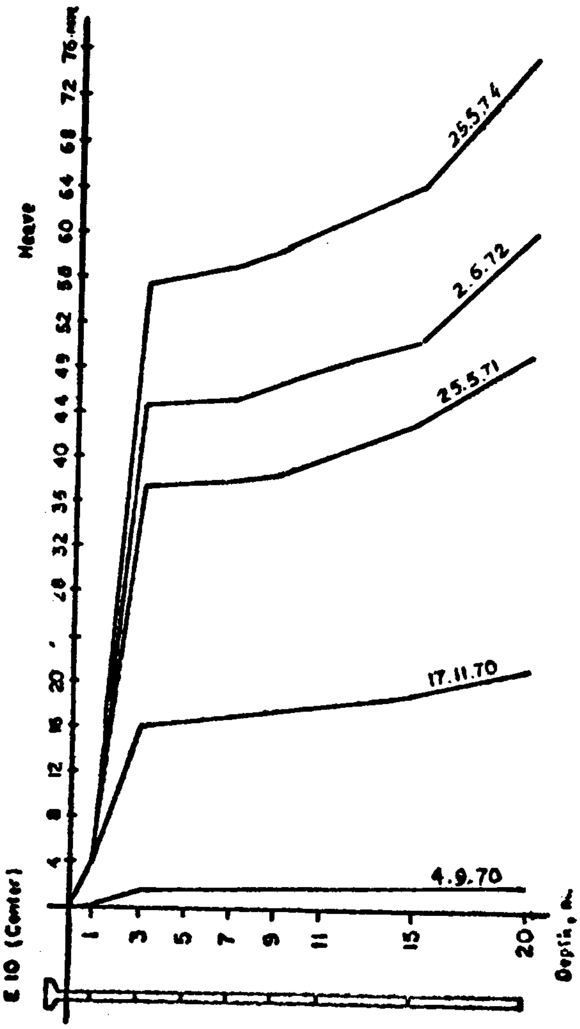

Figure 2.18 Storage Tunnel in Marl - Displacement measurements in unbolted section. (Einstein and Bischoff(1975))

such as 1/3 of the tunnel diameter and wall height (for large underground openings) have been suggested.

2. The fractured zones have to be protected as early as possible due to: (a) safety reasons especially when located in the roof of openings (rock falls, slab detachment), and (b) to arrest any propagation of these zones.
3. Time-dependent deformations are very small, maybe of a much less magnitude than the immediate response. Hence, the characteristics associated with the lining strategy are: (a) amount of required support will be a function of the depth of these zones, (b) support has to be designed in order to withstand further movements due to progression of the excavation and (c) supporting measures must also provide protective shield in order to avoid deterioration of the material around the opening.
4. Special attention must be paid to cases of large underground openings where walls must be protected as early as possible at the first sign of fracturing. These large openings are normally excavated in stages and before each stage is excavated, zones of overstressing must be protected ideally by rock reinforcement. Actual modelling of the excavation stages can be done and the sequence which best minimizes the size of overstressed zones should be followed.

- <u>Loosening</u>

1. The 'loosening' process was identified as a progressive loss of load-bearing capacity of the rock mass due to excessive deformations and which would eventually lead to failure of opening if appropriate measures were not taken.
2. Enough evidence in the literature indicates that this process is time-dependent and case-records were discussed which showed typical deformation versus time curves for the rock mass around the opening. For the case of the Kielder Water Scheme Experiment, radial deformations between 20 and 40mm occurred within a period of about 400 days.
3. The most important behavioral parameter associated with this mode of ground behavior is the total deformation which defines the start of the release of blocks. This is not readily evaluated. Safety reasons and economics require early installation of support measures.
4. The question of time-dependent deformations becomes secondary since all the efforts should be directed towards an early arrest of deformations.
5. This mode of ground behavior is particularly important for large underground openings at shallow depths. Multiple-face excavation has to be used in many instances and presupport technique to improve rock conditions and hold particular wedges in place may be essential to maintain a safe excavation.

- Squeezing

1. Cases reported seem to indicate that deformations can be very large as well as the time for reaching equilibrium. Excavation cannot proceed if large amounts of deformations occur during excavation. Therefore, initial support is installed in order to prevent initial failure of the hole. This support in order to be effective has to be flexible to take deformations due to face advance.
2. Support also has to be able to cope with delayed deformations. Now the question which seems to be appropriate is the relative order of magnitude between instantaneous and delayed deformations.
3. The main goal of the designer is to reinforce the rock mass around the opening in such a way that maximum advantage is taken from the rock mass. An extra step in this direction is the closure of the invert as soon as possible as well as installation of flexible lining on the roof and walls.
4. The time-dependent deformations after this event will be more or less a function of the initial state of stress around the opening as well as the disturbance in material properties.

- Swelling

1. The same set of general ideas discussed for the case of squeezing can be applied to swelling with now the special condition that the variation of the first invariant of the stress tensor is the controlling factor in generating time-dependent deformations.
2. It constitutes good practice to minimize the development of these stress relief zones which associated with delayed placement of the invert may lead to undesirable deformations and delayed deformations.
3. The special feature is that the longer one waits to support properly the invert the worse the situation gets since the accumulated deformations will generate more stress relief which in turn will lead to more swelling.

Chapter 3

REVIEW OF TIME-DEPENDENT PROPERTIES OF ROCKS

3.1 Introduction

The phenomenon of time-dependent behavior of rocks is a source of many problems in designing structures in rock. Foremost amongst them is the need for methods of predicting the performance of structures in creeping rocks. In order to address this problem it is necessary to have data on the stress-strain-time response of rock. The present review summarizes some of the ideas developed from previous investigations on time-dependent properties of rocks and, in so doing, it sets the stage for Chapter 4 which presents the results of creep tests on jointed coal.

The basis for the study of the time-dependent behavior of materials can be credited to Andrade(1910) who studied the behavior of metal wires subjected to constant tensile stress above the elastic limits to strains up to 30%. Andrade's results lead to the proposal of empirical laws describing the development of deformations with time and the separation of the creep deformations into three components :β-flow(transient or primary creep), viscous flow (secondary or steady-state flow) and tertiary creep. At the present time, almost seven decades later, an extensive literature on time-dependent behavior is available covering both a wide range of materials (such as metals, plastics, rubber, ice, soils and rocks) and applications (such as mechanical, civil and mining engineering, metallurgy, geological and geophysical studies).

The developments during this period of time with respect to the time-dependent behavior of rocks have been summarized by state-of-the-art reports given by Robertson(1964), Cruden(1969) and Wawersik(1973). These reviews have revealed a myriad of stress-strain-time relationships each credited with a good representation of experimental data on creep of rocks. This diversity certainly introduces some restrictions with respect to the usefulness of these relationships for practical applications. The present review summarizes the more recent data on creep of rocks and critically assesses the relevant information with respect to the analysis and interpretation of creep data. It also summarizes the relevant works on time-dependent failure and on the relaxation properties of rocks.

3.2 Creep behavior of rocks

At the laboratory scale, the study of time-dependent behavior of rocks has been carried out basically using three types of tests, namely:

a. <u>constant stress test or creep test</u> : a load, following a certain history, is applied to a rock specimen and maintained constant and the resultant deformations with time are measured. This test then measures the effect of stress history upon the deformations.

b. <u>constant strain test or relaxation test</u> : the rock specimen is deformed, following a certain strain history, up to a certain strain value which is maintained constant and the resultant change in stress with time is measured. This test then measures the influence of the strain history upon the stresses on the rock specimen.

c. <u>constant strain-rate test</u> : the rock specimen is deformed at a constant strain rate and the stresses are recorded throughout the test. The effect of time on the material properties is evaluated by performing tests at different strain-rates on similar specimens.

Figure 3.1 shows schematically the relationship among these three types of tests. Although both relaxation and constant strain-rate tests demonstrate the influence of time on the behavior of rocks, their interpretation requires the knowledge of a creep relationship which basically is the ultimate goal.

3.2.1 Stress-strain-time relationship

In this section, the time-dependent deformations of rocks under constant stress at room temperature are reviewed. This is done for two reasons. Firstly, information obtained from this simple test is relatively easy to collect

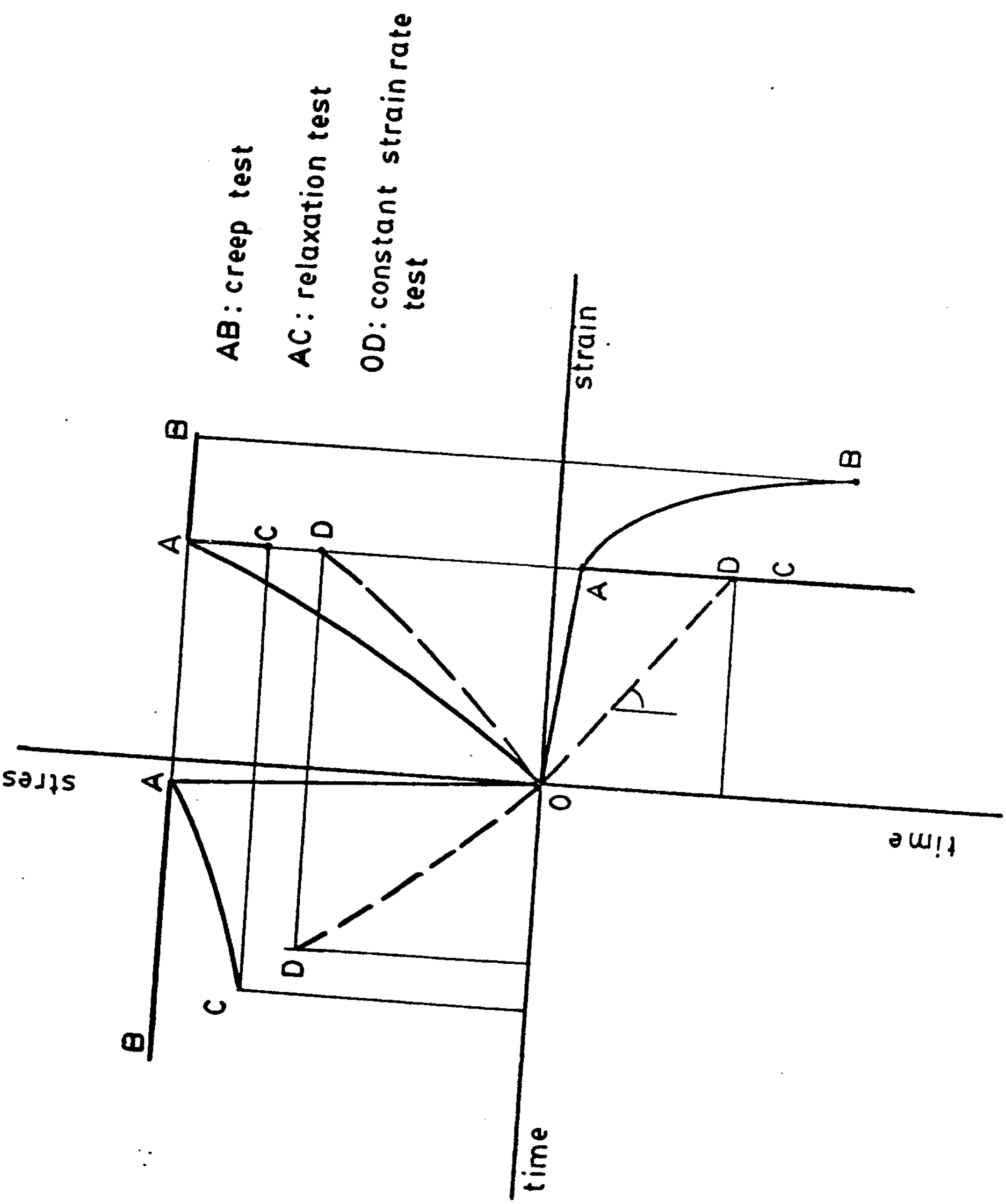

Figure 3.1 Schematic relationship among creep, relaxation and constant strain-rate tests

by careful testing and secondly, this is practically the only information available covering a wide range of rock types.

Figure 3.2 presents the common idealization of a creep curve as put forward by Andrade(1910) . In general, it is widely accepted that such a curve can be divided into three main regions. Initially, the process of creep deformations is characterized by a decreasing rate of strain represented by stage AB. This has been called primary or transient creep. Following this stage, there is a region where the rate of strain is constant. This is represented by stage BC and is the so-called secondary or steady-state creep. Finally, there follows a stage CD where the rate of creep strains increases with time eventually leading to failure. This region is known as tertiary creep.

The existence of these components, at least during the time of observation in a laboratory, depends on the stress level at which the test is carried out,e.g. Jaeger and Cook(1969) . Moreover, it is also accepted that these stages or 'processes' act independently of each other and at the same time. In the following only the first two stages are discussed. Data on tertiary creep are still very scarce and will not be discussed in this thesis.

The analytical convenience introduced by the separation and independence of the creep stages allows creep data to be described quantitatively by expressions such as equation (3.1) where $\varepsilon(t)$ represents the total strain, ε_0 is equal

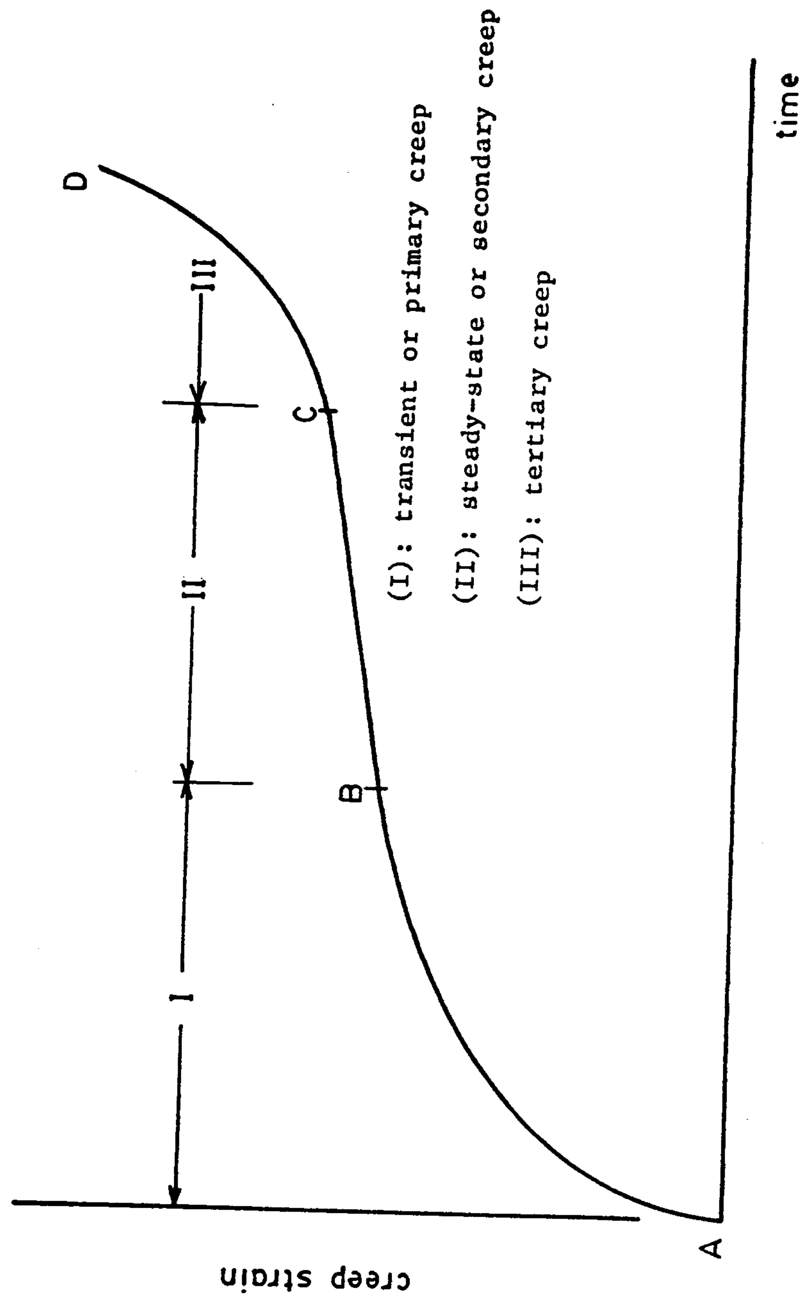

Figure 3.2 Idealized creep strain versus time curve

to the instantaneous or time-independent strain, $\varepsilon_p(t)$ represents the primary creep strain and $\beta \cdot t$ represents the secondary creep strain.

$$\varepsilon(t) = \varepsilon_o + \varepsilon_p(t) + \beta \cdot t \qquad \text{.... (3.1)}$$

Equation (3.1) constitutes the basis for the analysis of creep data by the so-called empirical approach which consists of selecting appropriate functions to describe both $\varepsilon_p(t)$ and β that best fit the experimental data. Alternatively, rheological models consisting of springs, dashpots and sliders , connected in series or parallel or both, can be used to fit the experimental data ,e.g., Maxwell, Kelvin and Burgers' models. Creep strains have also been described in terms of fundamental parameters which are determined from theories describing the creep process on a microcospic scale,e.g., rate process, dislocation, exhaustion and structural theories.

Table 3.1 displays a small sample of creep data on rocks covering both a wide range of rock types and different test conditions. This table clearly indicates the number of different stress-strain-time relationships which have been used to describe creep data on rocks.

Table 3.1 - CREEP TESTS ON VARIOUS TYPES OF ROCKS AT ROOM TEMPERATURE

Source	Type of Rock	Type of test	Stress-strain-time relationship	Remarks
Griggs(1939)	Limestone Talc Shale Mineral crystals	Uniaxial compression and Triaxial compression	$\varepsilon = \varepsilon_o + B\log t + ct$	
Pomeroy(1956)	Coal	bending	$\varepsilon = \varepsilon_o + B\log t + ct$	
Chugh(1974)	Indiana Lst. Tenessee Sst. Barre Granite	uniaxial tension and compression	$\varepsilon = \varepsilon_o + B\log t + ct$	
Afrouz and Harvey(1974)	Air-dried coal Dolomitic Lst. Sandstone	uniaxial compression	$\varepsilon = P_1 + P_2 t^{P_3} + P_4 \exp(-P_5 t)$	
	Air-dried underclay Saturated underclay Calcitic Lst	uniaxial compression	$\varepsilon = P_1 + P_2 \ln t + P_3 t^{P_4}$	
	Saturated coal Saturated underclay		$\varepsilon = P_1 + P_2 t^{P_3} + P_4 t^{P_5}$	
Cruden(1971a)	Pennant Sst. Carrare Marble	uniaxial compression	$\dot{\varepsilon} = b_1 t^{-b_2}$	
Wawersik(1972)	Westerly Granite Nugget Sst.	uniaxial compression	$\varepsilon = a_1 t^{a_2} + b_1 t$	
Hendron(1968) Nair and Deere(1970)	rock salt	extension triaxial test	$\varepsilon = a_1 t^{a_2}$	
Hardy(1967)	Wombeyan Marble	uniaxial compression test	$\varepsilon = \frac{\sigma}{E_1} + \frac{\sigma}{E_2}(1-\exp(-t/T)) + \frac{\sigma t}{N_1}$	Burger's rheological model $T = N_2/E_2$
Singh(1975)	Sicilian Marble	uniaxial compression test	$\varepsilon = a_1 t^{a_2}$	
Terry and Morgan(1958)	Coal	uniaxial compression	$\varepsilon = \frac{\sigma}{E_1} + \frac{\sigma}{E_2}(1-\exp(-t/T)) + \frac{\sigma t}{N_1}$	Burger's rheological model $T = N_2/E_2$

For early data on creep of rocks, Griggs (1939) suggested equation (3.2) as describing his experiments; the term Blogt represents the primary creep and the term Ct the secondary creep.

$$\varepsilon(t) = A + B \cdot \log t + C \cdot t \qquad \ldots.(3.2)$$

Griggs' data were plotted as strain versus the logarithm of time, as shown in Figures 3.3 and 3.4, and the parameters A,B were determined from the straight line describing the data at the early stages of the test. The departure from the initial straight line was assumed to constitute the secondary creep component, i.e. the term Ct in equation (3.2). The later data were subtracted from the straight line and the results plotted versus time. The slope of the new line yielded the value of the parameter C.

Griggs' approach can be criticized for two reasons. Initially, the departure from a straight line on a strain versus logt plot is not a sufficient condition to indicate the existence of a term such as Ct (see equation (3.2)), i.e., the presence of a secondary creep. This departure may simply mean a distortion caused by the semi-logarithmic plot. Moreover, this interpretation causes some difficulties

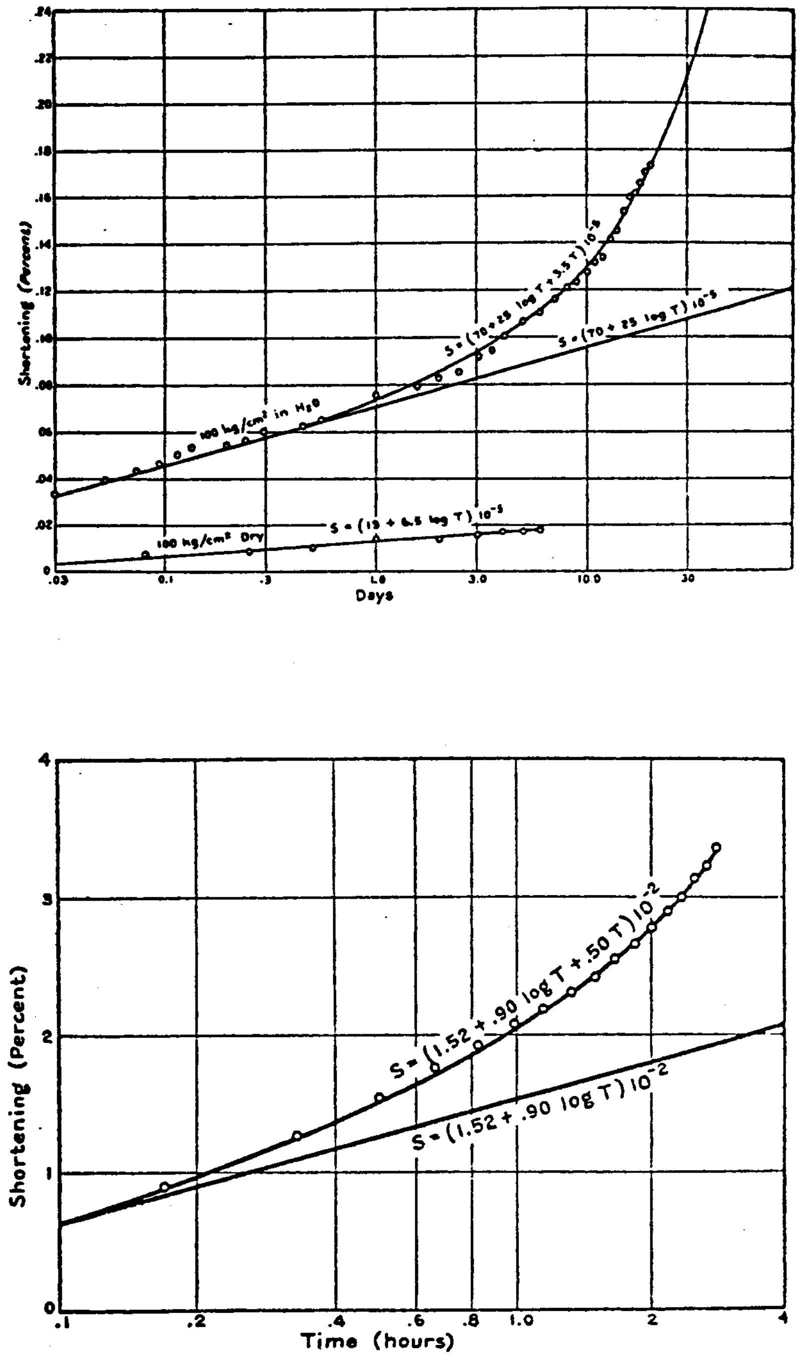

Figure 3.3 Early data on creep of rocks: Alabaster and Solenhofen Limestone (after Griggs(1939))

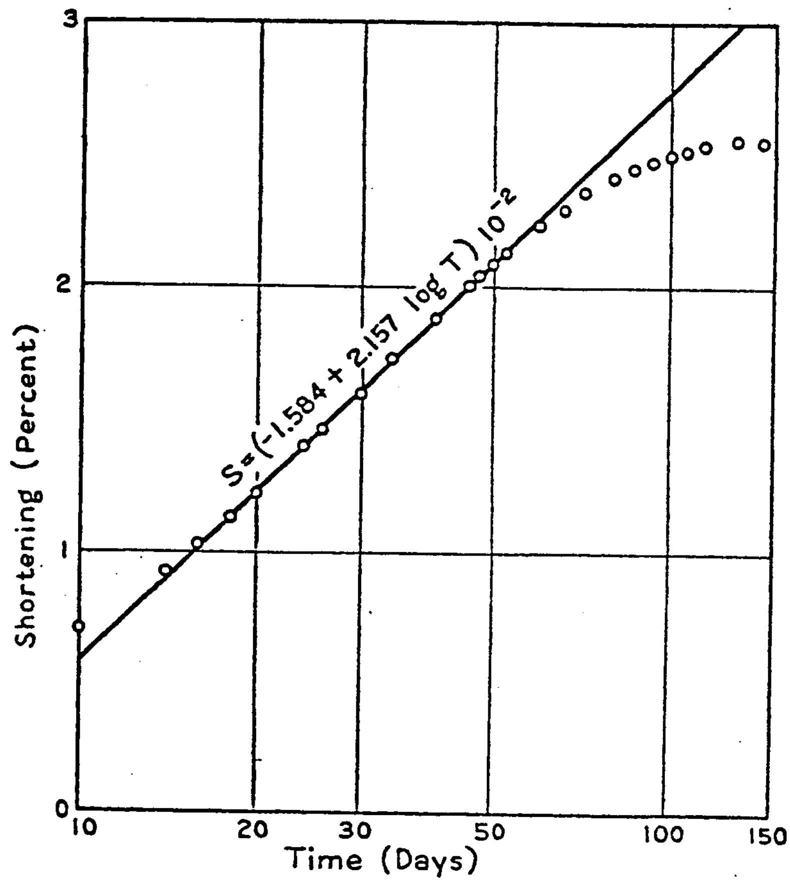

Figure 3.4 Early data on creep of rocks: Conchas shale (after Griggs(1939))

when analyzing data such as the ones indicated in Figure 3.4 where the departure from a straight line would indicate a negative secondary creep rate. In Figure 3.5 it is shown that functions such as a power law, $\varepsilon = \varepsilon_1 + at^b$, provide an explanation for both types of departures on Griggs' data without having to call for an extra term such as Ct. Actually, reanalyzing Griggs' data , Cruden(1969) indicated that such a power law provided a good representation of the data.

To avoid any misinterpretation, a much more satisfactory way of assessing both the existence and the value of a secondary creep rate is from a plot indicating the variation of the strain rate, obtained from the experimental data, with time.

3.2.1.1 Primary creep

Logarithm time laws as suggested by Griggs(1939) have also been used by other investigators for describing primary creep strain on rocks,e.g.,Hobbs(1970) for siltstones, shale, mudstone, limestone and sandstone under uniaxial compression,Chugh(1974) for limestone, sandstone and granite under both uniaxial tension and compression and Pomeroy(1956) for coal under bending.

Other investigators have suggested an exponential law to describe primary creep strain. This creep law is generally the result of the application of Burger's rheological model,e.g. Evans and Pomeroy(1966) for coal

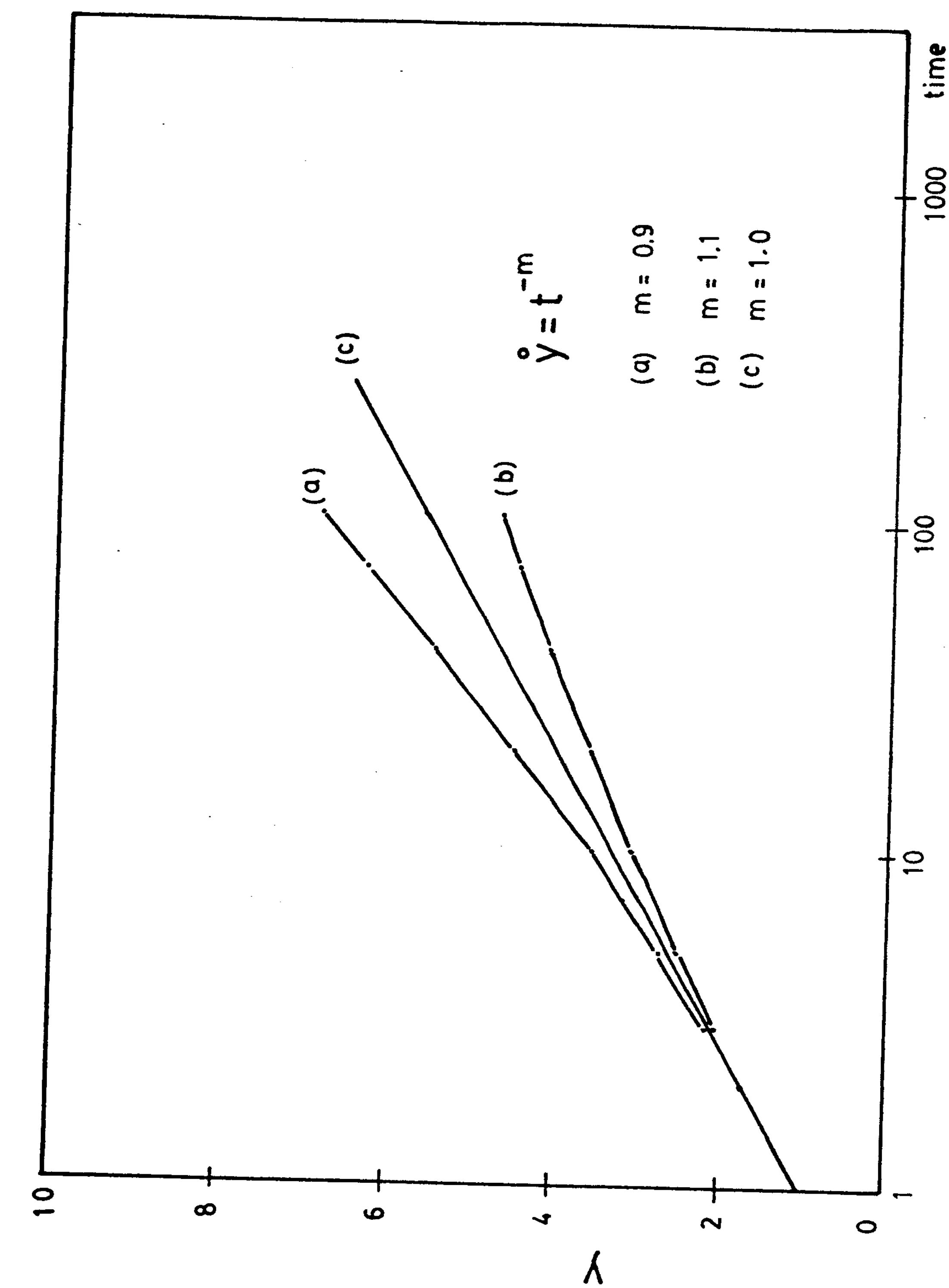

Figure 3.5 Creep strains as predicted from power law

under uniaxial compression and Hardy(1967) for marble under uniaxial compression. As suggested by Cruden(1971a), the time laws describing primary creep can be divided broadly into two groups consisting of exponential laws and power laws, equations (3.3) and (3.4) respectively.

$$\mathring{\varepsilon}_p = a_1 \exp(-a_2 t) \qquad \ldots.(3.3)$$

$$\mathring{\varepsilon}_p = b_1 t^{-b_2} \qquad \ldots.(3.4)$$

where $\mathring{\varepsilon}_p$ =primary creep rate and a_1, a_2, b_1, b_2, are constants. The logarithm law proposed by Griggs(1939) can be seen as a particular case of the power law for $b_2=1$.

The power law has also been preferred by Cottrell(1952) for a variety of materials; Boresi and Deere(1963), LeComte(1965) and Hendron(1968) for rock salt; Wawersik(1973) for sandstone and granite; Singh and Mitchell(1968) for several types of soils and Roggensack(1977) for frozen soils, etc. Cruden(1971a) submitted both exponential and power law to severe statistical tests for the representation of uniaxial compression creep tests on marble and sandstone and , for all the cases, the power law showed a better representation of the data.

Two important observations have been made with respect to the power law for describing primary creep in geological materials. Initially, the parameter b_2 in equation (3.4), which represents the hardening effect, has been found to vary within a very narrow range. Table 3.2 summarizes some of the b_2-parameters reported in the literature. Both the good approximation of the experimental data by the power law for a wide range of materials and the narrow range of variation of b_2 seem to suggest a common link between the hardening mechanisms for the materials considered.

Secondly, the value of b_2 has been found to be fairly constant within a large range of stress level, (Murayama and Shibata(1958) and Bishop and Lovenbury(1969)) for tests on clays, see Figure 3.6. Wawersik(1974) suggested a constant value of b_2 to describe the primary creep of Westerly granite for different stress levels and confining pressure, and results reported by Cruden(1970) do not show any sign of a particular dependence of b_2 upon the stress level for values up to 85% of the maximum compressive strength.

On the other hand, some creep tests carried out for long periods of time;i.e.,Bishop and Lovenbury(1969) up to 1000 days, and at high stress level ,Cruden(1971a) , have indicated a continuous decrease in strain rate with time and, in both instances, the power law yielded a good

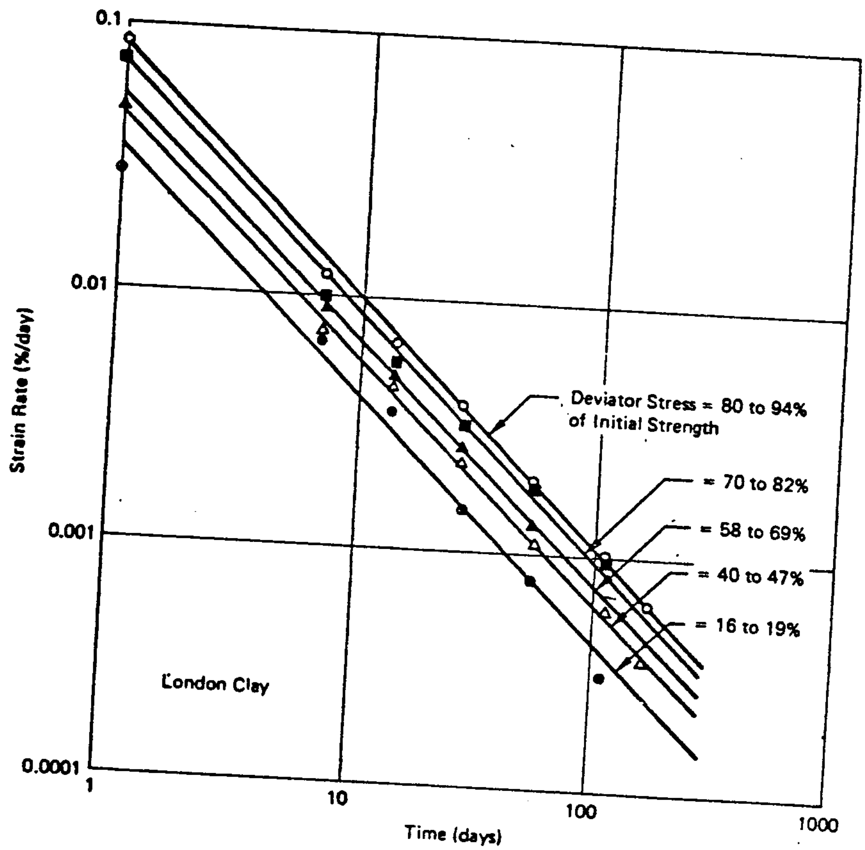

Figure 3.6 Strain rate vs. time curves for various stress levels during drained creep of London Clay (Bishop and Lovenbury(1969))

Table 3.2 Summary of b_2-values reported in the literature

Author	Rock type	b_2-values	Type of test
Misra(1962) (*)	Anhydrite	0.65 - 0.98	uniaxial compression test
	Olivine	0.71 - 0.74	
	Granodiorite	0.66	
	Darle Dale Sst	0.88 - 0.92	
	Pennant Sst.	0.88 - 0.98	
Griggs(1939) (*)	Solenhofen Lst	0.99	uniaxial compression test
	NaCl single crystals	0.79	
Cruden(1971a)	Sandstone	0.82 - 1.06	uniaxial compression test
	Marble	0.79 - 1.06	
Mitchell(1975)	several types of soils	0.65 - 1.0	triaxial compression tests
Wawersik(1972)	sandstone	0.71	uniaxial compression test
	granite	0.61	
Wawersik(1974)	sandstone	0.72	triaxial compression test
Nair and Deere(1970)	rock salt	0.55 - 0.68	extension triaxial

(*) Original data recalculated by Cruden(1969) representation of the creep data. These observations certainly constitute a threat to the well established idea of the existence of a secondary creep rate.

3.2.1.2 Secondary creep

A secondary creep stage has been reported by several authors,e.g., Wawersik(1973) for sandstone, Singh(1970) for marble, Afrouz and Harvey(1974) , etc. (see Table 3.1). However, it seems to be a common feature of all these analyses that such a secondary creep stage was assumed a priori: its determination being based on best judgment about the region of the creep curve representing the secondary creep stage and graphical methods being used to determine the rate of creep during this stage. This interpretation is open to strong criticism.

Methods to analyze creep data have been described extensively by Conway(1967) and, as suggested, the presence of secondary creep rate must be evaluated by using plots such as strain rate versus time. The secondary creep rate would then be indicated by a horizontal asymptotic value, see Figure 3.7.

The question of the existence of a true secondary creep rate cannot be resolved simply by considerations of analytical or graphical techniques. The available data in the literature as discussed before, cannot be used to either prove or disprove the validity of this concept. Even the longest tests on creep of rocks, Price(1964) duration of up

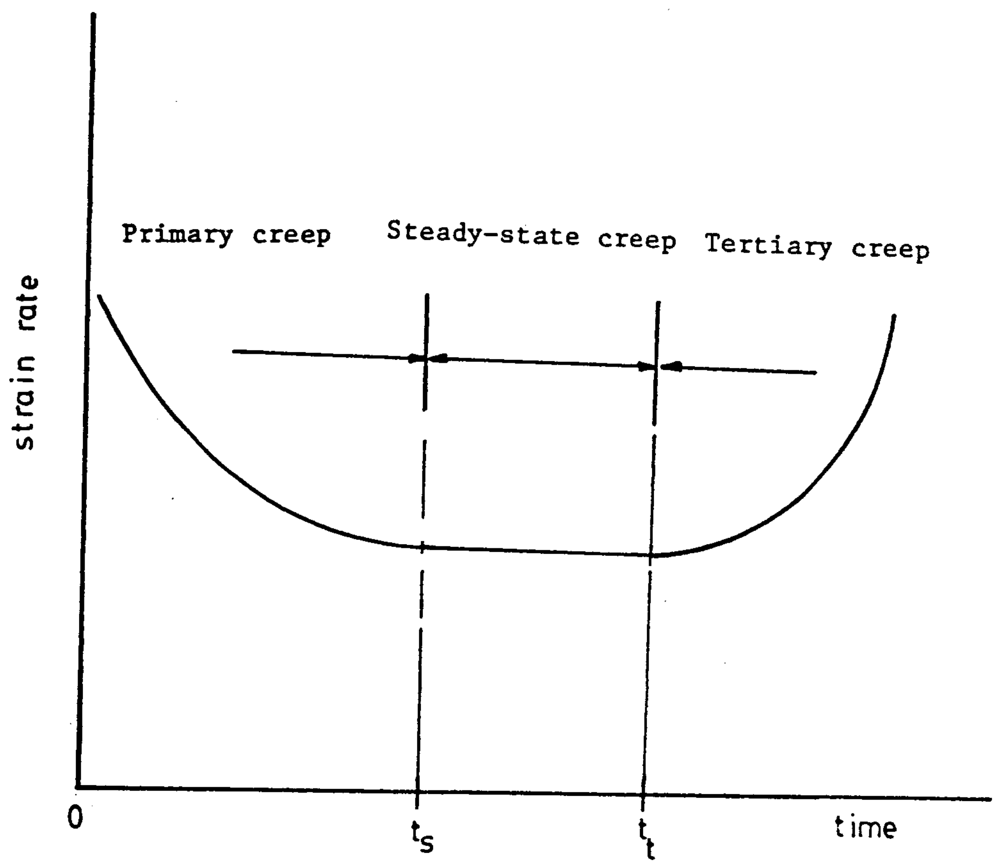

Figure 3.7 Typical strain rate versus time plot

to 1 year, do not seem to present a strong case for the validity of secondary creep rate in brittle rocks under a uniaxial state of stress. However, from the engineering point of view, it suffices to establish the degree of approximation one will obtain if effects associated with a secondary creep stage in rocks are neglected. The question certainly needs to be investigated in more detail in order that it can be answered by facts rather than opinions.

3.2.2 Factors controlling creep of rocks

The time-dependent deformations of rocks are themselves dependent upon a number of factors such as nature of stress or stress system, stress level, confining pressure, moisture and humidity and temperature. In the following , some of these factors will be discussed.

3.2.2.1 Stress system

As indicated in Table 3.1, most of the work on creep of rocks has been done under a stress state of uniaxial compression; other stress systems have been used such as bending (Pomeroy(1956) and Price(1964)), uniaxial tension (Wawersik(1973) and Chugh(1974)), triaxial compression (Boresi and Deere(1963) and Wawersik(1974)), and triaxial extension (Hendron(1968) and Nair and Boresi(1970)) .

Wawersik and Brown(1973) presented tests on granite which indicated that, in compression, creep accelerated gradually during tertiary creep providing some warning about imminent creep failure whereas in uniaxial tension, creep failure was reached suddenly. Results presented by Chugh(1974) on sandstone indicate that creep strains were about six times higher in tension than under compression for the same percentage of failure stress. These results seem to indicate that the stress system may have a considerable influence on the parameters describing the creep behavior of rocks.

More results would certainly be necessary before a better assessment of this influence can be made. Recently published data for clays(Cleveland varved clay and Nevada clay) suggest that the variations in creep properties measured under triaxial, plane strain and simple shear stress state are small enough to be masked by variations between samples, Wu et al(1978) .

3.2.2.2 Stress level

In equations (3.2), (3.3), (3.4) the constants B,C,a_1 ,b_1 are dependent upon the stress in which the test is carried out. Tests by Griggs(1940) on Alabaster indicated that both the rate of strain and the magnitude of strain at any time are dependent upon the stress level, see Figure 3.8. The term 'stress level' has been used in the literature sometimes implying the absolute value of stress at which the test is carried out. This definition is rather meaningless when dealing with stress systems other than uniaxial compression or tension, for geological materials are

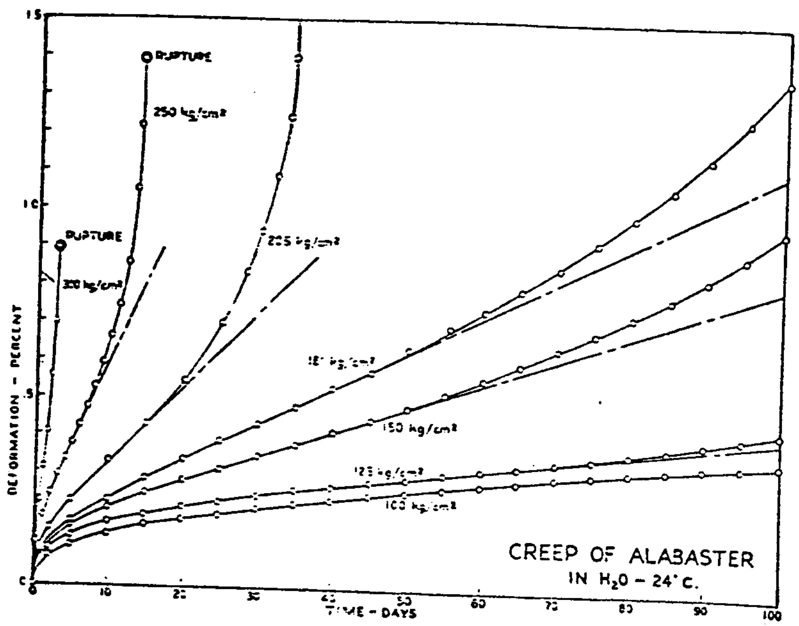

Figure 3.8 Creep curves of Alabaster for different stress levels (after Griggs(1940))

influenced by the confining pressure. Stress level in this thesis refers to the ratio between the stress at which the test is carried out and the strength of the rock both referring to the same state of confinement. The absolute value of stress is referred to simply as stress.

Hendron(1968) and Nair and Boresi(1970) suggest equation (3.5) for describing the creep strains on rock salt under both uniaxial compression and triaxial extension tests. They suggest a power law to describe the stress dependence of the creep strains where σ = stress difference, $(\sigma_1 - \sigma_3)$ in psi, $K=1.87 \times 10^{-16}$ and $n=2.98$:

$$\varepsilon(t) = k\sigma^{n} t^{m} \qquad \ldots. \ (3.5)$$

Comparing the creep rates at the same deviatoric stress, $\sigma_1 - \sigma_3$, Hendron(1968) concludes that the uniaxial compression test gives a higher strain rate than the triaxial extension test, and then, suggests that the uniaxial compression test is too severe to define creep parameters.

A structural theory for creep in brittle rocks at room temperature and uniaxial compression condition based on crack growth was developed by Cruden(1970) which suggests a power law ,such as equation (3.5), to describe the influence of the stress level on the strain rate. Experiments on Pennant Sandstone and Carrara Marble showed a good agreement, in the range between 0.1 and 0.7 of $\sigma_{max.}$, with this theory, see Figure 3.9. For stress levels above 80% the experiments seem to indicate an increase of the stress level dependence.

Wawersik(1973) suggested an exponential law such as equation (3.6) to describe the influence of the stress level on the strain rate. However, Wawersik points out that the scatter observed from his experiments was of the same order of magnitude for both equations (3.5) and (3.6).

$$b_1 = A e^{\bar{\alpha}\bar{\sigma}} \quad \text{.... (3.6)}$$

where A,$\bar{\alpha}$= material parameters and $\bar{\sigma}$ =stress level.

Applying the concept of creep as a thermally activated rate process, Mitchell et al(1967) predict a strain-rate variation which is dependent on a hyperbolic sine function of stress. As suggested by Singh and Mitchell(1968) such a variation could be approximated by an exponential law such as equation (3.6) within the range of 20-80% of the maximum strength, see Figure 3.10. Results by Bishop and

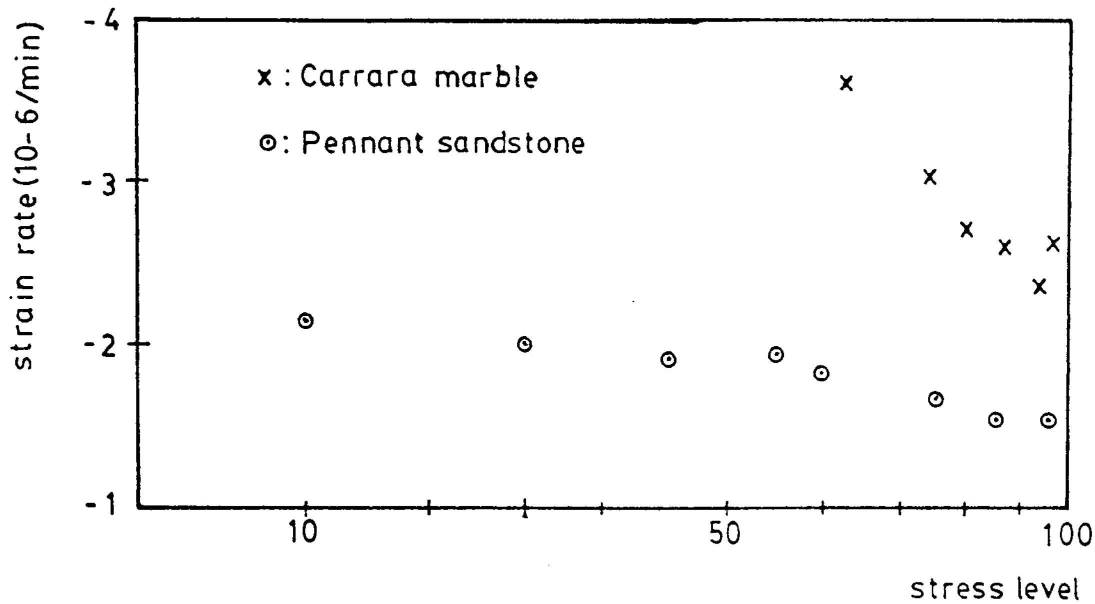

Figure 3.9 Strain rate versus the percentage of short-term failure stress(log scale) (after Cruden(1970))

Lovenbury(1969) for creep tests on London Clay suggest the same exponential law to measure stress dependence, see Figure 3.11.

3.2.2.3 Confining pressure

Few data have been reported in the literature aiming specifically at investigating the influence of confining pressure on the creep behavior of rocks. Robertson(1960) reported tests on Solenhofen limestone in compression for confining pressures up to 400 MPa and concluded that hydrostatic stress greatly reduces the creep rate. Unfortunately, Robertson's conclusion refers to data related to the same deviatoric stress and this result would be logical since the stress level would decrease with increase in confining pressure for the same deviatoric stress.

Other factors have been found to influence the creep behavior of rocks such as environmental conditions(humidity and temperature) and structural factors such as composition, orientation of grains, etc. However for the purpose of the present review it suffices to recognize the fact that the bulk of the influence of these factors is related with the constants which describe the relationships above discussed.

3.3 Time dependent failure of rocks

It has long been accepted that the strength of rocks depends amongst other factors, upon the rate of loading or elapsed time to reach failure. Also if the applied stress is unconfined compression tests on clay-shales, Bieniawski(1970) for uniaxial compression tests on fine-grained sandstone, Peng and Podnieks(1972) for uniaxial compression tests on tuff, etc. The decrease in strength with the rate of straining has been expressed by a logarithm law as equation (3.7) where σ_o =strength at unit strain rate, $\mathring{\varepsilon}$ =strain rate, σ =strength associated with $\mathring{\varepsilon}$ and m=constant.

$$\sigma = \sigma_o - m \log \mathring{\varepsilon} \qquad \ldots. \ (3.7)$$

Alternatively, the time-dependent strength of rocks has been investigated by static fatigue tests on which sustained loads are applied and time for failure are noted. In these tests, the failure process is indicated by the tertiary creep which is associated with a continuous increase of the strain rate. Griggs(1940) showed that for creep tests under uniaxial compression on Alabaster immersed in water there was a critical creep strain which marked the onset of tertiary creep.

Other parameters have been invoked to explain and characterize the onset of instability which leads to failure. Scholz(1968) and Cruden(1970) suggested that brittle creep in rocks under uniaxial compression was due to the formation and growth of cracks in the system by stress-aided corrosion. As the number and length of cracks increase the possibility that these cracks will intersect each other also increases. This gives rise to a new system of cracks which may well be in a more unstable situation and then accelerate the process leading eventually to the failure of the sample, Cruden(1974). This would imply the existence of a critical crack density at the onset of the instability process.

Cruden(1974) associates Griggs' critical creep strain as a measure of the critical crack density. Kranz and Scholz(1977) consider the onset of tertiary creep as occurring when a critical value of the inelastic volumetric strain has been reached. Kranz and Scholz's data refer to uniaxial compression creep tests on quartzite and granite and Figure 3.13 presents the total inelastic volumetric strain at the onset of tertiary creep as a function of stress level.

Using Griggs'(1940) data and assuming that at the onset of tertiary creep the power law defined by equation (3.4) is still valid, Cruden(1974) arrives at equation (3.8) which describes the strength decay with time for rocks under uniaxial compression.

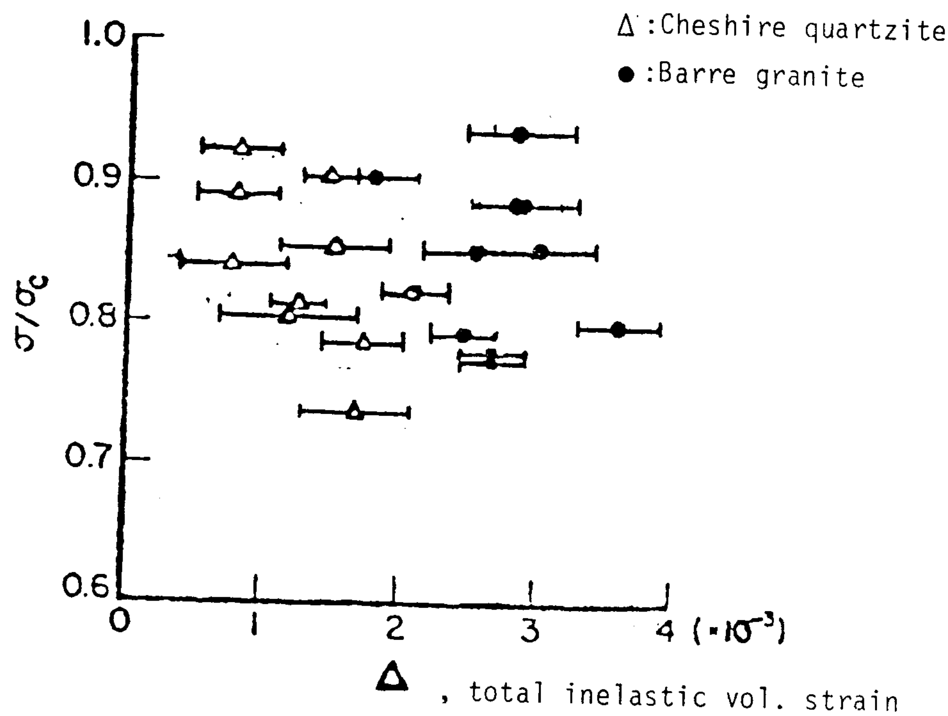

Figure 3.13 Total inelastic volumetric strain at the onset of tertiary creep as a function of stress(Kranz and Scholz(1977))

$$\frac{\sigma}{\sigma_o} = \left(\frac{t_f}{t_o} \right)^b \qquad \text{.... (3.8)}$$

where σ_o =uniaxial compressive strength at t_o , σ =uniaxial compressive strength at t_f , b =material constant. Kranz and Scholz(1977) have described the time for failure by a relation as equation (3.9)

$$\frac{t_f}{t_o} = A \frac{e^{\alpha\sigma}}{e^{\alpha\sigma_o}} \qquad \text{.... (3.9)}$$

A, α =material parameters. A similar relationship has been suggested by Mitchell(1975) as describing the time-dependent strength of clays.

Any dispute on the actual shape of the decrease in strength with time for rocks seems to be, at the present stage, of secondary importance due to the rather limited range of application(uniaxial state of stress) and its empirical nature. Further elaborations or assumptions such as critical crack density must be made in order to include situations other than uniaxial state of stress and to make possible its application to engineering works.

- Long-term strength

Of immediate need to the engineer, however, is the concept of long-term strength which by definition is the maximum stress sustained by the rock at which failure will not occur no matter how long the force has been applied. This long-term strength has been estimated by direct and indirect methods.

Griggs(1940) , Potts(1964) ,Price(1964) have suggested that the long-term strength of rock be represented by stress below which no steady-state creep is present. Unfortunately, this assumption cannot be verified experimentally due to the excessive time necessary for observation. A plot of secondary strain rate versus stress is helpful in defining the stress corresponding to a 'zero' secondary strain rate.

Another method, the dilatancy method, is based on Bieniawski's discussions on the brittle fracture of rocks (Bieniawski(1967) . The long-term strength is identified with the level of stress at which crack propagation becomes unstable. Wiid(1970) measured both the stress corresponding to fracture initiation and at unstable crack propagation for uniaxial compression tests on dolerite in dry and wet conditions. The decay in strength with time was obtained by actual strength tests and an estimative of the long-term strength was made. The long-term strength seemed to be much closer to the value of the stress defining crack initiation than the one at crack instability. Sangha and Dhir(1972) suggest the long-term strength is defined by the stress level at which the incremental Poisson's Ratio becames 0.50, which corresponds to the onset of significant dilatancy due to crack growth.

3.4 Creep behavior under variable stress

The previous discussion on creep of rocks has served to establish the basic dependence of time-dependent deformations with respect to stress and time under a constant state of stress. However, these stress-strain-time relationships are very specific and caution must be exercized when extending these relationships to the more common and general case of a variable stress condition. In the following, the available data on creep of rocks under variable stress as well as the concepts for their interpretation are discussed.

The creep of rocks under variable stress has been investigated by the so-called incremental creep test. This test has also been referred to as step-creep test or multiple-stage creep test. An incremental creep test consists in applying loads to a rock specimen in increments and the specimen is allowed to creep between these load increments, see Figure 3.14. This test procedure has the feature of providing several creep stages carried out on a single specimen which makes it very attractive from an economical point of view.

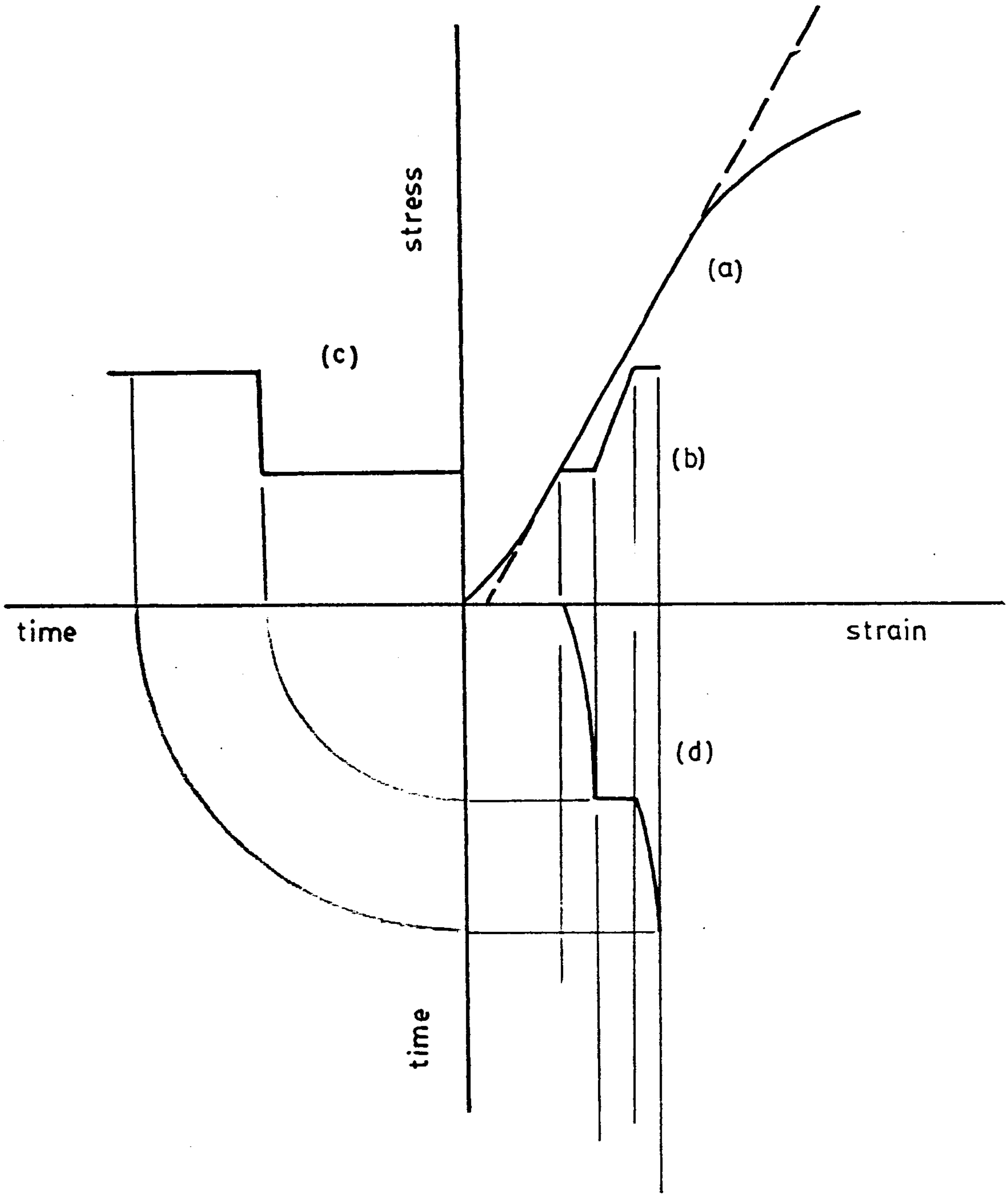

Figure 3.14 Schematic representation of incremental creep test

For the analysis of the creep data at a certain stress level the important question to be answered is how the prior deformation history of a specimen will influence the results. Several theories have been developed to analyze incremental creep , each one with a body of assumptions associated with this influence.

Hardy(1967) has used Burger's rheological model and the linear superposition principle for the analysis of incremental creep tests under uniaxial compression on Wombeyan marble. Moreover, Hardy considers a time, t, of creep between stress increments which is much larger than the term N_2/E_2. In this case, (3.10) which represents the governing equation for Burger's model at a constant can be written as (3.11) for an increment .

$$\varepsilon(t) = \frac{\sigma}{E_1} + \frac{\sigma}{E_2}\left(1 - \exp\left(-E_2 t/N_2\right)\right) + \frac{\sigma t}{N_1} \quad \ldots. \ (3.10)$$

$$\Delta\varepsilon(t) = \frac{\Delta\sigma}{E_1} + \frac{\Delta\sigma}{E_2}\left(1 - \exp\left(-E_2 t/N_2\right)\right) + \frac{\Delta\sigma \cdot t}{N_1} \quad \ldots. \ (3.11)$$

In making t much larger than the retardation time(N_2/E_2), the creep deformations at a particular stress are not influenced by the delayed deformations from the previous stages. Hardy also considers that 40 mins. is enough to erase the 'memory' component. However, his results show a continuous change in the parameters E_1, E_2, N_1 and N_2 with the stress.

Cruden(1971b) extended a structural theory for brittle creep (Cruden(1970)) to describe the behavior of a rock specimen under uniaxial compression when the stress is raised from S_o to S_1 after the specimen had been creeping for a time t_o under S_o. Equation (3.12) describes the time-dependent behavior of the specimen under S_o (in the original paper referred to as parent curve) in terms of the observed behavior after the increment was applied (referred as daughter curve) and the ratio (S_1/S_o).

$$\overset{\circ}{\varepsilon}_p = \overset{\circ}{\varepsilon}_d \left(\frac{S_o}{S_1}\right)^n \left[1 - \frac{t}{t_o + \left(\frac{S_o}{S_1}\right)^n \cdot t}\right]^{\frac{n-2m-2}{n-2}} \quad \ldots. \; (3.12)$$

Figure 3.15 shows schematically the relations between parent and daughter curve. Cruden(1971b) has estimated the part OC of the parent curve using both the observations for the daughter curve(at curve AB) and equation (3.12). The estimate of the parent curve was compared with the experimental observations, curve OA, for 16 experiments and no significant departure was observed at the 1 per cent level.

Mitchell et al(1969) has used the superposition principle shown in Figure 3.16 to analyze the results of incremental observations tests on San Francisco Bay mud under triaxial conditions. This method, described by equation (3.13), was applied to estimate the creep parameters, A and $\bar{\alpha}$, from equation (3.6) using a single specimen.

$$\frac{\dot{\varepsilon}(\sigma_2, t)}{\dot{\varepsilon}(\sigma_1, t)} = \left(\frac{t_i}{t_j - t'}\right)^m \cdot \left(e^{\alpha(\sigma_2 - \sigma_1)} - 1\right) + \left(\frac{t_i}{t_j}\right)^m \quad \ldots . \; (3.13)$$

According to this method, the creep behavior after the stress increment is independent of the time when the increment was applied. Mitchell <u>et al</u>(1969) present only one application of this method and the agreement between the experimental and predicted results seems to be very good. However, these authors point out that the parameters, A and α , obtained by this method may be different from the ones obtained from a sequence of single-stage creep tests on different samples.

Other theories have been proposed mainly in connection with the field of metals. The most common ones are the <u>time</u>

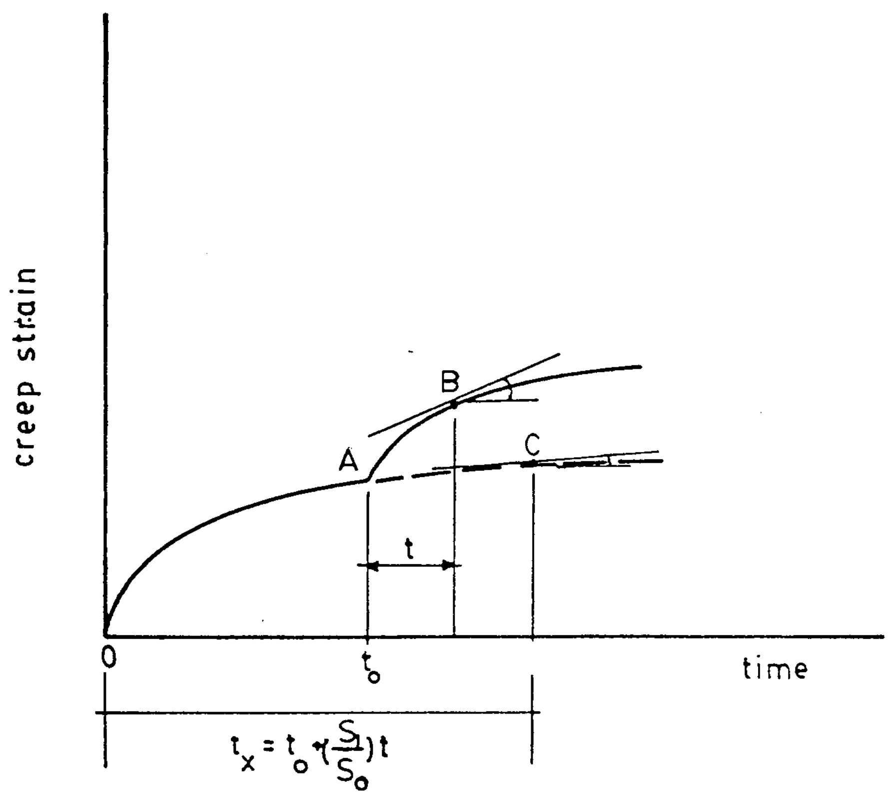

Figure 3.15 Prediction of incremental creep test by structural creep theory (Cruden(1969))

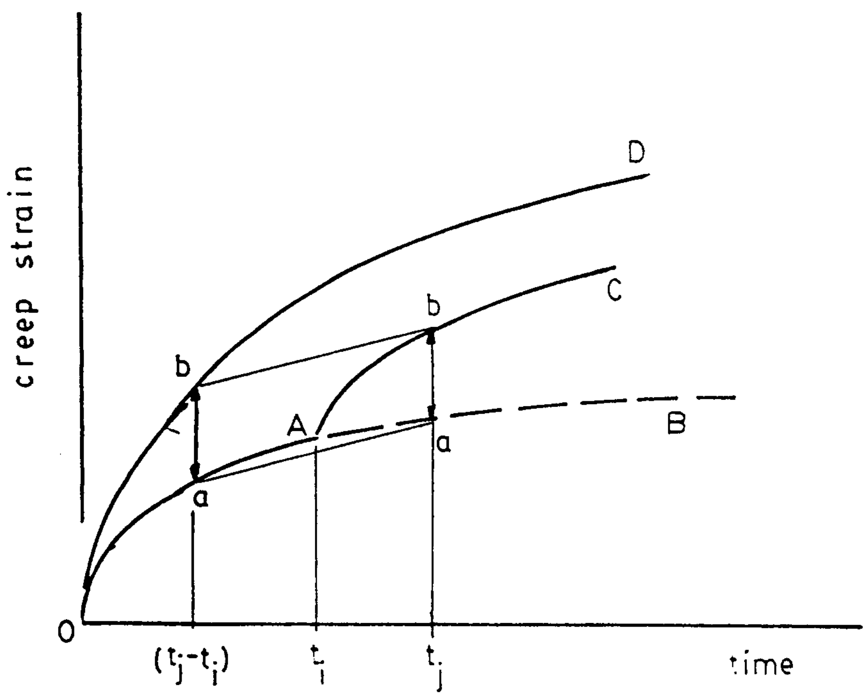

Figure 3.16 Prediction of incremental creep test by superposition principle (Mitchell et al(1967))

and strain hardening theories but they have not been used, to the best of the Author's knowledge, to analyze results of creep data from incremental tests on rocks. However, as will be discussed in Chapter 6, these theories have been used in association with analytical studies on the time dependent behavior of underground openings. Penny and Marriott(1971) describe the assumptions involved in both theories. Figure 3.17 shows schematically how each theory predicts the creep behavior after a stress increment. The time-hardening theory (figure 3.17a) predicts much lower strain rate than the ones observed for tests on metals (Penny and Marriot(1971)) and it has the inconvenience of predicting no time-dependent deformations after the stress increment if the specimen had been creeping for long periods under a previous increment. The strain-hardening theory seems to yield a better prediction of the experimental results for metals(Penny and Marriot(1971)).

3.5 Relaxation properties of rocks

As discussed earlier in section 3.2 the time-dependent behavior of rocks is also reflected by the phenomenon of stress drop under a restrained state of deformations which has been commonly known as relaxation of stress or simply relaxation. The use of relaxation tests as a mean for defining the time-dependent properties of rocks has not been explored in its full extent and only relatively few data are available in the literature. In the following a review of

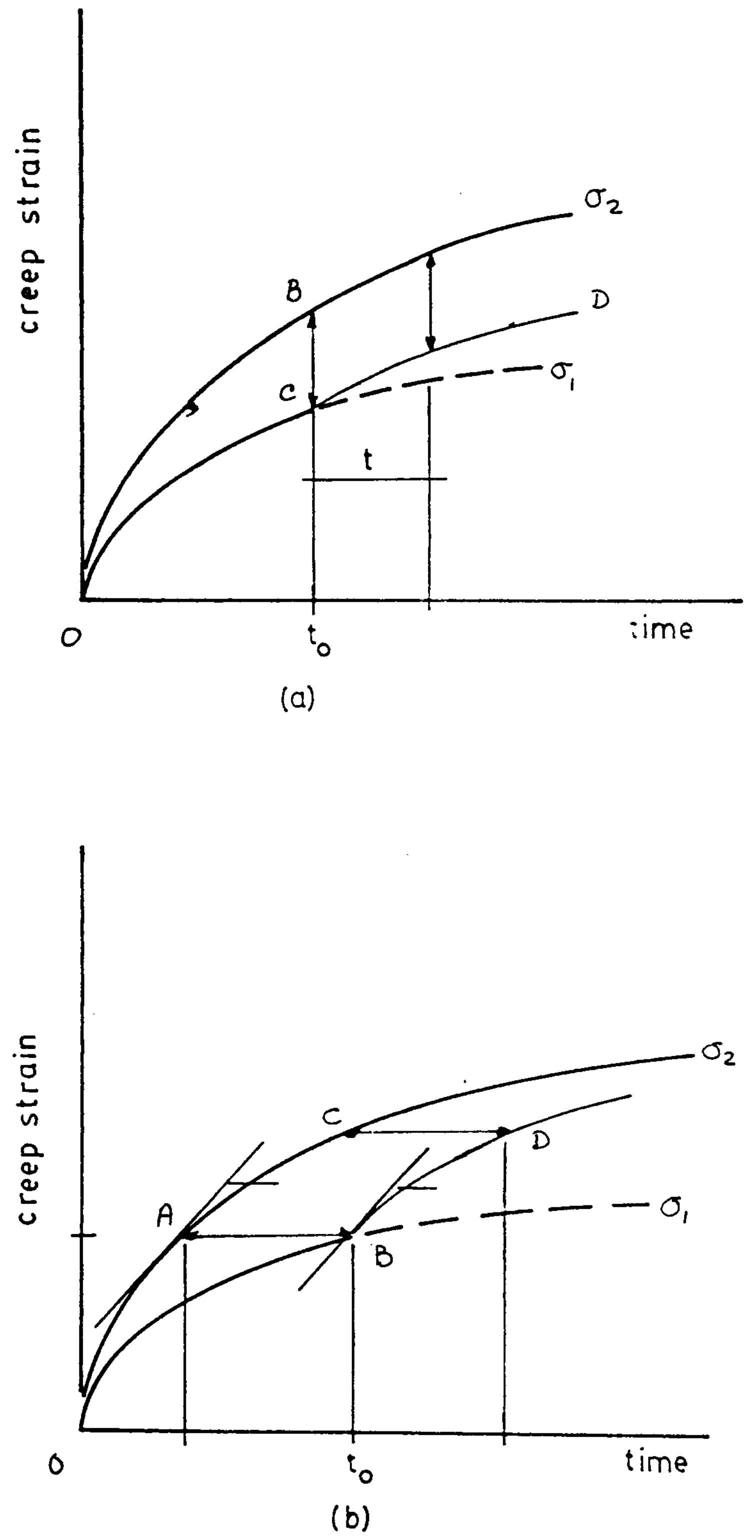

Figure 3.17 Prediction of incremental creep tests by (a)time-hardening and (b)strain-hardening

the previous attempts to describe the relaxation properties of rocks is presented. Lacerda and Houston(1973) presented data for relaxation behavior of Ygnacio Valley clay and during these tests the specimens have been loaded at a constant rate of strain varying from 1.1x10-3 to 9x10-5 min-1 and the stress relaxation has been observed from roughly the same initial stress. Figure 3.18 shows Lacerda and Houston's results and from them the following observations were made:

a. there is a delay in the stress relaxation response; the logarithm of this time delay being proportional to the time spent in reaching the initial stress;

b. the stress drop varies in a linear fashion with the logarithm of time and the slope of such a curve is approximately the same for all the curves.

The linear relationship between stress drop and the logarithm of time displayed in Lacerda and Houston's results have been observed for other materials such as unvulcanized rubber,Tobolski(1960) ; Murayama and Shibata(1961) for alluvial Osaka clay; Vialov and Skibitski(1961) on overconsolidated clays,etc. From these results the relaxation behavior seems to be described by equation (3.14) where t_o=delay time ,σ_o=stress associated with t_o ,t = total elapsed time ,σ=current stress and s = slope of the straight line.

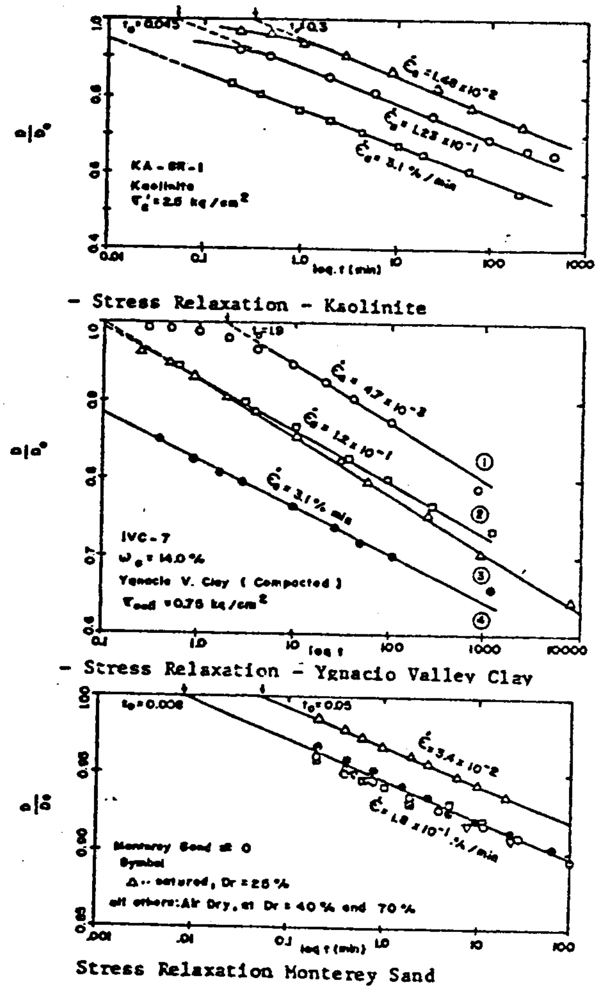

Figure 3.18 Stress relaxation curves for distinct types of soils (Lacerda and Houston(1973))

$$\sigma = \sigma_o - s \cdot \log \left(\frac{t}{t_o} \right) \qquad .... (3.14)$$

As the elapsed time becomes very large, Murayama and Shibata's(1961) results seem to suggest the existence of a stress level below which there is no relaxation, i.e., curve versus logt tends to a horizontal asymptotic value.

The work on relaxation of rocks has been very scarce. Hudson and Brown(1973) ,Bieniawski(1970) and Kaiser and Morgenstern(1979) have recognized the relaxation of rocks but there was no attempt to describe the stress drop with time. Peng and Podnieks(1972) have presented data on the relaxation behavior of tuff under uniaxial compression. Unfortunately, these were very short-term tests and the proposed relationship is valid only for the first 5 minutes of testing, see equation (3.15).

$$P = k \cdot t \cdot exp\,(-0.12t) \qquad .... (3.15)$$

$$t < t_{max.}$$

where P= load drop , t=time(sec), K=constant, $t_{max.}$=time required for load drop to approach asymptotic value.

Another useful characteristic of the relaxation behavior of materials is its ability to infer the long-term strength of a certain material. Vialov(1970) has postulated that if a relaxation test is started near failure, the equilibrium level reached by the stress can be considered as the long-term strength of the rock. Bieniawski(1970), Pushkarev and Afanasev(1973), suggest that the long-term stress strain curve would be obtained by connecting points representing relaxation stages at different stress levels, see Figure 3.19.

3.6 Final remarks

The preceeding review has discussed several aspects related to the time-dependent behavior of rocks and, whenever possible, similarities with the behavior of other materials has been pointed out. Based on this review the following observations can be made:

1. Even though most of the available data on creep of rocks refers to uniaxial compression tests, reported results under other stress systems seem to indicate a similar pattern of behavior.
2. Some investigations have not recognized the influence of the stress level, rather than the stress value, on the proposed stress-strain-time relationships. This concept is of particular importance when comparing results of creep deformations associated with different stress systems and also trying to generalize creep relationships to a multiaxial state of stress.

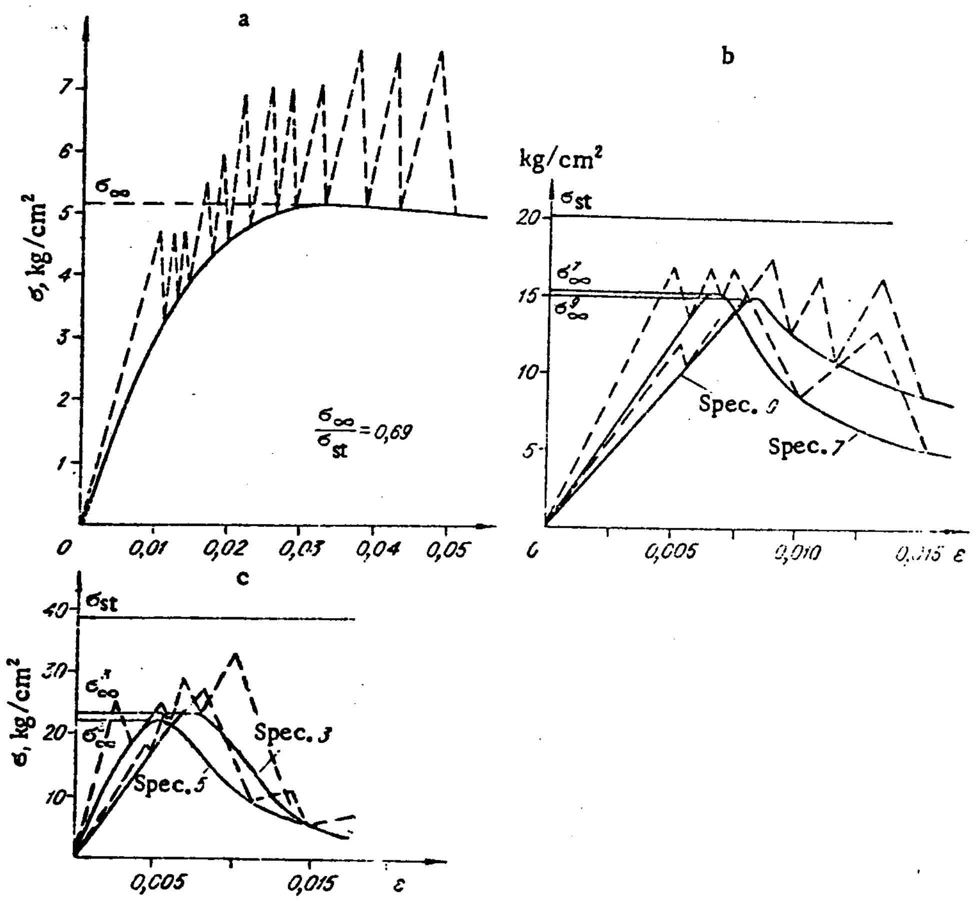

Figure 3.19 Determination of long-term strength using multiple relaxation tests (Pushkarev and Afanasev(1973))

3. Very little information on the influence of stress history on creep behavior is available. Experimental results describing the creep behavior under variable stress conditions are needed in order to develop more general creep relationships.
4. The large number of creep relationships encountered in the literature seems to be partly caused by a lack of uniformity in analyzing creep data.

Chapter 4

TIME-DEPENDENT BEHAVIOR OF A JOINTED COAL

4.1 Introduction

In order to pursue the study of time-dependent behavior of underground openings it was felt necessary to investigate the time-dependent response of a rock mass when subjected to a change in stress. It was also decided to concentrate on the rheological response rather than investigate other mechanisms, such as swelling, that cause delayed behavior of a rock. Therefore, the aim of the present investigation is to assess both the general features of the time-dependent behavior of a rock mass and the parameters describing this process at the laboratory scale.

To accomplish this goal two major steps have to be completed. In the first place, the question of which material should be used as a 'modelling' for a jointed rock mass had to be answered. It was decided to work with a natural rock-like material that would possess a well defined set of discontinuities and yet, where the effects of these discontinuities could be adequately represented in a sample of reasonable size; i.e; the spacing between discontinuities would be in the order of centimeters. For that purpose, coal from the deposits near Lake Wabamun was selected. A description of the structure and some properties of this coal is presented in section 4.2.

The second question to be resolved was concerned with the type of tests to be carried out to assess the creep behavior of the material in question. For that purpose, it was decided that constant load creep tests under triaxial conditions would be carried out.

Two main questions were set to be answered, namely:

a. the general pattern of the creep behavior of a fractured rock-like material

b. establishment of a relationship that could predict the creep deformations under a certain load and load history.

Eight constant load tests under triaxial conditions were carried out following different stress histories, giving a total of about 50 creep stages. To carry out these tests a simple rig was designed. Section 4.3 presents both the testing equipment and testing procedures. Section 4.4 presents a summary of results obtained, their analyses and interpretation, and in section 4.5 the main conclusions as well as recommendations for further research are given.

4.2 Sample description and material properties

4.2.1 Sampling site

The coal samples used in the present study were obtained from the coal seams exploited at the Highvale Mine which is situated on the south shore of Wabamun Lake. The Wabamun Lake district is west of Edmonton in Tps. 50-54, Rs 3-7, W.5th Mre., and is centered about Wabamun Lake. The acess from Edmonton is west via Highway 16.

The major geologic features as well as topography and drainage of the area in the proximity of the sampling site have been described by Pearson(1959) and Noonan(1972) . The bedrock of the Wabamun Lake district is formed by rocks of late Cretaceous and early Tertiary ages and consists of sandstones, shales and coal seams deposited in a fresh-water environment. The coal-bearing unit is continuous at the Wabamun Lake district and, in most places throughout the area, it can be divided into two main seams with a few thinner seams below, see Figure 4.1.

All the blocks of coal used to obtain the samples were obtained from the upper main seam in the west pit at the Highvale Mine, see Figure 4.2.

4.2.2 Sampling procedures

The coal seams at Highvale mine are exploited by a conventional strip-mining operation. The till cover is removed by a dragline leaving the coal seam exposed and light explosive charges are set in boreholes at a depth of 2.4 m on half of the exposed seam to loosen the coal thereby facilitating the mining operation. The coal is then loaded into trucks and transported to the Sundance Power Plant, see Figure 4.2.

Observations of the blast holes exposed along the face of the bench were made by Noonan(1972) and indicated that the shatter-zone extended in a fan-like arrangement only

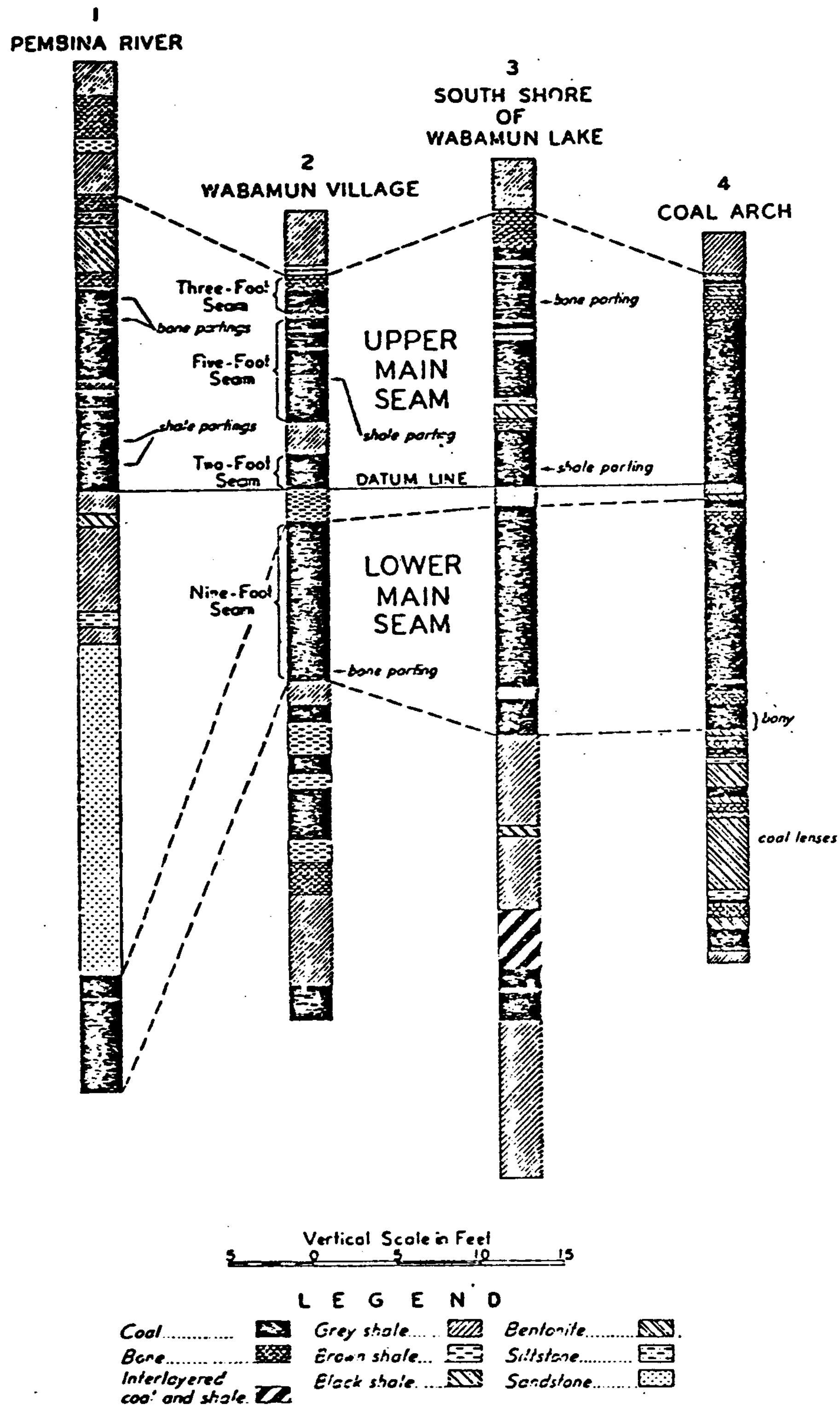

1. Pembina Peerless Coal Company pit and nearby outcrops. NW¼ Sec 2, Tp 54, R 7, W 5th
2. Alberta Coal Limited 1957-58 pit, Lsds 2 and 3, Sec 15, Tp 53, R 4, W 5th.
3. Mount Royal Collieries Limited pit, Lsds 4 and 5, Sec 23, Tp 52, R 4, W 5th.
4. Coal Arch, North Saskatchewan River, Lsd 1, Sec 32, Tp 50, R 3, W 5th

Figure 4.1 Section through the Pembina coal-bearing zone, (Pearson(1959)

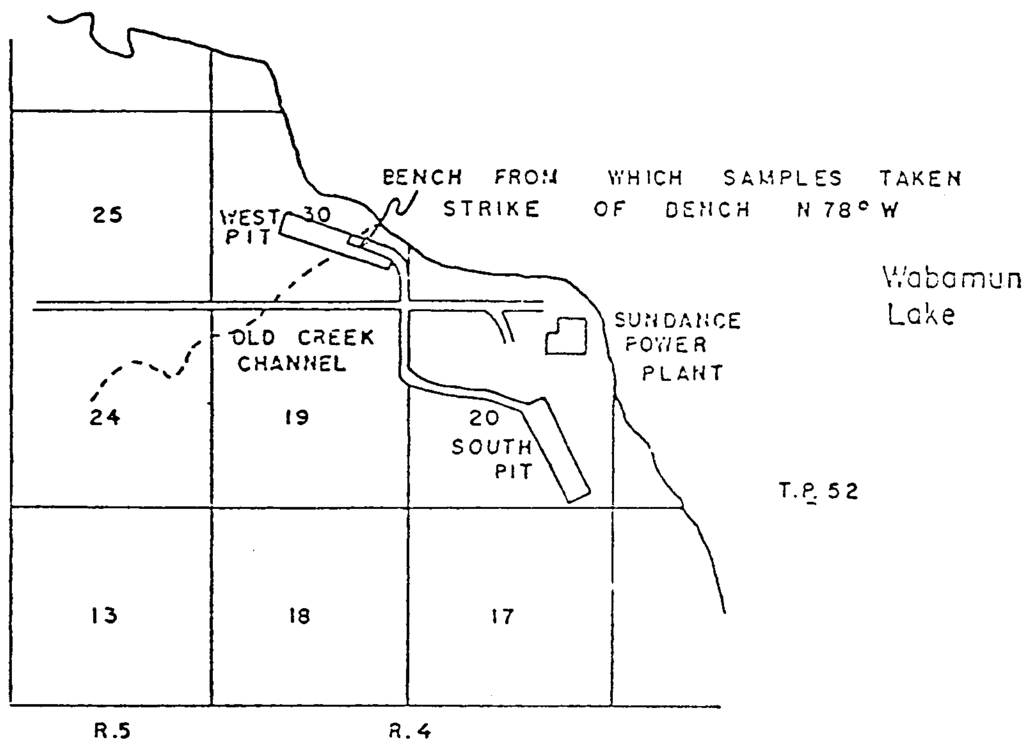

Figure 4.2 Sampling area at Highvale Mine (after Noonan(1972)

about 45 cm from the point where the charge was detonated. Hence, only few, if any, additional fractures would be created at the top of the seam as a result of blasting. Blocks from the top of the seam were selected to be brought to the laboratory from which the samples were later to be drilled. To avoid breakage during transportation only the blocks without any major apparent fracture were selected.

This rudimentary sampling procedure could be justified since it was not the aim of this study to produce results that would be representative of the in-situ coal but rather to use the samples as a modelling material. However, these blocks displayed the same structural characteristics and permitted the cutting of similar samples to the required dimensions.

4.2.3 Structure of the Wabamun coal

A detailed structural survey of the upper main seam at the west pit at the Highvale mine was carried out by Noonan(1972). Two main sets of discontinuities exist.

The first set consists of bedding planes which, at the location studied, are horizontal and consist of thin bands of both bright (vitrain) and dull (durain) coal. Noonan also described occasional thin bands of shale, discontinuous laterally and interbedded in the coal. This was also observed by the Author in one of the samples cut from the blocks collected at the site. It was also noted that these coal bands (vitrain and durain) were not continuous laterally.

The second set of discontinuities consists of planar, vertical, discontinuous joints or 'cleats' at right angles to the bedding planes and having an average orientation of N 45° E and average spacing of about 3 cm. The origin of 'cleating' in the Wabamun Lake coal was not investigated, being outside of the scope of this thesis, but the character of the jointing, i.e., almost perpendicular to bedding planes and being discontinuous, suggests tensile strains due probably to regional rebound. As discussed by Evans and Pomeroy(1966) , these vertical joints tend to concentrate in the bright bands while decreasing in density or even becoming non-apparent in the dull bands. This probably reflects the fact that vitrain is more brittle than durain and therefore more prone to tensile failure at a smaller value of strain. The rock bridges along the surface of a joint could then be associated with the presence of dull coal. This fact together with the lateral and vertical variations in coal properties suggest the difficulties in estimating the percentage of rock bridges in a particular joint.

Noonan(1972) also suggested the presence of a non-planar system of fractures which are not as consistent as the joints described previously, running prependicular to both bedding planes and major cleats. These features have been described in the literature as 'cross-cleats', e.g., Evans and Pomeroy(1966) . The Author observed the existence of such fractures along the samples but their density was low enough to be of no concern.

4.2.4 Material properties

The Wabamun Lake district coal has been classified as a sub-bituminous coal B according to the Canadian Classification, Pearson(1959). Table 4.1 presents a summary of some index properties for the Wabamun coal, extracted from Pearson(1959) and Noonan(1972).

Both deformation and strength properties of the Wabamun coal have been described previously by Noonan(1972). Noonan's results refer to direct shear tests on both precut and 'intact' samples. Shear tests on pre-cut planes parallel to the bedding planes yielded an ultimate frictional angle of 30°. The experimental program for 'intact' samples included direct shear tests under normal stresses below 1.0 Mpa on samples with discontinuities (bedding planes, joints) oriented differently with respect to the shearing direction. Table 4.2 summarizes the peak strength parameters determined, for several test configurations, assuming the Mohr-Coulomb criterion as valid. The small values of the vertical displacement at peak lead to the conclusion that no geometric component of the shear strength associated with dilatancy was mobilized.

Additional mechanical properties for the Wabamun coal have been reported recently by Kaiser(1979) and Guenot(1979). For Kaiser's data on direct shear tests along

Table 4.1 Wabamun coal - Summary of index properties

moisture content (%)	21.3 - 26.9
specific gravity	1.58
void ratio	0.340 - 0.484
degree of sat. (%)	85.4 - 100
bulk density (t/m3)	1.36 - 1.38
ash content (%)	11.9 - 14.9
volatile matter (%)	24.4 - 27.4
fixed carbon (%)	38.9 - 42.3
gross (btu/lb)	8000 - 8720

Table 4.2 Shear strength parameters at peak for the Wabamun coal

Sample configuration	c (Kpa)	ϕ (degree)
shear plane // bedding; joints vertical and different orientations with respect to shearing direction	386 - 524	40.5 - 41.7
shear plane // joints; bedding vertical and // to shearing direction	172.5	67.8
bedding plane vertical and // to shearing direction; joints at different orientations	117.3 - 345	64 - 65.5

joints, the Mohr-Coulomb criterion was also assumed as valid. Moreover, it also assumed that the internal friction was fully mobilized at peak and its value being numerically equal to 30°, i.e., the ultimate frictional angle determined by Noonan(1972) on precut samples. Cohesive components were determined as ranging from 0.85 - 1.92 MPa for normal stresses between 1 and 4 MPa. The variation in the cohesive component at peak strength was ascribed to differences in the degree of continuity of rock bridges along joints (shearing planes). As in Noonan(1972) geometric components such as dilation were neglected.

Kaiser(1979) also discusses the behavior of Wabamun coal under triaxial tests at low confining pressures. Sample configuration was such that joints were oriented at about 30° with the vertical and bedding planes parallel to the major principal stress. The reported modes of failure for all the samples indicate that generally the shear surface followed the joints with tensile fractures developing along the bedding planes in one occasion. Degrees of separation[3] or continuity of the joints estimated by eye after the test (Kaiser(1979) , ranged between 50% - 80%. Again, the Mohr-Coulomb criterion was used to analyze the strength data and the frictional component was assumed to be 30°. The cohesive component varied between 0.7 to 2.05 MPa at the peak strength. Young's modulus obtained from the linear part of the stress-strain curve varied from 870 - 1300 MPa.

----

[3]Degree of separation herein is defined as the ratio between area of open joint and total area.

Guenot(1979) presents data for high confining pressure triaxial tests (σ_3 : 3.5 to 10 MPa) on 3.71cm diameter samples and joints at different orientations with respect to the vertical stress. Using the Mohr-Coulomb failure criterion, Guenot suggests a cohesive component between 1.9 and 2.4 MPa assuming a frictional component of 30°.

4.3 Testing procedure

4.3.1 Sample preparation

Large lumps of coal were collected in the field, as described in section 4.2.2, and, after the arrival at the laboratory, these blocks were coated with latex to avoid drying and then stored in a moist room. Cylindrical cores of about 6.90 cm in diameter and different length were drilled from these blocks. A laboratory drilling machine with a core barrel of about 7.5 cm in external diameter and water-operated was used for the drilling operations. Reaction against the ceiling was provided to the drilling machine in order to avoid unwanted vibrations of the core-barrel that could damage the core.

All the samples were drilled with their long axis parallel to the bedding planes and at an angle of 30 with the joints. This configuration would correspond to a horizontal sample in the field. Figure 4.3 shows the relative orientation of discontinuities and sample axis during drilling operations.

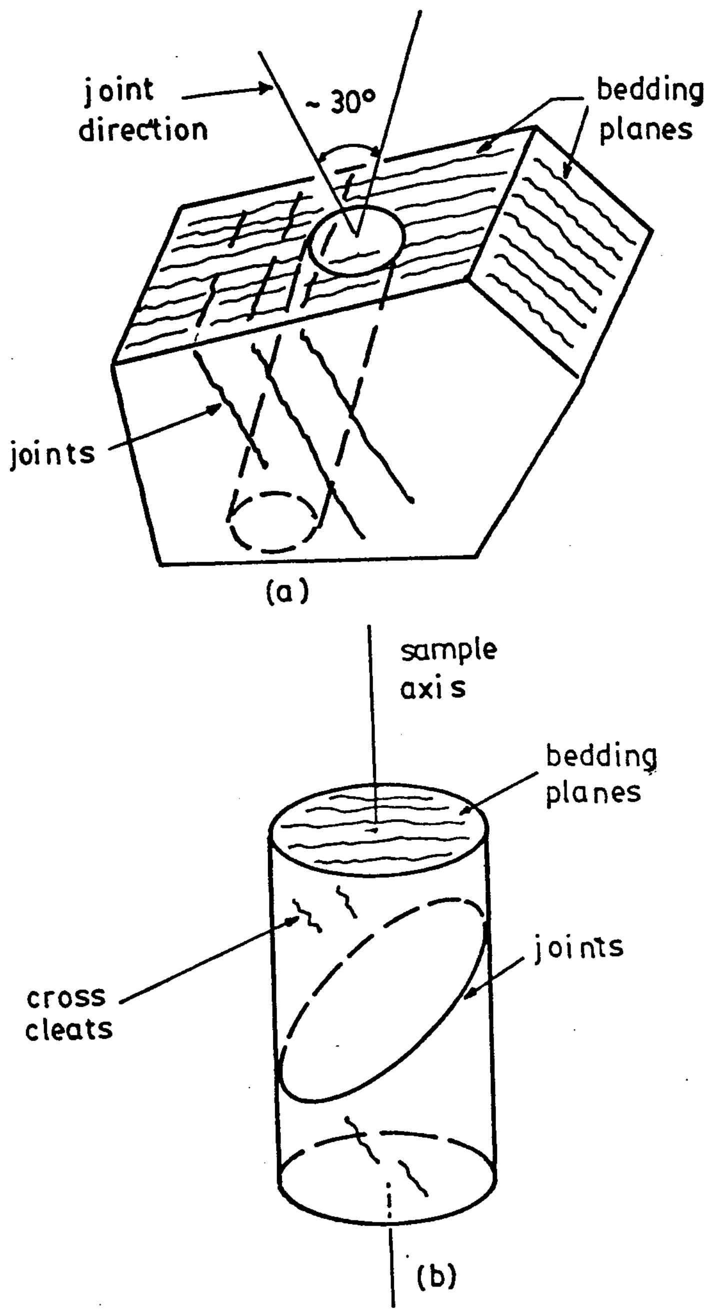

Figure 4.3 Relative orientation of core barrel and coal structure

Many problems occurred during the coring operations. The high degree of fracturing encountered in zones inside the blocks prevented, in many cases, the sucessful coring of the samples because of breakage of the core. Also, attempts to drill cores perpendicular to the bedding planes failed consistently due to shearing and separation along these planes.

After removing the core from the core barrel, the samples were cut to a convenient length using a water-cooled circular diamond saw. Two criteria were used in selecting the length of the samples: first, the ratio length/diameter was kept around 2.5 and second, it was attempted to keep at least one joint intercepting the sample along its length and to avoid joints intercepting the ends. Due to the small spacing of the joints the latter was not always possible.

The ends were further trimmed in order to ensure a minimum of non-parallelism between the ends. A sand-paper belt was used initially without great sucess because pieces at the periphery were broken off very easily, especially when joints intercepted the ends. This operation was then carried out by manually sanding the ends. The 'parallelism' of the end surfaces was controlled by measuring the length of the sample in at least four different positions and in all cases it was possible to limit the maximum deviation to less than 0.05°.

4.3.2 Testing equipment

A simple double-lever arm rig capable of applying a constant axial load was designed and built for the series of creep tests reported herein. The decision to select a mechanical system was based mainly on simplicity and the time for construction. The rig consists of a reaction frame and two lever-arms (I-section) which would transfer loads applied at their ends through a loading ram to the sample. The mechanical magnification for the double-lever arm system was about 10. Figure 4.4 shows a sectional view of the rig when assembled.

A conventional triaxial cell for 10-cm diameter samples was modified in order to accommodate 7-cm diameter samples by changing both top cap and bottom pedestal. Special Thompsom linear bushings were used to guide the loading ram with minimal shaft friction. The triaxial cell used had a capacity of withstanding confining pressures up to 1380 Kpa and provision for drainage of the sample provided at both top-cap and bottom pedestal.

A unit for monitoring axial load, displacement and confining pressure complemented the laboratory set up. This unit consisted of a Fluke data-acquisition system with a printer unit, a recording device (Techtran #8410), capable of storing all the information on a cassete tape, and two power-supplies to provide input voltage to feed the measuring units. The axial displacements were measured with linearly variable differential transformer (LVDTs), the

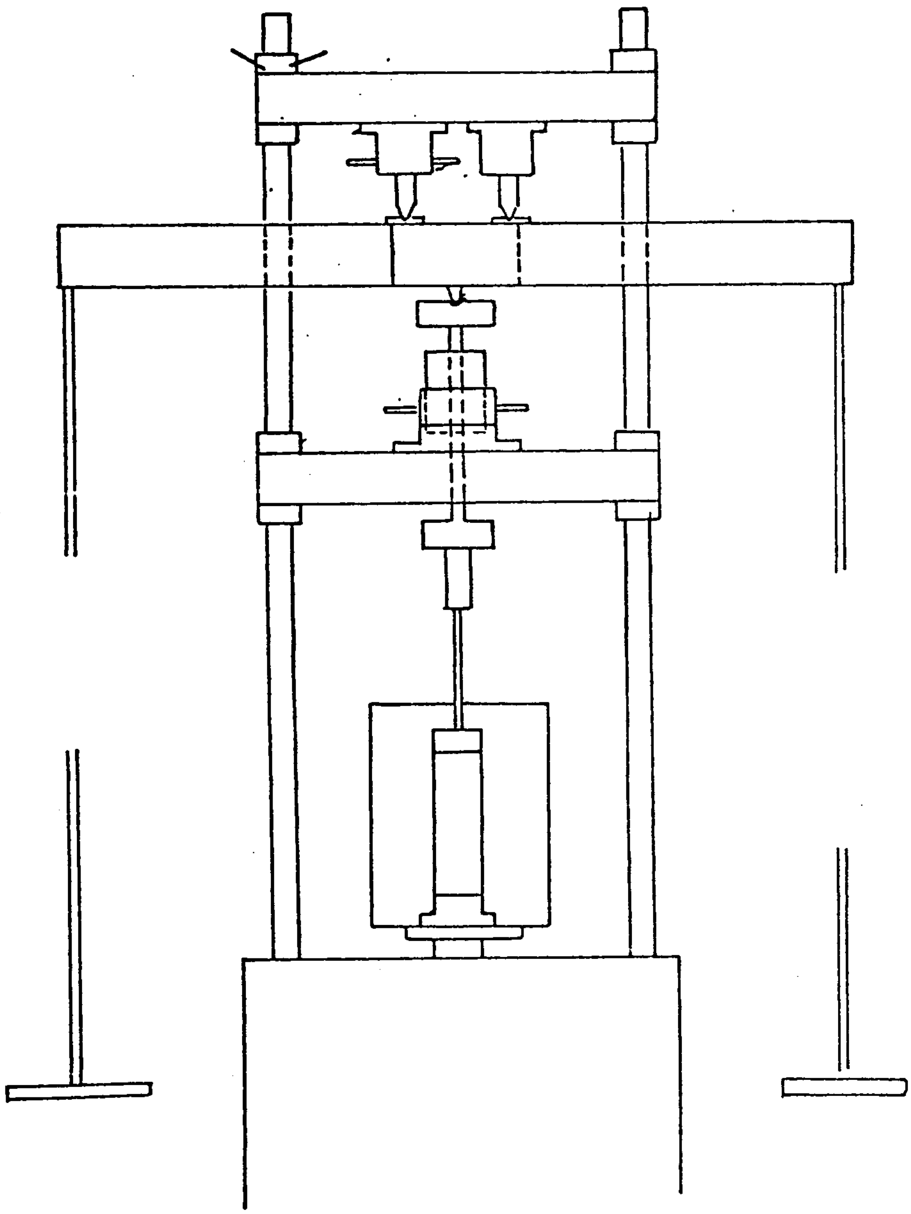

Figure 4.4 Sketch of creep rig when assembled

axial load was measured with a temperature compensated electrical resistance strain gauged load-cell and the confining pressure with a transducer. These units were calibrated regularly and no change in the calibration factors was observed during the experimental program. The whole apparatus was kept in a temperature and humidity controlled room capable of maintaining the temperature variations within about 0.5 $^{\circ}$C and the humidity within 5%.

4.3.3 Testing procedures and sample properties

Specimen weight, dimensions and a sketch of externally visible discontinuities for all the samples were recorded prior to testing. Water content from pieces trimmed from the ends of the core were determined and, for some samples, the water content at the end of the test was obtained by using the whole sample. Each sample prior to set up was enclosed within a filter cloth and a double rubber membrane as an extra precaution to avoid leakage in case one membrane was punctured during the test. Double O-ring and screw-clamps were used at each end to provide extra sealing along the contacts between membrane and both pedestal and top cap.

After the application of both confining and back-pressure, the sample was allowed to consolidate for a period of 24 hrs. For all tests a small axial load was applied to seat the load plattens against the sample. Following these preliminary stages, the axial load was increased up to the level where a creep test was to be carried out. The recording of the axial displacement was initiated in all the cases within 10 sec after the load was increased. Readings were taken automatically by the data acquisition system and the time interval varied throughout the test. At the early stages, readings were taken at every minute up to the first 10 min of test, changing to 10 min intervals up to the first 2 hrs. Subsequently, the strain-rate was small enough to allow for a large time interval and then, readings were taken at every hour up to the end of the test.

For the multiple-stage creep tests, after a creep test terminated, the load was again incremented up to a new level and another creep test was carried out. This procedure continued until failure occurred. For the single-stage creep tests, after the creep test terminated, the sample was unloaded and the creep recovery was observed for a maximum period of 24 hrs. After that the sample was loaded, at a high rate of loading, up to failure.

Table 4.3 summarizes the index properties and the sample dimensions for the creep tests. The variation of water content, void ratio and unit weight displayed in this Table is well within the previously reported data by Noonan(1972) and Kaiser(1979). For all the calculations a specific gravity of 1.58 was assumed as suggested by Pearson(1959). Also indicated in Table 4.3 are both confining and back pressure for each test as well as estimated values for maximum deviatoric stress and Young's

Table 4.3 Summary of sample and test characteristics

Sample	CT1	CT2	CT3	CT4	CT6	CT7	CT8	CT9
diameter(cm)	6.890	6.890	6.905	6.863	6.875	6.872	6.882	6.863
length(cm)	17.556	18.469	20.312	20.088	20.149	19.062	20.048	19.713
unit weigth (t/m3)	1.350	1.381	1.377	1.378	1.356	1.383	1.371	1.376
water content (%)	22.1	22.4	20.5	21.8	24.9	23.5	21.3	22.5
void ratio	0.430	0.400	0.382	0.396	0.456	0.411	0.398	0.406
degree of sat. (%)	81.4	88.5	84.6	86.8	86.4	90.3	84.5	87.9
conf. pressure (Kpa)	346	208	553	415	415	415	415	415
back pressure (Kpa)	70	70	70	70	70	70	70	70
$(\sigma_1 - \sigma_3)f$ (*)	3801	4642.2	6050	3800	4950	6180 6700	5340 5700	6700
E(Mpa)	1080	670	1185.2	849.1	571.3	942.4	891.4	1200

(*) best estimative from stress-strain curve moduli for the sample tested. These moduli correspond to the linear section of the stress-strain curves, see Figures 4.5 to 4.9.

Figures 4.5 to 4.9 present the stress-strain curves for the tests reported herein and the stress level at which creep tests were carried out are also indicated in these figures. The stress history followed by each particular test is indicated in Figure 4.10.

The values of maximum deviatoric stress indicated in Table 4.3 constitute the best estimate extracted from the corresponding stress-strain curve for each test. Unlike a strain controlled test, a stress controlled test does not allow an accurate measurement of stress and associated strain near failure, let alone any measurement of the post failure region.

4.4 Creep behavior from laboratory tests

4.4.1 Analysis of creep data

The analysis of a constant deviatoric stress test consists basically of two steps: first, data-handling or processing of the obtained raw data and second, the presentation and interpretation of the processed data. The overall shortening of the sample, ΔL, was measured at convenient time intervals after the load application and transformed into engineering axial strain by the expression $\varepsilon = \Delta L / L$, where L represents the initial length of the sample. The variation in strain with time can be displayed

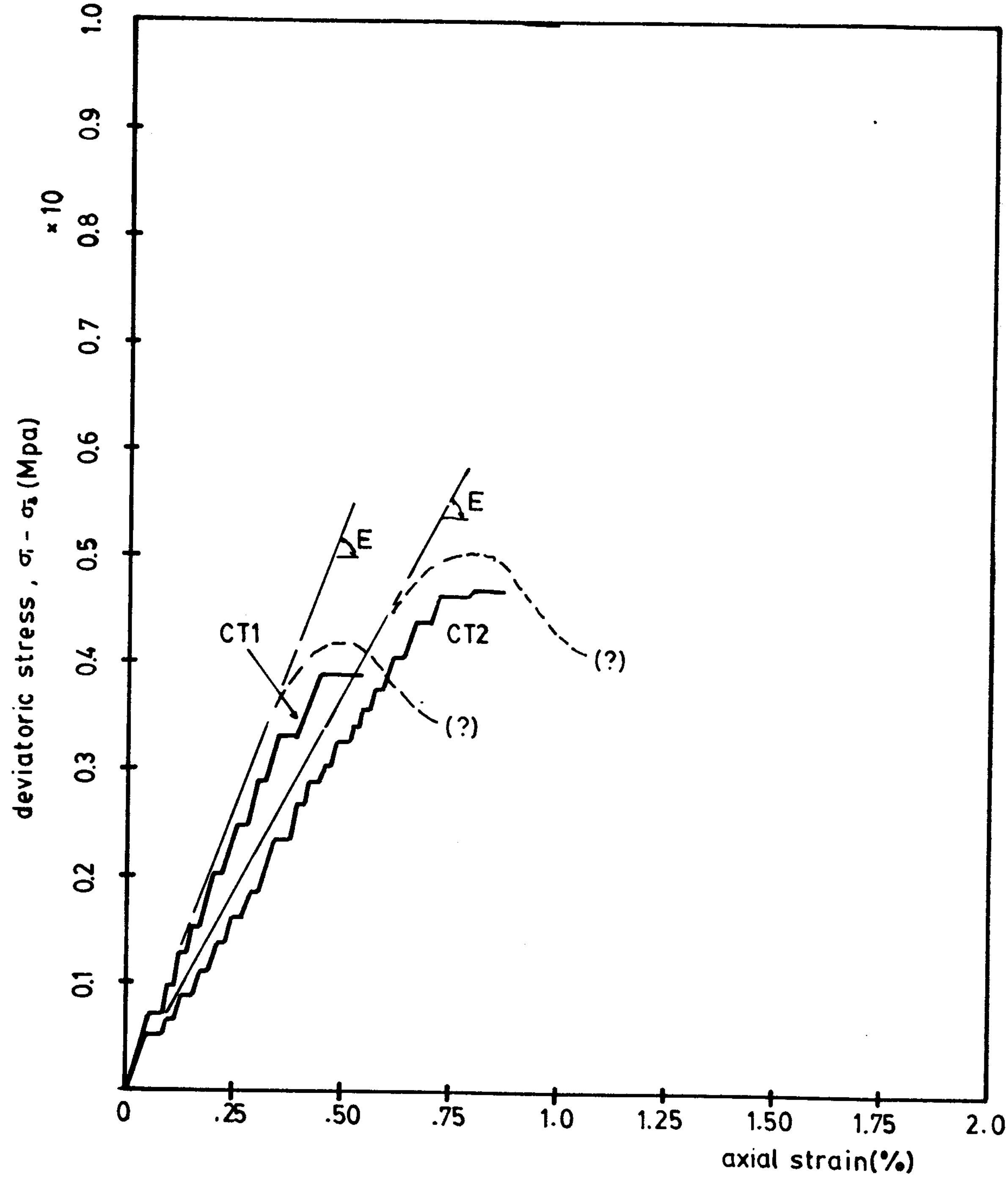

Figure 4.5 Stress-strain curve for tests CT1 and CT2

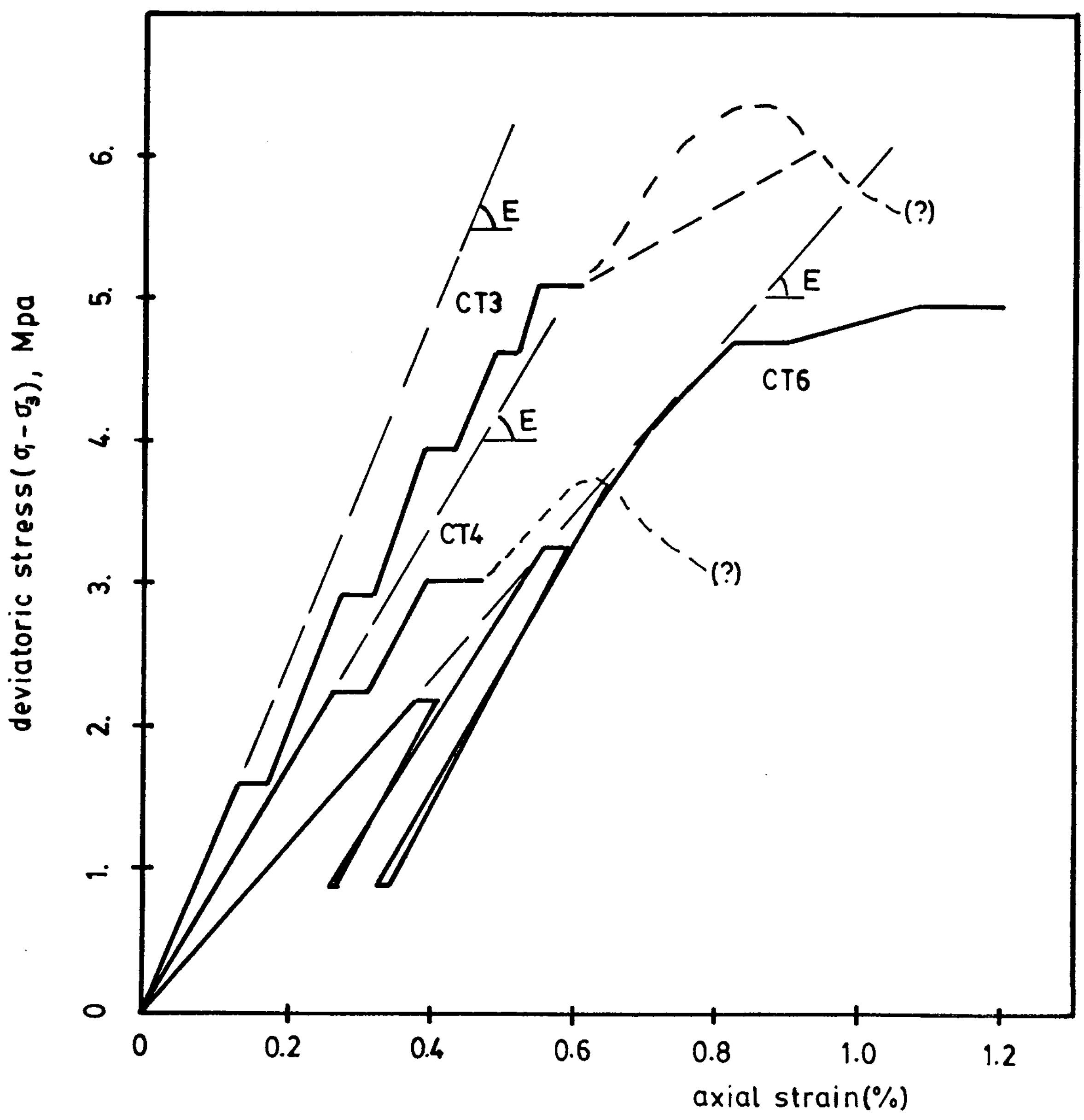

Figure 4.6 Stress-strain curves for tests CT3, CT4, CT6

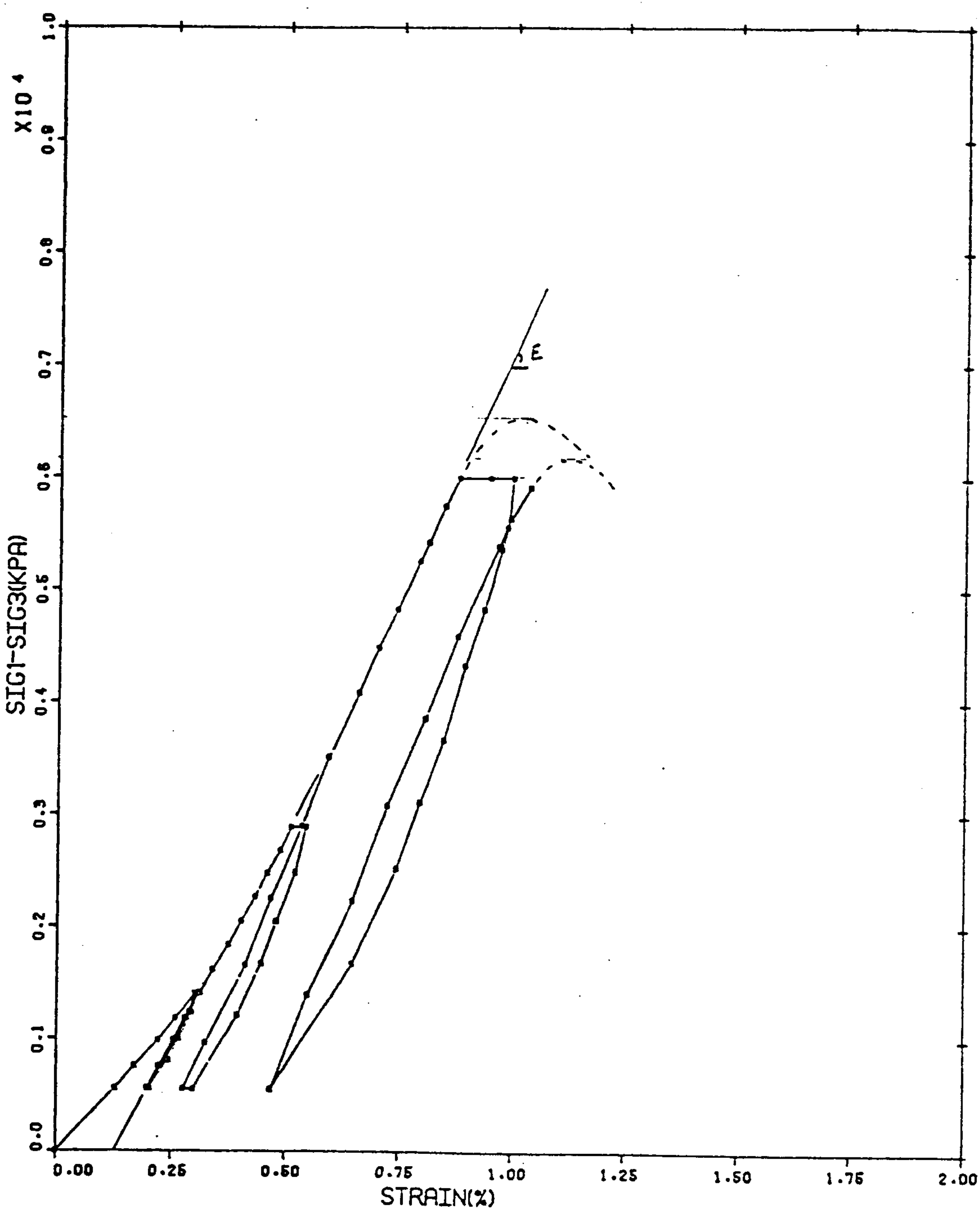

Figure 4.7 Stress-strain curve for test CT7

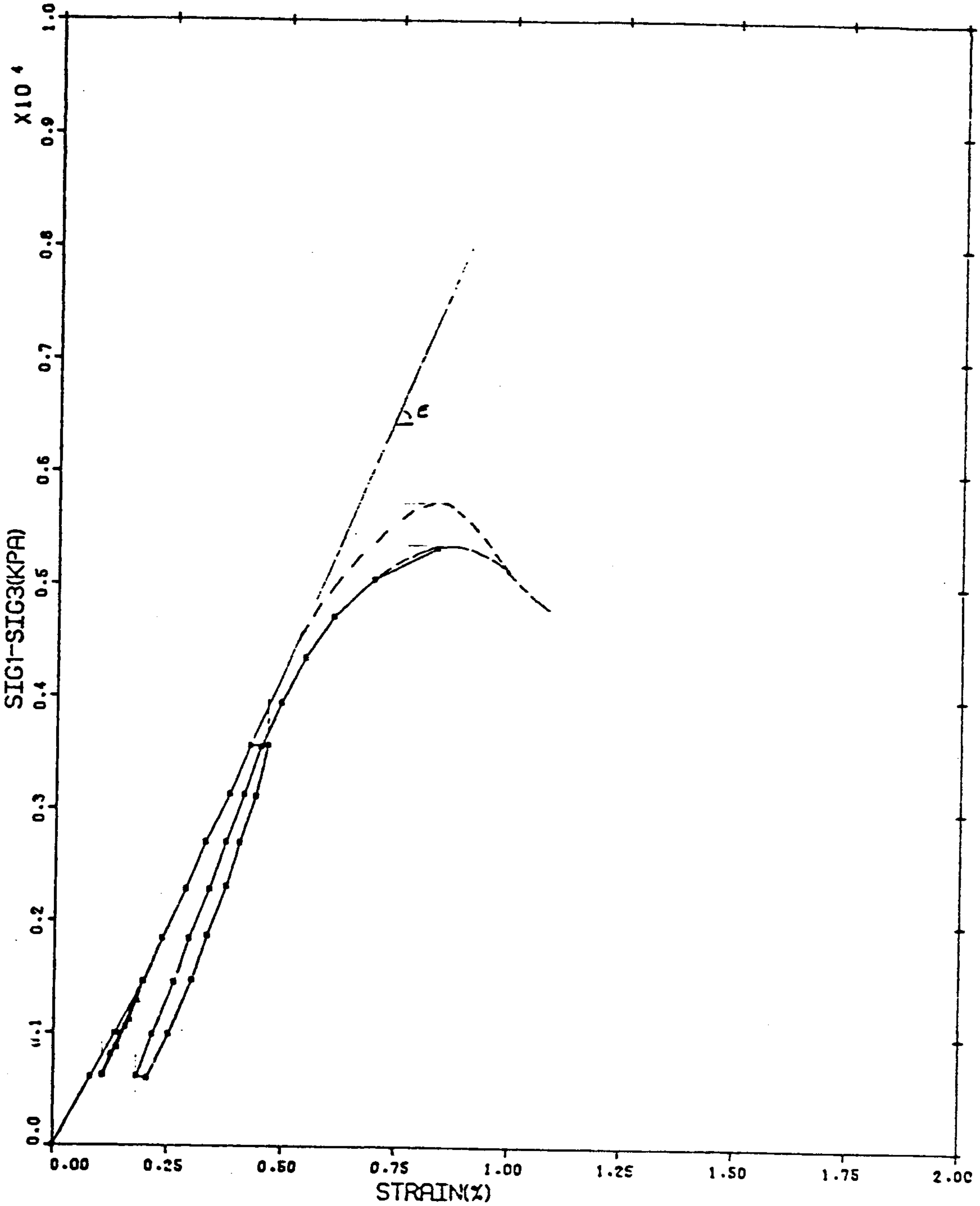

Figure 4.8 Stress-strain curve for test CT8

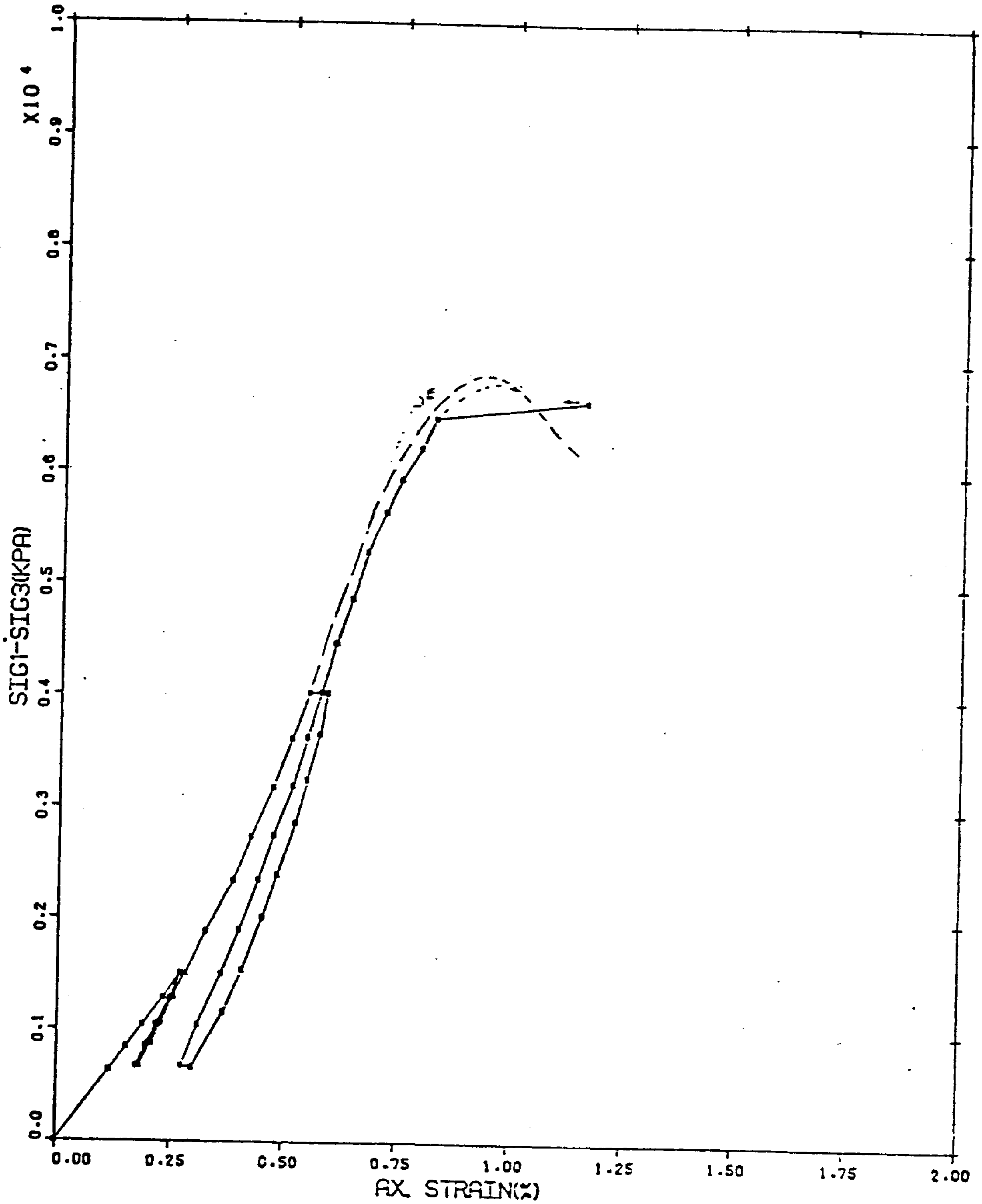

Figure 4.9 Stress-strain curve for test CT9

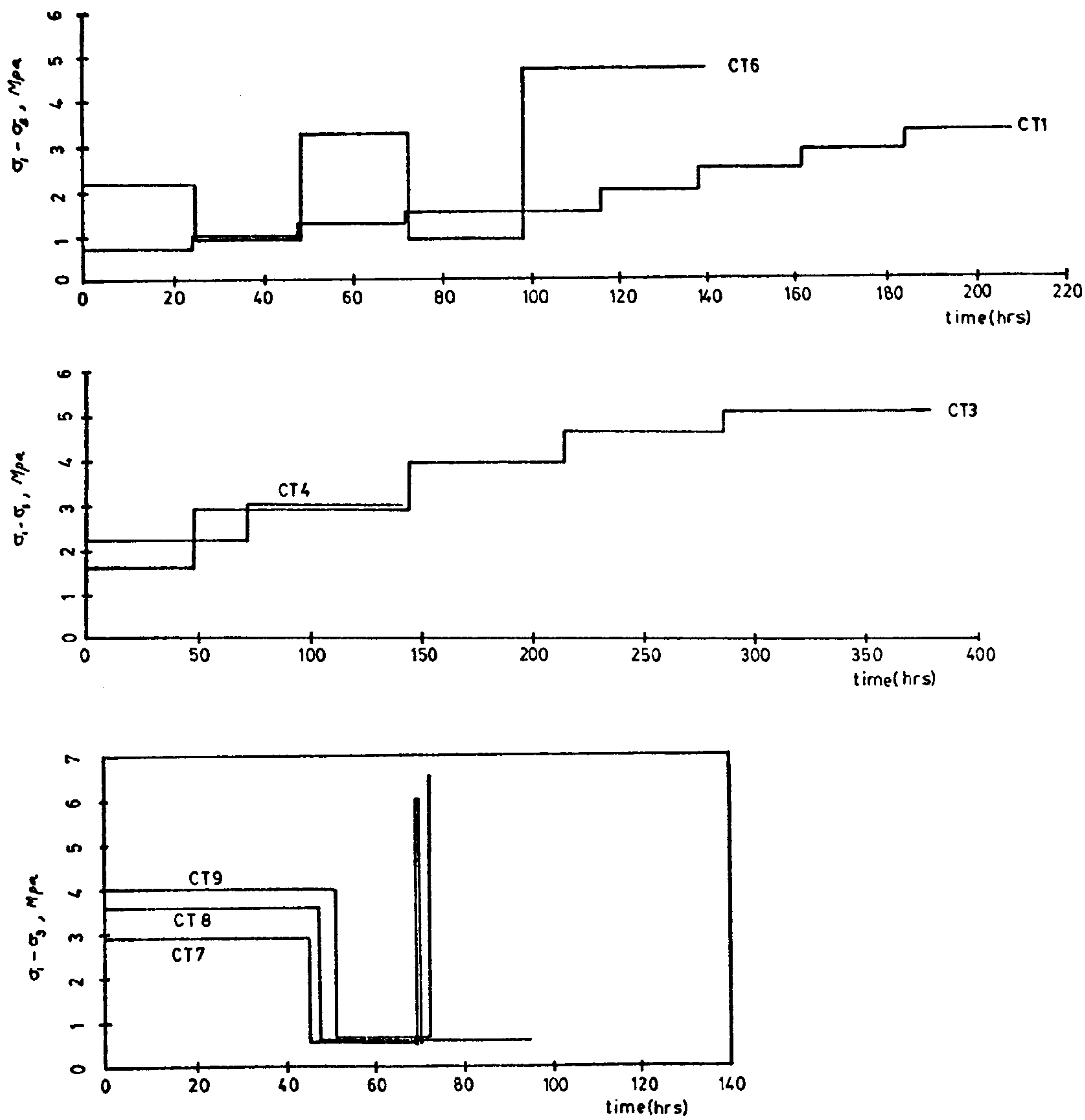

Figure 4.10 Stress history for the reported tests

graphically by several plots as ε vs. t, ε vs. logt and log ε vs. logt, the most common one being ε vs. t. At this stage, it is convenient to make a few remarks about this set of data, i.e., the creep strains and elapsed time.

The time-dependent strains during a creep test cannot be evaluated with complete confidence. Figure 4.11 shows an idealized total strain versus time curve for one typical creep test where t_1 represents the elapsed time between the load application and the time when the first measurement was observed, $(\varepsilon_t)_1$. The value of t_1 depends on the nature of the available measuring unit and the methodology of the test.

For all tests reported it was possible, in using an automatic reading and recording unit (data acquisition), to cut this first reading time down to less than 15 sec. However, the assumption that $(\varepsilon_t)_1 - (\varepsilon_t)_o$ would be equivalent to an 'instantaneous deformation' cannot be supported. Experimental data obtained by Evans(1958) at high rates of loading suggest that the amount of time-dependent strain involved in the value of $(\varepsilon_t)_1 - (\varepsilon_t)_o$ can reach the 40% range. Evans reported variations from 15%, 19% and 40% for respectively granite, concrete and sandstone. Based on Evans' results, Cruden(1969) suggested the range of 0 to 40% of the immediate deformations as being part of the time-dependent strains. Therefore, caution must be exercised when analyzing data based on creep strain as they are normally underestimated.

The interpretation of creep data can be done basically

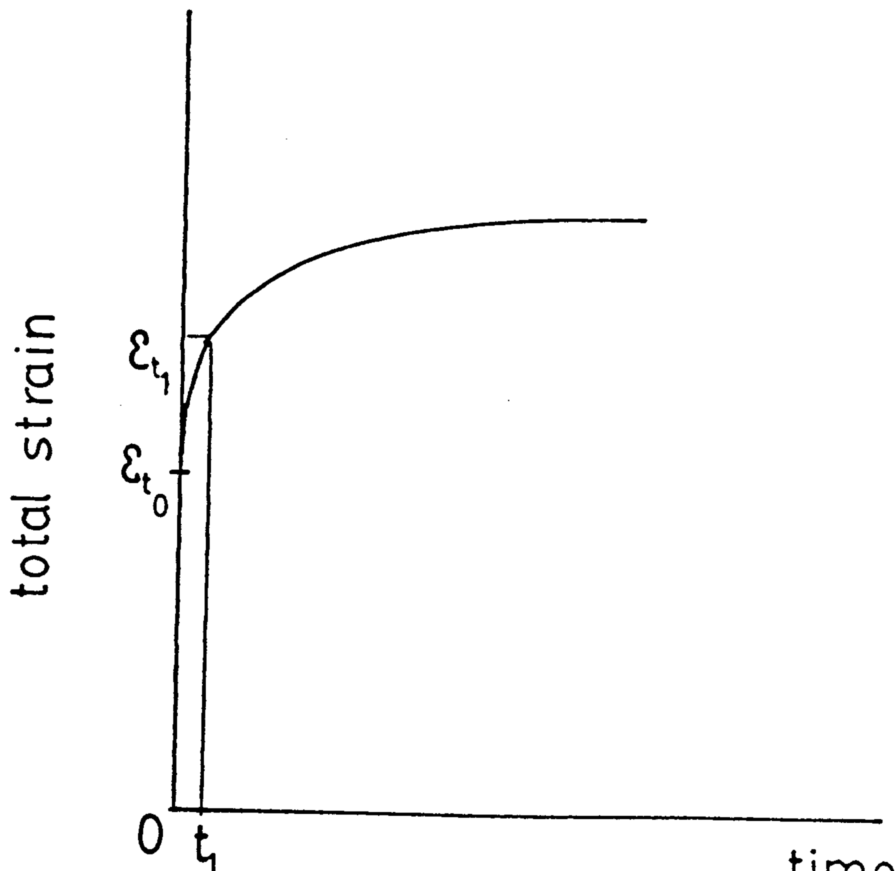

Figure 4.11 Idealized total strain vs. time curve for an increment of deviatoric stress

by two approaches: (a) in terms of creep strains or (b) in terms of strain rate. This step consists of finding a convenient mathematical relationship involving stress level and elapsed time to fit the experimental data. The use of creep strain data or analysis in terms of strain is subjected to the restrictions imposed by the uncertainties with respect to the time-dependent component of strain as discussed above. On the other hand, the analysis of creep data in terms of strain-rate involves the estimation of the strain-rate from the initial data. The strain-rate at a certain instant of time is independent of uncertainties with respect to the actual amount of creep strain provided it is treated as the rate of change of total strain (which is known accurately).

The strain-rate at a particular instant of time, t, is, by definition, the first derivative of the function relating the total strain, ε, with the time. Since the total strain is known only at certain times, t , the estimation of the strain-rate has to be done by numerical differentiation. Figure 4.12 presents a typical set of measurements, (ε_i , t_i) , from which strain-rate has to be estimated. The simplest approach would be to approximate the strain-rate at time $t^* = (t_{i-1} + t_i)/2$ by $(\varepsilon_i - \varepsilon_{i-1})/(t_i - t_{i-1})$.

This approach, however, presents some difficulties. Small fluctuations in the output voltage of the LVDT and also temperature caused some observations of strain at time t_i to be smaller than the observations at time, t_{i-1}, which

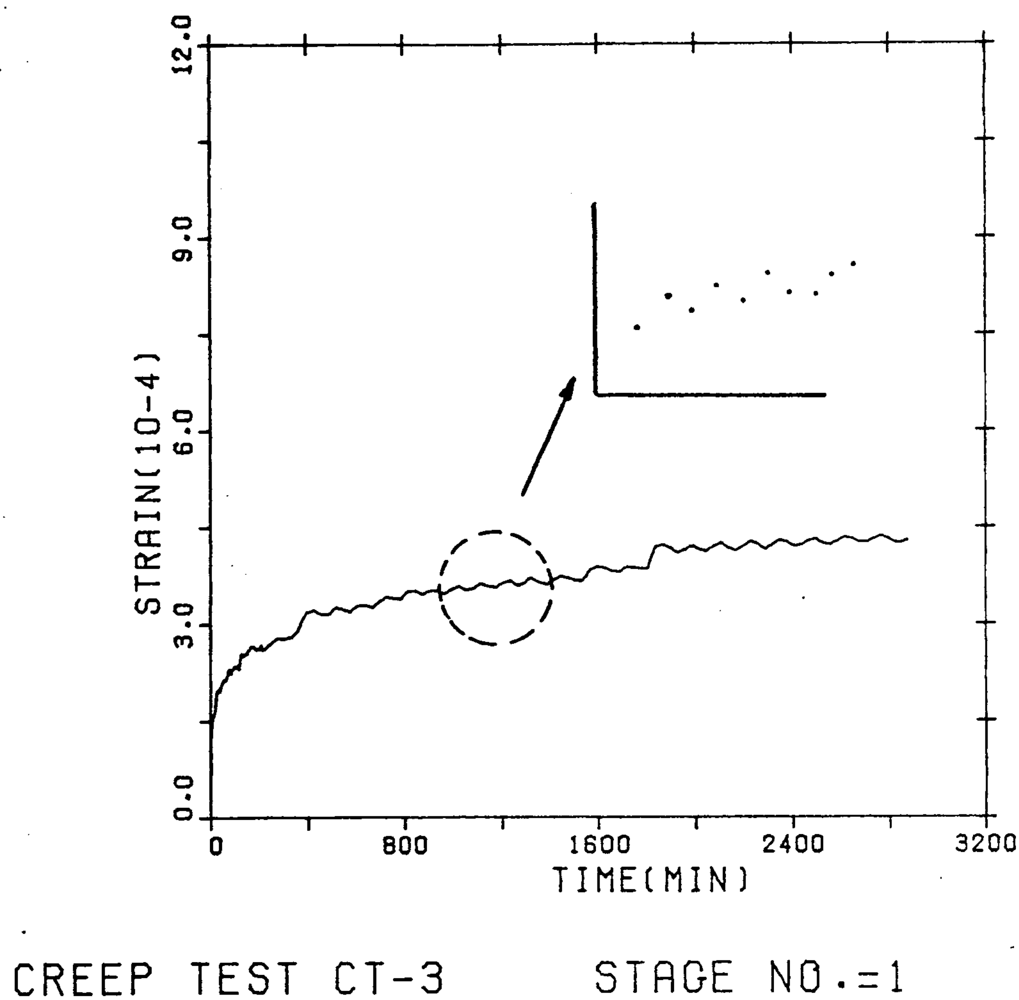

Figure 4.12 Typical set of measurements in a creep test

corresponds to a negative strain-rate which is not physically possible for the present test conditions. This started to happen more frequently when the increase in strains during the interval $[t_i, t_{i-1}]$ was of the same order of magnitude as the accuracy of the measuring system. A possible way of avoiding such inconvenience is to progressively increase the time interval between observations in order to compensate for these fluctuations in the measurements.

Cruden(1969) proposed a technique which 'corrects' the original data in the following way. If a situation occurs that $\varepsilon_i < \varepsilon_{i-1}$, a new observation $\varepsilon^* = (\varepsilon_i + \varepsilon_{i-1})/2$ is defined associated with a time $t^* = (t_i + t_{i-1})/2$. The new observation, ε^*, is given a weight, w^*, which is equal to the sum of w_i and w_{i-1}. For the original data, all the observations have a weigth, w_i, equal to unity. This process is followed until all the 'observations' are such that every strain is greater than the previous ones. From the new set of observations the strain-rate is calculated using the simple approach mentioned earlier.

A new technique was introduced which allowed the estimation of the strain-rate using the original set of data without having to correct them. This technique consists of approximating the strain-rate in the interval (t_{i-1}, t_{i+1}), i.e., at $t^* = (t_{i-1} + t_{i+1})/2$ by the slope of a least-squares straight line fit to the observations at t_{i-1}, t_i and t_{i+1}. As the time of testing increases, an interval such as (t_{i-2}, t_{i+2}) can be used and in this case 5 points are involved in the regression analysis. The computer program written to handle these calculations was set up in such a way that lines of zero or negative slope were neglected.

This method proved to be very sucessful smoothing the creep data obtained, as indicated by the relative small scatter observed in plots of strain-rate vs time to be discussed later. Strains rates obtained by this method were compared with the ones obtained using Cruden's approach described previously and similar results were obtained but with a small scatter. For all future reference in this thesis, this technique will be referred to as the linear-regression method.

4.4.2 Single stage creep tests

This section describes the results and interpretation of nine single-stage creep tests carried out under a triaxial state of stress.

4.4.2.1 Typical results

Natural materials usually exhibit considerable variations in properties between samples. Carefully conducted experiments on creep properties of materials have indicated that in spite of all the precautions with respect to sample quality, reproducibility and testing procedures the variations between results can be very large, e.g., Wu et al.(1978).

Without entering into considerations about the mechanisms leading to creep to explain the quantitative differences in a creep experiment program, it is reasonable to assume that the creep response is greatly affected by the structure of the material. In particular, for the highly fractured coal used in this experimental program one should expect quantitative variations between samples.

Based on these considerations, the major aim of the experimental program was to investigate the general pattern of creep response and the possibility of expressing this behavior in a simple relationship suitable for engineering applications. For all the results obtained, the raw data were reduced and strain-rate was estimated according to the linear-regression method described in the previous section.

In order to avoid any preconceived idea about the particular creep relationship to be used in attempting to match the experimental results, logarithmic plots of the axial strain-rate vs time were prepared for all tests including the ones corresponding to first-stage loading in the multiple-stage creep tests. This form of presenting the results is particularly suitable for analyzing the general pattern of creep behavior of a particular test.

Results of a typical test are displayed in Figure 4.13 as curves of strain vs time and logarithm of strain-rate versus time. Even though one could be tempted to assume that a region of constant strain-rate had been reached by considering strain-time data on Figure 4.13a, the

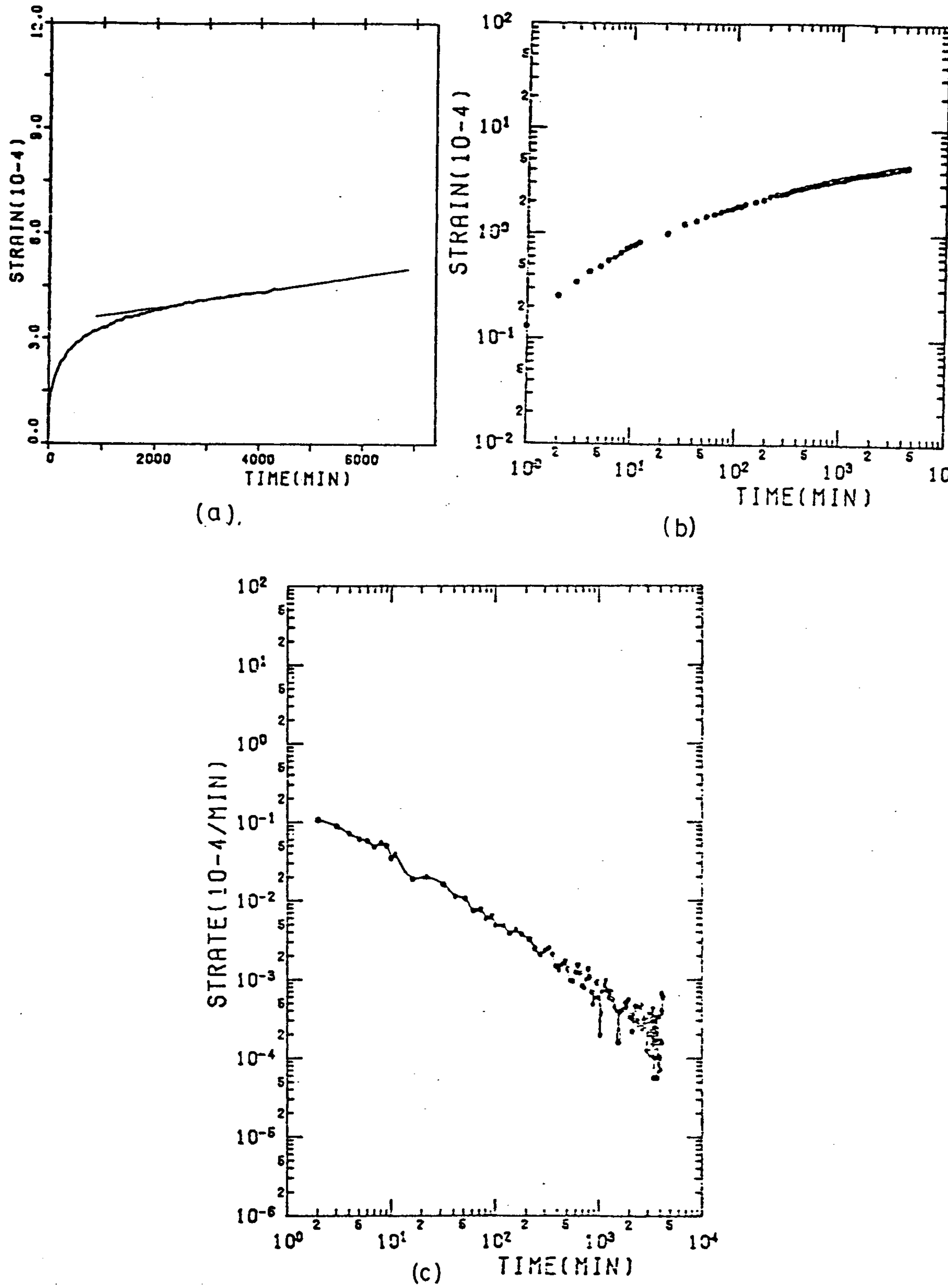

Figure 4.13 Typical result of creep test in jointed coal - Test CT4

strain-rate versus time plot shows a continuous decrease of the strain-rate with time.

As discussed in Chapter 3, the methods to analyze creep data can be divided into three categories: rheological methods, physical theories and empirical methods. The application of physical theories such as dislocation, rate process or structural theories of creep to the time-dependent behavior of rocks which are heterogeneous and complex in composition and structure would require a very sophisticated experimental program. The use of rheological model (e.g., Kelvin, Burgess model, etc.) requires determination of a large number of parameters thereby losing a valuable element of simplicity. The empirical approach constitutes a natural alternative which could be used readily for engineering purposes and which requires only a limited number of parameters to describe behavior during a creep test.

The empirical approaches assume the existence of three different creep processes, the so-called transient or primary creep, steady-state or secondary creep and tertiary creep, acting independently and at the same time, which can be included in a single expression describing the creep deformations or creep rate under a constant state of stress as equations (4.1) and (4.2).

$$\varepsilon_c = \varepsilon_p + \varepsilon_{ss} + \varepsilon_t \qquad \ldots. \ (4.1)$$

$$\mathring{\varepsilon}_c = \mathring{\varepsilon}_p + \mathring{\varepsilon}_{ss} + \mathring{\varepsilon}_t \qquad \ldots. \ (4.2)$$

where,

ε_c , $\mathring{\varepsilon}_c$ = creep strain and creep strain rate

ε_p , $\mathring{\varepsilon}_p$ = primary creep strain and strain rate

ε_{ss} , $\mathring{\varepsilon}_{ss}$ = secondary creep strain and strain rate

ε_t , $\mathring{\varepsilon}_t$ = tertiary creep strain and strain rate

The tertiary component of creep is normally not considered in empirical relationships. This is primarily due to the lack of experimental data on this component. Equation (4.2) can be simplified and rewritten as equation (4.3) which now assumes that both components $\mathring{\varepsilon}_p$ and $\mathring{\varepsilon}_{ss}$ are a function of stress. For a particular value of stress, σ, the question is to determine the function $f_2(t)$ which best describes the experimental data.

$$\mathring{\varepsilon}_c = f_1(\sigma) \cdot f_2(t) + g_1(\sigma) \qquad \ldots. \ (4.3)$$

From logarithm plots of strain-rate versus time the secondary creep rate, $g_1(\sigma)$, is indicated by an asymptotic value approached at large times. Alternatively, other forms of plots of strain-rate versus time could be used for the same purposes. Rigorously, at any instant of time both components act independently of each other but their relative importance for the overall process at small times and at large times are very different. At small time the secondary creep rate has a small influence on the creep strain-rate while at large time it overcomes this difference and must be considered. On the other hand, the separate existence of a secondary creep stage has been severely criticized , Mitchell(1975). Even for materials such as ice and frozen soils the concept of secondary creep rate has been subjected to criticism, Roggensack(1977).

The logarithmic plots of strain-rate versus time for eight different tests at various confining pressures displayed in Figures 4.14 to 4.17 indicate no sign of an asymptotic value of strain-rate during the time the test was carried out. The longest test was carried out for about 120 hrs. Therefore, no attempt was made to separate the primary and secondary component of the creep strains for the tests reported in this section.

In Chapter 3 the use of power law or exponential representation of strain rate versus time was discussed and it was concluded that the power law relations are more suitable for the purposes of this research. The power law relationship between strain-rate and time is represented by equation (4.4) where $\overset{\circ}{\varepsilon}$ = strain rate and 'a' is a constant for a certain stress level.

$$\overset{\circ}{\varepsilon} = a \cdot t^{-m} \qquad \ldots . \ (4.4)$$

This equation is represented by a straight line in a logarithm plot of strain-rate versus time. The pattern of the experimental data displayed in Figures 4.14 to 4.17 seems to suggest the use of the power law to fit these results. A computer program to carry a regression analysis based on the least-squares method was employed to analyze the data. The results of these regressions are summarized in Table 4.4 which displays, for each test, the two coefficients, 'a' and 'm', characterizing the power law.

The goodness of fit indicated by the coefficient of correlation for most of the tests indicates the validity of the power law as providing a good approximation to the experimental data. For test CT3, which indicates the lowest coefficient of correlation, the output voltage at the data-acquisition was not set properly at the beginning of the test and there was a loss in accuracy of the results due to this fact.

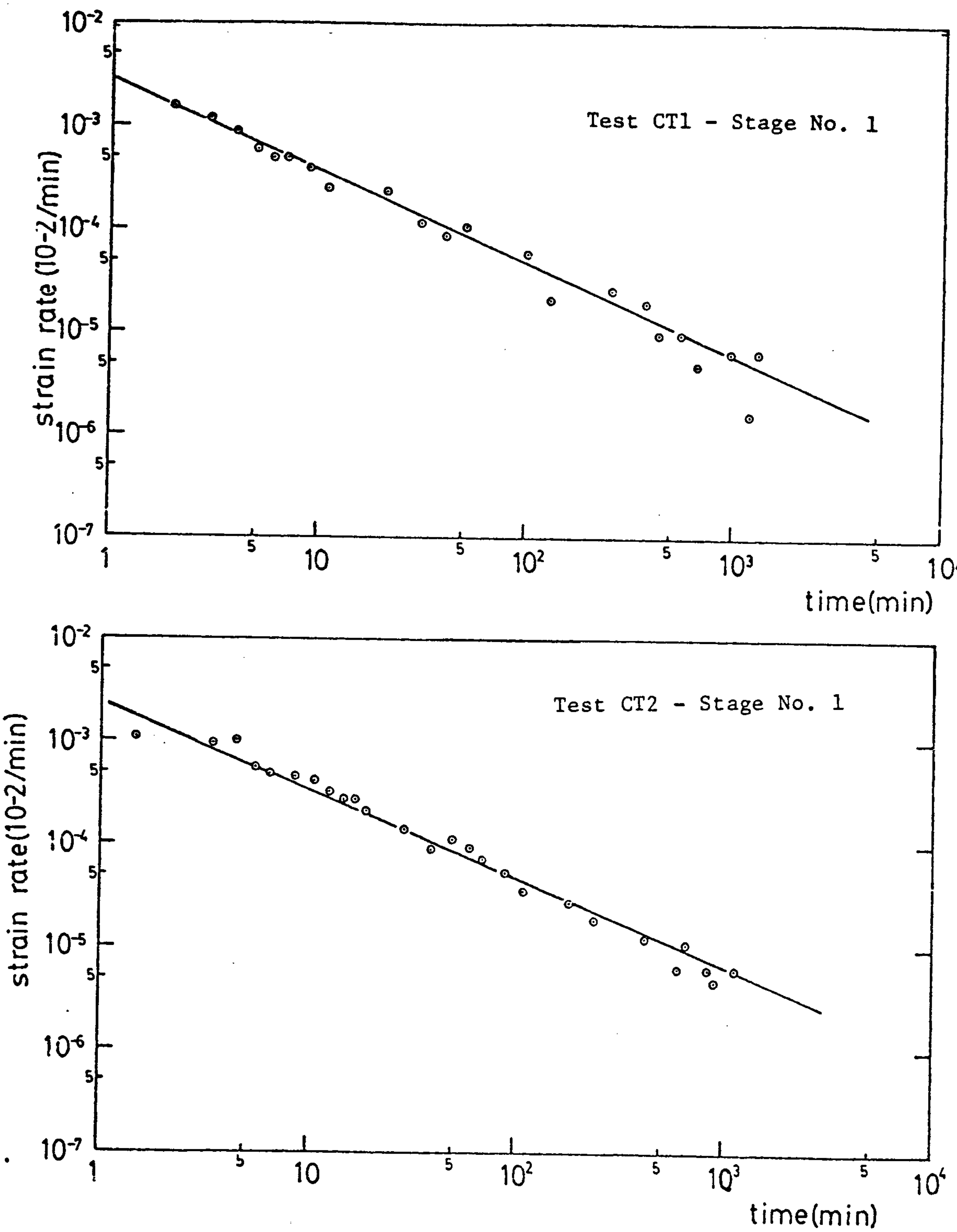

Figure 4.14 Logarithm plots of strain-rate versus time. First loading. Tests CT1 and CT2

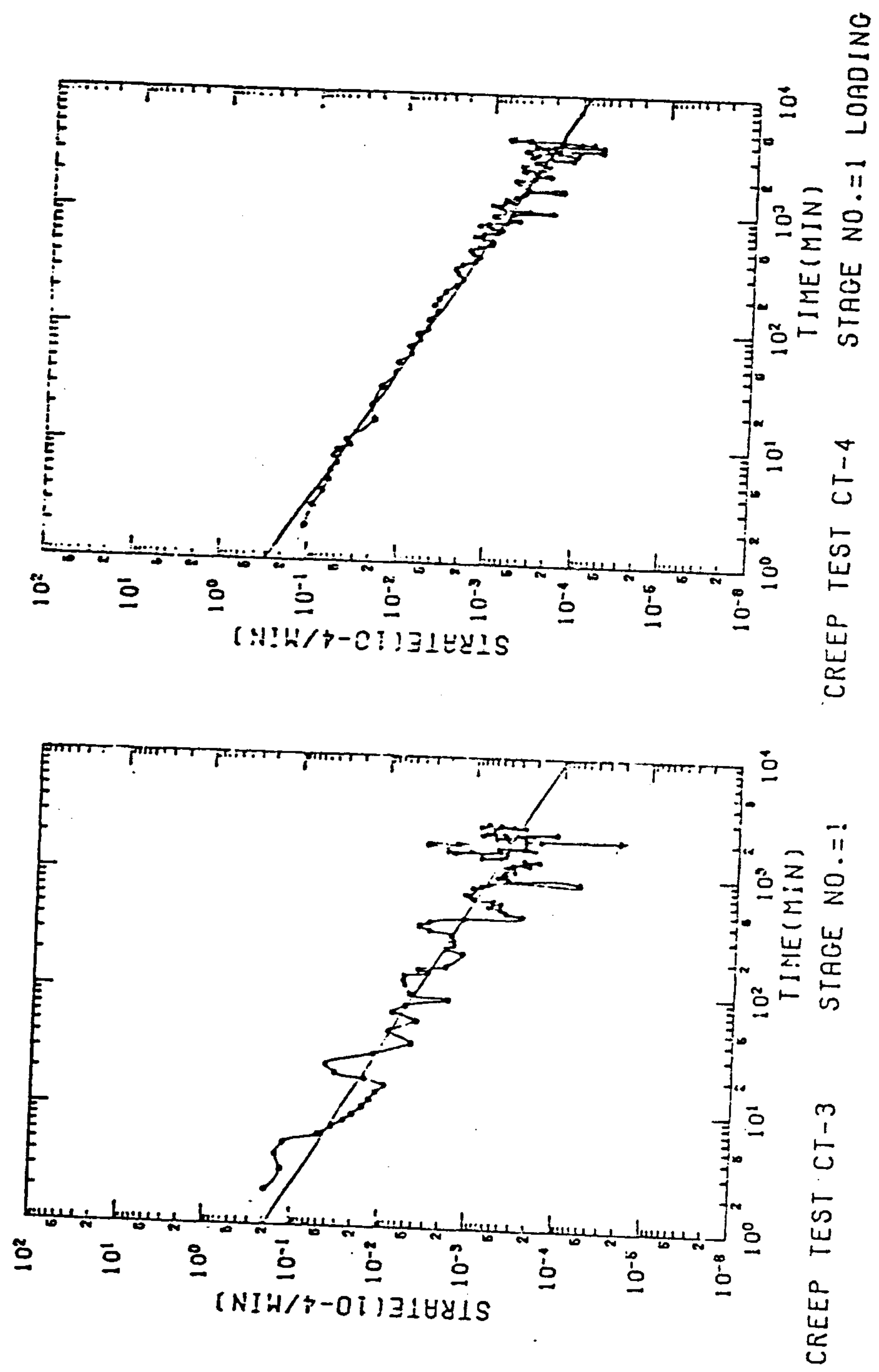

Figure 4.15 Logarithm plots of strain-rate versus time.
First loading. Tests CT3 and CT4

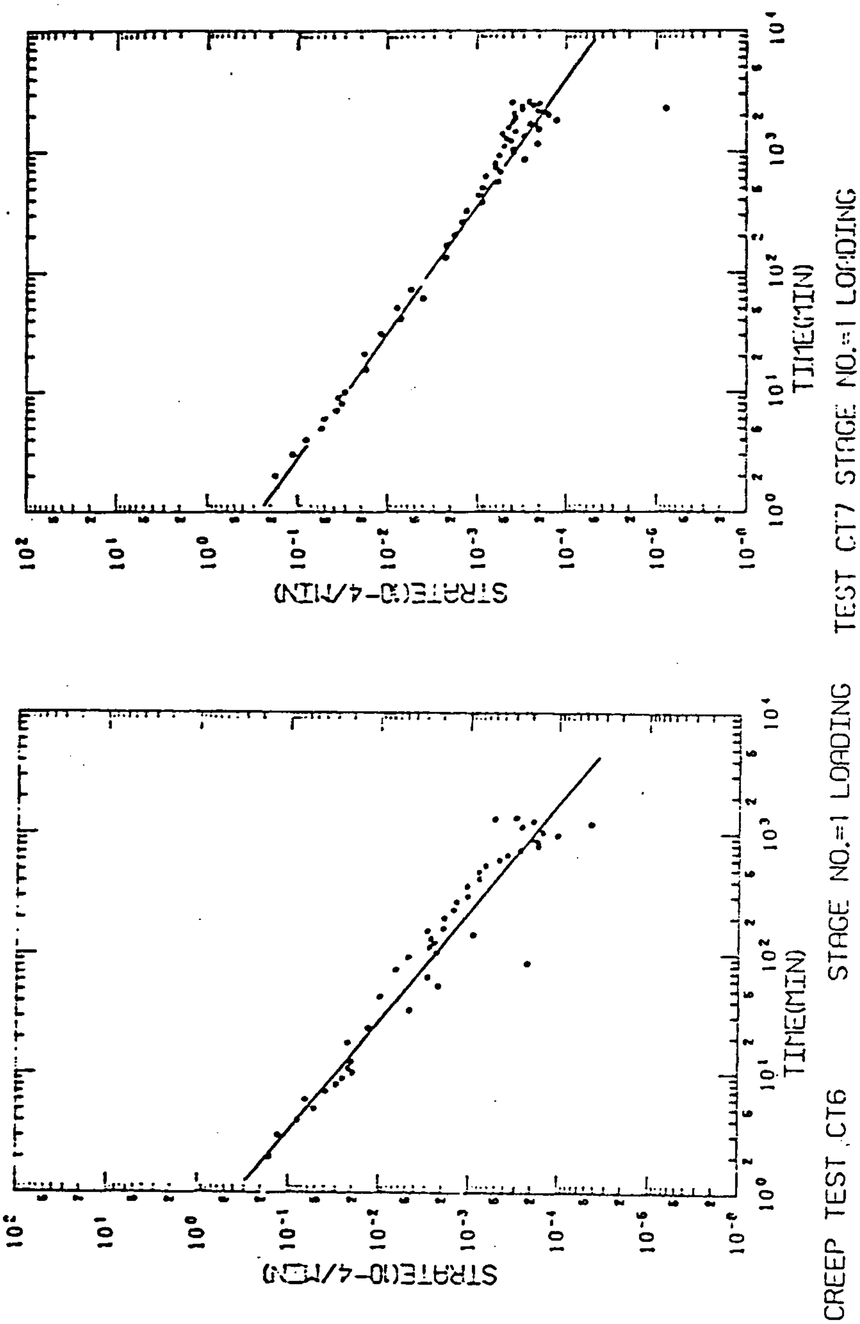

Figure 4.16 Logarithm plots of strain-rate versus time. First loading. Tests CT6 and CT7

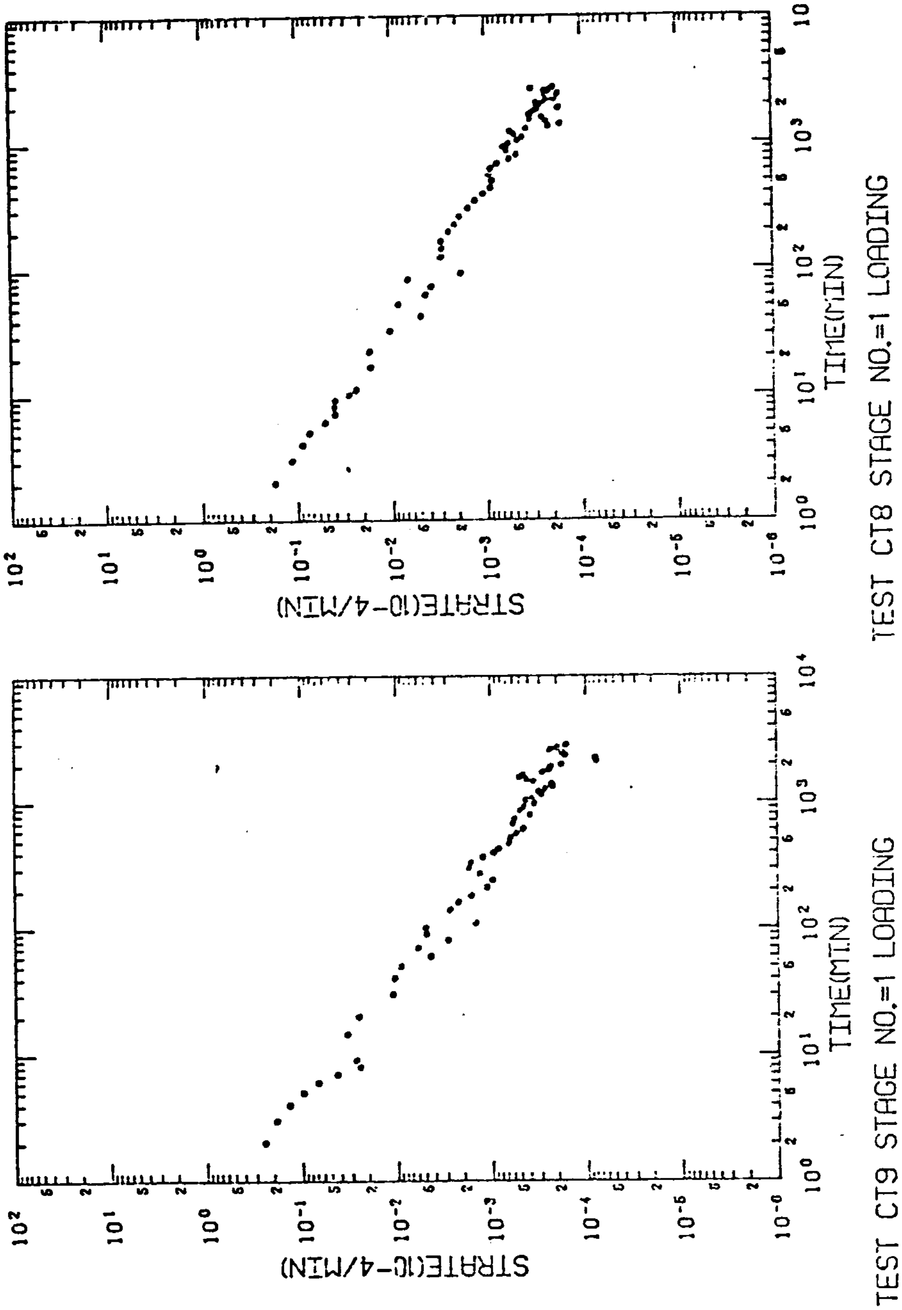

Figure 4.17 Logarithm plots of strain-rate versus time. First loading. Tests CT8 and CT9

Table 4.4 Single-stage creep tests - Summary of regression analysis

Test	Dev. Stress $(\sigma_1 - \sigma_3)$,Mpa	Stress level (*)	a (10-4/min)	m	coefficient correlation
CT1	0.70	.184	0.275	0.896	- 0.976
CT2	0.50	.11	0.240	0.856	- 0.991
CT3	1.60	.26	0.188	0.819	- 0.894
CT4	2.20	.58	0.297	0.882	- 0.971
CT6	2.18	.44	0.301	1.040	- 0.958
CT7/st1	2.88	.43 - .47	0.261	0.931	- 0.969
CT7/st2	6.00	.95	2.100	0.810	- 0.955
CT8	3.57	.63 - .67	0.268	0.919	- 0.992
CT9	4.02	.60	0.368	0.994	- 0.986

(*) calculated based on estimative displayed in Table 4.3

The two parameters, 'a' and 'm', representing the power law are constants for a certain stress level. The parameter 'a' represents the potential for creep, or strain-rate at unit time, during or under a certain stress level whereas 'm' represents a hardening-parameter describing the rate of decrease of the strain-rate with time.

The hardening-parameter 'm' varied between 0.82 and 1.07 as tabulated and there was no indication of any relationship between 'm' and the stress level as indicated in Figure 4.18. Based on these results an average value of 0.9 is recommended for the Wabamum coal. This result seems to be in agreement with other investigations which suggest that m is very much independent of the stress level, e.g.,Singh and Mitchell(1968) and Bishop and Lovenbury(1969) . The scatter in the results certainly can be associated with the differences between samples. However, it may be argued that Figure 4.18 shows a weak dependence on stress level. Table 3.2 presents a summary of m-values reported in the literature for rocks and soils which indicates a range of variations similar to the one obtained here.

Even though the experimental data are not sufficient to allow more elaborate discussion, it is important to realize the qualitative value of the reported findings. A highly fractured rock-like material can also be described by a power law which suggest that whatever mechanism has lead to creep, the overall effect can be described by a simple time law. This result complements the observation of

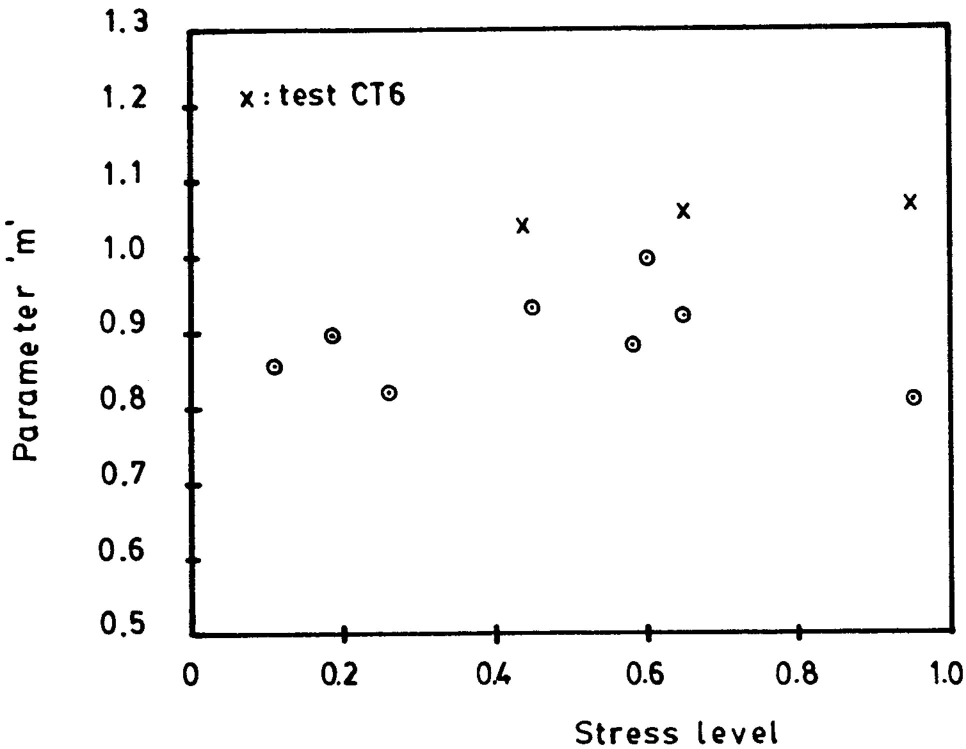

Figure 4.18 Variation of parameter m with stress level

Cottrell(1952) who discusses the validity of a power law for a wide variety of materials.

As indicated in equation (4.4), the primary creep rate has been considered as a combination of two terms, one depending only on the elapsed time, t , and another depending on the stress level, 'a' . From the previous discussions in Chapter 3, two types of stress functions have been used to describe the time-dependent deformations of geological materials, i.e, the power law (Deere and Boresi(1963); Cruden(1971)) and the exponential law (Singh and Mitchell(1968) and Wawersik(1972)) respectively represented by equations (4.5) and (4.6).

$$a = k \left(\frac{\sigma}{\sigma_o} \right)^{n} \qquad \ldots . \; (4.5)$$

$$a = A \, e^{\bar{\alpha} \bar{\sigma}} \qquad \ldots . \; (4.6)$$

where K,n and A, $\bar{\alpha}$ are material constants. The parameter $\bar{\sigma}$ in equation (4.6) represents the stress level. Singh and Mitchell(1968) have shown that equation (4.6) can actually be obtained by convenient simplifications of a more general equation based on the rate process theory.

The variation of the parameter 'a', tabulated in Table 4.4, with the stress level is displayed in Figure 4.19. This figure also includes some of the results of multiple-stage tests. The general pattern of the data suggests a trend very similar to the simplifications proposed by Mitchell, especially the fast increase of the parameter a for values of $\bar{\sigma}$ above 80%. Unfortunately, the variation for low values of $\bar{\sigma}$ could not be observed from the experimental data and the only two tests carried out at values of $\bar{\sigma}$ less than 20% have given a rather high strain-rate. These high strain-rates were probably caused by crack closure since, for these two tests, a sequence of loading and unloading was not applied. The departure from the straight line indicated in Figure 4.19 by the dotted line simply means that a progressive reduction in strain rate for values of stress level approaching zero must be expected.

The limited number of tests and the scatter present in Figure 4.19 certainly precludes a more conclusive discussion about the stress function controlling the creep behavior for the fractured coal. As a first approximation, the results seem to indicate a promising similarity with experimental data reported for soils, Singh and Mitchell(1968), and therefore, eligible for representation in terms of an exponential law. Values for A=1.0x10-5/min and '$\bar{\alpha}$'= 1.9 are recommended for the Wabamum coal.

Combining both equations (4.5) and (4.6) one obtains

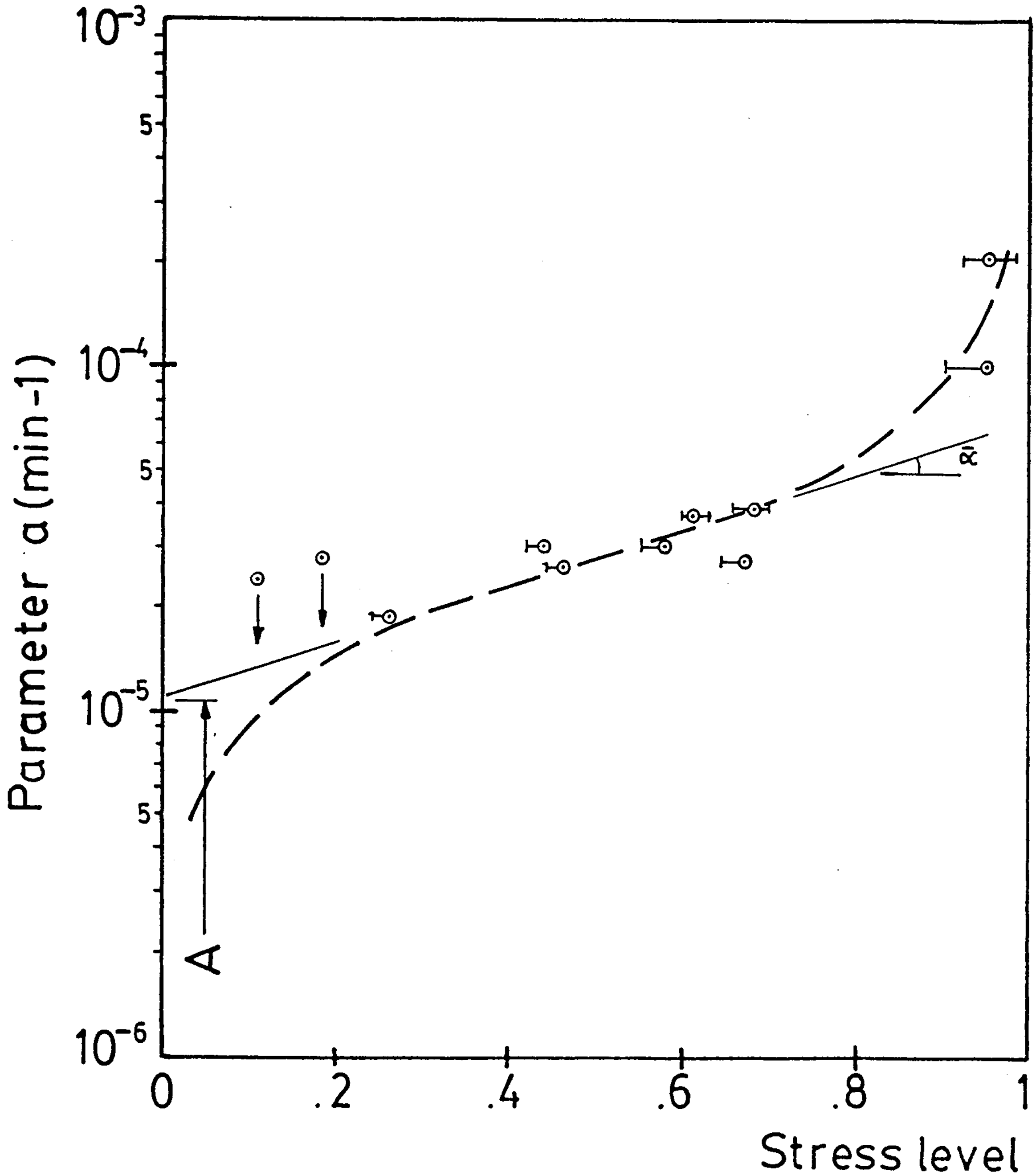

Figure 4.19 Variation of parameter a with stress level

equation (4.7) which, from the previous discussions, represents a good approximation for the creep data reported here.

$$\mathring{\varepsilon} = A\, e^{\bar{\alpha}\bar{\sigma}}\, t^{-m} \qquad \text{.... (4.7)}$$

The use of empirical equations such as (4.7) to describe the creep behavior of a natural material represents a great simplification of a highly complex process and no attempt was made to link the material parameters, 'A', '$\bar{\alpha}$', and 'm' with physical properties. Any further discussions about the validity of such an equation to describe creep behavior must be put in an engineering perspective. Such an equation fullfils the basic requirements of engineering applications, i.e, describes the behavior of the materials for a large range of stress level, 20% to 80%, using a small number of parameters determined from a reduced number of experiments.

4.4.3 Multiple-stage creep tests

This section describes the results and interpretation of five multiple-stage creep tests under different confining pressures, carried out on the jointed coal for a total of 38 creep stages. The testing procedures followed have been described in section 4.3.3. The aim of these tests has been to provide general information concerning the response of the material when subjected to a change in stress after the sample had been creeping for a certain period of time under a lower stress level.

This question is a necessary consideration in order to establish creep relationships which are able to predict the creep behavior under a general stress history. The tests discussed next constitute only a first step towards this goal.

4.4.3.1 Typical results and discussions

Indicated in Figure 3.14 is an idealized representation of a multiple-stage creep test. The sample is loaded up to an arbitrary stress level and allowed to creep for a certain period of time. Then the stress level is increased and again the sample is allowed to creep under the new deviatoric stress. Figure 4.10 indicates the stress history followed by these tests.

For each creep stage the axial deformations were recorded and reduced in a manner similar to that reported in section 4.4.1., i.e., the strain rate was estimated and logarithmic plots of strain-rate versus elapsed time after the stress level was incremented were prepared. Figure 4.20 displays a typical result, test CT4, showing the variation of strain-rate with time after the stress level was

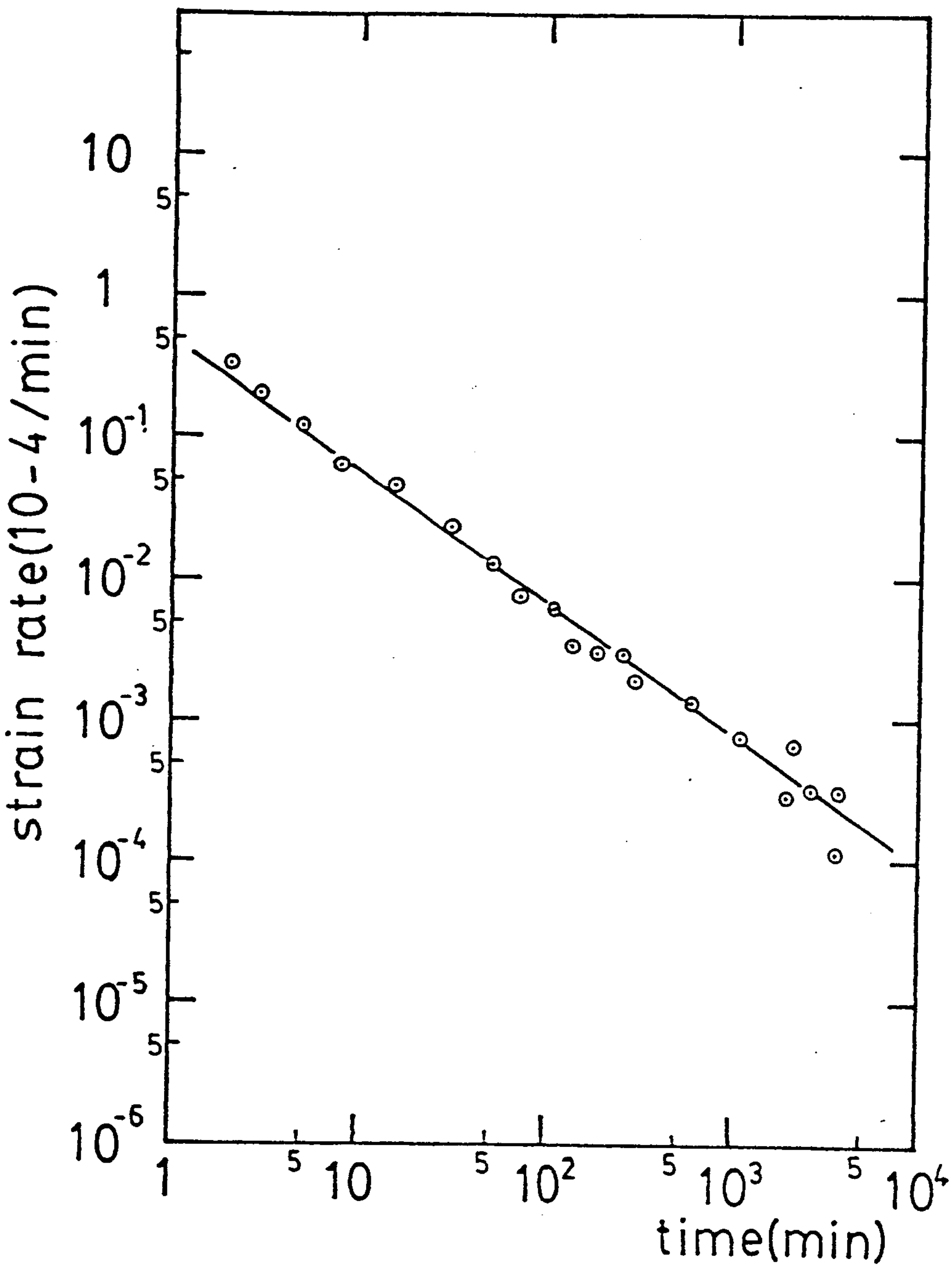

Figure 4.20 Strain-rate vs time after stress increment - Test CT4 - Stage no. 2

increased from 58% to 79% of the maximum deviatoric stress. The sample had been creeping for 4 days before the stress level was raised.

For most of the stages a great similarity was observed between the results of the variation of strain rate with time and the equivalent results for the single-stage creep tests reported in section 4.4.2. The strain-rate showed a continuous decrease with time and also the pattern of this decrease seemed to suggest the same power law relationship obtained for single-stage creep tests. These findings are in full agreement with previously reported results of multiple-stage creep tests on rocks (Marble and sandstone; Cruden(1971b)) and soils (Semple et al.(1973)).

For the interpretation of the results of a multiple-stage creep test, i.e., to relate the results of the several stages with each other, some additional hypotheses are necessary. These hypotheses basically consist in defining the influence of the previous stress level, stress increment and elapsed time before the stress level was raised.

Initially the experimental data were analyzed assuming that, for each creep stage, equation (4.4) would be a reasonable approximation for the data. A regression analysis was performed in order to obtain the parameters a and m describing that equation. The results for all the creep stages are summarized in Table 4.5 which also shows the coefficient of correlation for the regression. For most of the creep stages the tabulated results indicate that equation (4.4) provides a good approximation for the data, e.g., tests CT1, CT4, CT6.

However, some of the creep stages, especially for test CT2 equation (4.4) provided a poor representation of the variation of the strain-rate versus time. This occurred consistently every time the stress increment was very small which suggests that the new stress level did not erase or overcome the effects of the previous increment.

Another interesting feature about the results of this interpretation was that the value of the parameter 'm' lay within the same range obtained for the single-stage creep tests, see Table 4.5.

4.4.3.2 Stress-strain-time relationship

The previous discussion lead to the conclusion that the power law given by equation (4.4) provided a good approximation for most of the creep stages. However, this does not answer the question about the relationship between stages , i.e., how one stage can be predicted from the previous ones, if this is possible.

Several theories have been developed to take into account the influence of the stress history upon the creep behavior of a material. From the study of creep in metals, theories such as time-hardening and strain-hardening have been suggested. Penny and Marriott(1971) provide a good outline of these theories.

Table 4.5 Summary of multiple-stage creep tests

Test	Dev. Stress $(\sigma_1 - \sigma_3)$,Kpa	Stress level	a (10-4/min)	m	coefficient correlation
CT1					
cs1	700	.184	0.275	0.896	- 0.976
cs2	1000	.263	0.058	0.714	- 0.844
cs3	1300	.342	0.152	0.939	- 0.923
cs4	1500	.394	0.071	0.816	- 0.896
cs5	2000	.526	0.526	0.960	- 0.953
cs6	2500	.658	0.192	0.953	- 0.927
cs7	2900	.763	0.097	0..745	- 0.949
cs8	3300	.868	0.370	0.965	- 0.967
CT2					
cs1	500	.107	0.240	0.856	- 0.991
cs2	630	.135	0.058	0.746	- 0.898
cs3	900	.194	0.114	0.810	- 0.942
cs4	1100	.237	0.082	0.812	- 0.951
cs5	1350	.291	0.114	0.843	- 0.954
cs6	1600	.345	0.065	0.763	- 0.912
cs7	1800	.387	0.055	0.703	- 0.928
cs8	2300	********** data not recorded ********			
cs9	2350	.506	0.030	0.947	- 0.512
cs10	2650	.571	0.045	0.719	- 0.916
cs11	2850	.614	0.043	0.680	- 0.970
cs12	3000	.646	0.020	0.609	- 0.942
cs13	3200	.689	0.033	0.653	- 0.916
cs14	3270	.704	0.016	0.600	- 0.890
cs15	3240	.698	0.018	0.626	- 0.880
cs16	3550	.765	0.030	0.642	- 0.874
cs17	3700	.797	0.038	0.684	- 0.962
cs18	4000	.862	0.090	0.744	- 0.946
cs19	4350	.937	0.107	0.740	- 0.990
cs20	4500	.970	0.133	0.625	- 0.993
cs21	4640	** increment caused immediate failure ******			
CT3					
cs1	1600	0.264	0.188	0.819	- 0.894
cs2	2900	0.479	0.176	0.866	- 0.880
cs3	3950	0.652	0.169	0.843	- 0.957
cs4	4650	0.768	0.140	0.877	- 0.784
cs5	5100	0.842	0.229	0.812	- 0.966
CT4					
cs1	2200	0.578	0.297	0.882	- 0.971
cs2	3000	0.790	0.474	0.924	- 0.994
CT6					
cs1	2200	0.444	0.301	1.040	- 0.958
cs2	3250	0.656	0.381	1.060	- 0.959
cs3	4700	0.950	1.010	1.070	- 0.958

Alternatively, the incremental form of a rheological model, generally applying the principle of superposition, has been used for rocks, e.g., Hardy(1967). More elaborate procedures are described by Cruden(1971b) who applied three formal theories and one structural theory of creep to describe the results of incremental creep tests on Marble and sandstone.

Equation (4.8) and (4.9) represents the time-hardening and strain-hardening theories associated with the power law described by equation (4.4). Figure 3.17 illustrates how these theories consider the effect of the stress history assuming the behavior under a single-stage test. For time-hardening theory the behavior after the stress level is increased, can be represented by curve CD whereas the strain-hardening theory states that curve BD is a better approximation for the creep behavior for the second creep stage.

$$\mathring{\varepsilon} = A\, e^{\bar{\alpha}\bar{\sigma}_2}\, t^{-m} \qquad \ldots.\ (4.8)$$

$$\mathring{\varepsilon} = (1-m)\left[\frac{A e^{\bar{\alpha}\bar{\sigma}}}{1-m}\right]^{\frac{1}{1-m}} \varepsilon^{-\frac{m}{1-m}} \qquad \ldots.\ (4.9)$$

The strain-hardening theory expresses the current strain-rate as a function of the current strain, i.e., after increasing the stress to another level, the strain-rate follows the original curve but is corrected for the accumulated creep strain which occurred during the previous stage. As discussed previously in this Chapter, the values of creep strains are not as reliable as the strain-rate due to the difficulties in establishing the instantaneous strain. The use of the strain-hardening theory to adjust the experimental results would be subjected to a certain discrepancy once the key parameter, the accumulated creep strain could not be defined accurately. Therefore, the use of this theory was disregarded while analyzing the results of the step-creep tests reported herein.

Both time-hardening and strain-hardening theories were discarded when analyzing the results of the multiple-stage creep tests. Both theories predict a strain-rate versus time behavior which is strongly non-linear on a logarithm plot and therefore incompatible with the observed linear results.

In order to study the possible relations between creep stages, an incremental form of equation (4.7) associated with the superposition principle was adopted. Figure 4.21 displays the concepts involved in translating the creep strain curve after the stress increment in terms of the creep strain curve corresponding to the previous stress level('memory function') and the stress increment. Equation (4.10) describes the creep strain rate at any time, t, after the increase in stress.

$$\dot{\varepsilon} = A e^{\bar{\alpha}\bar{\sigma}_1} t^{-m} + A e^{\bar{\alpha}\Delta\bar{\sigma}} (t-t_o)^{-m} \qquad \ldots . \ (4.10)$$

To analyze the data for a particular multiple-stage creep test the following procedure was adopted. Initially, the results of the first creep stage are analyzed following the methodology in section 4.2.2 and equation (4.9) is fitted to the data. At the end of this step, the parameter m is known as well as the term $A e^{\bar{\alpha}\bar{\sigma}_1}$ for the particular value of σ_1.

Next, the results of the subsequent increment are reduced and the strain-rate versus time plot is obtained. Equation (4.10) can be used at a particular value of ($t - t_o$) and a second equation is obtained which allows for the determination of a set of parameters 'A' and '$\bar{\alpha}$'. Equation (4.10) can be extended to include more increments and therefore all the other other stages can be predicted. During this process the parameters A, m and $\bar{\alpha}$ are assumed constant for any increment. This hypothesis will be discussed later in this section.

Table 4.6 summarizes the creep parameters obtained by using this method of analysis. Figures 4.22 and 4.23 show typical predictions of the experimental data using equation (4.10) and the tabulated parameters. These results seem to indicate that such an approach predicted the experimental data rather well. In Appendix C, the results of the predictions of the experimental tests by using this approach are indicated in Figures C1 through C11. In particular for the test CT3 and CT1 the predictions are acceptable for stress levels up to 80% of the maximum deviatoric stress.

However, two points must be considered before any further discussions. First, the parameters tabulated in Table 4.6 must be compared with the ones obtained in section 4.4.2 for single stage tests and second, the particular stress-history followed by the multiple-stage tests must be considered.

As indicated in Table 4.6, the estimated parameters, 'A' and ' $\bar{\alpha}$ ', for tests CT1 and CT2 showed a large departure from the predicted ones using single-stage tests. This departure reflects the fact that for stress levels below 20%, equation (4.7) does not provide a good approximation for creep behavior if the parameters are maintained.

The behavior at low stress levels can be represented by a power law but with a different set of parameters. This fact indicates that in order to obtain creep parameters from multiple-stage creep tests, the increments of stress level as well as the initial stress level (first creep stage) have to be greater than 20%. Test CT3 indicates this observation.

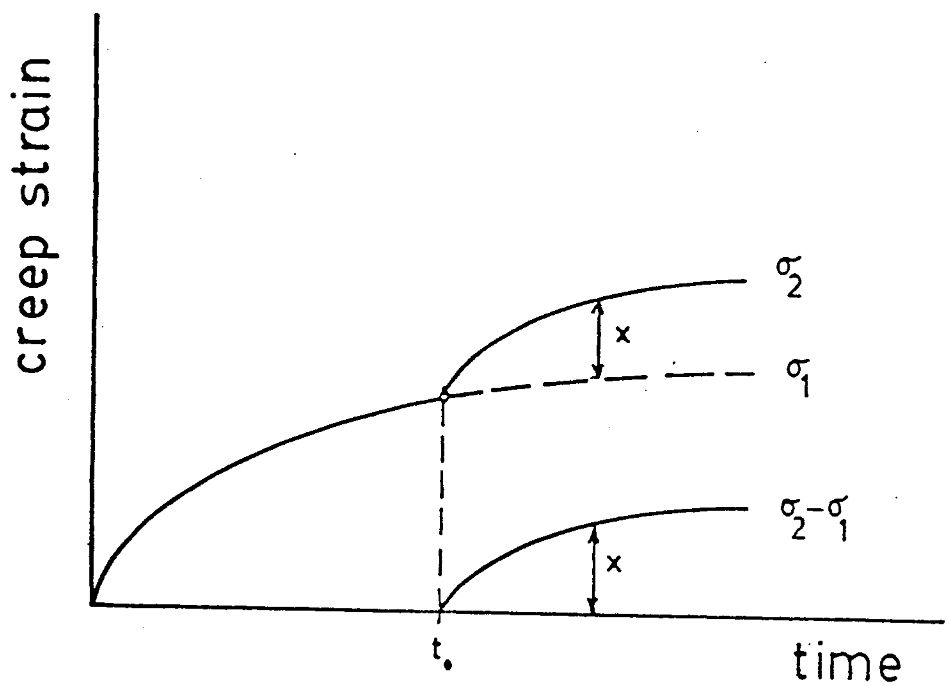

Figure 4.21 Schematic representation of superposition principle for incremental creep tests

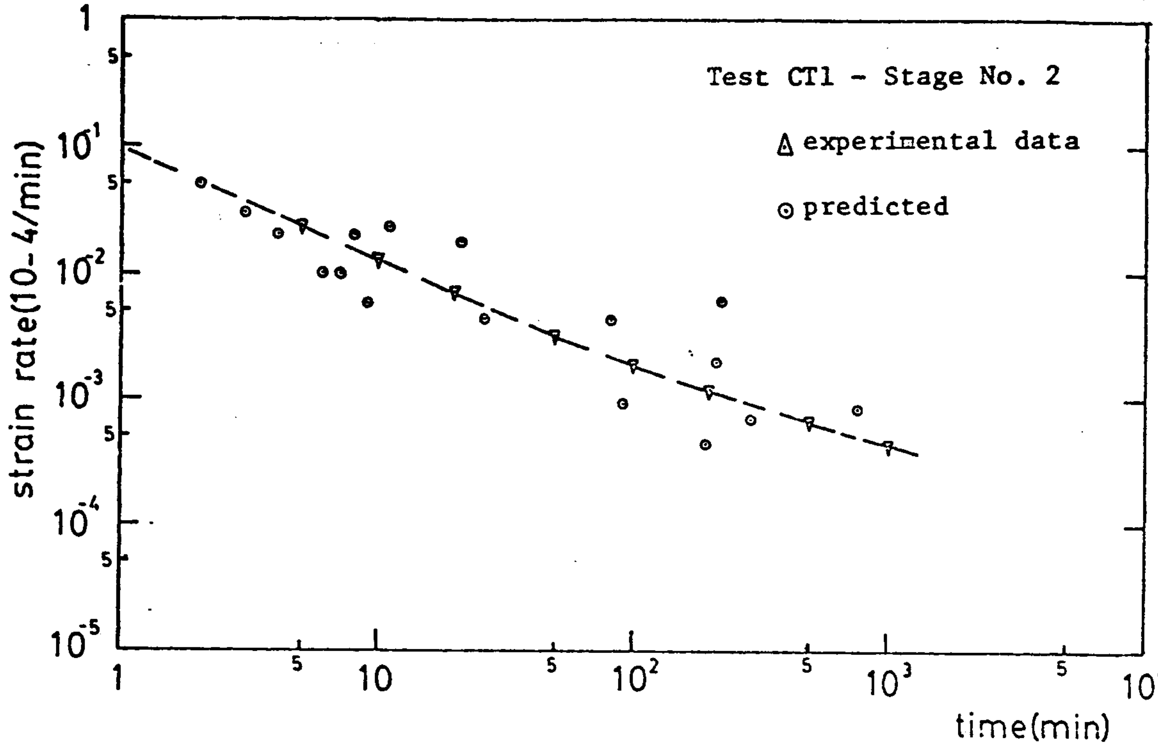

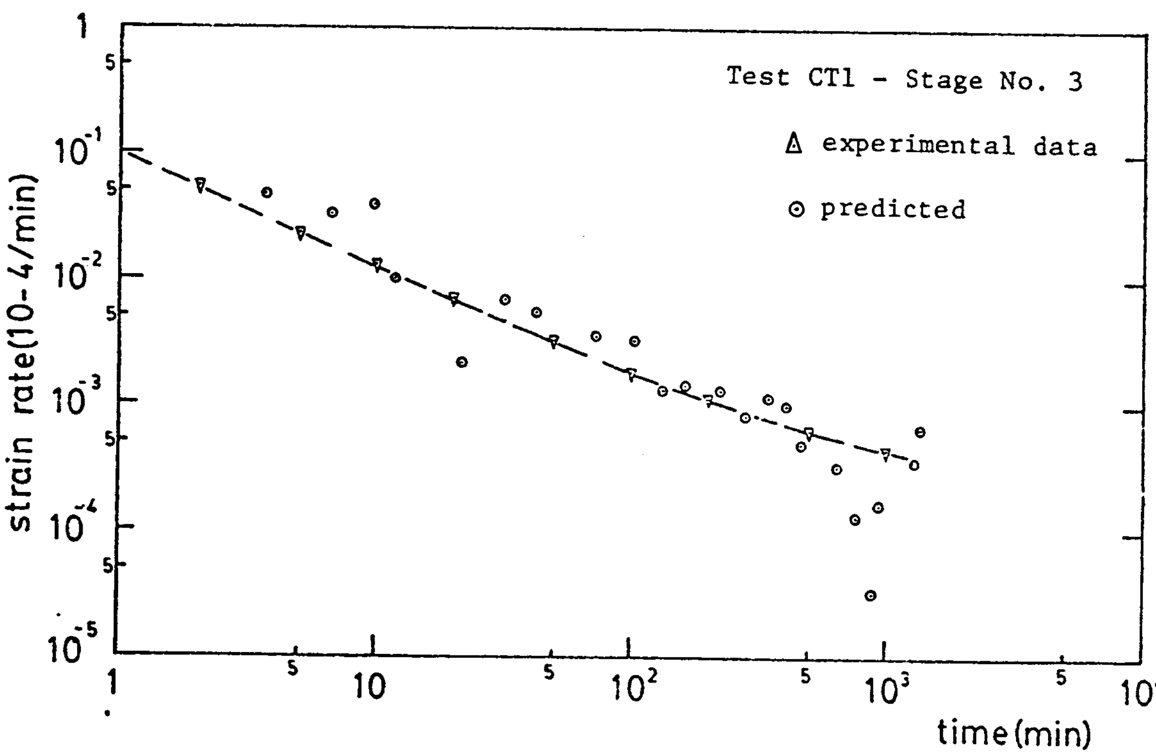

Figure 4.22 Typical prediction of incremental creep test - Test CT1

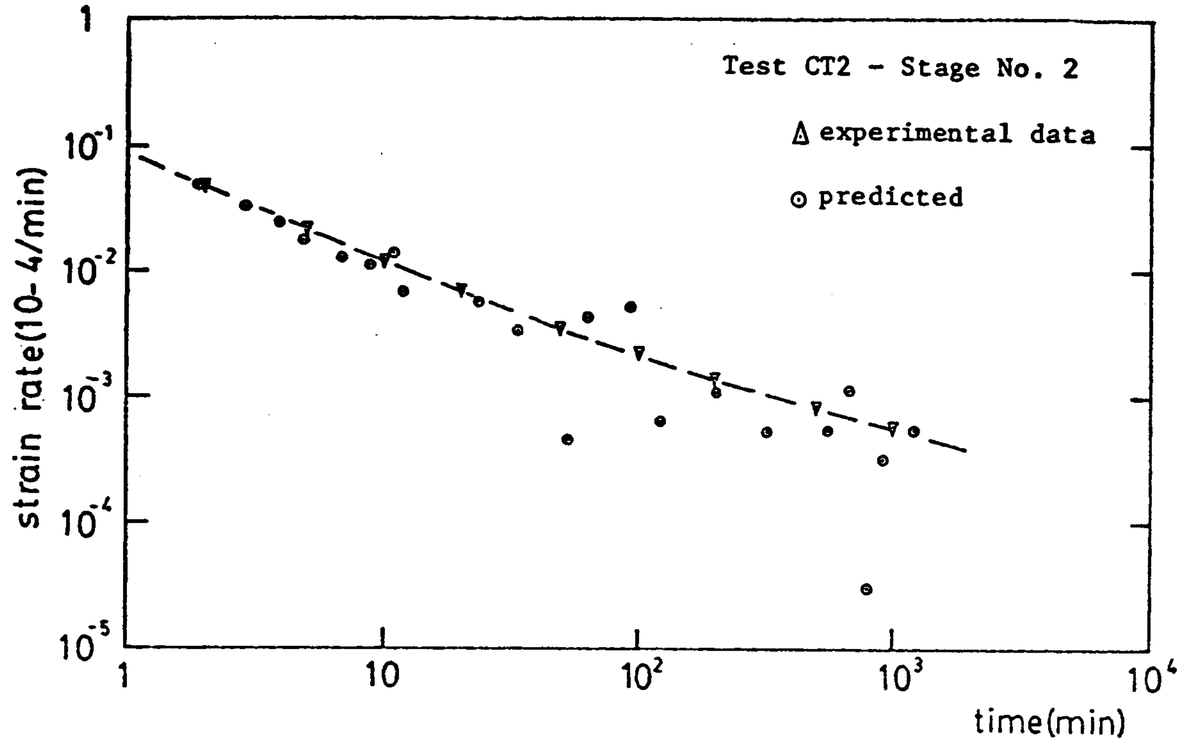

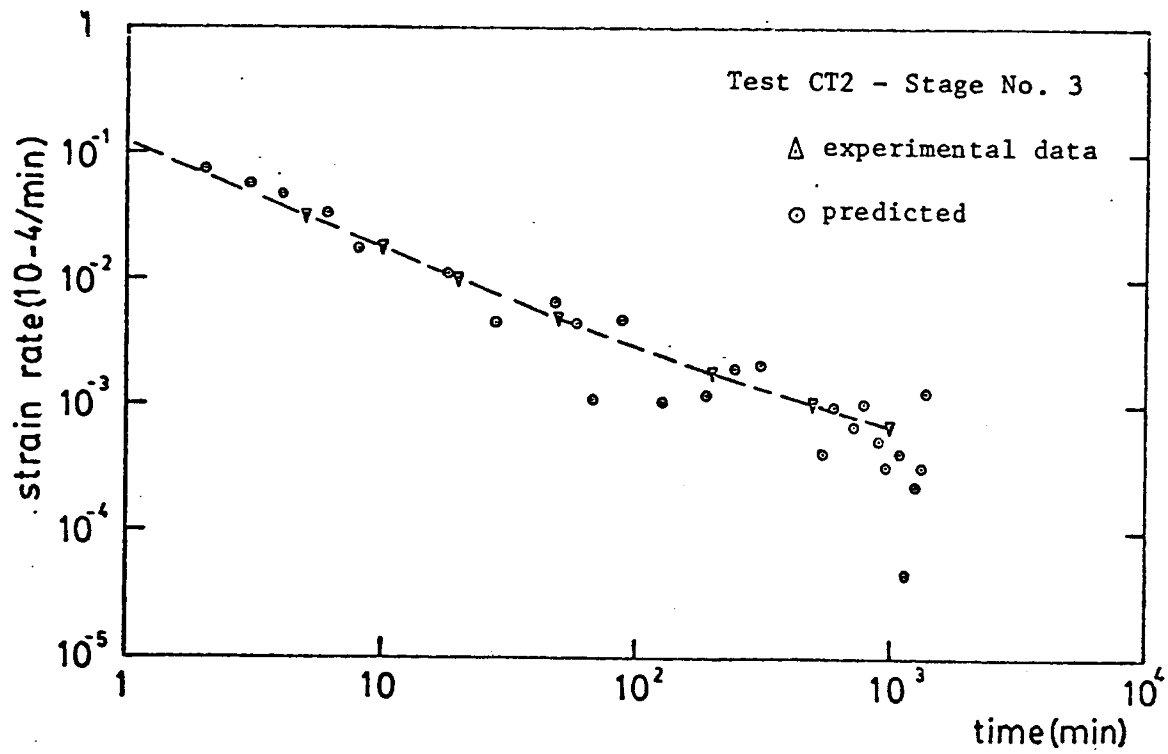

Figure 4.23 Typical prediction of incremental creep test - Test CT2

Table 4.6 Summary of creep parameters obtained from multiple-stage creep tests

Test	m	A (10-6/min)	alpha
CT1	0.90	4.036	10.51
CT2	0.85	5.531	13.44
CT3	0.82	16.430	0.52

(*) tests CT4 and CT6 were analyzed as single-stage creep tests

This finding represents a reduction on the efforts to establish creep parameters by carrying out several single-stage creep tests on different samples.

In general, one should expect that the creep behavior of a material is greatly influenced by the stress history. For the tests discussed here, a very particular stress history was followed. For each creep stage enough time was allowed for the strain-rate to decrease by a factor of more than 1000, which implies a comparatively slow process by the end of the stage. This means that after a new load increment, the contribution from the previous increment to the new rate will not be felt at the early stages of the test.

In order to extend the validity of equation (4.10) to describe incremental creep tests, more experiments have to be carried out following other stress histories such as, for instance, decreasing the time allowed for creep under a particular load.

4.4.3.3 Time-dependent failure process

As is well known, rock specimens subjected to a constant and high stress level will eventually fail after a certain period of time. The failure process under creep conditions is characterized by an increase in the strain-rate and this stage is known as tertiary creep.

Very few quantitative results on failure of rocks under creep have been reported. Work by Wawersik(1973) and Kranz and Scholz(1977) seem to suggest a criterion to mark the onset of the failure process but no attempt was made to describe the process afterwards.

In order to investigate the time-dependent failure for coal, all the test reported here were carried out to failure by adding stress increments. Unfortunately, in only one of the experiments, test CT2, could the failure process be observed within a reasonable length of time, i.e., about 400 min. For all the other tests, the samples failed abruptly after the load increment was applied.

Two important features could be observed during the analysis of these tests. For all the tests which failed abruptly, the strain-rate was still decreasing with time at the moment of the load application. For the particular test during which failure could be observed, the zone of transition between the regions of decreasing and accelerating strain-rate was very narrow, Figure 4.24.

It is of particular interest to compare these results which reported failure processes for soils. Test results on both overconsolidated and normally consolidated clays have indicated that the transition zone between decreasing and increasing strain-rate presented the same feature, e.g., Singh and Mitchell(1968) and Bishop and Lovenbury(1969). Even though there is a scale effect on logarithm plots of strain-rate versus time on this interpretation, these results seem to support the concept of equation (4.7) being applicable up to the onset of failure. However, more

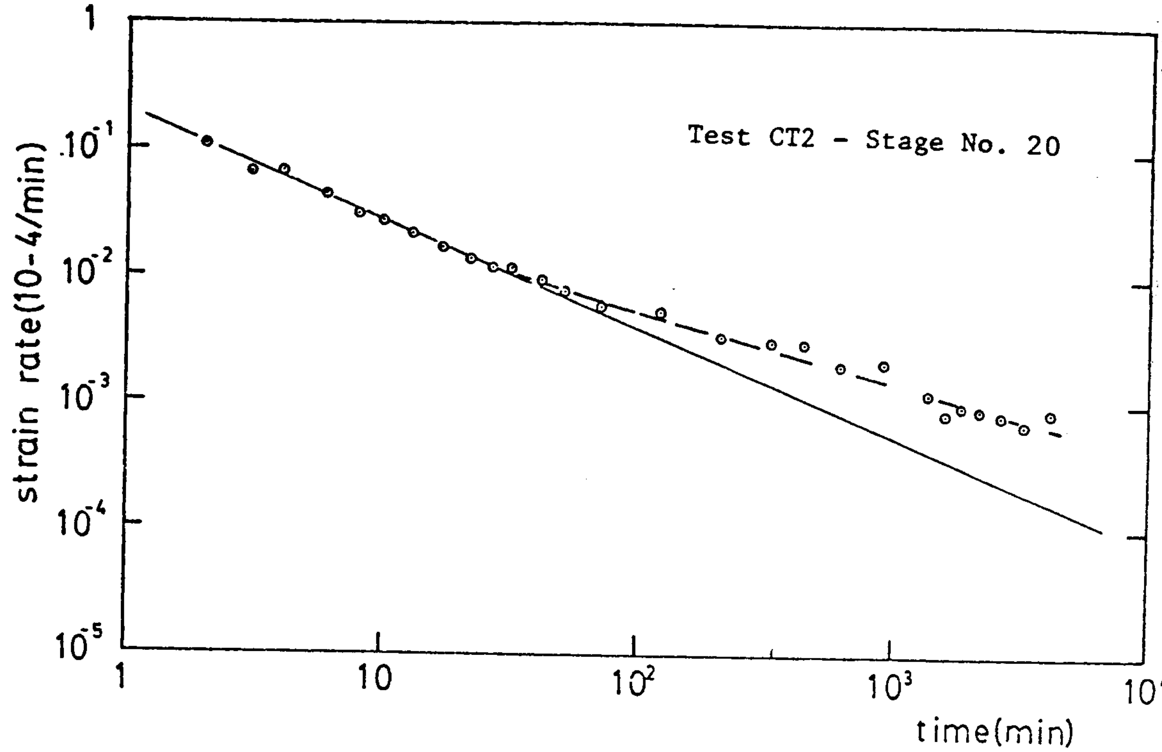

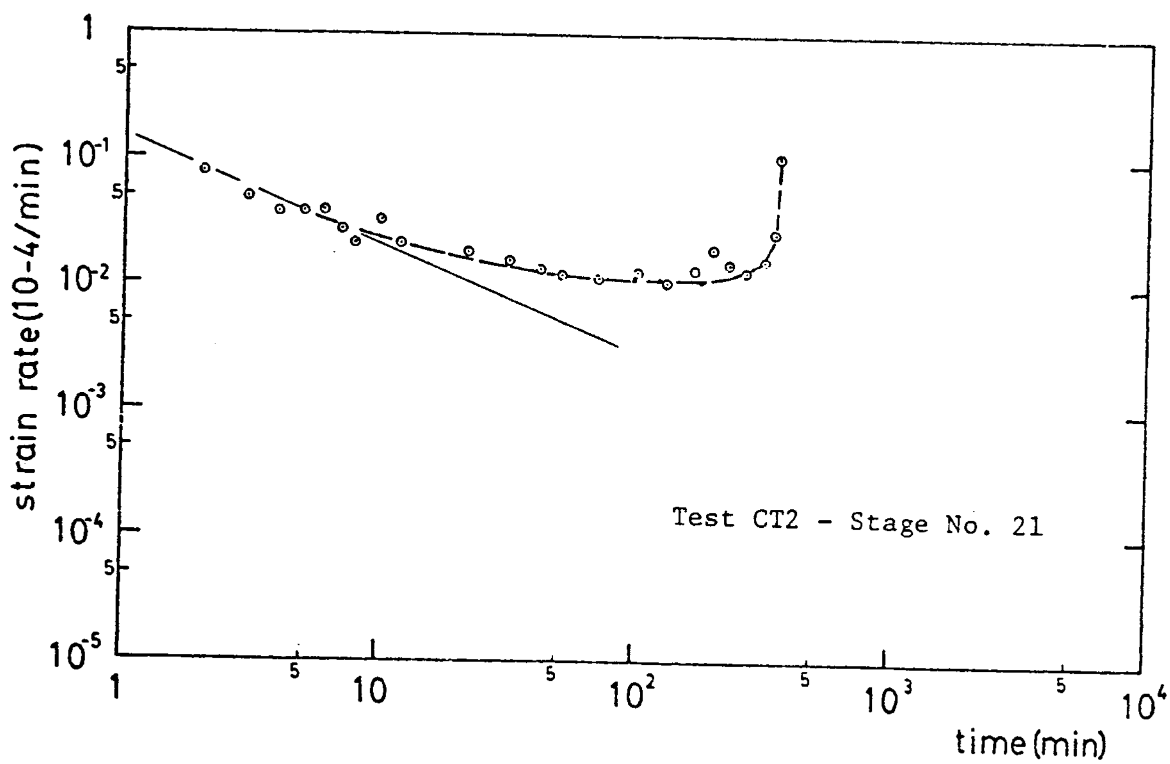

Figure 4.24 Strain rate vs time curve illustrating failure during creep - Test CT2

experimental results are needed before a more substantial body of conclusions can be drawn with respect to the quantitative representation of the time-dependent failure process in rocks.

4.5 Final remarks and recommendations

The previous sections described a limited experimental program on the creep behavior of a jointed coal. The analysis of the data have suggested a very close qualitative similarity between the creep behavior of this coal and other materials. Quantitatively, it seems that an empirical relationship as equation (4.7) describes the creep behavior of the jointed material.

This relationship was shown to be valid for a region of stress level between 20% and 80% of the maximum compressive strength and it also has the advantage of being described by only three parameters easily determined in an experimental program. For stress levels below 20% and above 80%, the behavior of the material cannot be described by the same set of parameters.This suggests, at least, three different modes of behavior which need to be distinguished more clearly.

Time-dependent strains were observed under different stress histories and the results were reasonably approximated by an incremental form of equation (4.7) and the superposition principle. A method for determining creep parameters from multiple-stage creep tests was presented and it is suggested that the results can only be compared with single-stage creep tests if the increments are within the range of stress from 20% to 80% of the short-term strength. Further investigations are necessary to evaluate this question mainly with respect to the influence of the stress history.

Chapter 5

REVIEW OF ANALYTICAL STUDIES ON THE TIME-DEPENDENT BEHAVIOR OF UNDERGROUND OPENINGS

5.1 Introduction

This Chapter presents a survey of the currently available solutions for the time-dependent behavior of underground openings. This survey concentrates on both reviewing and summarizing the main body of assumptions introduced in order to solve this class of boundary-value problems.

In section 5.2, the modelling of the time-dependent behavior of an underground opening is discussed. Three stages in the modelling process are considered, each with its own set of necessary simplifying assumptions. They are: statical system, load quantities and material modelling. In section 5.3, some of the relevant theoretical studies on the time-dependent response of openings are reviewed. Published results of comparisons between measured and predicted performance are described. Finally, in section 5.4, a summary of the discussions is presented and relevant conclusions for further research are indicated.

5.2 Modelling of time-dependent behavior of openings

As indicated previously in Chapter 2, two basic causes lead to time-dependent behavior of an opening, namely time-dependent change in boundary conditions and time-dependent response of the rock mass. Among the mechanisms leading to time-dependent response of the rock mass one can distinguish between rheological properties (e.g, creep and relaxation) and hydrodynamic properties (e.g, consolidation and swelling). Obviously, these mechanisms are governed by different equations and are physically distinct. In this Chapter, only the situations dealing with the rheological properties of the rock mass will be considered, unless noted otherwise.

Ideally, in the modelling of the rock mass behavior, all the factors which are known to influence time-dependent behavior should be taken into account. However, this would generally not be practical nor feasible. Substantial simplifying assumptions must usually be made in order to solve the boundary-value problem. To organize the concepts involved in this question, it is important to break down the modelling process into three stages, namely: statical system, load quantities and material modelling. In the following, the main assumptions related to each one of these stages are discussed.

5.2.1 Statical system and load quantities

In principle, the excavation process (i.e., rate and sequence of excavation) as well as the initial state of stress within the rock mass have to be simulated to correspond as closely as possible to reality. The simulation of both the statical system and the load quantities for the analytical modelling of the time-dependent behavior of openings follows from the same considerations as the case of time-independent solutions.

The simulation of excavation through a stressed medium is illustrated in Figure 5.1 and it consists of unloading the medium along the excavated perimeter. Chang and Nair(1973) discussed the techniques to simulate an excavation sequence, or unloading process, when the medium is modelled by finite elements. External boundaries should be chosen so as to include the zone within which stress changes would occur due to excavation and Kulhawy(1974) suggested the use of 7 to 10 times the diameter of the excavation. Aiyer(1969) suggested the same distance for studies of stress redistribution around openings in creeping ground.

Openings are usually considered as 2-dimensional, which cannot model the typically 3-dimensional effects that occur adjacent to an excavation face or near portals.

The in-situ state of stress before the excavation represents the most important type of loading to be considered. However, the determination of the state of stress in rock masses is not simple. The most common procedure is to consider σ_v , the vertical stress, as the

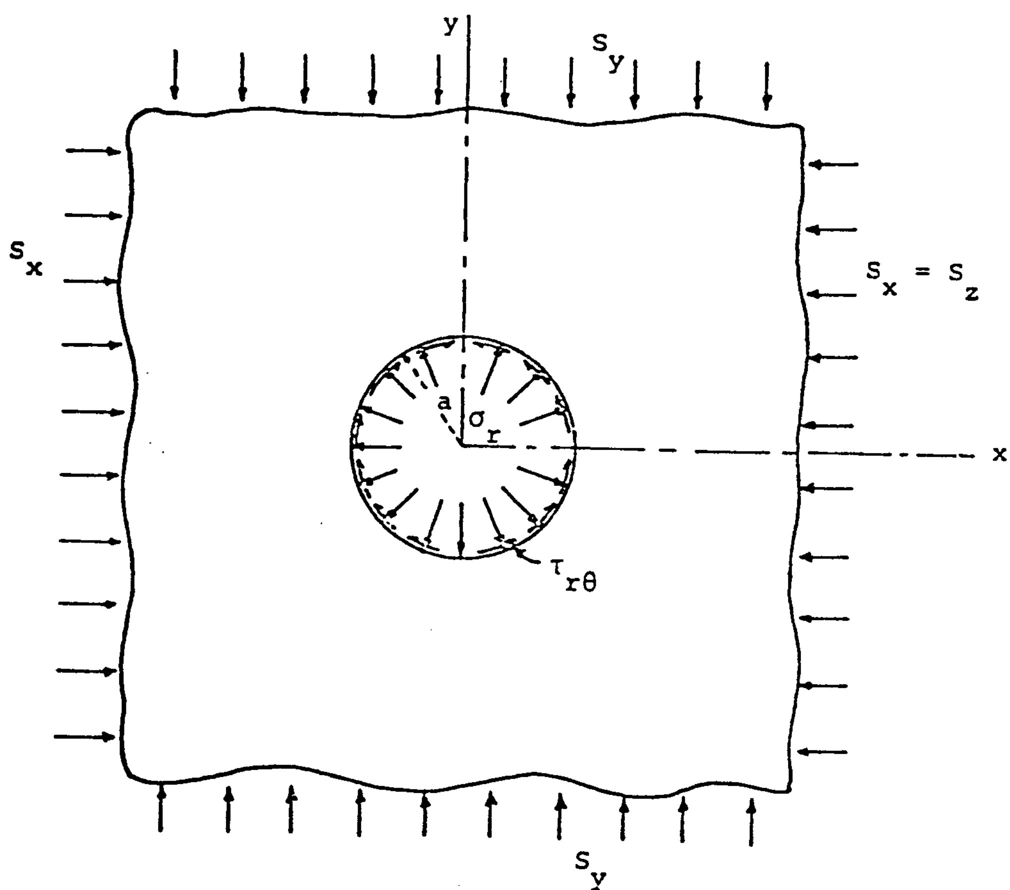

Figure 5.1 Unloading of stressed medium to simulate excavation

overburden pressure, $\gamma \cdot h$, and σ_h , the horizontal stress, as being some fraction of σ_v . However, exceptions to this are expected to occur due to rock structure and topography.

5.2.2 Material modelling

Ideally, a model for a rock mass should take into account all the discontinuities and planes of weakness. In addition, such a model should provide the means to consider the influence of stress system and stress history as well as strain history on the response of a rock mass. Evidently, such a model is far from being developed and its apparent complexity would preclude its application. In order to make the problem soluble, simplifying assumptions relative to particular aspects of the rock mass are necessary. The role of these assumptions has to be understood otherwise there is the risk of overestimating the practical use of the analytical solutions.

A complete review of the models used to generate time-dependent deformations in rocks was presented in Chapter 3. Those results basically described the behavior of rocks under very particular state of stresses (such as uniaxial). However, the solution of a boundary-value problem requires that more general stress-strain-time relationships be used. In the following, the generalizations leading to the formulation of a 3-dimensional relationship of models to describe the time-dependent behavior of rock masses are discussed.

In general, deformations or strains associated with a change in stress are separated into two components. For simplicity, let us consider first the situation where this stress change occurs in a small time interval and the stresses remain constant afterwards. Thus, after a certain period of time, Δt, the change of total strains can be written as in equation (5.1).

$$\{\Delta\varepsilon\}_t = \{\Delta\varepsilon\}_i + \{\Delta\bar{\varepsilon}\} \qquad \ldots . (5.1)$$

where,

$\{\Delta\varepsilon\}_t$ = change in total strain

$\{\Delta\varepsilon\}_i$ = change in instantaneous strain

$\{\Delta\bar{\varepsilon}\}$ = time-dependent strain

5.2.2.1 Instantaneous strain component

For the solution of a boundary-value problem, constitutive relationships have to be provided to solve for the 'instantaneous' component of strains. A number of models have been described in the literature to simulate this rock mass response and its discussion is outside the scope of this thesis. These models include: elastic, elasto-plastic (strain-hardening and strain-softening). Daemen(1975) presented a good review of these models and applications.

5.2.2.2 Time-dependent strain components

The time-dependent deformations are normally considered as the sum of two components : volumetric and deviatoric, see equation (5.2).

$$\{\Delta\bar{\varepsilon}\} = \{\Delta\bar{\varepsilon}\}_v + \{\Delta\bar{\varepsilon}\}_d \qquad \ldots\ldots (5.2)$$

One assumption has been to consider $\{\Delta\bar{\varepsilon}\}_v$ as being zero. This assumption is borrowed from the theory of classical plasticity because the creep strains are considered to be essentially plastic.

The validity of this assumption for rocks has not yet been fully established. Wawersik(1974) presented the results of creep tests on sandstone under triaxial compression in which volumetric creep was measured. Wawersik's results showed a considerable change in volume with time during creep. These results indicate that the volumetric component of the creep strain tensor may not be zero for certain cases. Assuming a zero volumetric change it is implied also that changes in the hydrostatic component of the stress tensor are irrelevant and do not produce time-dependent deformations. It is possible however that certain rocks such as weathered and soft rocks show a time-dependent response for a change in the hydrostatic stress component.

For brittle, fissured rock masses, volumetric creep can occur during crack closure and also due to compression of bedding surfaces and closure of joints. Kaiser(1979) considered the volumetric creep of coal as being represented by a 3-parameter solid with a long retardation time. However, no experimental data have been produced to indicate the validity of this law. This question certainly deserves more investigation, especially the relative order of magnitude of volumetric and deviatoric creep strain.

The deviatoric creep component, $\{\Delta\bar{\varepsilon}\}_d$, has been described by a large variety of models most of which have been reviewed in Chapter 3. Next, the generalization to a multiaxial state of stress of some of the models previously considered will be described.

- <u>linear viscoelasticity</u>

This theory has been used very frequently to solve time-dependent boundary-value problems in rocks. Essentially, this theory assumes that the time-dependent deformations are a linear function of the stresses, which for the uniaxial compression creep test is expressed by equation (5.3).

Table 5.1 - Solutions for Time-Dependent Behavior of Underground Openings

Sources	Material Modeling	Solution Procedure	Types of problems Considered	Remarks
Nair et al(1968)	- isotropic and homogeneous	- iterative finite method (elasticity matrix 'C' is a function of time)	stress and disp. for elements near the wall of the und. open. in time-dependent material	stress-strain-time for salt t=0 solution is linear elastic
Hannafy(1976)	isotropic and homogeneous strain-hard. creep law	incremental f.e.m procedure	radial displ. vs. time comparison with measurements stress distr. with time deformations and loads after lining installation	stress-strain-time for shale; t=0 sol. is linear elast. radial conv. rate const. after a short time
Aiyer(1969)	isotropic and homogeneous	incremental solution	radial disp. vs. time; stress distr. with time; influence of time of lining installation	t=0 solution is linear elastic
Winkle(1970)	isotropic and visco-elasto-plastic model(10 parameters)	finite element method(incremental)	study of closure of cyl. openings in deep potash mines	solution to describe behavior of openings in salt and potash
Nair et al(1971)	isotropic and time-hardening law	incremental f.e.m	deformations and stresses around deep unlined spher. openings	stress-strain-time law salt t=0 sol. lin. elastic
Ladanyi(1974)	isotropic and homogeneous	closed-form solution	stresses and disp. around circular opening in hydrostatic stress field; increase in load with time on linings	

material behavior. For instance, Figure 5.2 displays a typical time-dependent closure for the case of an unlined opening and hydrostatic state of stress. This figure shows a continuous decrease in the rate of closure with time. Hannafy(1976) presented results (see Figure 5.3) which indicated a constant rate of tunnel closure after a brief period of rate decrease. That may well be due to the particular stress-strain-time relationship used by Hanafy (see Table 5.1). Further reference to studies describing patterns of and the influence of several parameters on the time-dependent behavior of underground openings can be made to Nair _et al._(1968) ,Aiyer(1969) and Semple _et al_(1973) .

Comparisons between results of actual measurements of the time-dependent deformations of underground openings and the predicted performance by using methods such as the ones displayed in Table 5.1 constitute a necessary condition to assess the soundness of the combination of assumptions involved in each of these methods. Winkle(1970) described the results of time-dependent closure of a 10-in diameter hole drilled into a large pillar at a 1050m deep potash mine in Moab, Utah. This hole was drilled parallel to the ground surface and the closure was measured at a distance of about 10-in from the opening wall.

Figure 5.4 shows the measured deformations as well as the results of the predictions made by using a visco-elasto-plastic model and three different sets of parameters. The results labelled as Carlsbad parameters

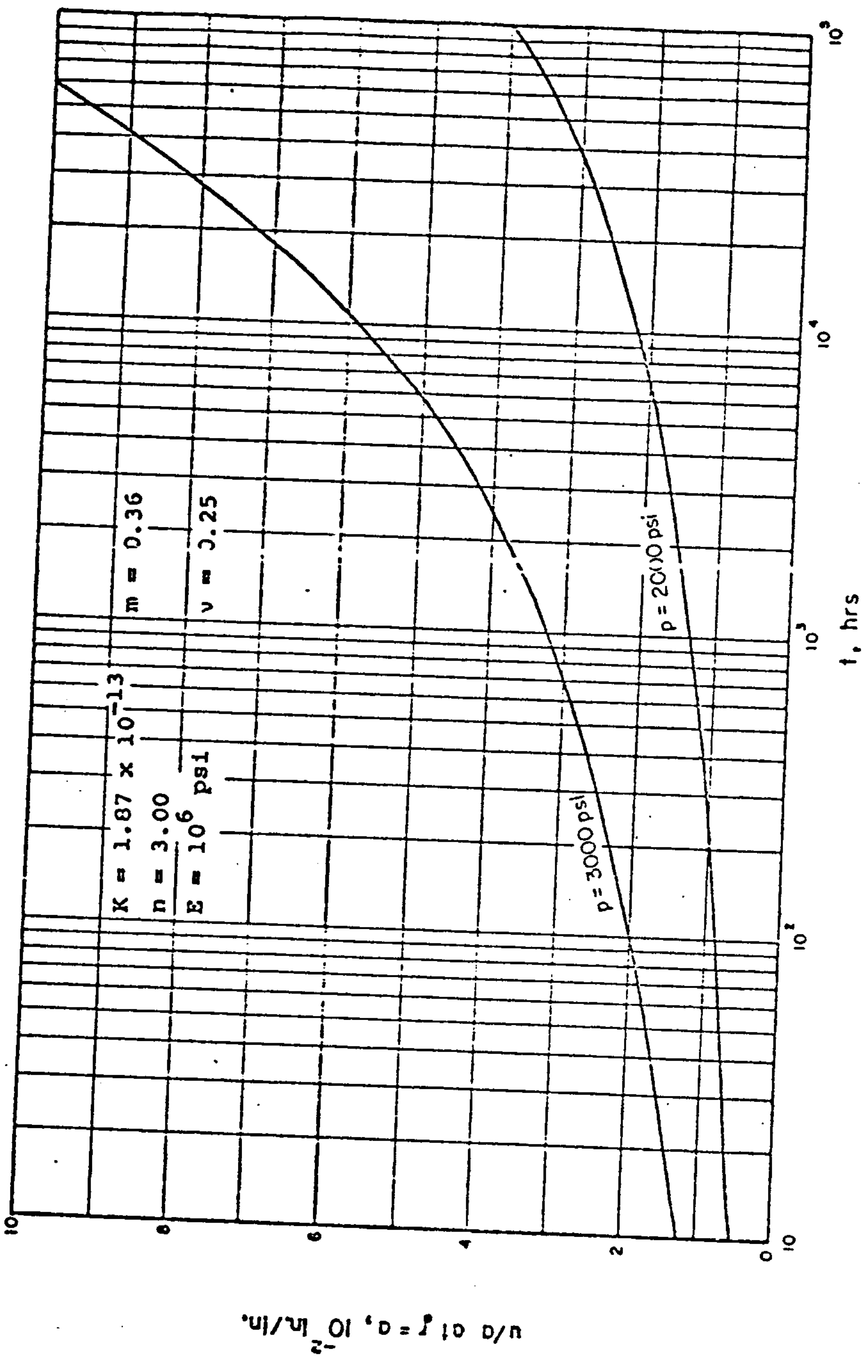

Figure 5.2 Typical time-dependent closure of cylindrical opening (after Aiyer(1969))

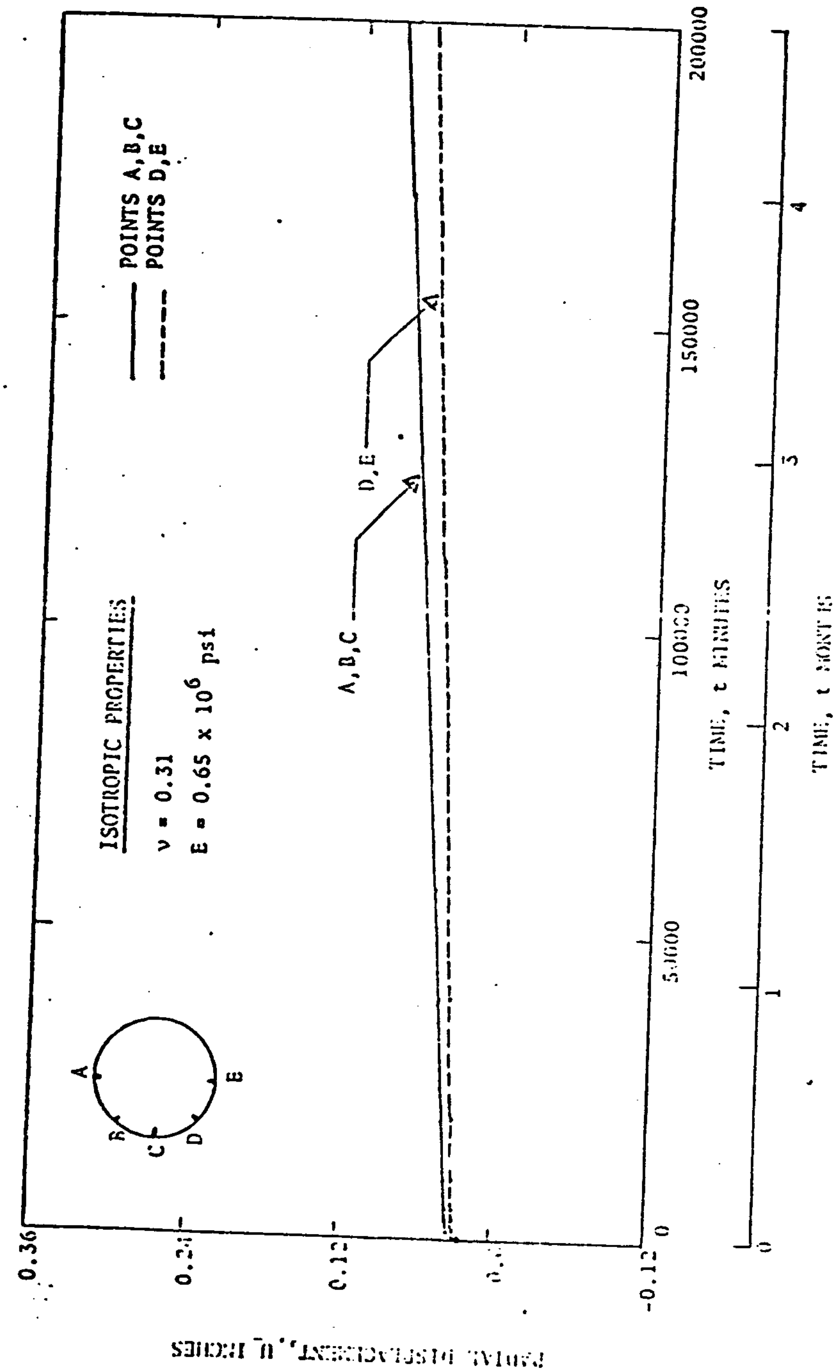

Figure 5.3 Time-dependent closure of circular tunnel (after Hanafy(1976))

constituted the prediction when using the creep parameters obtained from uniaxial compression creep tests on samples of Carlsbad potash. These particular predicted results lead to a very different pattern of deformations as can be observed in Figure 5.4 by comparing the variations of rate of opening closure with time and to a large difference in the amount of deformations especially for short times.

Also indicated in figure 5.4 are the predicted deformations by using a set of creep parameters obtained by Serata(1968) for rock salt and associated with the same visco-elasto-plastic model. Again, large differences in the amount of deformations can be observed, the deformations being overestimated by as much as 300%. Also, the rate of tunnel closure seems to be much higher than the one actually observed. Finally, the results of the predicted deformations using 'improved' parameters are shown to compare well with the observed deformations.

Hanafy(1976) described the results of time-dependent deformations of an underground intake tunnel for a large filtration plant near Toronto, Ontario. This tunnel is a circular opening of 4m diameter at a depth of 61m and located in Collingwood Shale. Figure 5.5 shows the results of comparisons between the observed creep closure 9 days after the installation of the instruments and the predicted deformations by using the creep law described in Table 5.1 and for distinct values of the stress ratio K ($\sigma h/\sigma v$). Large differences of up to 200% were observed for the creep

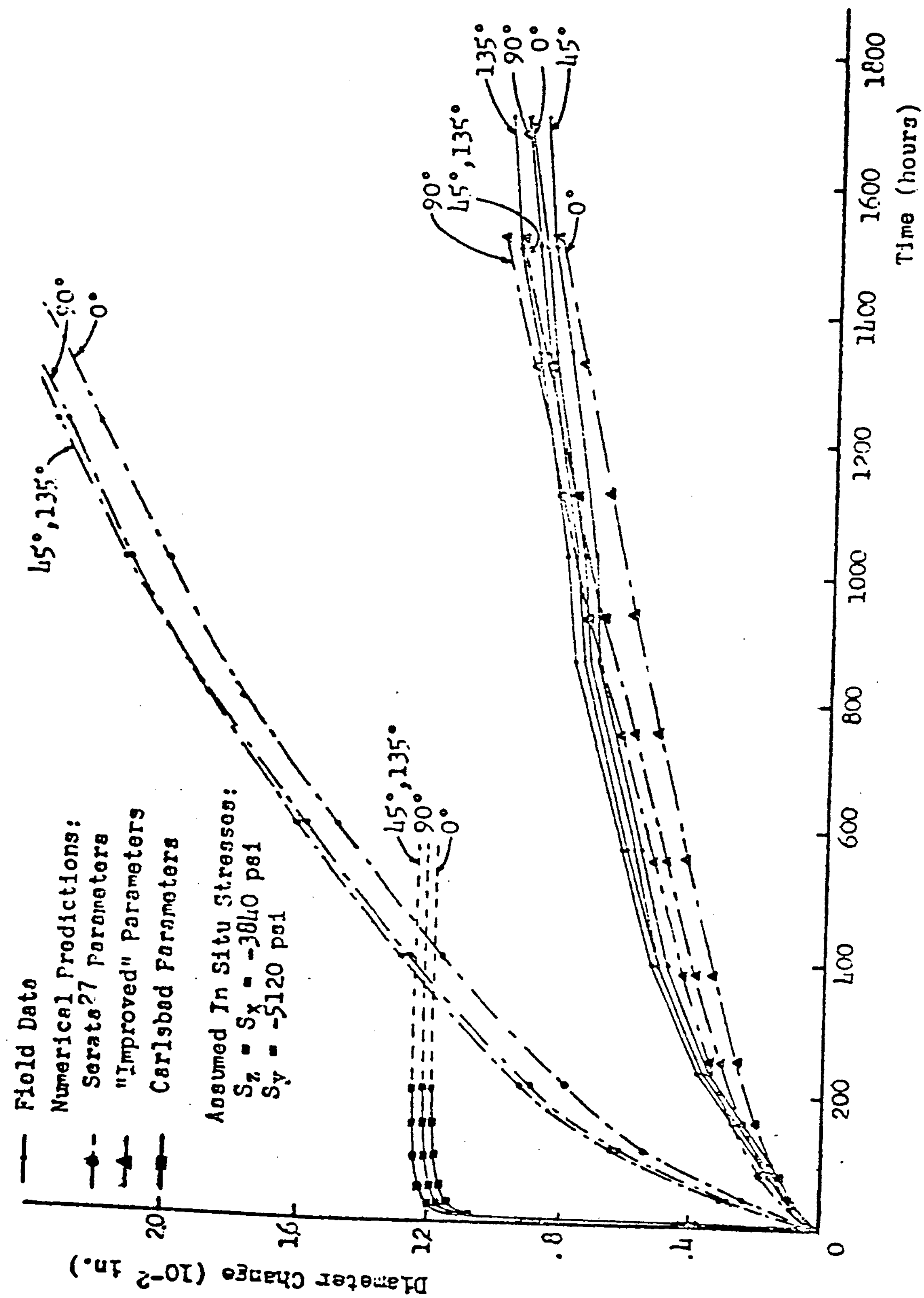

Figure 5.4 Comparison of predicted and measured closure of 10-in circular opening in potash (Winkle(1970))

closure and the difference diminished for points inside the rock mass.

The comparisons described in the previous examples seem to discourage the use of such approaches for evaluating creep deformations of underground openings. However, it is important to recognize that actual measurements can only be started some time after the excavation has passed through the measuring section and this fact generally leads to the inevitable loss of an unknown amount of deformation. This very often neglected feature makes comparisons between absolute magnitude of deformations sometimes very questionable. As concluded in Chapter 2 a much more important and reliable source of informations is the rate of tunnel closure which does not depend, for a particular time, on the values of the initial deformations. Therefore, comparisons between predicted and actual performance as a means of evaluating the adequacy of the use of analytical models to predict time-dependent behavior of underground openings must consider the rate of tunnel closure as a reliable parameter.

5.3.2 Time-dependent stress distribution

Another feature associated with the time-dependent behavior of an opening is the progressive stress redistribution which occurs as a result of creep deformations. Even though stresses do not contribute as a directly observable quantity, it is of paramount importance

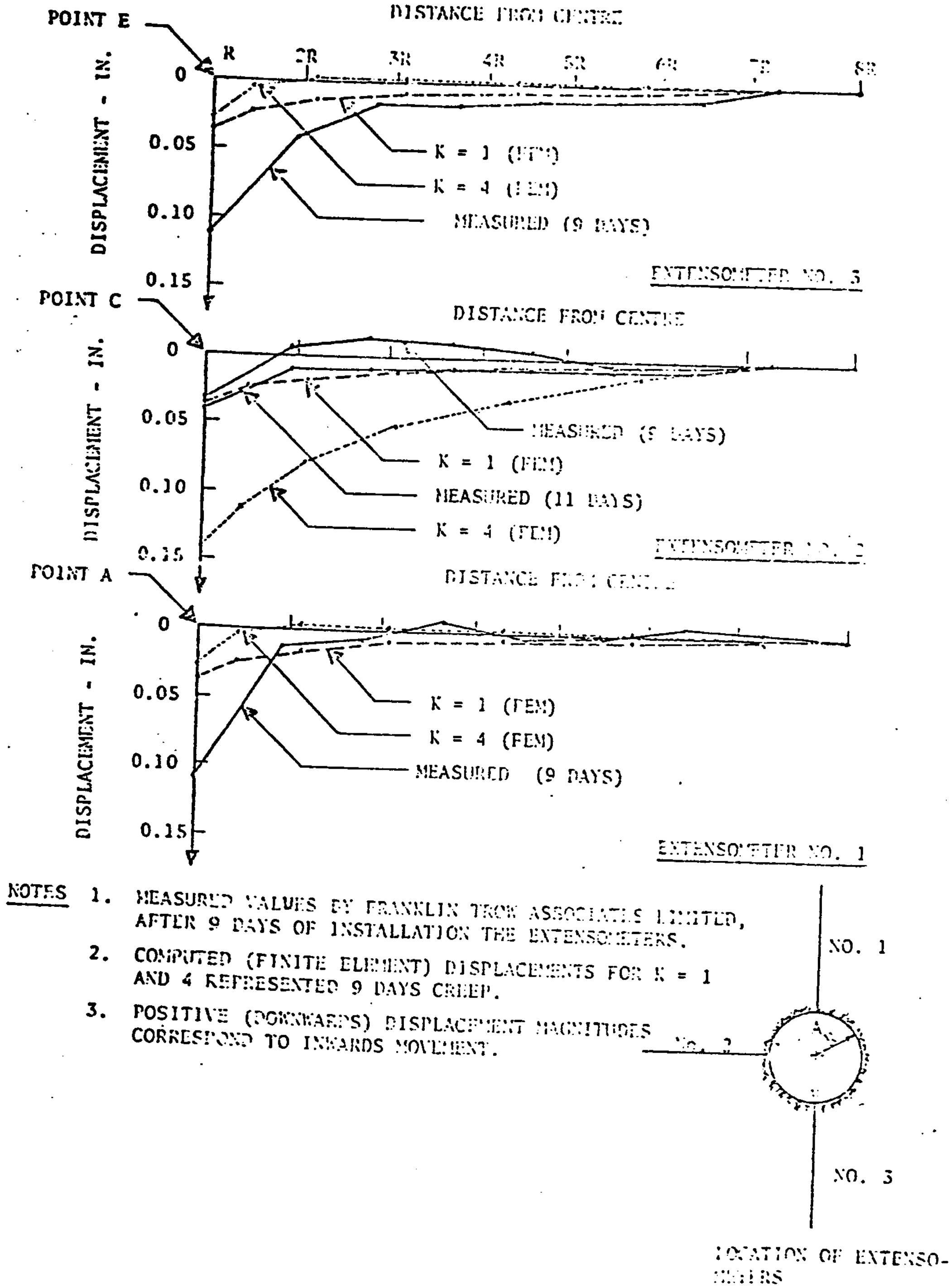

Figure 5.5 Comparison of predicted and measured creep displacements of circular tunnel in shale (Hanafy(1976))

to recognize the transfer mechanism associated with time-dependent deformations and to discuss its effect on the overall equilibrium of an underground opening. The main features of the process can be illustrated in Figure 5.6 which shows the variation with time of tangential, radial and 'effective' creep stress around a cylindrical opening for the situation of an isotropic medium and hydrostatic state of stress. Initially, stress redistribution occurs in such a way that there is a decrease in the tangential stress near the opening wall and an increase for the zones further away from the wall (Aiyer(1969)). This decrease in stress leads to the creation of a relaxation or unloading zone[4] around the opening. This stress transfer process occurs at a decreasing rate as indicated in Figure 5.6 where the bulk of stress change occurred within the first day of creep. Also both radial and 'effective' stress change with time but by a smaller amount than the tangential stress.

Parametric studies showing the influence of creep parameters, stress field and shape of opening on the stress redistribution with time have been reported by Nair <u>et al</u>(1968), Aiyer(1969) and Semple <u>et al</u>(1973). The process is similar to the one described above and displayed in Figure 5.6 the only difference being one of scale. On the other hand, this stress redistribution process has been described differently by Hanafy(1976) who indicated an increase of

----

[4]As discussed previously in Chapter 2, the creation of such relaxation or unloading zones can be caused by factors other than time-dependent deformations.

tangential stress around the opening wall, i.e., the opposite trend presented by the other methods. That may well be due to approximation effects of the stress at the center of the finite element. Also, this process is not recognized by the theory of visco-elasticity when solving this class of boundary-value problem.

More important is to recognize that stress distributions are rarely measured which precludes the use of comparisons between predicted and measured performances to assess the validity of the obtained results. Osmanagic and Jasarevic(1976) reported the results of tangential stress measurements around a 2.0m diameter circular opening at a 400m deep salt mine in Yugoslavia. These results reproduced in Figure 5.7 show a reduction of the tangential stress near the wall which indicates a pattern similar to the results of stress redistribution displayed in Figure 5.6.

5.3.3 Time-dependent loading of linings

Deformations imposed on the lining will cause an increase in load on those linings. The final load to act on the permanent lining was studied by Aiyer(1969) who considered the effect of both time of installation and stiffness of the lining on the final load on the lining. Figure 5.8 shows typical results. Aiyer concluded that for values of h/a greater than 0.04, where h=thickness of lining and a=radius of the opening, there is no remarkable reduction on the time-dependent deformations around the

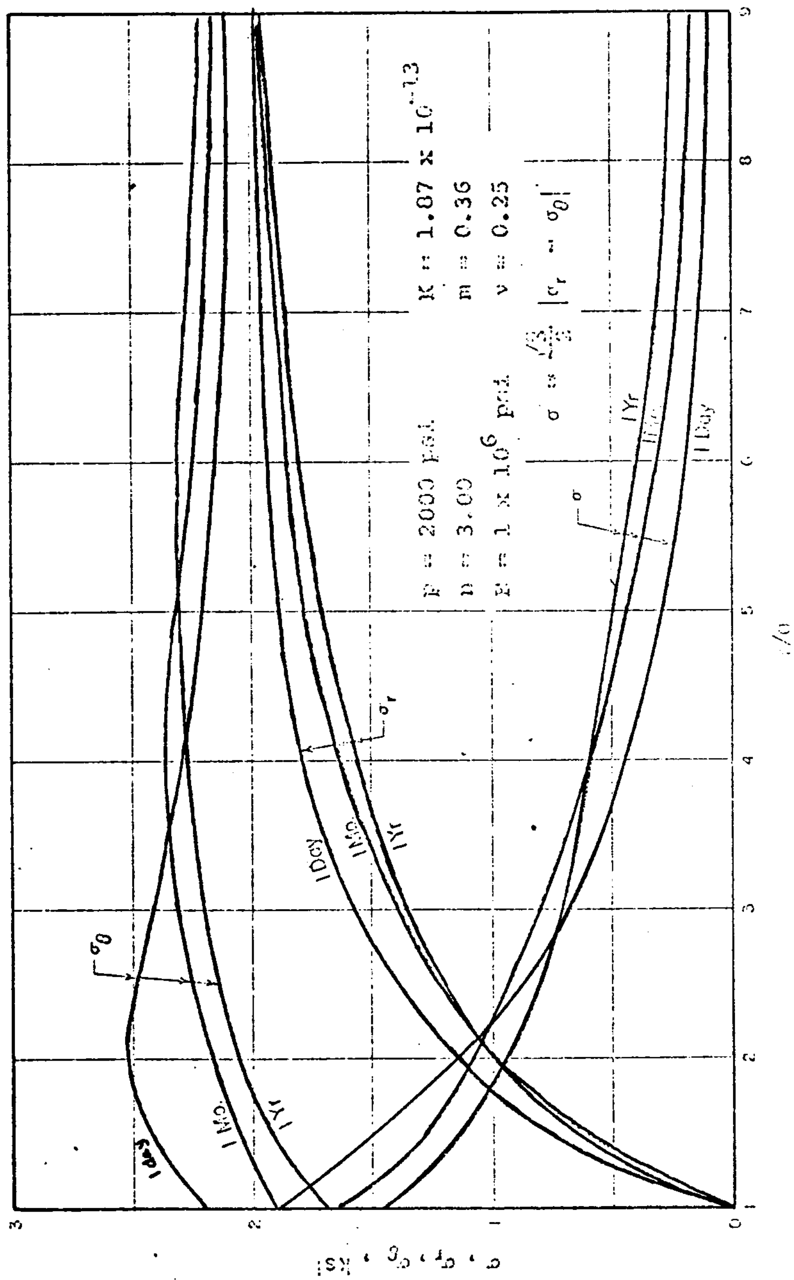

Figure 5.6 Stress distribution around an unlined cylindrical opening (Aiyer(1969))

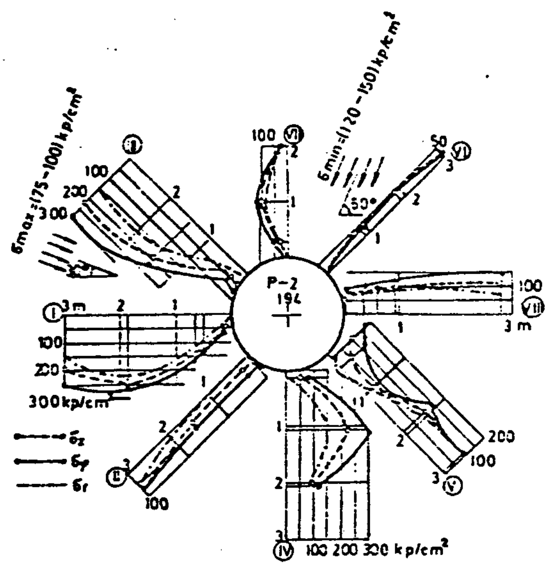

Figure 5.7 Tangential stress around an opening in salt (Osmanagic and Jasarevic(1976))

opening.

Ladanyi(1974) presented a closed-form solution for the determination of the time-variation of the 'true ground pressure' acting on the rock mass. Figure 5.9 illustrates Ladanyi's approach which consists in establishing the equation of the ground reaction curve assuming a number of simplifying assumptions. The variation of each material parameter with time is assumed to be known and lines of equal time or isochrones can be drawn up to the values defined by the long-term ground reaction curve. Associated with this, the lining installation can be considered by taking into account stiffness, gaps and time of installation. Ladanyi's approach considers the case of a circular opening, hydrostatic stress field, lining in a form of ring and a homogeneous and isotropic medium.

5.4 Final remarks

As seen in the previous sections, several studies on the time-dependent behavior of openings have been carried out. Even though these studies have attempted to describe the behavior of openings several drawbacks can be pointed out associated with them.

1. The description of the material modelling is still very limited and based on too many assumptions. A more general stress-strain-time relationship for rocks is needed which embraces both effects of volumetric and shear creep.

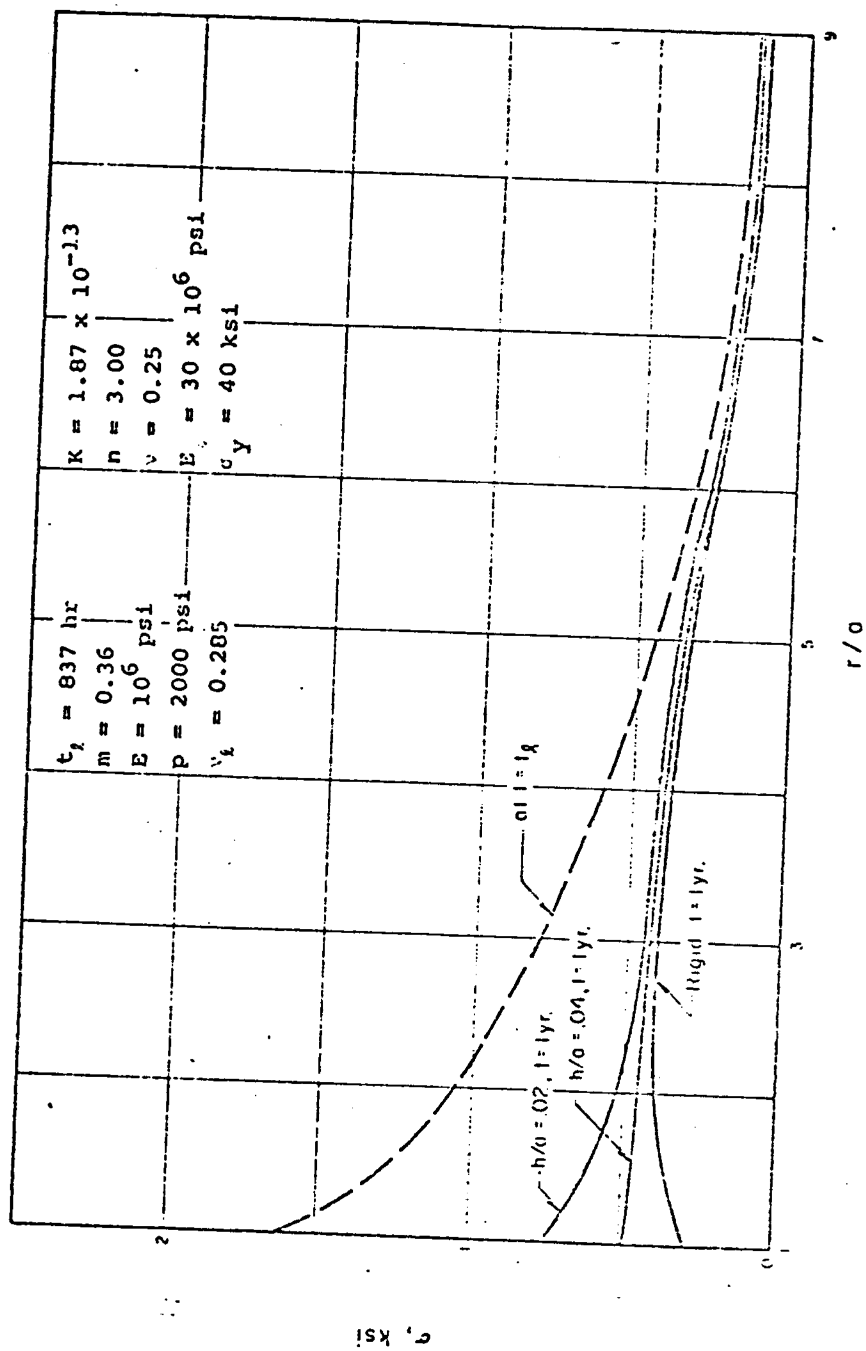

Figure 5.8 Distribution of stresses around a cylindrical opening for liners of different stiffnesses (Aiyer(1969))

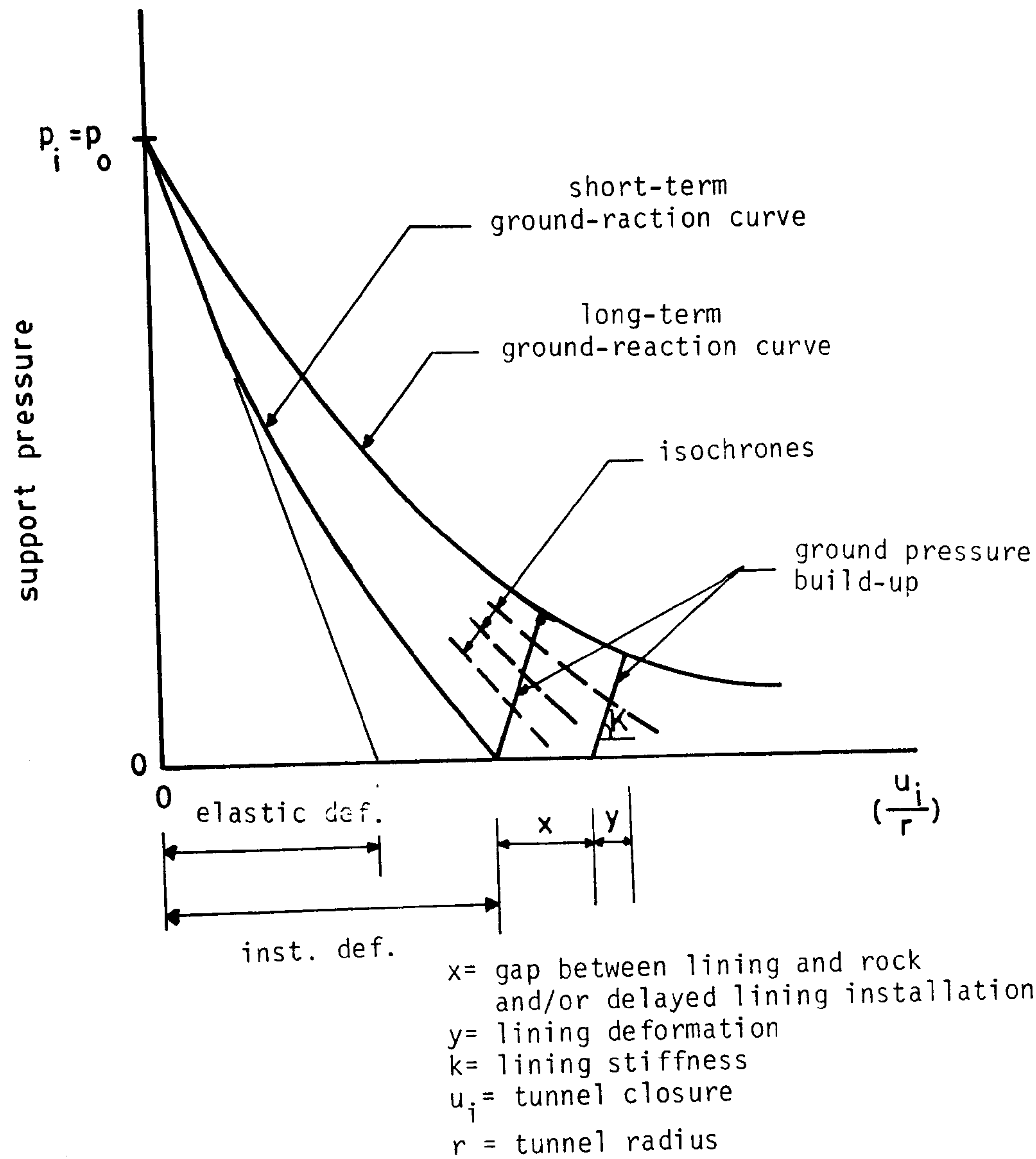

Figure 5.9 Schematic representation of the ground-reaction curve for ground pressure determination (Ladanyi(1974))

2. The present available solutions describe the change in both stresses and deformations around the opening as a function of an equivalent creep stress. However, as suggested in Chapters 3 and 4, the creep deformations seem to be a function of the stress level which describe the ratio of mobilized shear strength of the material. To understand the real effect of creep behavior of the rock mass on the overall time-dependent response of the opening, this concept has to be included in the final solution.
3. Several attempts have been made to describe the deformations occurring around the opening and comparisons between observed performance and predicted deformations. These attempts have not provided good correlation which leads to the discouraging feeling of not being able to represent the physics of the process. On the other hand, the discrepancy may well be due to the fact deformations are normally measured only a certain time after the excavation is done.

Chapter 6

THEORETICAL STUDY OF TIME-DEPENDENT BEHAVIOR OF UNDERGROUND OPENING

6.1 Introduction

To generate solutions for the time-dependent behavior of an underground opening, analytical methods of different degrees of complexity can be formulated. In order to assess the factors which ought to be considered in the formulation as well as the relevant parameters and features describing the time-dependent behavior of an opening, it is advisable to start with a simple formulation and increase, progressively, the complexity of the analytical model.

In this Chapter, a solution for the time-dependent behavior of a long hollow-cylinder under hydrostatic stresses and plane strain conditions was obtained. This solution consists of essentially three steps: the elaboration of a 3-dimensional stress-strain-time relationship; the development of a governing differential equation and its solution by a numerical technique. In the following, the necessary steps for the solution as well as the assumptions made are discussed.

Section 6.2 presents the proposed solution. The formulation of the material modelling as well as the development of the governing differential equation are discussed. This section also presents the solution procedure and the computer program written to solve the differential equation. Section 6.3 presents an analysis of the validity and accuracy of the proposed solution. This is done by comparing the measured tunnel closure in a model test carried out by Guenot(1979) and the results predicted by the analytical procedure outlined in section 6.2.

Section 6.4 presents the results of a parametric study carried out to assess the influence of factors such as size of the opening, creep parameters and time-independent properties on the time-dependent behavior of an opening. Especial attention is paid to the rate of tunnel closure and some aspects of the stress path and strain history for the material around the opening. Finally, section 6.5 presents the summary and the conclusions obtained from this chapter.

6.2 Proposed solution

The nature of the assumptions associated with the formulation of material modelling calls for the use of a simple model for the time-independent solution. Therefore, it was decided at this stage, to study the case of a linear elastic medium with a coupled rheological behavior, under plane strain conditions and using a 2-dimensional formulation.

6.2.1 Material modelling

In order to describe the time-dependent deformations occurring around an opening, the empirical creep relationship developed in Chapter 4 and described by equation 6.1 was used.

$$\mathring{\varepsilon} = A \cdot e^{\bar{\alpha}\bar{\sigma}} \cdot t^{-m} \qquad \text{.... (6.1)}$$

In equation 6.1, the term $\bar{\sigma}$ represents the stress level which is defined as the ratio between the current deviatoric stress and the short-term strength. For the purpose of modelling a 3-dimensional state of stress, the material was assumed to follow the Mohr-Coulomb criterion, i.e., the maximum shearing strength being defined by two parameters, c and ϕ. In that case, the stress level can be calculated as indicated by equation 6.2 where σ_1 and σ_3 are respectively the maximum and minimum principal stresses.

$$\bar{\sigma} = \frac{\sigma_1 - \sigma_3}{f(\sigma_1, \sigma_3)} = \frac{\sigma_1 - \sigma_3}{2c \cos\phi + (\sigma_1 + \sigma_3) \sin\phi} \qquad \text{.... (6.2)}$$

In this formulation the intermediate principal stress, σ_2 , is assumed as having no influence on the shear strength and therefore is not considered. Even though this hypothesis constitutes an over-simplification of this question, the Author considers it justifiable in order to maintain a simple model. As defined by equation (6.2), the stress level can be calculated without any difficulty in accommodating alternate failure criteria.

Equation (6.1) only describes the maximum principal strain rate. In order to consider the strains which occur in other directions, equation (6.3) was used to describe the volumetric strains which occur during creep. Even though no consistent experimental evidence exists which describes the volumetric strain during creep, the use of such a relationship is believed to be a convenient approximation. At the same time, equation (6.3) is general enough to allow for further improvements when more updated relationships are developed.

$$\varepsilon_1^c + \varepsilon_2^c + \varepsilon_3^c = k\,\varepsilon_1^c \qquad \ldots\ldots (6.3)$$

For the case of k=0, the common assumption of no-volume change due to creep is recovered. In addition, the creep strains which occur in the principal directions are related to creep strain ε_1^c as described by (6.4)., where Pn and

Pm are assumed to be constants. Again, available experimental data is not enough to provide a consistent picture for the actual relationship between strain components and so, (6.4) is considered as being reasonable.

$$\varepsilon_2^{\,c} = -\,P_m\,\varepsilon_1^{\,c}$$
$$\varepsilon_3^{\,c} = -\,P_n\,\varepsilon_1^{\,c} \qquad \text{.... (6.4)}$$

6.2.2 Governing equation

In Appendix A, equation (6.5) was developed. This differential equation constitutes the governing equation describing the change in radial stresses with time for the case of a 2-dimensional axisymmetric plane-strain boundary-value problem.

$$k_{11}\,\frac{d^2}{dr^2}(\Delta\sigma_r) + k_{12}\,\frac{d}{dr}(\Delta\sigma_r) = k_{13} \qquad \text{.... (6.5)}$$

In this equation, the terms k_{11} , k_{12} and k_{13} are a function of both $\Delta\sigma r$ and $d/dr(\Delta\sigma r)$ and they are defined in

Appendix A. The solution of this type of differential equation has been discussed by Fox(1957) . In order to solve (6.5), a numerical scheme based on finite differences was used. This scheme consists of writing (6.5) in terms of finite differences for points in an equally spaced mesh. For three subsequent points along the mesh, i.e., (i-1), i and (i+1) and replacing $\Delta\sigma r$ by 'y', equation (6.5) can be written as equation (6.6).

$$a_j\, y_{i-1} + b_j\, y_i + c_j\, y_{i+1} = d_j \qquad \ldots.\ (6.6)$$

where,

$$a_j = \frac{k_{11}}{h^2} - \frac{k_{12}}{2h}$$

$$b_j = -\frac{2k_{11}}{h^2}$$

$$c_j = \frac{k_{11}}{h^2} + \frac{k_{12}}{2h}$$

$$d_j = k_{13}$$

The boundary conditions for the problem in question, i.e., an unlined opening, are that $(\sigma_r)_1$ =0; y1=0 and

$(\sigma_r)_n$ =po; yn=0 at any time, t, where $(\sigma_r)_1$ = radial stress at the opening wall, $(\sigma_r)_n$ = radial stress at the external boundary, and y1 and yn are the changes in the radial stress at the same locations. Subject to these boundary conditions and using equation (6.6) for each point along the finite difference mesh, a system of (n-2)x(n-2) equations can be set up for each time step, Δt, and solved by trial-and-error by assuming an initial set of values for yi. This process continues until the difference between the values of yi's obtained in consecutive iterations reaches a pre-established value or a maximum number of iterations is exceeded which indicates a non-convergence of the solution.

A computer program was written to solve equation (6.6) according to the scheme just discussed. The listing of this program is presented in Appendix B which also describes the input data and their format.

6.3 Accuracy of proposed solution

Due to the highly non-linear nature of the equation (6.1), no closed-form solution which uses this equation to solve the boundary-value problem in question could be found in order to compare with the solution procedure outlined in the previous section. The results of the model tests reported by Guenot(1979) constituted an alternative to check out both the accuracy and validity of such a procedure.

In these tests, blocks of jointed coal with dimensions of 60x60x20 cm with a circular opening of 12 cm diameter at the center were loaded at the block surfaces and plane strain conditions were maintained. The external loads were maintained constant for a period of time during which measurements of tunnel closure as well as internal radial deformations were taken. A complete description of testing equipment and methodology as well as discussion of results is presented in Kaiser(1979) and Guenot(1979). For these tests, the coal used was essentially the same as that used by the Author in the creep tests described in Chapter 4.

6.3.1 Performance of model tests

The prediction of the results obtained in these tests involved two steps. Initially, the parameters to be used during the analysis were selected and secondly these parameters were employed in the computer program listed in Appendix B.

The test selected for analysis was the loading of the model test to a stress of 4.8 MPa with a ratio between horizontal and vertical stresses of about 1.06. Using Guenot's numbering system, this test will be referred to as MC-3.1.

Figure 6.1 shows the results of tunnel closure versus the external stress during the loading of the sample. Following an initial clearly non-linear stage, the stress-strain curves show a linear trend. This fact lead to the choice of a linear elastic model for the initial behavior. For the Young's modulus a value of E equal to 1000

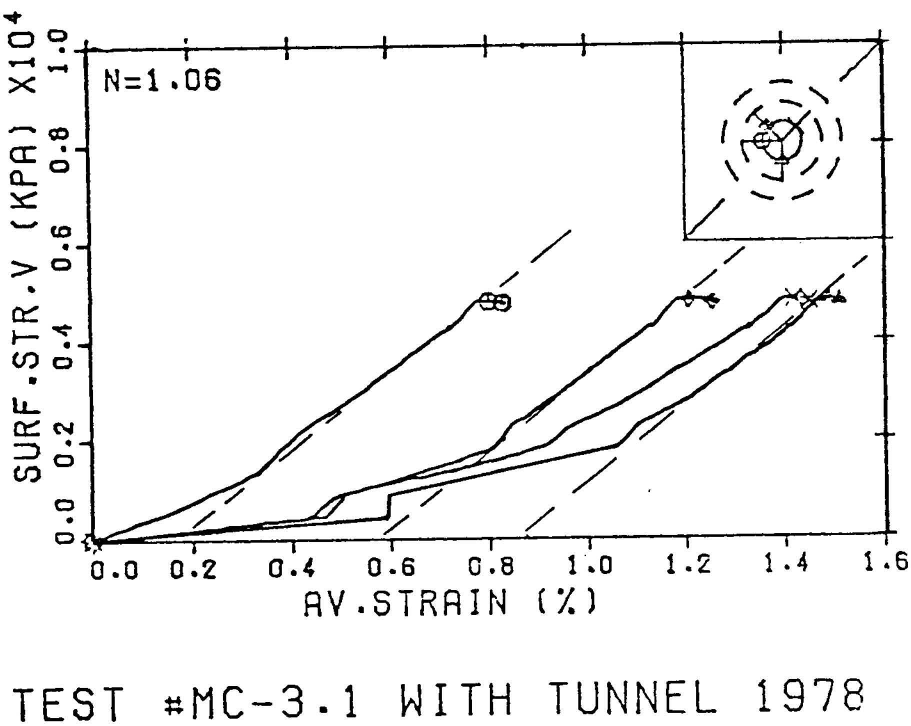

Figure 6.1 External stress vs. tunnel closure - model test MC-3.1 - (after Guenot(1979))

MPa was chosen which corresponds to an average value of E obtained in the laboratory tests by Kaiser(1979) and the ones reported in Chapter 4 of this thesis. A value of u=0.30 was selected on the basis of calculations of the initial strain for the model test. This value is also close to the one used by Noonan(1972).

The selection of the shear strength parameters was made by initially assuming that the Mohr-Coulomb failure criterion would represent the short-term strength of the coal. Based on the previous results of direct shear tests (Noonan(1972)) and triaxial compression tests (Kaiser(1979)) on the Wabamum coal, the following parameters were selected as representing average conditions: c=2.0 MPa and $\phi=50^\circ$.

The time-dependent behavior of this coal was described in Chapter 4 based on the results of triaxial tests. The parameters describing the creep behavior were the ones obtained from the results of the laboratory tests and summarized in Figure 4.19. They correspond to A=1.0x10-5/min and $\bar{\alpha}$ =1.9 and m=0.9.

The assumption of no-volumetric creep strain was made, i.e., in equation (6.3) k=0, and the value of Pm was also assumed to be zero. The Pm=0 assumption is equivalent to considering the value of ε_2^c as zero. However, for plane strain conditions, it is the total strain in that direction and not the creep strain which is zero. To check the sensitivity of the solution to this assumption, preliminary runs were carried out and for the cases associated with

Pm+Pn=1 (equivalent to k=0). The results indicated n and time-dependent closure for values of pm in the range between 0 and 0.3. Even though, no experimental data has been produced to suggest the range of Pm, there is no reason to believe that Pm assumes values greater than 0.2. Therefore, it was concluded that to use pm=0 would not have any noticeable influence on the present study.

Figure 6.2 shows the model test and the finite difference mesh used during the prediction of the results. The comparisons were made for the 1st. loading stage of the test MC-3.1 as described by Guenot(1979), which corresponds to a 4.8 MPa stress applied at the boundary and a ratio between stresses of 1.06. In the simulation a ratio of 1.0 was used.

Figure 6.3 presents the results of tangential and radial stress distribution around the opening as well as the stress level variation with time. As can be observed from these figures, the stress distribution hardly changed with time which seems to indicate that the creep tests carried out at constant stress level are a good representation of the stress condition around this particular opening.

Figure 6.4 presents a comparison of the measured and predicted time-dependent tunnel closure for the model test. In this figure, curve (1) represents the results obtained if only the creep strains due to shear stresses are considered. Four measurements in different extensometers are indicated in that figure and the predicted ones falls at just about

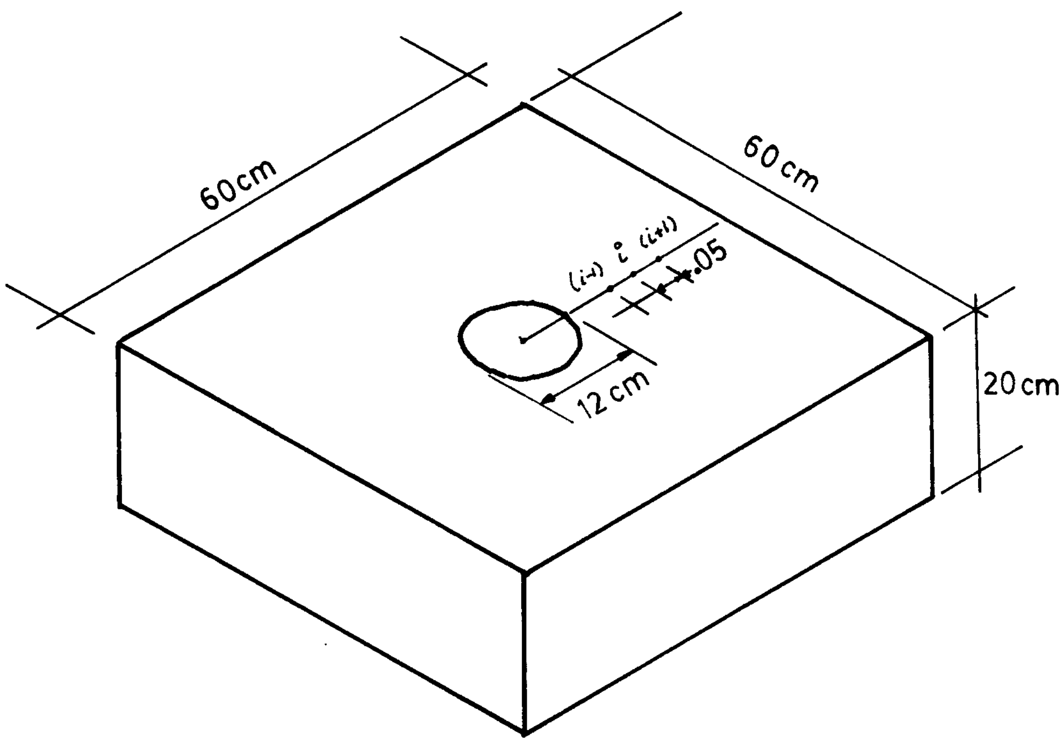

Figure 6.2 Model test and finite difference mesh

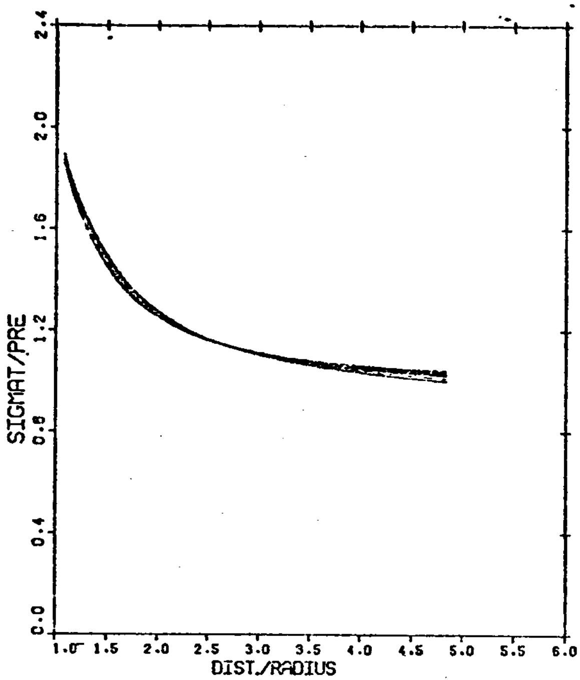

(a)
TIME-DEPENDENT TANG. STRESS DISTRIBUTION

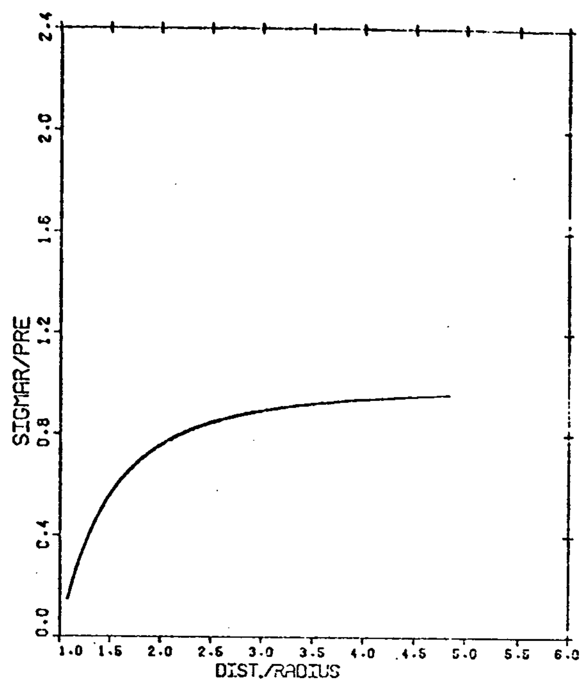

(b)
TIME-DEPENDENT RADIAL STRESS DISTRIBUTION

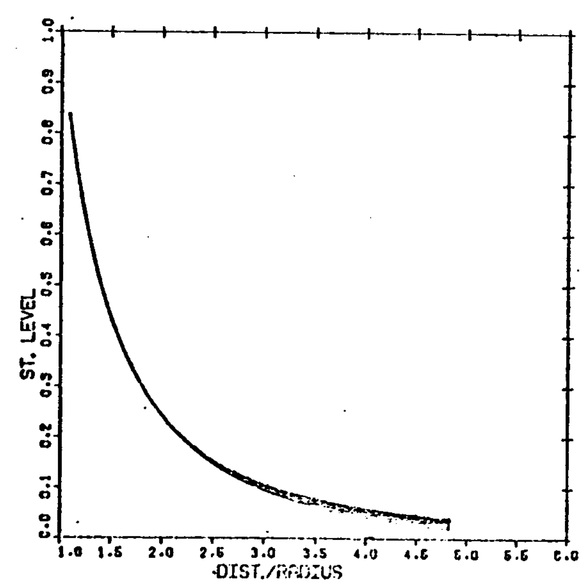

(c)
TIME-DEPENDENT STRESS LEVEL DISTRIBUTION

Figure 6.3 Time-dependent stress distribution - predicted results

the average between the measured values which indicates a good approximation of the order of magnitude of the time-dependent deformations.

At the same time, as discussed in Chapter 5, it is of value to describe not only the deformations but also the rate of tunnel closure. Figure 6.5 displays a comparison between the measured rate of tunnel closure and the predicted rate. Again, in this figure, curve (1) indicates the results obtained if only creep strains due to shear stresses are considered. These results suggest that the proposed solution procedure yields results which are representative of the actual deformations and therefore describe quite well the physics of the deformation processes around the opening in the model test.

In addition, values for the internal measurements were interpreted by the proposed method. The observed time-dependent radial strains were compressive at all times whereas the predicted radial creep strains, based on creep strains due to shear stress, were extensive. According to Kaiser(1979) this behavior is due to the fact that creep components due to both hydrostatic as well as deviatoric components of the stress tensor act on the sample. For the values around the opening the value of creep due to the hydrostatic component would be greater than the creep due to the deviatoric component which would yield a net compressive radial creep strain.

In order to verify the assumption of hydrostatic creep

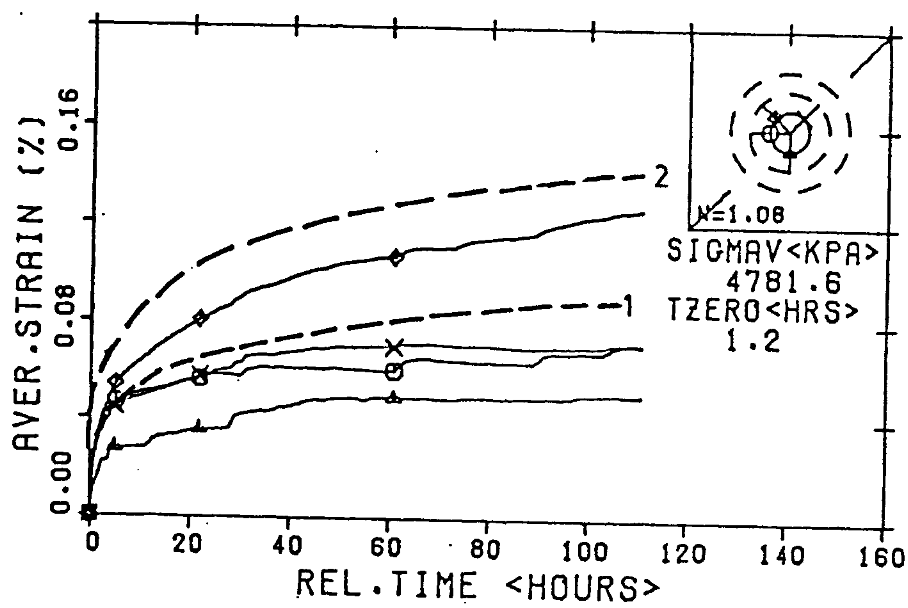

Figure 6.4 Comparison of measured and predicted tunnel closure

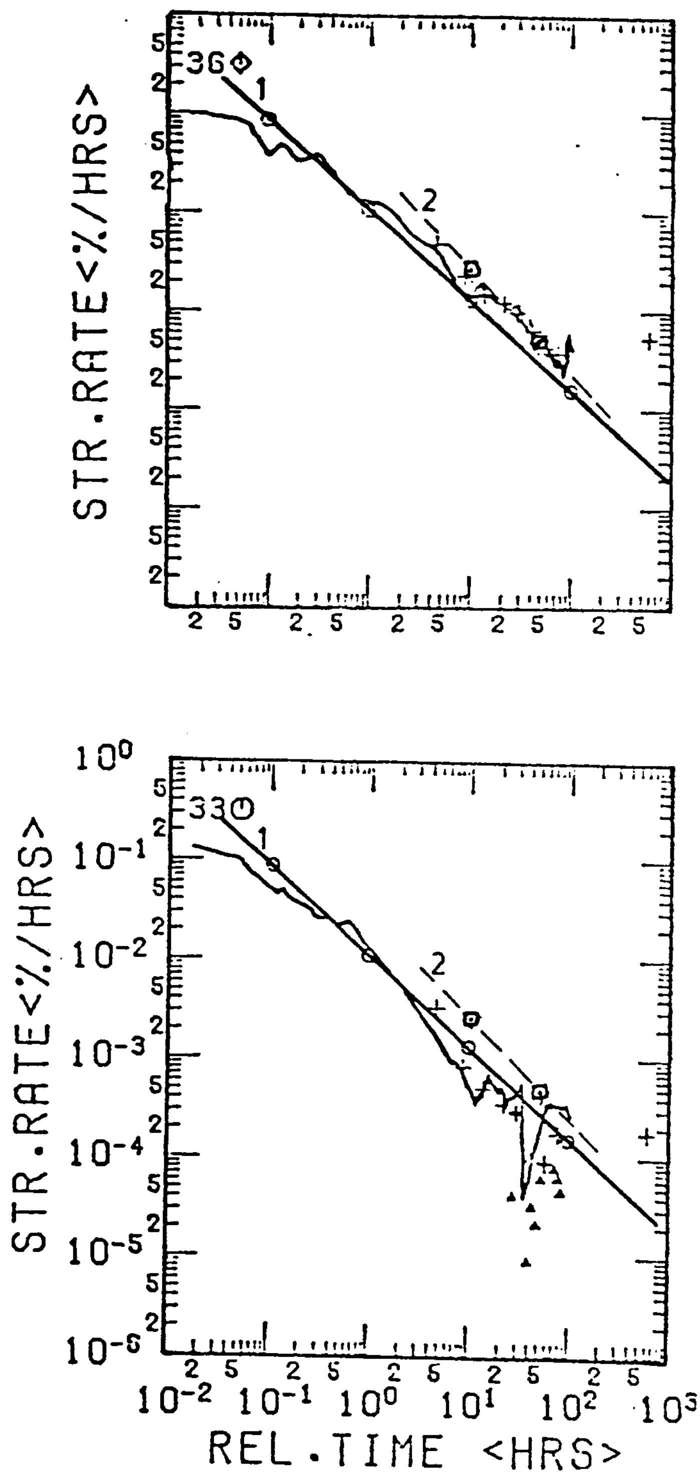

Figure 6.5 Comparison of measured and predicted rate of tunnel closure

strain, the results presented by the computer program were corrected to include such a component. The following strategy was used to evaluate the necessary correction. The values of the radial creep strains obtained from the first row of extensometers, at about 3.5 cm from the opening wall, were used as the results to be matched after applying the correction. This is indicated in Figure 6.6.a as curve (a). Curve (b) represents the results predicted by the solution procedure which predicts extension at the position in question. If curve (a) is to be reproduced after applying the correction to the results, a radial creep strain versus time curve as indicated by curve (c) has to be superimposed on the obtained results.

This correction was compared with the values of creep deformations measured at the end of the block during the experiments which represents a situation of almost hydrostatic state of stress. As can be observed in Figure 6.6b, the value of the correction is within the same order of magnitude as the observed measurements. This procedure was further checked now as a way to obtain the value of the radial creep strain for the second row of extensometers, i.e., at about 8.5 cm from the tunnel wall. Curve (e) in Figure 6.6a is the result of the correction applied to curve (d) which is the radial creep strain predicted by the computer program. This curve compares well with the obtained experimental data.

Assuming that the value of the creep radial strain due to the hydrostatic component is equal to the tangential creep strain, the value of the tunnel closure presented in Figure 6.4 was corrected and is shown as curve (2) in that figure. In Figure 6.5, points were plotted to illustrate the new rate of tunnel closure as compared with the experimental data. This comparison shows that even though the correction strategy may be considered too crude, the results indicate a good agreement between observation and prediction.

However,no experimental data describing the creep behavior of coal under hydrostatic condition was reported and therefore further analysis cannot be carried out. Also the analytical solution used in this thesis does not consider the creep behavior due to hydrostatic component of the stress tensor. More data may be necessary before further elaboration of this question.

6.4 Results of parametric studies

The present section describes further investigations on the time-dependent stress and strain distribution around a circular opening within a hydrostatic stress field. Initial investigations were made to assess aspects of the time-dependent behavior of an opening such as the stress redistribution process and the increase in deformations with time and their dependence upon factors such as size of opening, creep and time-independent parameters of the rock mass. Table 6.1 presents a summary of the runs of the implemented program in which some parameters were varied in

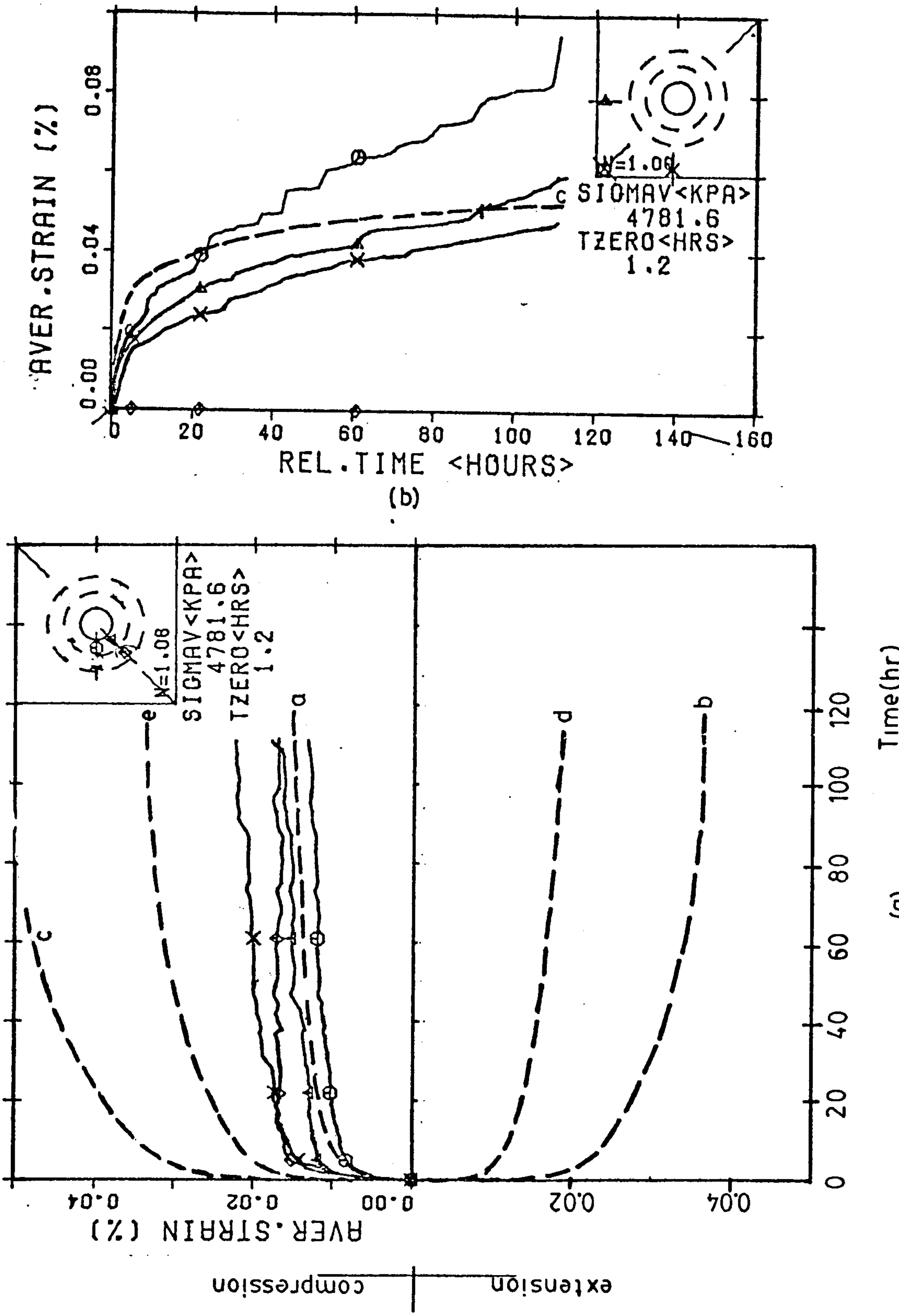

Figure 6.6 Comparison of measured and predicted radial creep strain versus time

order to assess the influence of these factors. At the present stage, the analysis has been carried out considering unlined openings.

6.4.1 Time-dependent stress distribution

Figure 6.7 shows the stress distribution versus radial distance from the tunnel wall for different times for the set of parameters corresponding to case C1. Times up to about 6 days were considered. In this figure, two aspects relative to the time-dependent behavior of an underground opening are illustrated. Initially, the change in the tangential stress with time must be considered. There is a progressive stress transfer towards the inside of the rock mass which represents physically the tendency to reduce the shear stress causing creep.

The process of stress redistribution can be characterized by two variables, namely:

4. the time after which variations in stresses are negligible and
5. the size of the unloading zone.

Both variables are a direct function of the creep properties of the medium, i.e., the magnitude of creep parameters and stress level. The results presented in Figure 6.7 show a reduction of 31% in the first hour for the tangential stress at the wall whereas this drop reaches 47% for the first day of creep. After the first day, say to the first week, only 49% of the drop occurs which indicates that most of the drop

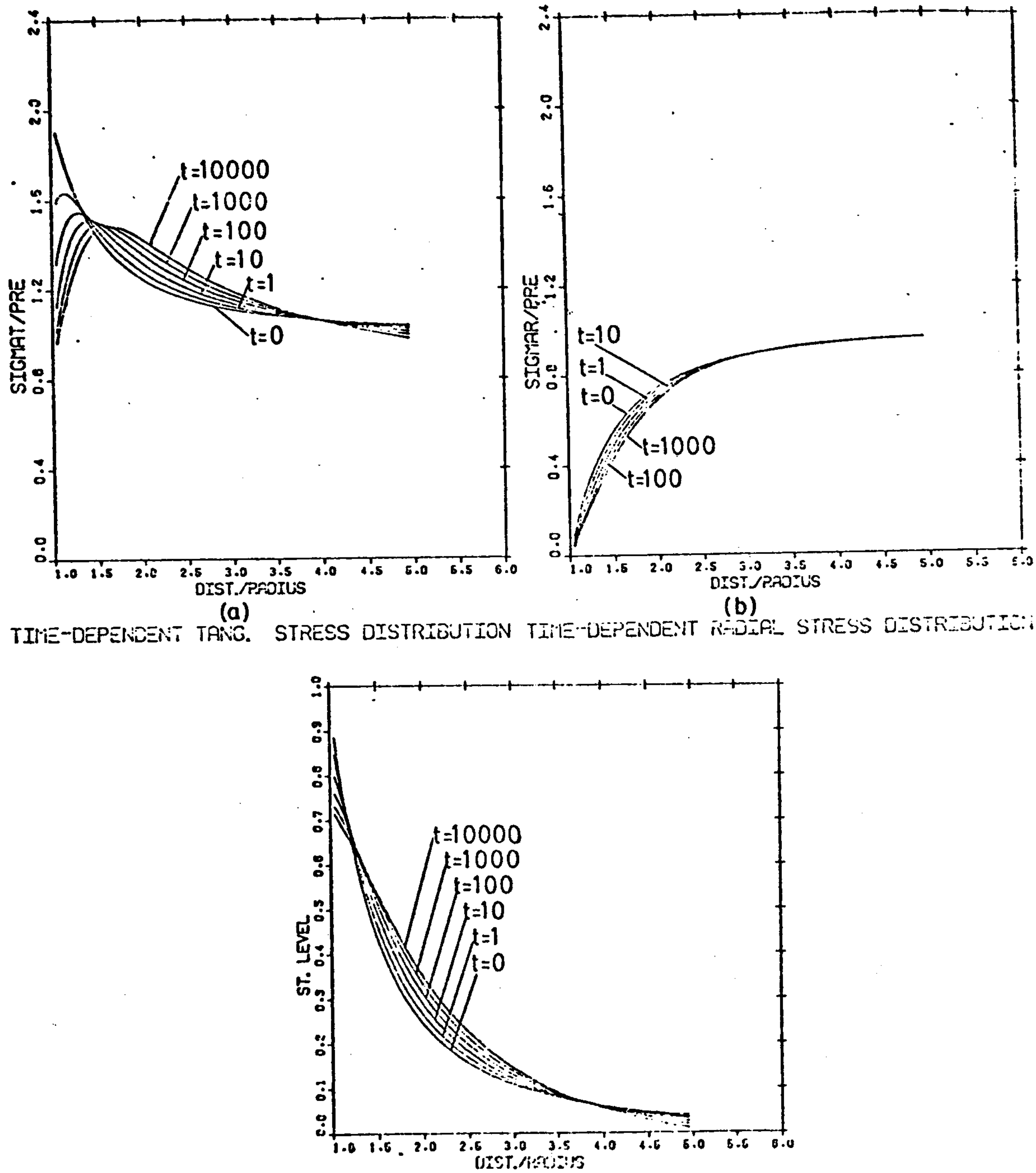

(a) TIME-DEPENDENT TANG. STRESS DISTRIBUTION

(b) TIME-DEPENDENT RADIAL STRESS DISTRIBUTION

(c) TIME-DEPENDENT STRESS LEVEL DISTRIBUTION

Figure 6.7 Time-dependent stress distribution - Case C1

Table 6.1 Summary of the cases analyzed during the parametric study

Case Run	Material Parameters(*)				Geom. Characteristics		Remarks(**)
	A(min-1)	Alpha	m	E(kg/cm2)	R(m)	Ah(m)	
C1	5x10-5	4.0	0.9	10000	5	0.25	$\dot{\delta}= 10^{-2} t^{-0.90}$
C2	5x10-5	4.0	0.9	10000	2	0.10	
C3	1x10-5	2.0	0.9	10000	5	0.25	$\dot{\delta}= 0.72\times10^{-4} t^{-0.91}$
C4	1x10-5	2.0	0.9	50000	5	0.25	

(*) For all cases : u=0.30 ; c=20 kg/cm2 ; 0=50

(**) $\dot{\delta}$ = rate of tunnel closure/ tunnel radius

Po=50 kg/cm2 E=50000 kg/cm2

A	Alpha	K	EK
(10-4/min)		(%/hr)	(10+4xkgx%/hrxcm2)
0.2	4.0	6.55	32.75
0.6	4.0	19.65	98.25
0.7	4.0	22.92	114.60
0.1	4.0	3.27	16.35
0.05	4.0	1.63	8.15
0.01	4.0	0.327	1.635

Po=20 kg/cm2 E=10000 kg/cm2

A	Alpha	K	EK
(10-4/min)		(%/hr)	(10+4xkgx%/hrxcm2)
0.5	4.0	16.37	16.37
0.7	4.0	22.37	22.37
0.2	4.0	6.55	6.55
0.01	4.0	0.327	0.327

Table 6.1 Summary of cases studied (contn.)

Po=50 kg/cm2 E=10000 kg/cm2

A	Alpha	K	EK
(10-4/min)		(%/hr)	(10+4xkgx%/hrxcm2)
0.5	4.0	16.37	16.37
0.1	4.0	3.27	3.27
0.033	4.0	1.08	1.08
0.2	4.0	6.55	6.55
0.05	4.0	1.63	1.63
0.0135	4.0	0.442	0.442

Po=30 kg/cm2 E=10000 kg/cm2

A	Alpha	K	EK
(10-4/min)		(%/hr)	(10+4xkgx%/hrxcm2)
0.5	4.0	16.37	16.37
0.7	4.0	22.93	22.93
0.2	4.0	6.55	6.55
0.01	4.0	0.327	0.327

or stress redistribution occurs within the first day of creep. It is interesting to compare the stress redistribution process indicated in Figure 6.7 with the one obtained for the case of Figure 6.3 where a different set of creep parameters was used. In this case, no important stress redistribution occurs which indicates the sensitivity of the system with respect to the creep behavior of the medium. The change in the creep parameters is equivalent to a change in the creep rate of about 40 times.

The size of the 'unloading zone' as shown by the comparison of the cases displayed in Figures 6.7 and 6.3 is also a function of the creep parameters. For the first case, the zone of rock located within about one radius from the opening wall is unloaded. This unloading process corresponds to a loss in ring stress and may lead to a reduction in the self-support ability of the rock mass around the opening.

As also indicated in Figure 6.7, the radial stress distribution does not show much variation as compared with the variation in tangential stress. A reduction in the radial stress contributes to a loss in the ability of carrying load by the ring of rock in the immediate vicinity of the opening. This fact suggests that the radial stress distribution is much less sensitive to the creep deformations than the associated tangential stress distribution.

The influence of the creep parameters on the stress redistribution is further illustrated in Figure 6.8. This consists of a plot of the ratio between the drop in tangential stress at the end of one hour of creep and the external applied stress (which represents a measure of of the stress redistribution) and the parameter $K=Ae^{\bar{\alpha}}$ which is a measure of the creep potential of the material. Two curves are shown in this figure, each associated with a different value of the Young's modulus, E. For the same set of creep parameters, the greater the modulus E (the stiffer the system) the more stress redistribution will occur. In Figure 6.9, a new plot is presented for the same set of data now considering the parameter EK defined as the 'system creep potential' which represents a combined effect of the stiffness of the system and the material creep potential. The two curves now coincide showing that regions of stress redistribution potential can be assessed for a given value of EK. In the same figure, is also illustrated the effect of the opening size which does not affect the previous relationship.

As would be expected due to the highly non-linear term $e^{\bar{\alpha}\bar{\sigma}}$, the time-dependent behavior is influenced by both $\bar{\alpha}$ and the strees level, $\bar{\sigma}$, which in turn is defined by the external pressure, po, and the shear strength parameters. In Figure 6.9, a number of curves relating the stress redistribution parameter, Sr, and the system creep potential, EK, is shown to illustrate the effect of the stress level. During the course of this study the parameter $\bar{\alpha}$ was shown to influence sets of curves such as the one

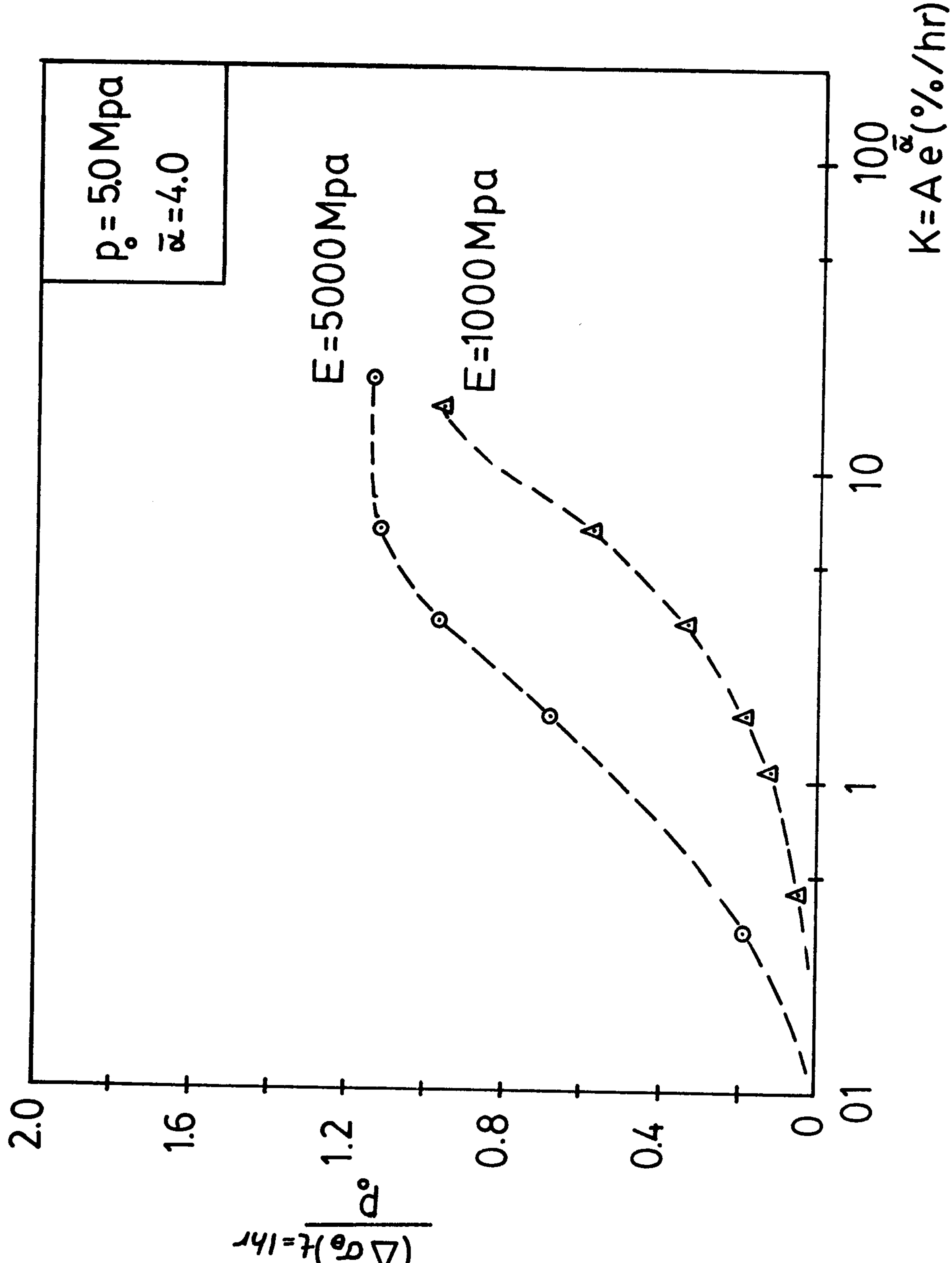

Figure 6.8 Drop in tangential stress versus creep potential of material

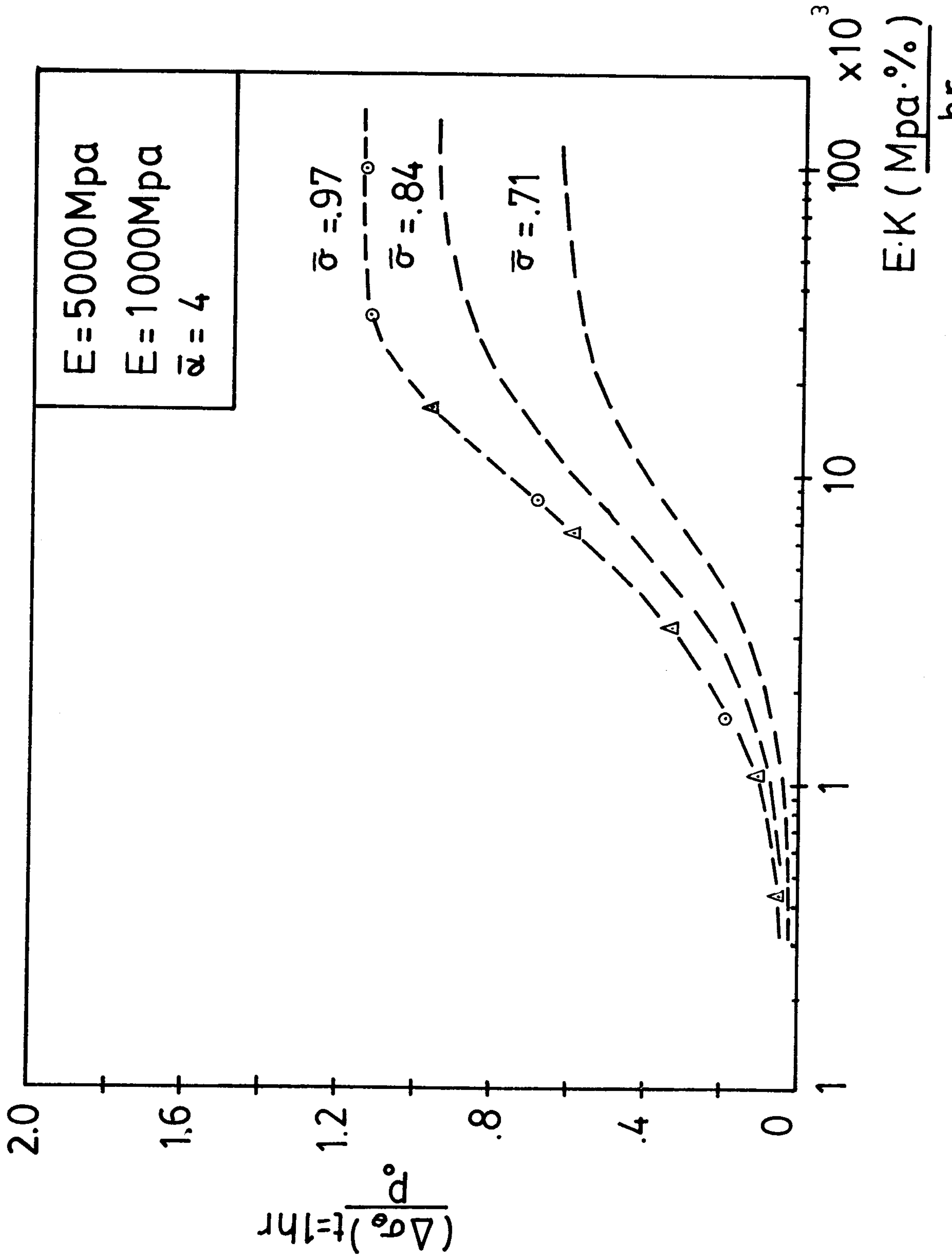

Figure 6.9 Stress redistribution factor versus the system creep potential

presented in Figure 6.8.

In Figure 6.10 another aspect of the influence of the creep parameters and stress level on the stress redistribution is illustrated by plotting the ratio between the total closure at the end of one hour and the initial tunnel closure versus the stress redistribution factor. This relationship also proved to be independent of both the Young's modulus and the opening size. Again, the effect of the stress level is indicated by the three curves also illustrated in this figure.

6.4.2 Stress level

Considering that the behavior of a rock mass is controlled basically by the stress level, it is important to consider the variation of the stress level around the opening for various times. Figure 6.7c presents the stress level plotted against radial distance for different values of time for the set of parameters corresponding to case C1. This definition of stress level has been given previously in section 6.2. At the same time, the parameters controlling the failure envelope are assumed constant with time. Under those circumstances the variation of stress level with time may be considered as one way of measuring the disturbance in equilibrium of the medium and its rate as the reestablishment of the equilibrium process.

Considering an initial 'elastic' stress distribution, the stress level reaches values of less than 25% at points

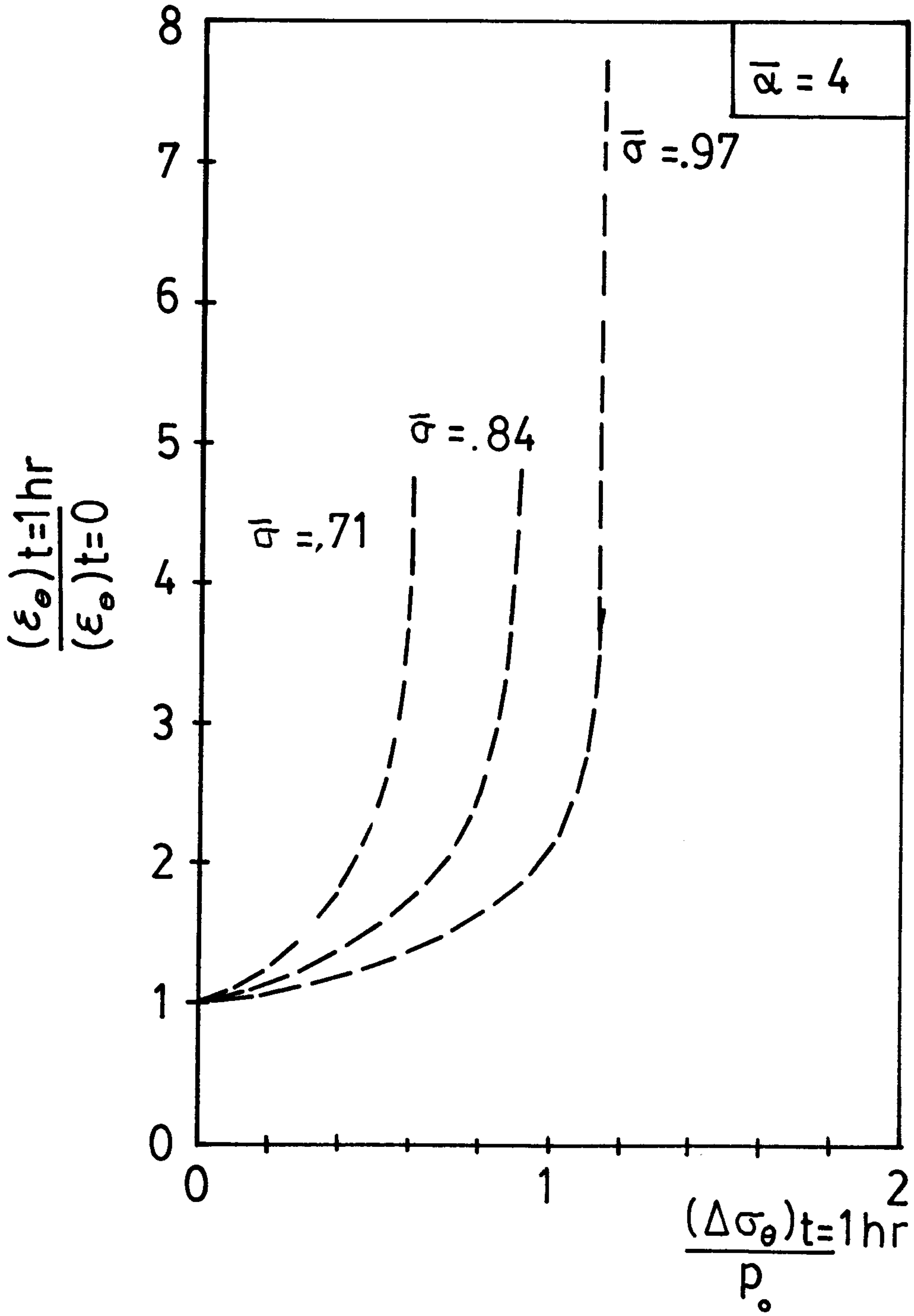

Figure 6.10 Stress redistribution factor versus ratio of tunnel closure

as close as one radius from the wall. If it is considered that such a small stress level does not cause appreciable creep strains, the area of both movements and stress redistribution is more or less concentrated around the opening. With time the area of relevant creep movements does not change considerably and the unloading process is more or less concentrated around the cavity.

The variation of the stress level with time is also a function of the creep parameters in such a way that the larger the creep movements, the greater the change in stress level. This fact can be readily observed by comparison of Figures 6.7c and 6.3c. For these two cases, a change in creep parameters equivalent to a 40-fold variation in strain rate was used.

As indicated in Figure 6.7c, the maximum change in stress level occurs very near the opening wall and, for case C1, this change corresponds to about 25%. For points outside this range the change is smaller not reaching values greater than 15% and shows an increase in stress level with time as a result of the stress redistribution process.

6.4.3 Strain accumulated during creep

The third question related to the time-dependent behavior of an opening is the one considering the state of straining undergone by each element around the excavation. It is particularly important to consider the deformations during the transition period, i.e., from the pre- to post-excavation equilibrium. The validity of the assumptions made previously with respect to stress path and strain history can now be adjusted on the basis of these results.

Figure 6.11 presents the variation of the stress level with the tangential strains for different values of times for the set of parameters associated with case C1. As can be seen from this figure, for elements near the wall the stress level decreases even though the tangential strain increases. The decrease in stress level tends to stabilize after a certain period of time. Elements in different positions behave in a somewhat different way from each other.

The diagram presented in Figure 6.11 also suggests that the tangential strain more or less follows a path which certainly does not take into account any limitation from the rock point of view in terms of accumulated displacements. The rock is considered as able to take the calculated displacements. This question has not yet been fully investigated but some previously reported data supports the idea that long duration loads tend to increase the ability of rock to deform without failing in a brittle manner e.g., Bieniawski(1970) and Kaiser and Morgenstern(1979) .

It is also interesting to notice that several curves can be plotted as isochrones of stress level versus tangential strain for different times. The curves demonstrate the reduction in stiffness with time especially for the areas near the opening.

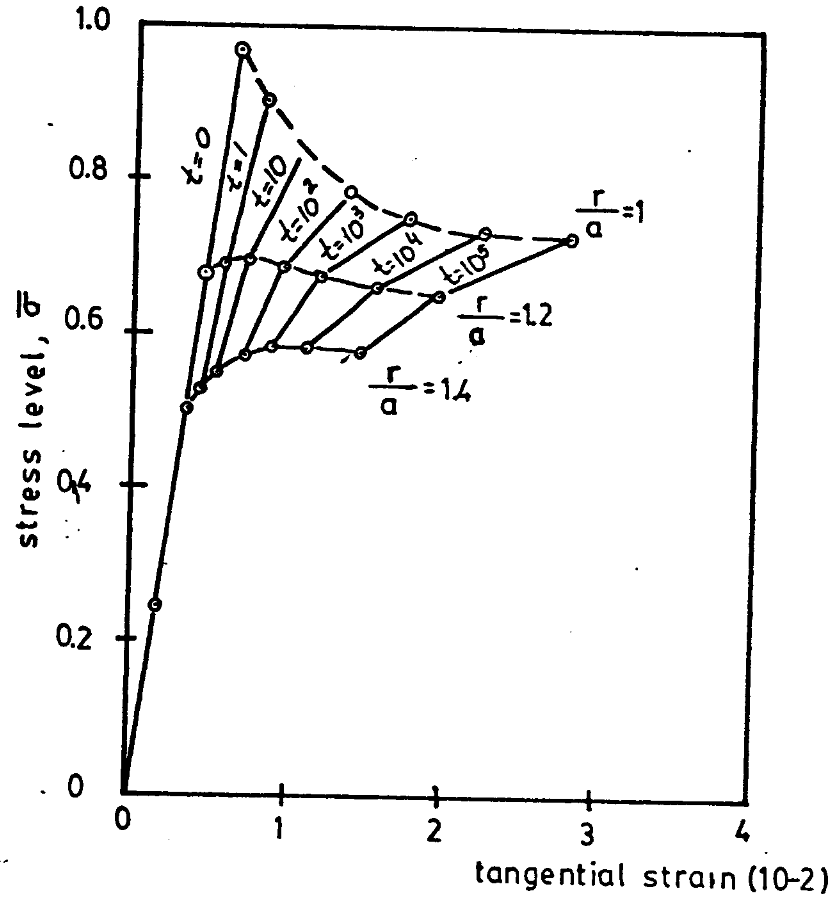

Figure 6.11 Stress level versus accumulated total tangential strain - case C1

6.4.4 Time-dependent deformations

Another important aspect of the time-dependent response of an opening is the variation of both tunnel closure and internal radial displacements with time.

Figure 6.12 gives the curve of tunnel closure versus time for case C1 and Figure 6.13b shows the same data plotted as rate of tunnel closure versus time in a double log-scale. Two important features are illustrated in these figures. Initially, the rate of tunnel closure shows a continuous decrease with time for the model used and secondly, this decrease can be conveniently represented by a power law with respect to the elapsed time. This power law corresponds to a straight line when the data are plotted in a double-log scale.

The continuous decrease in rate of tunnel closure displayed by this solution procedure indicates a time-dependent stable process where an equilibrium position is finally approached. This process certainly reflects some situations in the field. As the model which was used does not provide for any deterioration of rock mass properties such as decrease in strength with accumulated displacement or creep acceleration due to this decrease in strength, it is not possible to model the onset of an unstable situation.

The final aspect considered is illustrated in Figure 6.13a which displays the variation of the radial displacements versus radial distance for different values of time. It is also encouraging to note the similarity in

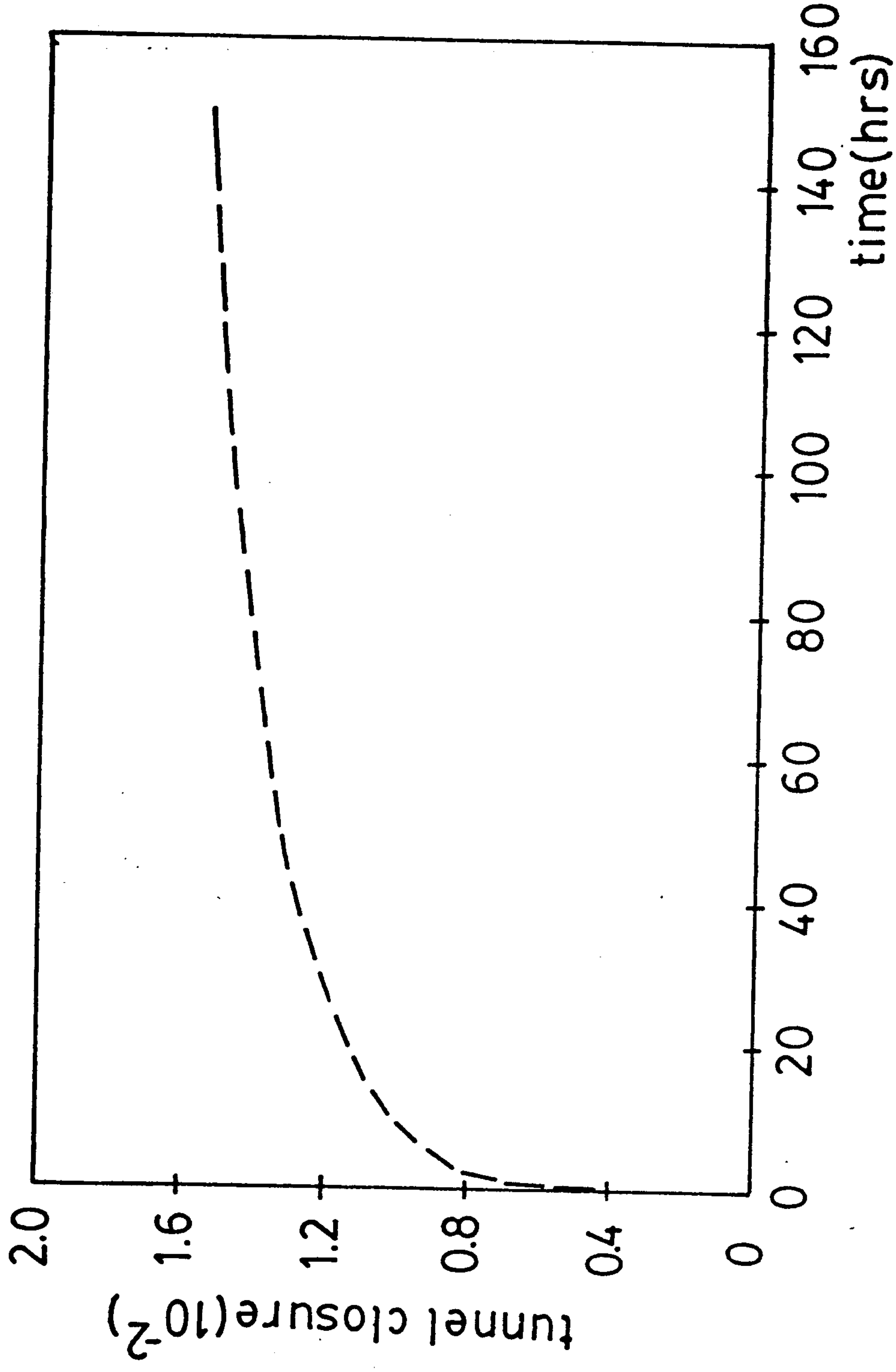

Figure 6.12 Time-dependent tunnel closure - case C1

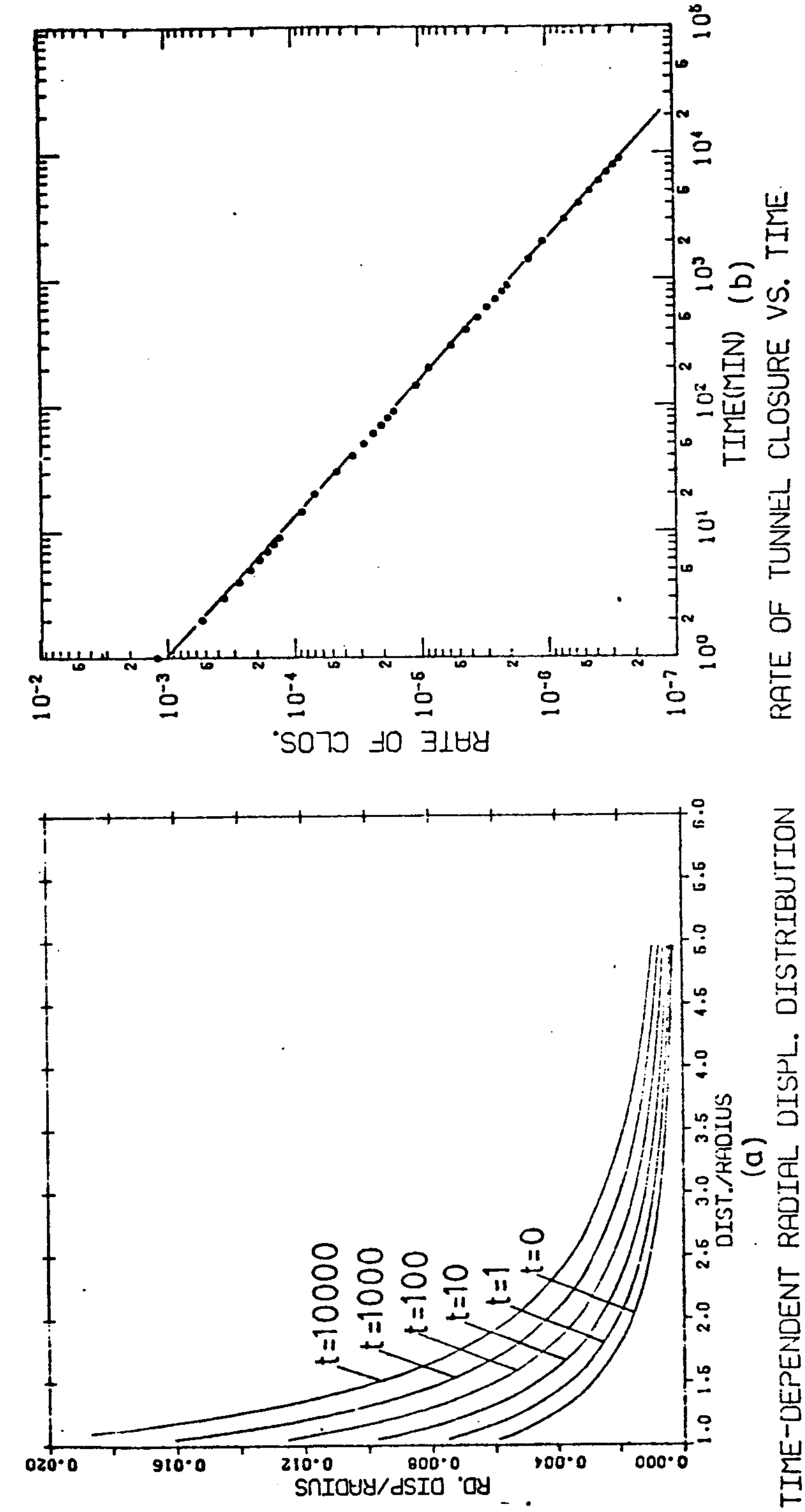

Figure 6.13 Time-dependent strain-distribution and rate of tunnel closure vs. time - case C1

pattern of deformations with the reported measurements of variation of radial displacement with time for the Yarbo No.1 Shaft described in Chapter 2.

6.5 Summary and conclusions

The following conclusions were reached from the analyses presented in this Chapter:

1. The creep behavior of rock mass is related to how close the material is to the short-term failure strength. If the failure criterion is expressed in terms of stresses, the creep behavior can be expressed in terms of stress level. A method to describe the creep behavior in terms of stress level is presented and its inclusion in an analytical technique is discussed.
2. A solution for the time-dependent stress distribution and the time-dependent deformations around an opening was presented. The case considered took into account the creep law described previously and a differential equation was developed. This differential equation was solved nummerically and a computer program was written.
3. This solution procedure was checked against a set of measurements of opening closure and the results of comparison between predicted and obtained closure were satisfactory.
4. The time-dependent behavior was described as being associated with a time-dependent stress redistribution and a time-dependent deformation. The stress

redistribution process was seen to be highly dependent on the creep properties of the medium. High creep behavior leads to a considerable redistribution around the opening especially with respect to the tangential stress.

5. The time-dependent deformations were described by both deformations and rate of deformations. The rate of tunnel closure was shown to decrease in a linear manner with the time when plotted in a double log scale. This pattern is similar to measurements described in the literature for the behavior of model pillars in salt (King(1974)) and the early stages of closure of openings in salt (Baar(1975)).

6. Based on the comparisons of measured and predicted deformations for the model test, it was concluded that the solution procedure suggested provides results which are within the range of the expected behavior. The assumptions made in order to solve this boundary-value problem have to be understood specially the limitation regarding the elastic behavior of the medium immediately after the excavation. However, this does not invalidate the use of the creep relationship described as well as the solution procedure.

More research has to be done in order to include cases such as non-hydrostatic state of stress and non-circular openings.

Chapter 7

FINAL REMARKS

7.1 Conclusions

The aim of this thesis is to provide a contribution towards understanding the time-dependent processes associated with the excavation of tunnels in rocks. This is achieved in three ways:

a. investigations of the process leading to time-dependent behavior of underground openings;

b. experimental data describing the time-dependent response of rock masses;

c. analytical modelling of excavations in creeping rock.

In the light of the discussions presented throughout this thesis the following conclusions were reached.

(a) In-situ time-dependent response of rock tunnels

The understanding of the processes involved in the passage from a pre- to a post excavation equilibrium is of fundamental importance in advancing our current tunnel design practice . The evaluation of these processes is of great value if it is done through the observation of the performance of actual case-records. From the outset of this research, the Author was aware of the many difficulties in undertaking such a study due to the lack of a sufficient number of well documented case-records. A common feature of reported cases is that many of the factors which control the opening behavior such as rock mass properties, stress field, sequence of excavation and lining strategy are not properly described.

Four different modes of ground behavior were postulated initially. The mechanisms leading to these modes were described and illustrative case-records associated with each one of them were presented. From these considerations the following observations with respect to the role of the time-factor associated with each mode can be made.

For the cases of 'fracturing' and 'loosening' the discussions suggested that the role of time-factor is secondary since prompt protection of the excavated rock is normally required. This need is due to the difficulty in predicting accurately the weakening process associated with increasing deformations (or increasing delay in lining installation) of the tunnel wall. Also, failure in this type of ground may occur without warning and the size of blocks and slabs which may detach from the roof certainly justify strong safety measures.

Many of the reported cases considered as squeezing are associated with very weak ground (fault zones and weathered rocks) at great depths (see Table 2.2). In these cases, the ground around the opening is overstressed and the deformations associated with the excavation must be expected to be high. The main concern in these circumstances is to control the deformations during the excavation which is normally done by choosing a convenient excavation sequence and lining strategy. Cases such as Tauern and Giri tunnels demonstrate the need to account for large deformations by using flexible linings. More informations relative to the size of the overloaded zone around the opening are needed as well as measurements of time-dependent deformations after the effects of the face advance can be neglected. An understanding of these deformations is considered essential before the loading of the supports and time of ring closure can be assessed with more confidence.

Also included in the category of squeezing ground are the cases of openings in rocks which do not present any problems of overall stability immediately following excavation but deform continuously with time. Measurements of tunnel closure versus time, such as the ones shown for the Yarbo No.1 shaft, are more or less creep-like curves. This class of squeezing ground is addressed during the analytical section where the effects of creep behavior are modelled.

Some of the case-records described as swelling also reveal the same characteristics of weak ground (fault zones and weathered rocks) and at relatively great depths. These cases present the same general set of problems of stability during excavation as discussed earlier for squeezing ground. Again, the initial stability is the main concern which is demonstrated by a number of case-records in Japan (see Table

2.3). Also, information on the deformations which occur after the effect of excavation advance becomes negligible are needed in order to understand the loading of the lining which occurs afterwards. Cases where the initial stability of the opening is not the main concern, such as some cases in Eastern Canada and Germany, have suggested that changes in the first stress invariant and hydration must be accounted for to explain the time-dependent deformations. However, these classes of case-records have yet to be described effectively as far as the stress-strain-time laws for these materials are concerned.

(b) Rheological response of rock mass

A review of the stress-strain-time relationships which have been used to describe the time-dependent behavior of rocks was presented in Chapter 3. Many of these relationships refer to uniaxial compression tests and relatively intact rock samples. A very large number of different expressions was noticed that may be associated with different ways of analyzing and interpreting the experimental data. It was also observed that for the interpretation of the data an arbitrary relationship (either empirical or associated with a rheological model) is often assumed a priori and the parameters are adjusted to the data by curve fitting techniques. The analysis of the data is normally done in terms of creep strains despite experimental evidences that suggest that creep strains are not accurately known due to the question of obtaining the proper zero reading. On the basis of these findings, the Author feels that the establishment of a standard way of analyzing creep data would provide means to compare the results of creep behavior either for the same rock group or within different groups.

Several constant axial load tests were carried out under triaxial conditions in order to assess the creep behavior of a fractured coal. The results were analyzed in terms of strain rate. This approach is more reliable since the strain rate value is not sensitive to error in the creep strains.

An empirical stress-strain-time relationship was obtained which described in a satisfactory manner the experimental data. A continuous decrease in strain rate with time was observed in all tests. This empirical relationship consists in the combination of a power law describing the dependence of the strain rate with time and an exponential law describing the dependence of the strain rate on the stress level.

This relationship was found to describe the experimental data in the range of 20-80% of the short-term strength and only three parameters are necessary to describe the material behavior. This is of great value from the engineering point of view due to the reduced number of parameters and the relatively large range of application. No attempt was made to attach any physical meaning to the parameters even though the time-exponent 'm' clearly indicates a 'strain-hardening' effect whereas the term '$Ae^{\bar{\alpha}}$' reflects the creep potential of the material.

Only one test was carried out up to a stress level where creep failure occurred. This test indicated that the strain rate was decreasing with time until the acceleration process occurred. This fact is in aggreement with previous observations both in rocks and soils. Another implication of this fact is the absence of a period of steady-state creep.

A series of multiple-stage creep tests was also described and an incremental form of the stress-strain-time relationship obtained from single-stage creep tests was found to fit the results very well. The use of this type of test to describe the creep properties must be explored in more depth due to its attractiveness in providing considerable information by using only one sample.

(c) <u>Analytical modelling of openings in creeping rocks</u>

The analytical capabilities to evaluate the time-dependent behavior of underground openings were discussed in Chapter 5. Several formulations have been presented and some were used to match results of observations. However, these formulations have failed to properly take into account the influence of the stress level on the time-dependent behavior.

Based on the empirical relationship obtained during the experiments, a solution procedure was formulated which included the elaboration of a 3-dimensional stress-strain-time relationship. In order to assess the validity of the assumptions made during the developments of the 3-dimensional relationship, this solution procedure was used to describe the behavior of a 12-cm opening in coal. The comparison between the predicted results and the measurements obtained by Guenot(1979) showed that both tunnel closure and rate of tunnel closure can be represented quite well by the solution procedure outlined in Chapter 6.

Due to the nature of this model test (load applied at the ends of the block) and the fractured nature of the coal, compressive radial creep strains were measured during the tests. These strains could not be reproduced by the solution procedure since the creep relationship used did not take into account the creep due to the hydrostatic component of the stress tensor. The correction procedure applied to the results predicted previously proved to be reasonable in order of magnitude and the changes in both tunnel closure and rate of tunnel closure did not modify the initial aggreement between predicted and measured deformations.

A modest parametric study was carried out in order to display some of the general features of the time-dependent behavior of an underground opening. For this study, all the cases were modelled as actual excavations, i.e., loads were reduced at the opening walls.

It is shown that the stress distribution around the opening changes with time and that this redistribution process is more pronounced the greater the creep properties of the medium. This dependence is by no means obvious due to the highly non-linear nature of the creep relationship. However, it is expected to reflect the combination of the system stiffness (represented by E-value), the creep parameters and the initial stress level. A unique relationship was shown to exist between the creep strain number, CSN, (defined as the ratio of the tunnel closure at t=1hr. and the tunnel closure at t=o) and the system creep potential, EK, (defined as the product $E.A.e^{\bar{\alpha}}$ where E=Young's modulus and A, $\bar{\alpha}$ = creep parameters) for the same initial stress level and $\bar{\alpha}$. This relationship is independent of the size of the opening and the Young's modulus.

The rate of tunnel closure was found to vary linearly with the time when plotted in a double log-scale with the results being also independent of E and the opening size. The predicted 'strain-hardening' for the relationship between rate of tunnel closure and time is very similar to the value obtained in the laboratory.

Even though the solution procedure is not general enough to consider cases other than circular openings and ratios between stresses differing from 1.0, the previous comparison suggests the validity of the approach and this procedure is bound to give good results when other solution methods are used such as finite elements in order to include more general cases.

7.2 Suggestions for further research

The investigation of the performance of available case-records must continue. Only through these observations can one assess the influence of the many factors on the overall behavior of the opening. The concept of modes of tunnel behavior can be used to classify the case-records and also to direct the attention to the questions associated with each mode and which must be addressed (see Figure 7.1). More effort must be spent when publishing or organizing data relevant to tunnel behavior by describing rock mass parameters (either Barton's or Bieniawski's) and both excavation sequence and lining strategy. The experience gained from previous excavations can only be readily used by other if the data are well codified. The use of the modes of ground behavior may be helpful in achieving this goal.

Even though much progress has been attained in the past, the knowledge about the rheological behavior of rock masses is still quite limited mainly due to the lack of experimental data covering stress systems other than uniaxial and triaxial compression. In particular, creep deformations must be recorded not only in one direction in order to evaluate the relationship between strains in principal directions and but also to assess the amount of volumetric creep. Experiments describing the time-dependent volumetric changes associated with a hydrostatic state of stress are of immediate need in order to both isolate the ammount of creep due to shear stress and to include the

1. **Characteristic of the mode**

   (i) mechanisms leading to this particular mode
   (ii) combination of factors which describes the mode, e.g, rock type, stress field, etc.

2. **Behavioral parameters associated to each mode**

   (i) tunnel closure, rate of tunnel closure (order of magnitude and pattern)
   (ii) warning parameters

3. **Excavation strategy associated with each mode**

   (i) excavation method
   (ii) type and time of lining installation

4. **Validity of analytical techniques**

   (i) type of required tests
   (ii) numerical modelling

5. **Remedial measures associated with each mode**

Figure 7.1 Questions associated with each mode of ground behavior relationship in analytical techniques. The cases of fractured rocks at low stress level as well as weathered rocks may be examples showing this need.

Both material modelling and analytical techniques must be extended to include the cases where the material around the opening is overstressed or fails immediately after excavation. These conditions are particularly important in weak ground (fault zones and weathered rocks) at medium to great depths. Studies on these aspects would contribute to the understanding of the factors such as optimum excavation sequence and lining strategy in order to minimize stability problems of both ground and lining structures.

The study of other aspects of the time-dependent behavior of openings such as 'stand-up' deserves special attention in the future. The analytical study must concentrate on the amount of creep strain which is actually tolerated by the material, in particular the tensile strains near the opening wall. This question is of particular importance when associated with the stability of unlined openings.

References

Afrouz,A. and Harvey,J.M.,1974. 'Rheology of rocks within the soft to medium strength range', Int. Journal of Rock Mech. and Min. Sci. & Geom. Abstracts, Vol.11, no.7, pp.281-290

Aiyer,A.K., 1969. "An Analytical Study of The Time-Dependent Behavior of Underground Openings " Ph.D. Thesis, Dept. of Civil Engineering, University of Illinois, Urbana, Illinois, 264pp.

Andrade,E.N. da C.,1910. 'On the viscous flow in metals, and allied phenomena',Proc. of the Royal Society Series A, Vol.84, pp.1-12

Austin,W.G. and J.W.Fabry, 1974. "Rock behavior studies during drill-blast and machine-bored tunnelling" Proc. 3rd. Cong. ISRM, Vol.II-B, pp.1242-1249

Baar,C.A., 1975. "The deformational behavior of salt rocks in-situ: hypothesis versus measurements" Bull. Int. Assoc. Engng. Geol., no.12, pp.65-72

Barron,K. and Toews,N.A., 1963. "Deformation around a mine shaft in salt" Proc. 2nd. Can. Rock Mech. Symp., Kingston, Ont., pp.115-134

Barton,N., R.Lien and J.Lunde, 1974. "Engineering classification of rock masses for the design of tunnel support" Norwegian Geot. Inst. Pub. No. 106, 48pp.

Barton,N., 1976a. "Recent experiences with the Q-system of tunnel support design" In: Proc. of the Symp. on Exploration for Rock Engineering, Johannesburg, Nov.1976, Vol.1, pp.107-117

Bawa,K.S. and A.Bumanis, 1972. "Design considerations for underground structures in rocks" Proc. 1st. RETC, Chicago, Vol.I, pp.393-417

Bieniawski,Z.T., 1974. "Geomechanics classification of rock masses and its application in tunnelling" Proc. 3rd. Int. Congr. Rock Mech., IRSM, Denver, Vol. II-A, pp.27-32

Bieniawski,Z.T., 1979. "Introductory lecture of a Short-Course on Tunnelling in Rocks" Unpublished notes, Penn. State Univ. May 22-25, 1979

Bieniawski,Z.T.,1967. "Mechanism of brittle fracture of rock", <u>International Journal of Rock Mechanics and Mining Sciences</u>, Vol.4, pp.395-430

Bieniawski,Z.T.,1970. 'Time-dependent behavior of fractured rock', <u>Rock Mechanics</u>, Vol.2, pp.123-137

Bishop,A.W. and Lovenbury,H.T.,1969. 'Creep characteristics of two undisturbed clays', Proc. of 7th. Int. Conf. on Soil Mech. and Found. Engineering, Mexico City, Vol.1, pp.29-37

Blake,W., 1972. "Rock-burst mechanics" <u>Quart. Colorado School of Mines</u>, Vol.67, no.1, 64pp.

Boresi,A.P. and Deere,D.U.,1963. 'Creep closure of a spherical cavity in an infinite medium with special applications to Project Dribble, Tatum Salt dome, Mississippi', for Holmes Narver, Inc., Las Vegas Division

Casagrande,A. and Wilson,S.D.,1951. 'Effect of rate of loading on the strength of clays and shales at constant water content', Geotechnique, Vol.2, pp.251-263

Chang,C-Y and Nair,K., 1973. "Developments and applications of theoretical methods for evaluating stability of openings in rock" Final report submitted to U.S. Bureau of Mines under contract No. H0220038

Chugh,Y.P.,1974. 'Viscoelastic behavior of geologic materials under tensile stress', Transactions A.I.M.E., Vol.256, pp.259-264

Conway,J.B.,1967. 'Numerical Methods for Creep and Rupture Analysis', Gordon and Breach, Sci. Publishers, 204pp.

Cook,N.G.W., Hoek,E., Pretorius,J.P.G., Ortlepp,W.D. and Salamon,M.D.G., 1966. "Rock mechanics applied to the study of rockbursts" Journal of S. Afr. Inst. Min. Metall., Vol.66, pp.435-528

Cook,N.G.W., 1973. "The siting of mine tunnels" Assoc. of Mine Managers, No.3/73

Cording,E.J. and J.W. Mahar, 1978. "Index properties and observations for design of chambers in rock" Engineering Geology, Vol.12, pp.113-142

Cording,E.J., A.J.Hendron Jr. and D.U.Deere, 1971. "Rock Engineering for underground caverns" Proc. Symp. on Underground Rock Chambers, ASCE, Phoenix, Arizona, pp.567-600

Cording,E.J., Mahar,J.W. and Brierley,G.S., 1977. "Observations for shallow chambers in rock" Proc. of Int. Symp. on Field Meas. in Rock Mechanics, Vol.II, pp.485-508

Cottrell,A.H.,1952. "The time laws of creep" _J. Mech. Phys. Solids_, Vol.1, pp.53-63

Cruden,D.M.,1969. 'A Laboratory Study of the Strain Behavior and Accoustic Emission of Stressed Rock', Ph.D. Thesis, Univ. of London

Cruden,D.M.,1970. 'A theory of brittle creep in rocks under uniaxial compression', _Journal of Geophysical Research_, Vol.75, No. 17, pp.3431-3442

Cruden,D.M.,1971a. 'The form of creep law for rock under uniaxial compression', _Int. Journal of Rock Mech. Min. Sci._, Vol.8, pp.105-126

Cruden,D.M.,1971b. 'Single-increment creep experiments on rock under uniaxial compression', _Int. Journal of Rock Mech. Min. Sci._, Vol.8, No.2, pp.127-142

Cruden,D.M.,1974. 'The static fatigue of brittle rock under uniaxial compression', _Int. Journal of Rock Mech. Min. Sci. & Geom. Abst._, Vol.11, No.2, pp.67-73

Daemen,J.J.K.,1975. "Tunnel Support Loading Caused by

Rock Failure", Ph.D. thesis in Civil Engineering, University of Minnesota

Deere,D.U., R.B.Peck, J.E.Monsees and B.Schmit, 1969. "Design of tunnel liners and support systems" National Tech. Inf. Service, PB 183799, 287pp.

Einstein,H.H. and Bischoff,N., 1975. "Design of tunnels in swelling rocks" Proc. 16th. Symp. on Rock Mechanics, publ. ASCE pp.185-195

Evans,I. and Pomeroy,C.D.,1966. "The Strength, Fracture and Workability of Coal",Pergamon Press

Evans,R.H., 1958. "Effect of rate of loading on some mechanical properties of concrete" in "The Mechanical Properties of Non-Metallic Brittle Materials", ed. W.H.Walton, Butterworths, London, 492pp.

Fluegge,W.,1967. "Viscoelasticity", Blaisdell Publishing Company

Fox,L., 1957. "The Numerical Solution of Two-Point Boundary Problems in Ordinary Differential Equations" Oxford, Clarendon Press, 371pp.

Gioda,G. and J.Ghaboussi, 1977. "A study of time-dependent behavior of tunnels" Technical Report No.1/77Dept. of Civil Eng., Univ. of Illinois at Urbana-Champaign, Urbana, Illinois, 66pp.

Griggs,D.T.,1939. 'Creep of rocks',<u>Journal of Geology</u> Vol.43, No.3, pp.225-251

Griggs,D.T.,1940. 'Experimental flow of rocks under conditions favouring recrystallization', Geol. Soc. America Bulletin, Vol.51, pp.1001-1022

Guenot,A.,1979. "Investigation of Tunnel Stability by Model Tests", M.Sc.Thesis, Department of Civil Engineering, University of Alberta

Hannafy,E.A., 1976. "Finite Element Simulation of Tunnel Excavation in Creeping Rock" M.Eng. Thesis, Dept. of Civil Engineering, McMaster University, 131pp.

Hardy,H.R.,1967. 'Determination of the inelastic parameters of geologic materials from incremental creep experiments', Proc. of 3rd. Conference on Drilling and Rock Mechanics, A.I.M.M.P.E., pp.105-120

Hayashi,M. and Hibino,S.,1968. "Progressive relaxation of rock masses during excavation of an underground cavity", Proceedings of the International Symposium on Rock Mechanics, Madrid, Spain, pp.343-349

Heard,H.C.,1963. 'The effect of large change of strain rate in the experimental deformation of rocks', Journal of Geology, Vol.71, No.2, pp.162-195

Hendron,A.J.,1968. 'Mechanical properties of rocks' in 'Rock Mechanics and Engineering Practice' edited by Stagg,K.C. and Zienkiewicz,O.C., London, 442pp.

Heuer,R.E. and Hendron,A.J.,1971. "Geomechanical model study of the behaviour of underground openings in rock subjected to static loads",U.S.Corps of Engineers Report N-69-1, Report 2, Contract No.

DACA39-67-C-0009

Hobbs,D.W.,1970. 'Stress-strain-time behavior of a number of coal measure rocks',Int. Journal Rock Mech. and Min. Sci., Vol.7, no.2, pp.259-264

Hoek,E. and E.T. Brown, 1978. "Underground Excavations in Rock" Restricted Circulation Draft, to be published by The Inst. of Min. and Met., London

Hudson,J.A. and Brown,E.T.,1973. "Studying time - dependent effects in failed rock", Fourteenth Symposium on Rock Mechanics, Pennsylvania State University, ASCE, pp.25-34

Jaeger,J.C. and Cook,N.G.W.,1969. 'Fundamentals of Rock Mechanics', Methuen and Co. Ltd., 515pp.

Kaiser,P.K. and Morgenstern,N.R.,1979. "Time-dependent deformation of jointed rock near failure", Proceedings of the Fourth International Congress on Rock Mechanics, Montreux, Switzerland, Vol.1, pp.195-202

Kaiser,P.K., 1979. "Time Dependent Behavior of Tunnels in Jointed Rock Masses" PhD thesis, Dept. of Civil Eng., Univ. of Alberta, 360pp.

King,M.S., 1974. "Creep in model pillars of Saskatchewan potash" Int. J. of Rock Mech. Min. Eng. & Geom. Abst., Vol.10, no.4, pp.363-371

Kranz,R.L. and Scholz,C.H.,1977. "Critical dilatant volume of rocks at the onset of tertiary creep", Journal of Geophysical Research, Vol.82, No.30, pp.4893-4898

Kulhawy,F.H., 1974. "Finite element modelling criteria for underground openings in rocks" Int. Journal of Rock Mech. and Mining Science & Geom. Abst., Vol.11, No.12, pp.465-472

Lacerda,W.A. and Houston,W.N.,1973. "Stress relaxation in soils", Proceedings of the Eighth International Conference on Soil Mechanics and Foundation Engineering, Moscow, USSR, pp.221-227

Ladanyi,B.,1974. "Use of the long-term strength concept in the determination of ground pressure on tunnel linings", Proceedings of the Third Congress of the International Society of Rock Mechanics, Denver, Colorado, Vol 2B, pp.1150-1156

Lauffer,H., 1958. "GebirgsKlassiferung fur den Stolenbau" Geologie und Bauwessen, Vol.24, pp.46-51

LeComte,P.,1965. 'Creep in rock salt', Journal of Geology, Vol.72, pp.469-484

Lee,C.F. and Klym,T.M., 1978. "Determination of rock squeeze potential for underground power projects" Engineering Geology, Vol.12, pp.181-192

Lindner,E., 1976. "Swelling rock: a review" Proc. Specialty Conf. on "Roch Eng. for Found. and Slopes", Boulder, Colo. ASCE, Vol.I, pp.141-181

Lo,K.Y., 1979. "Draft Working Document for Discussion - Task C - Identification of Problem Areas" ISRM Commission on on Swelling rock , Unpublished report

Lombardi,G. 1977. "Long term measurements in underground openings and their interpretation with special consideration to the rheological behavior of the rock" Proc. Int. Symp. on Field Measurements in Rock Mechanics, Zurich, April 4-6, Vol.II, pp.839-858

Lombardi,G., 1970. "The influence of rock characteristics on the stability of rock cavities" Tunnels and Tunnelling, Vol.2, No.2, pp.19-22 and No.3, pp.104-109

Mitchell,J.K. et al.,1967. 'Soil creep as a rate process',Journal of Soil Mech. and Found. Div., ASCE, Vol.94, No. SM1, pp.231-253

Mitchell,J.K. et al.,1969. 'Bonding, effective stress and strength of soils', Journal of Soil Mech. and Found. Div., ASCE, Vol.95, SM5, pp.1219-1246

Mitchell,J.K.,1975. 'Fundamentals of Soil Behavior', John Wiley and Sons, Inc., 422pp.

Murayama,S. and Shibata,T.,1958. 'On the rheological characteristics of clays',Part I, Bulletin No.26, Disaster Prevention Res. Institute,Kyoto, Japan (cited in Mitchell,1975)

Murayama,S. and Shibata,T.,1961. 'Rheological properties of clays', Proc. 5th. Int. Conf. Soil Mech. and Found. Eng., Paris, Vol.I, pp.269-273

Myer,L.R., Brekke,T.L., Korbin,G.E., Kavazangian,E. and Mitchell,J.K., 1977. "Stand up time of tunnels in squeezing ground" Final report, DOT OS 50108, U.S.

Dept. of Transportation, Vol.I

Nair,K. and Boresi,A.P.,1970. "Stress Analysis for time-dependent problems in rock mechanics", Proceedings of the International Society for Rock Mechanics, Beograd, Vol.2, paper 4-21

Nair,K., Sandhu,R.S. and Wilson,E.L.,1968. "Time-dependent analysis of underground cavities under an arbitrary initial stress field", Tenth Symposium on Rock Mechanics, Texas, Chapter 27, pp.699-730

Nakano,R.,1979. "Geotechnical properties of mudstone of Neogene Tertiary in Japan with special reference to the mechanism of squeezing swelling rock pressure in tunneling", International Symposium on Soil Mechanics, Mexico, Vol.1, pp.75-92

Noonan,D.K.J.,1972. "Fractured Rock Subjected to Direct Shear", M.Sc.Thesis,Department of Civil Engineering, University of Alberta, Edmonton

Odqvist,F.K.G., 1966. "Mathematical Theory of Creep and Creep Rupture" Oxford, Clarendon Press, 170pp.

Osmanagic,M. and Jasarevic,I., 1976. "Stresses and strains around underground openings in rock with viscous elasto plastic properties" Proc. of Int. Symp. on Investigations of Stress in Rock , Sydney, Aust., pp.107-114

Pearson,G.R.,1959. "Coal reserves for strip mining, Wabamun Lake District Alberta", Research Council of

Alberta, Geology Division, Preliminary Report 59-1, 37pp.

Peng,S.S. and Podnieks,E.R.,1972. "Relaxation and the behaviour of failed rock", International Journal of Rock Mechanics and Mining Sciences, Vol.9, No.6, pp.699-712

Penny,R.K. and Marriott,D.L., 1971. "Design for Creep" , McGraw-Hill, New York, 291pp.

Pomeroy,C.D.,1956. "Creep in coal at room temperature", Nature, Vol.178, pp.279-280

Potts,E.L.J.,1964. 'An investigation into the design of room and pillar workings in rock salt', Min. Eng., No.49, pp.27-44

Price,N.J.,1964. 'A study of time-strain behavior in Coal Measure rocks', Int. Journal of Rock Mech. Min. Sci., Vol.1, no.2, pp.277-303

Pushkarev,V.I. and Afanesev,B.G.,1973. "A rapid method of determining the long-term strength of weak rocks", Soviet Mining Science, Vol.9, pp.558-560

Rabcewicz,L.v. and J.Golser, 1974. "Application of the NATM to the underground works at Tarbela" Water PowerVol.26, No.9, pp.314-321 (part I) and Vol.26, No.10, pp.330-335 (part II)

Robertson,E.C.,1960. 'Creep of Solenhofen limestone under moderate hydrostatic pressure', Geol. Soc. of America, Memoir 79, pp.227-244

Robertson,E.G.,1964. 'Viscoelasticity of rocks', Proc.

of the Int. Conf. State of Stress in the Earth's Crust , pp.180-224

Roggensack,W.D.,1977. 'Geotechnical Properties of Fine-Grained Permafrost Soils', Ph.D. Thesis, Dept. of Civil Engineering, University of Alberta, 449pp.

Sangha,C.M. and Dhir,R.K.,1972. 'Influence of time on the strength, deformation and fracture properties of a lower devonian sandstone', Int. Journal of Rock Mech. Min. Sci., Vol.9, No.3, pp.343-354

Scholz,C.H.,1968. 'Mechanism of creep in brittle rocks', Journal of Geophysical Research, Vol.73, No.10, pp.3295-3302

Semple,R.M., Hendron,A.J. and Mesri,G., 1973. "The effect of time dependent properties of altered rock on tunnel support requirements" Report FRA-ORDD-74-30, Dept. of Civil Eng., Univ. of Illinois, also NTIS PB 230307

Serata,S., 1968. "Application of continnum mechanics to deep potash mines in Canada" Int. J. Rock Mech. and Mining Sci., Vol.5, pp.293-314

Singh,A. and Mitchell,J.K.,1968. 'General stress-strain-time functions for soils', Journal of the Soil Mech. and Found. Div., A.S.C.E., Vol.94, no.SM1, pp.21-46

Singh,D.P.,1970. 'A study of time-dependent properties and other properties of rocks', Ph.D. thesis, Univ. of Melbourne, Melbourne, 219pp.

Sperry,P.E. and R.E.Heuer, 1972. "Excavation and support of Navajo tunnel no. 3" Proc. 1st. RETC, Vol.I, pp.539-571

Terzaghi,K., 1946. in: "Rock Tunnelling with Steel Supports" Proctor and White, ed., Commercial Shearing and Stamping,Co., Youngstown, Ohio, 292pp.

Tobolski,A.V., 1960. "Properties and Structures of Polymers" J. Wiley and Sons., 331pp.

Vialov,S.S. and Skibitsky,A.M.,1961. 'Problems of the Rheology of soils', Proc. 5th. Int. Conf. Soil Mech. and Found. Eng., Paris, Vol.I, pp.387-391

Vialov,S.S., 1970. "Creep in rocks" Proc. of 2nd. Cong. ISRM, Belgrade, Vol.1, pp.305-312

Ward,W.H., D.J.Coats and P.Tedd, 1976. "Performance of tunnel support in the Four Fathom Mudstone" Tunnelling 76, M.J.Jones, ed., pp.329-340

Ward,W.J., 1978. "Ground support for tunnels in weak rock" Rankine lecture in Geotechnique, Vol.28, No.2, pp.135-171

Wawersik,W.R. and Brown,W.S., 1973. "Creep fracture of rock" Report No. UTEC-ME-73-197, Mech. Eng. Dept., Univ. Utah, Salt Lake City, July

Wawersik,W.R.,1973. "Time-dependent rock behaviour in uniaxial compression", Proceedings of the Fourteenth Symposium on Rock Mechanics, Pennsylvania, pp.85-106

Wawersik,W.R.,1974. 'Time-dependent behavior of rock in compression', Proc. 3rd. Cong. ISRM, Vol. 2A, pp.357-363

Whalstrom,E.E., 1973. "Tunnelling in Rock" Series Development in Geot. Engineering, Vol.3, Elsevier Scientific Publ. Co., 250pp.

Wiid,B.L.,1970. 'The influence of moisture on the pre-rupture fracturing of two rock types', Proc. 2nd. Congress ISRM, Belgrade, Vol.2, pp.239-245

Winkle,B.v, 1970. "Time-dependent Analysis of Rock Mechanics Problems" Ph.D. Thesis, Dept. of Civil Engineering, Univ. of Colorado, 167pp.

Wittke,W. and Rissler,P., 1976. "Dimensioning of the lining of underground openings in swelling rock applying the finite element method" Publ. Inst. Found. Eng., Soil Mech., Rock Mech. and Water Ways Const., RWTH Aachen, Vol.2, pp.7-48

Wittke,W., 1978. "Fundamentals for the design and construction of tunnels located in swelling rock and their ... " Inst. Found. Eng., Soil Mech., Rock Mech. and Water Ways Const.,RWTH Aachen, Vol.6, 131pp.

Wu,T.H. et al.,1978. 'Creep deformation of clays',<u>Proc. of ASCE, Journal of the Geot. Eng. Div.</u>, Vol.104, GT1, pp.61-76

Zienkiewicz,O.C., 1977. "The Finite Element Method" McGraw-Hill Book Co., 3rd. Edition, 787pp.

Uncited references

Ayres,M.O., 1969. "Case history - Berkeley Hills twin transit tunnels" Proc. 2nd. Symp. on Rapid Excavation, Sacramento H.C.Hartman, ed., pp.10-26 to 10-37

Bowen,C.F.P., F.I.Hewson, D.H.MacDonald and R.G.Tanner, 1976. "Rock squeeze at Thorold tunnel" Can. Geot. Journal, Vol.13, no.2, pp.111-126

Brekke,T.L. and Howard,T.R., 1972. "Stability problems caused by seams and faults" Proc. 1st. RETC, Eds. K.S. Lane and L.A. Garfield, Vol.1, pp.25-39

Crocker,E.R., 1955. "Hottest wettest tunnel holed through" Civil Engineering, ASCE, March,

Czurda,K. and Quigley,R.M., 1973. "Cracking of a concrete tunnel in the Meaford-Dundas Formation" Research report SM-3-73, Faculty of Engineering Science, University of Western Ontario, Canada

Dubnie,G.F. and Geller,L., 1975. "Canadian tunnel register" Report DS75-9, Tunnelling Office of Canada, EMR, Ottawa, Canada

Franklin,J.A., 1976. "Rock stresses in Canada, their relevance to engineering projects" Proc. 25th. Geomechanical Colloquy, Salzburg, Austria

Hogg,A.D., 1959. "Some engineering studies on rock movement in the Niagara area" Engineering Geology

Case-Histories No.3, Geological Society of America, pp.1-12

Lee,C.F. and Lo,K.Y., 1976. "Rock squeeze study of two deep excavations at Niagara Falls" ASCE Specialty Conference on Rock Engineering, Boulder, Colorado, Vol.1, pp.116-140

Lo,K.Y. and J.D.Morton, 1976. "Tunnels in bedded rock with high horizontal stresses" Can. Geotechnical Journal, Vol.13, no.3, pp.216-230

Lo,K.Y. and Yuen,C.M.K., 1978. "Stress measurements in rock at Heart Lake Tunnel" Repot No. GEOT-4-78, Faculty of Engineering Science, University of Western Ontario, Canada

Lo,K.Y., Devata,M. and Yuen,C.M.K., 1979. "Performance of a shallow tunnel in shaly rock with high horizontal stresses" Proceedings of Tunnelling'79, London, March

Lo,K.Y., Lee,C.F., Palmer,J.H.L. and Quigley,R.M., 1975. "Stress relief and time-dependent deformations of rocks in Southern Ontario" Research Report to the National Research Council of Canada, Special Research Grant No. 5-7307

Lo,K.Y., 1978. "Regional distribution of in situ horizontal stresses in rocks in Southern Ontario" Canadian Geotechnical Journal, Vol.15, No.3, pp.371-381

Morton,J.D., K.Y.Lo and D.J.Belshaw, 1975. "Rock performance considerations for shallow tunnels in bedded shales with high lateral stresses" Proc. 12th. Can. Rock Mech. Symp., Kingston, Ont.

Quigley,R.M., Thompson,C.D. and Fedorkiw,J.P., 1978. "A pictorial case history of lateral rock creep in an open cut into Niagara Scarpment rocks at Hamilton, Ontario" Canadian Geotechnical Journal, Vol.15, No.1, pp.128-133

Rabcewicz,L.v., 1975. "Tunnel under Alps uses new cost saving lining method" Civil Eng., ASCE, Vol.45, no.10, pp.69-74

Sandborn,J.F., 1950. "Engineering geology in the design and construction of tunnels" Berkey Volume, Geological Society of America, New York

Smith,C.B., 1905. "Construction of Canadian Niagara Company's 100,000 h.p. hydroelectric plant at Niagara Falls, Ontario" Transactions, Canadian Society of Civil Engineers, Vol.19

Trefzger,R.E., 1966. "Tecolote tunnel" Eng. Geology in Southern California, Assoc. of Eng. Geologists, Los Angeles

Varello,P.J., 1970. "Difficult excavation at Carley Porter tunnell" Civil Engineering, ASCE, June

Widerhofer,R., 1972a. "Methods of recent Japanese tunnel constructions through ground of expansive character" International Symposium on Underground Openings, Lucerne, pp.146-161

Widerhofer,R., 1972b. "Ground pressure measurements and interpretation of the results of recent Japanese tunnel constructions" International Symposium on Underground Openings, Lucerne, pp.526-537

Wilson,R.R. and H.S. Mayeda, 1969. "The first & second Los Angeles Aqueducts" Eng. Geology in Southern California, Assoc. of Eng. Geologists, New York

Appendix A

Development of governing differential equation

General

In the following, a differential equation is developed which describes the time-dependent change in stresses as well as the time-dependent deformations for a circular unlined opening in an isotropic and homogeneous material subjected to a hydrostatic state of stress. Two-dimensional, plane strain and axisymmetric conditions are also assumed.

To solve a time-dependent boundary problem, both compatibility and equilibrium equations must be valid at all times. For the case of small displacements these equations are described as (A.1) and (A.2) for the conditions imposed above.

$$\varepsilon_r = \varepsilon_\theta + r \frac{d\varepsilon_\theta}{dr} \qquad \text{....(A.1)}$$

$$\frac{d\sigma_r}{dr} + \frac{1}{r}(\sigma_r - \sigma_\theta) = 0 \qquad \text{....(A.2)}$$

In the above equations, ε_r and ε_θ are the total strains at the radial and tangential directions and σ_r and σ_θ are the total stresses at the same directions. The longitudinal total strain, ε_z , is assumed to be zero at all times. It is also assumed that at any particular instant of time, t, the creep strains are such that volumetric strains due to creep caused by shear stress may occur and are described by equation (A.3) below.

$$\bar{\varepsilon}_r + \bar{\varepsilon}_\theta + \bar{\varepsilon}_z = k\,\bar{\varepsilon}_\theta \qquad \text{....(A.3)}$$

where $\bar{\varepsilon}_r$, $\bar{\varepsilon}_\theta$ and $\bar{\varepsilon}_z$ are creep strains at radial, tangential and longitudinal direction respectively and 'K' is a proportionality parameter assumed constant.

Governing differential equation

Consider the i-th time increment, Δt, such that $t_i = t_{i-1} + \Delta t$. At the end of the (i-1)-th time increment, $(\sigma_r)_{i-1}$ and $(\sigma_\theta)_{i-1}$ are the current total stresses and $(\varepsilon_r)_{i-1}$ and $(\varepsilon_\theta)_{i-1}$ are the current total strains which include both a time-independent and a time-dependent component. Assuming that the time-independent component can be described by the theory of elasticity, it follows that:

$$(\varepsilon_r)_{i-1} = (\varepsilon_r)^e_{i-1} + (\varepsilon_r)^c_{i-1} \qquad \ldots .(A.4)$$

$$(\varepsilon_\theta)_{i-1} = (\varepsilon_\theta)^e_{i-1} + (\varepsilon_r)^c_{i-1} \qquad \ldots .(A.5)$$

During the i-th time increment, there will be a change in stresses which are followed by both elastic and creep deformations. These changes will occur in every direction, i.e., radial, tangential and longitudinal. If $\Delta\sigma_r$, $\Delta\sigma_\theta$ and $\Delta\sigma_z$ are the changes in stresses during this time increment, it follows from the elastic theory that the time-independent components are:

$$(\Delta\varepsilon_r)^e = \frac{1}{E}\left[\Delta\sigma_r - \nu\,(\Delta\sigma_\theta + \Delta\sigma_z)\right] \qquad \ldots .(A.6)$$

$$(\Delta\varepsilon_\theta)^e = \frac{1}{E}\left[\Delta\sigma_\theta - \nu\,(\Delta\sigma_r + \Delta\sigma_z)\right] \qquad \ldots .(A.7)$$

$$(\Delta\varepsilon_z)^e = \frac{1}{E}\left[\Delta\sigma_z - \nu\,(\Delta\sigma_r + \Delta\sigma_\theta)\right] \qquad \ldots .(A.8)$$

From plane strain considerations, it follows that $\Delta\varepsilon_z = 0$ or,

$$(\Delta\varepsilon_z)^e + (\Delta\varepsilon_z)^c = 0 \qquad \text{....(A.9)}$$

In addition, the Author has introduced the possibility of volumetric change due to creep caused by shear stress. This has been done by assuming that the creep strain increments in the radial and longitudinal directions can be written in terms of the tangential creep strain increment as follows:

$$(\Delta\varepsilon_r)^c = -p_n(\Delta\varepsilon_\theta)^c \qquad \text{....(A.10)}$$

$$(\Delta\varepsilon_z)^c = -p_m(\Delta\varepsilon_\theta)^c \qquad \text{....(A.11)}$$

where pn and pm are assumed as constants. Due to the lack of experimental results describing this type of relationship, the expressions (A.10) and (A.11) are considered to be acceptable for initial discussions. More investigations can be made and these expressions may be changed without many additional complications.

Applying equations (A.1) and (A.2), i.e., compatibility and equilibrium equations, at the end of the i-th time increment, it follows that:

$$(\varepsilon_r)_{i-1} + (\Delta\varepsilon_r) = (\varepsilon_\theta)_{i-1} + \Delta\varepsilon_\theta + r\frac{d}{dr}\left[(\varepsilon_\theta)_{i-1} + \Delta\varepsilon_\theta\right] \qquad \text{....(A.12)}$$

$$\frac{d}{dr}\left[(\sigma_r)_{i-1} + \Delta\sigma_r\right] + \frac{1}{r}\left[(\sigma_r)_{i-1} + \Delta\sigma_r - (\sigma_\theta)_{i-1} - \Delta\sigma_\theta\right] = 0 \qquad \text{....(A.13)}$$

Equations (A.13) and (A.14) can both be rewritten as:

$$(\varepsilon_r)_{i-1} - (\varepsilon_\theta)_{i-1} - r\frac{d}{dr}\left[(\varepsilon_\theta)_{i-1}\right] + \Delta\varepsilon_r = \Delta\varepsilon_\theta + r\frac{d}{dr}(\Delta\varepsilon_\theta) \qquad \text{....(A.14)}$$

$$\frac{d}{dr}(\sigma_r)_{i-1} + \frac{1}{r}\left[(\sigma_r)_{i-1} - (\sigma_\theta)_{i-1}\right] + \frac{d}{dr}(\Delta\sigma_r) + \frac{1}{r}\left(\Delta\sigma_r - \Delta\sigma_\theta\right) = 0 \qquad \text{....(A.15)}$$

As both the strains and stresses at the end of the (i-1)th time-increment obey the compatibility and equilibrium equations, equations (A.14) and (A.15) can be further simplified to:

$$\Delta\varepsilon_r = \Delta\varepsilon_\theta + r\frac{d}{dr}\left(\Delta\varepsilon_\theta\right) \qquad \ldots.(A.16)$$

$$\frac{d}{dr}\left(\Delta\sigma_r\right) + \frac{1}{r}\left(\Delta\sigma_r - \Delta\sigma_\theta\right) = 0 \qquad \ldots.(A.17)$$

where $\Delta\varepsilon_r$ and $\Delta\varepsilon_\theta$ are the total strain increments during Δt and $\Delta\sigma_r$ and $\Delta\sigma_\theta$ are the change in stresses during Δt. Equation (A.16) can be further developed as:

$$(\Delta\varepsilon_r)^e + (\Delta\varepsilon_r)^c = (\Delta\varepsilon_\theta)^e + (\Delta\varepsilon_\theta)^c + r\frac{d}{dr}\left[(\Delta\varepsilon_\theta)^e + (\Delta\varepsilon_\theta)^c\right] \qquad \ldots.(A.18)$$

where the superscripts 'e' and 'c' mean elastic and creep respectively. Combining (A.6) and (A.7) into (A.18), it follows that:

$$\frac{1}{E}\left[\Delta\sigma_r - \nu(\Delta\sigma_\theta + \Delta\sigma_z)\right] + (\Delta\varepsilon_r)^c = \frac{1}{E}\left[\Delta\sigma_\theta - \nu(\Delta\sigma_r + \Delta\sigma_z)\right]$$

$$+ \quad (\Delta\varepsilon_\theta)^c + \frac{r}{E}\frac{d}{dr}\left[\Delta\sigma_\theta - \nu(\Delta\sigma_r + \Delta\sigma_z)\right] + r\frac{d}{dr}(\Delta\varepsilon_\theta)^c \qquad \text{....(A.19)}$$

Combining equations (A.8), (A.9) and (A.11) it follows that:

$$\Delta\sigma_z = \nu(\Delta\sigma_r + \Delta\sigma_\theta) + P_m E(\Delta\varepsilon_\theta)^c \qquad \text{....(A.20)}$$

Using (A.20) and (A.10) into (A.19), the following expression can be obtained:

$$\frac{(1+\nu)}{E}\left[\Delta\sigma_r - \Delta\sigma_\theta\right] = (1+P_n)(\Delta\varepsilon_\theta)^c + \frac{r}{E}(1-\nu^2)\frac{d}{dr}(\Delta\sigma_\theta)$$

$$- \frac{\nu r}{E}(1+\nu)\frac{d}{dr}(\Delta\sigma_r) + r(1-P_m\nu)\frac{d}{dr}(\Delta\varepsilon_\theta)^c \qquad \text{....(A.21)}$$

The creep strain increment , $(\Delta\varepsilon_\theta)^c$, during the time increment is estimated by assuming that the stresses at the time $(t_{i-1} + \Delta t/2)$ remain constant during the time interval and also that these stresses can be approximated by $(\sigma_r + \Delta\sigma_r/2)$ and $(\sigma_\theta + \Delta\sigma_\theta/2)$. Additionally, the time-strain hardening is assumed to be valid in order to describe the effects of the previous strain history on the creep behavior of materials. Based on these considerations and also on the fact that creep strain rates depend on the current stress level it follows that:

$$(\Delta\varepsilon_\theta)^c = A\, e^{\bar{\alpha}\,\bar{\sigma}_i} \left(t_{i-1} + \frac{\Delta t}{2}\right)^{-m} \cdot \Delta t \qquad \ldots.(A.22)$$

where 'A',' $\bar{\alpha}$ ', and 'm' are creep parameters (see Chapter 4 for discussions on the creep law) and $\bar{\sigma}_i$ represents the current stress level. Finally, using (A.17) and (A.22) into (A.21), it follows that:

$$-\frac{r^2(1-\nu^2)}{E}\frac{d^2}{dr^2}(\Delta\sigma_r) - 3r\,\frac{(1-\nu^2)}{E}\frac{d}{dr}(\Delta\sigma_r) = (1+p_n)\,A e^{\bar{\alpha}\bar{\sigma}_i}\left(t_{i-1}+\frac{\Delta t}{2}\right)^{-m}\Delta t\; +$$

$$+\; r(1-p_m\nu)A\bar{\alpha}\, e^{\bar{\alpha}\bar{\sigma}_i}\left(t_{i-1} + \frac{\Delta t}{2}\right)^{-m}\cdot \Delta t \cdot \frac{d}{dr}\bar{\sigma}_i \qquad \ldots.(A.23)$$

Equation (A.23) constitutes the governing differential equation for the time-dependent boundary-value problem.

This equation can be further extended by substituting the stress level, $\bar{\sigma}_i$, by its proper value. Assuming that the Mohr-Coulomb criterion is valid, it follows that:

$$\bar{\sigma}_i = \frac{2\left\{(\sigma_\theta)_{i-1} - (\sigma_r)_{i-1}\right\} + (\Delta\sigma_\theta) - (\Delta\sigma_r)}{4\, c\cos\phi + 2\sin\phi\left\{(\sigma_\theta)_{i-1} + (\sigma_r)_{i-1}\right\} + \sin\phi\left\{\Delta\sigma_\theta + \Delta\sigma_r\right\}} \quad \text{....(A.24)}$$

where c and ϕ are the shear stength parameters. Equation (A.24) can be rewritten as:

$$\bar{\sigma}_i = \frac{k_1 + \Delta\sigma_\theta - \Delta\sigma_r}{k_2 + \sin\phi\left(\Delta\sigma_\theta + \Delta\sigma_r\right)} \quad \text{....(A.25)}$$

where:

$$k_1 = 2\left\{(\sigma_\theta)_{i-1} - (\sigma_r)_{i-1}\right\}$$

$$k_2 = 4c\cos\phi + 2\sin\phi\left\{(\sigma_\theta)_{i-1} + (\sigma_r)_{i-1}\right\}$$

Also equation (A.23) can be rewritten as:

$$-k_3 \frac{d^2}{dr^2}(\Delta\sigma_r) - k_4 \frac{d}{dr}(\Delta\sigma_r) = k_5\, e^{\bar{\alpha}\bar{\sigma}_i} + k_6\, e^{\bar{\alpha}\bar{\sigma}_i} \frac{d}{dr}\bar{\sigma}_i \qquad \text{....(A.26)}$$

where:

$$k_3 = r^2(1-\nu^2)/E$$

$$k_4 = 3r\,(1-\nu^2)/E$$

$$k_5 = (1+p_n)\,A\,(t_{i-1} + \Delta t/2)^{-m}\,\Delta t$$

$$k_6 = r\,(1-p_m\nu)\,A\,\bar{\alpha}\,(t_{i-1} + \Delta t/2)^{-m}\,\Delta t$$

To further extend equation (A.26), the term $\frac{d}{dr}\bar{\sigma}_i$ has to be calculated. Thus, using (A.24) it follows that:

$$\frac{d\bar{\sigma}_i}{dr} = \frac{\left[\frac{dk_1}{dr} + \frac{d}{dr}(\Delta\sigma_r) + r\frac{d^2}{dr^2}(\Delta\sigma_r)\right]\left[k_2 + \sin\phi\left\{2\Delta\sigma_r + r\frac{d}{dr}\Delta\sigma_r\right\}\right]}{k_{10}^{\,2}} -$$

$$- \frac{\left[k_1 + r\frac{d}{dr}\Delta\sigma_r\right]\left[\frac{dk_2}{dr} + \sin\phi\left\{3\frac{d}{dr}\Delta\sigma_r + r\frac{d^2}{dr^2}\Delta\sigma_r\right\}\right]}{k_{10}^{\,2}} \qquad \text{....(A.27)}$$

where

$$K_{10} = k_2 + \sin\phi \left\{ \Delta\sigma_r + r \frac{d}{dr} \Delta\sigma_r \right\}$$

Equation (A.27) can be rewritten as:

$$\frac{d\bar{\sigma}_i}{dr} = \frac{k_7 \frac{d}{dr}\Delta\sigma_r + k_8 \left\{ \frac{d}{dr}\Delta\sigma_r \right\}^2 + k_9 \frac{d^2}{dr^2}\Delta\sigma_r + k_{14}}{k_{10}^{\,2}} \qquad \ldots.(A.28)$$

where:

$$k_7 = r \sin\phi \frac{dk_1}{dr} + k_2 + 2\,\Delta\sigma_r \sin\phi - 3k_1 \sin\phi - r \frac{dk_2}{dr}$$

$$k_8 = -\,2r\sin\phi$$

$$k_9 = k_2\, r + 2r\sin\phi\,\Delta\sigma_r - r\,k_1 \sin\phi$$

$$k_{14} = k_2 \left(\frac{dk_1}{dr}\right) + 2\sin\phi \left(\frac{dk_1}{dr}\right) \Delta\sigma_r - k_1 \left(\frac{dk_2}{dr}\right)$$

Using equation (A.28) into (A.26), it follows that:

$$-k_3 \frac{d^2}{dr^2}\Delta\sigma_r - k_4 \frac{d}{dr}\Delta\sigma_r = k_5\, e^{\bar{\alpha}\bar{\sigma}_i} +$$

$$+ k_6\, e^{\bar{\alpha}\bar{\sigma}_i} \left[\frac{k_7 \frac{d}{dr}\Delta\sigma_r + k_8 \left\{ \frac{d}{dr}\Delta\sigma_r \right\}^2 + k_9 \frac{d^2}{dr^2}\Delta\sigma_r + k_{14}}{k_{10}^{\,2}} \right] \qquad \ldots.(A.29)$$

or,

$$k_{11} \frac{d^2}{dr^2} \Delta\sigma_r + k_{12} \frac{d}{dr} \Delta\sigma_r = k_{13} \qquad \text{....(A.30)}$$

where:

$$k_{11} = -k_3 - \frac{k_6 \cdot k_9 \cdot e^{\bar{\alpha}\bar{\sigma}_i}}{k_{10}^2}$$

$$k_{12} = -k_4 - \frac{k_6 \cdot k_7 \cdot e^{\bar{\alpha}\bar{\sigma}_i}}{k_{10}^2}$$

$$k_{13} = k_5\, e^{\bar{\alpha}\bar{\sigma}_i} + k_6\, e^{\bar{\alpha}\bar{\sigma}_i} \left[\frac{k_8 \left\{ \frac{d}{dr} \Delta\sigma_r \right\}^2 + k_{14}}{k_{10}^2} \right]$$

Equation (A.30) represents the short form of the governing differential equation which describes the change in radial stress with time. To evaluate the components $\Delta\sigma_\theta$, $\Delta\sigma_z$ and $(\Delta\epsilon_r)$ and $(\Delta\epsilon_\theta)$, equations (A.2), (A.22) and (A.6) through (A.8) have to be used.

Appendix B

Computer program to integrate the developed differential equation

In the following, a computer program is described and its listing presented, where the differential equation (A.30) described in Appendix A is integrated numerically.

```
C**********************************************************************
C   CYLINDRICAL OPENING: PROGRAM FOR TIME-DEPENDENT STRESS AND STRAIN  *
C                         DISTRIBUTION - CASE 1
C**********************************************************************
      IMPLICIT REAL*8(A-H,O-Z)
      DIMENSION R(200),STRR(200),STRT(200),STRNR(200),STRNT(200),
     1          Y(200),DY(200),YY(200),STLEV(200),A(200),B(200),
     2          C(200),D(200),STRZ(200),STRNZ(200)
      REAL*8 K1,K2,K3,K4,K5,K6,K7,K8,K9,K11,K10,K12
      REAL*8 K13,K14,K15
C**********************************************************************
C*                      LIST OF INPUT DATA                             *
C*                                                                     *
C* RD  = RADIUS OF OPENING(METERS)                                     *
C* EPRES = EXTERNAL PRESSURE (KG/CM**2)                                *
C* E     = YOUNG'S MODULUS (KG/CM**2)                                  *
C* PR    = POISSON'S RATIO                                             *
C* CHO   = SHORT-TERM COHESIVE COMPONENT OF SHEAR STRENGTH ENVELOPE    *
C*         (KG/CM**2)                                                  *
C* PHIO  = SHORT-TERM FRICTIONAL COMPONENT OF SHEAR STRENGTH ENVELOPE  *
C* AAO,ALPO = CREEP PARAMETERS FOR STRESS LEVEL LESS THAN .25          *
C*            AAO (MIN-1)                                              *
C* AA1,ALP1 = CREEP PARAMETERS FOR STRESS LEVEL BETWEEN.25 AND .80     *
C*            AA1 (MIN-1)                                              *
C* AA2,ALP2 = CREEP PARAMETERS FOR STRESS LEVEL GREATER THAN .80       *
C*            AA2 (MIN-1)                                              *
C* XM        = TIME EXPONENT                                           *
C* XM1      = PARAMETER DESCRIBING LOSS OF SHEAR STRENGTH WITH TIME    *
C*  H       = THICKNESS OF F.D. MESH                                   *
C* DT       = TIME INTERVAL (MIN)                                      *
C* TMAX     = MAXIMUM TIME FOR SOLUTION (MIN)                          *
C* IMAX     = NO. MAXIMUM OF ITERATIONS                                *
C* ICASE    = PARAMETER DESCRIBING LOADING CASE                        *
C*          = 1 SIMULATING EXCAVATION- INFINITE CASE                   *
C*          = 2 LOAD APPLIED EXTERNALLY- INFINITE CASE                 *
C*          = 3 SIMULATING EXCAVATION   - HOLLOW CYLINDER              *
C*          = 4 LOAD APPLIED EXTERNALLY - HOLLOW CYLINDER              *
C*                                                                     *
C**********************************************************************
      READ(5,500) RD,RD1,EPRES,E,PR,CHO,PHIO
      READ(5,505) AAO,ALPO,AA1,ALP1
      READ(5,507) AA2,ALP2,XM,XM1
      READ(5,510) H,DT,TMAX,IMAX
      READ(5,508) PN,PM
  508 FORMAT(2F10.4)
      READ(5,506) ICASE
  506 FORMAT(I3)
      WRITE(6,700)
      IF(ICASE.EQ.1) GO TO 1
      IF(ICASE.EQ.2) GO TO 2
      IF(ICASE.EQ.3) GO TO 3
      WRITE(6,705)
      GO TO 4
    1 WRITE(6,702)
      GO TO 4
    2 WRITE(6,701)
      GO TO 4
    3 WRITE(6,706)
    4 CONTINUE
      ROMAX=5.*RD
```

```
      IF(ICASE.GE.3) RDMAX=RD1
      WRITE(6,703) RD,RDMAX,EPRES
      WRITE(6,704) CHO,PHIO,AA1,ALP1,XM,E,PR
      WRITE(6,707) AAO,ALPO,AA2,ALP2
  707 FORMAT(2(2X,E15.8,2X,F10.4))
C
C
      PHIO=PHIO*3.1416/180.
      PHI=PHIO
C
C** DEFINITION OF FINITE DIFFERENCE MESH
C** H = THICKNESS MUST BE SELECTED SUCH THAT
C** RDMAX - RD IS A MULTIPLE OF H
C
      I=1
   11 R(I)=RD+H*FLOAT(I-1)
      IF(R(I).GT.RDMAX) GO TO 10
      I=I+1
      GO TO 11
   10 N=I-1
      NN=N-1
C
C
      TO=O.
      WRITE(1,790) NN,RD,EPRES
  790 FORMAT(I4,2F10.2)
      WRITE(1,800) TO
C
C
C
      IF(ICASE.EQ.1.OR.ICASE.EQ.2) GO TO 7
      GO TO 8
C******************************
C** STRESSES FOR INFINITE CASE *
C******************************
    7 DO 100 I=1,N
      AUX=(RD**2)/(R(I)**2)
      STRR(I)=EPRES*(1.-AUX)
      STRT(I)=EPRES*(1.+AUX)
      STRZ(I)=2.*EPRES*PR
      IF(ICASE.LE.1) GO TO 16
      IF(ICASE.GE.2) GO TO 12
      WRITE(6,601)
  601 FORMAT(5X,'ERROR INPUT DATA CHECK ICASE VALUE END OF EXECUTION')
      STOP
C
C** STRAINS FOR INFINITE CASE : SIMULATING EXCAVATION
C
   16 STRNR(I)=-EPRES*(1.+PR)*AUX/E
      STRNT(I)=-STRNR(I)
      STRNZ(I)=(STRZ(I)-PR*(STRR(I)+STRT(I)))/E
      GO TO 13
C
C** STRAINS FOR INFINITE CASE : LOAD APPLIED EXTERNALLY
C
   12 STRNR(I)=EPRES*(1+PR)*(1.-2.*PR-AUX)/E
      STRNT(I)=EPRES*(1.+PR)*(1.-2.*PR+AUX)/E
      STRNZ(I)=(STRZ(I)-PR*(STRR(I)+STRT(I)))/E
   13 AUX1=2.*CHO*DCOS(PHIO)+DSIN(PHIO)*(STRR(I)+STRT(I))
      STLEV(I)=(STRT(I)-STRR(I))/AUX1
```

```
   100 CONTINUE
       GO TO 9
C*******************************
C** STRESSES FOR HOLLOW CYLINDER *
C*******************************
     8 DO 150 I=1,N
       AUX=(RD1**2)-(RD**2)
       AUX1=1.-((RD/R(I))**2)
       STRR(I)=EPRES*(RD1**2)*AUX1/AUX
       AUX2=1.+((RD/R(I))**2)
       STRT(I)=EPRES*(RD1**2)*AUX2/AUX
       STRZ(I)=PR*(STRR(I)+STRT(I))
   150 CONTINUE
       IF(ICASE.EQ.4) GO TO 98
       GO TO 99
C
C** STRAIN FOR HOLLOW CYLINDER : LOAD APPLIED EXTERNALLY
C
    98 DO 151 I=1,N
       STRNR(I)=(1.+PR)*((1.-PR)*STRR(I)-PR*STRT(I))/E
       STRNT(I)=(1.+PR)*((1.-PR)*STRT(I)-PR*STRR(I))/E
       STRNZ(I)=0.
   151 CONTINUE
     . GO TO 89
C
C** STRAIN FOR HOLLOW CYLINDER : SIMULATING EXCAVATION
C
    99 DO 152 I=1,N
       AUX=1. -2.*PR-((RD1/R(I))**2)
       AUX1=1.-2.*PR+((RD1/R(I))**2)
       AUX2=(RD**2)/((RD1**2)-(RD**2))
       STRNR(I)=EPRES*AUX2*(1.+PR)*AUX/E
       STRNT(I)=EPRES*AUX2*(1.+PR)*AUX1/E
       STRNZ(I)=0.
   152 CONTINUE
    89 DO 153 I=1,N
       AUX1=2.*CHO*DCOS(PHIO)+DSIN(PHIO)*(STRR(I)+STRT(I))
       STLEV(I)=(STRT(I)-STRR(I))/AUX1
   153 CONTINUE
C
C
     9 WRITE(6,600)
       DO 105 I=1,N
       WRITE(6,605) R(I),STRNR(I),STRNT(I),STRNZ(I),STRR(I),STRT(I),STRZ(
      1I),STLEV(I)
   105 CONTINUE
       DO 107 I=2,NN
       WRITE(1,810) R(I),STRNR(I),STRNT(I),STRNZ(I),STRR(I),STRT(I),STRZ(
      1I),STLEV(I)
   107 CONTINUE
C
C***** TIME DEPENDENT SOLUTION STARTS HERE *****************
C
       T=0.
       II=1
       NPRINT=1
       NN=N-1
    21 CONTINUE
       DO 110 I=2,NN
       Y(I)=0.0
```

```
  110 CONTINUE
      Y(1)=0.
      Y(N)=0.
      IF(T.GE.0..AND.T.LT.100.) DT=1.
      IF(T.GE.100..AND.T.LT.1000.) DT=10.
      IF(T.GE.1000..AND.T.LT.10000.) DT=10.
      IF(T.GE.10000..AND.T.LT.100000.) DT=100.
      IF(T.GE.100000.) DT=1000.
      CH=CH0-XM1*DLOG10(1.+T)
      INT=1
   40 DO 115 I=1,N
      YY(I)=Y(I)
  115 CONTINUE
C
      DO 120 I=2,NN
      EAUX=R(I)*(Y(I+1)-Y(I-1))/(2.*H)
      EAUX1=DSIN(PHI)*(2.*Y(I)+EAUX)
      K1=2.*(STRT(I)-STRR(I))
      K2=4.*CH*DCOS(PHI)+2.*DSIN(PHI)*(STRT(I)+STRR(I))
      EAUX2=(K1+EAUX)/(K2+EAUX1)
      IF(EAUX2.LT.0.20) GO TO 9000
      IF(EAUX2.GT.0.80) GO TO 9001
      GO TO 9002
 9000 AA=AA0
      ALPHA=ALP0
C     IF(EAUX2.LE.0.05) AA=0.
      GO TO 9003
 9001 AA=AA2
      ALPHA=ALP2
      GO TO 9003
 9002 AA=AA1
      ALPHA=ALP1
 9003 CONTINUE
      EAUX3=DEXP(ALPHA*EAUX2)
      K3=(R(I)**2)*(1.-PR**2)/E
      K4=3.*R(I)*(1.-PR**2)/E
      K5=(1.+PN)*AA*((T+DT/2.)**(-XM))*DT
      K6=R(I)*(1.-PM*PR)*ALPHA*AA*((T+DT/2.)**(-XM))*DT
      K7 = K2+2.*DSIN(PHI)*Y(I)-3.*K1*DSIN(PHI)
      DK1 = (STRT(I+1)-STRT(I-1)-STRR(I+1)+STRR(I-1))/H
      DK2 = DSIN(PHI)*(STRT(I+1)-STRT(I-1)+STRR(I+1)-STRR(I-1))/H
      K7 = K7+R(I)*DSIN(PHI)*DK1-R(I)*DK2
      K8=-2.*DSIN(PHI)*R(I)
      K9=K2*R(I)+2.*R(I)*DSIN(PHI)*Y(I)
      K9=K9-K1*R(I)*DSIN(PHI)
      K10=K2+EAUX1
      K11 = -K3-(K6*K9*EAUX3)/(K10**2)
      K12 = -K4-(K6*K7*EAUX3)/(K10**2)
      K13 = K5*EAUX3
      K14 = K2*DK1-K1*DK2+2.*DSIN(PHI)*DK1*Y(I)
      K15 = (Y(I+1)-Y(I-1))/(2.*H)
      K15 = K15**2
      K13 = K13+K6*EAUX3*(K8*K15+K14)/(K10**2)
      A(I) = K11/(H**2)-K12/(2.*H)
      B(I) = -2.*K11/(H**2)
      C(I) = K11/(H**2)+K12/(2.*H)
      D(I) = K13
  120 CONTINUE
      D(2)=D(2)-A(2)*Y(1)
      D(NN)=D(NN)-C(NN)*Y(N)
```

```
C
      CALL TRIDIA(N,A,B,C,D,Y)
C
      DO 125 I=2,NN
      DY(I)=DABS(Y(I)-YY(I))
  125 CONTINUE
      DO 126 I=2,NN
      IF(DY(I).GT.0.00001) GO TO 15
  126 CONTINUE
C
      TO=T+DT
      IF(II.EQ.NPRINT) GO TO 37
      GO TO 20
   37 WRITE(6,620) TO,INT
      WRITE(1,800) TO
  800 FORMAT(F10.2)
      WRITE(6,625)
C
C
   20 DO 130 I=2,NN
      EAUX=R(I)*(Y(I+1)-Y(I-1))/(2.*H)
      EAUX1=DSIN(PHI)*(2.*Y(I)+EAUX)
      K1 = 2.*(STRT(I)-STRR(I))
      K2 = 4.*CH*DCOS(PHI)+2.*DSIN(PHI)*(STRT(I)+STRR(I))
      EAUX2 = (K1+EAUX)/(K2+EAUX1)
      IF(EAUX2.LT.0.20) GO TO 9005
      IF(EAUX2.GT.0.80) GO TO 9006
      GO TO 9007
 9005 AA=AA0
      ALPHA=ALP0
C     IF(EAUX2.LE.0.05) AA=0.
      GO TO 9008
 9006 AA=AA2
      ALPHA=ALP2
      GO TO 9008
 9007 AA=AA1
      ALPHA=ALP1
 9008 CONTINUE
      EAUX3= DEXP(ALPHA*EAUX2)
      SAUX1 = AA*EAUX3*((T+DT/2.)**(-XM))*DT
      DSIGT = Y(I)+EAUX
      SAUX2 = (1.+PR)*((1.-PR)*DSIGT-PR*Y(I))/E
      SAUX3 = (1.+PR)*((1.-PR)*Y(I)-PR*DSIGT)/E
      STRNR(I) = STRNR(I)+SAUX3-PN*SAUX1
      STRNT(I) = STRNT(I)+SAUX2+SAUX1
      DEPZ=-PM*SAUX1
      STRNZ(I)=DEPZ
      STRZ(I)=STRZ(I)+PR*(Y(I)+DSIGT)-E*DEPZ
      STRR(I) = STRR(I)+Y(I)
      STRT(I) = STRT(I)+DSIGT
      K1=2.*CH*DCOS(PHI)+DSIN(PHI)*(STRT(I)+STRR(I))
      STLEV(I)=(STRT(I)-STRR(I))/K1
  130 CONTINUE
C
C
      IF(II.EQ.NPRINT) GO TO 36
      GO TO 22
   36 CONTINUE
      IF(T.GE.0..AND.TO.LT.10.) NPRINT=NPRINT+1
      IF(TO.GE.10..AND.TO.LT.1000.) NPRINT=NPRINT+10
```

```
      IF(TO.GE.1000.) NPRINT=NPRINT+100
      DO 135 I=2,NN
      WRITE(6,630) R(I),STRNR(I),STRNT(I),STRNZ(I),STRR(I),STRT(I),STRZ(
     1I),STLEV(I)
      WRITE(1,810) R(I),STRNR(I),STRNT(I),STRNZ(I),STRR(I),STRT(I),STRZ(
     1I),STLEV(I)
  810 FORMAT(F7.3,3(E15.8),3(F10.4),F6.3)
  135 CONTINUE
C
   22 STRT(1)=2.*STRT(2)-STRT(3)
      STRT(N)=2.*STRT(N-1)-STRT(N-2)
      II=II+1
      T = T+DT
      IF(T-TMAX)21,21,25
   25 WRITE(6,635)
      TT=-999.
      WRITE(1,800) TT
      STOP
   15 IF(INT-IMAX)30,35,35
   30 INT = INT+1
      GO TO 40
   35 WRITE(6,640) II,IMAX
      STOP
C***************************************************************
C*                   LIST OF FORMATS                           *
C***************************************************************
  500 FORMAT(7F10.2)
  505 FORMAT(2(E15.8,F15.8))
  507 FORMAT(E15.8,3F15.8)
  510 FORMAT(3F10.2,I6)
  600 FORMAT(//,5X,'***** INITIAL ELASTIC SOLUTION *****',//,5X,'RADIUS'
     1,5X,'RAD. STRAIN',5X,'TAN. STRAIN',5X,'RAD. STRESS',5X,'TAN. STRES
     2S',5X,'STR. LEVEL',/,6X,'(M)',10X,'(M/M)',12X,'(M/M)',8X,'(KG/CM**
     32)',5X,'(KG/CM**2)'/)
  605 FORMAT(4X,F7.3,3(2X,E12.5),3(4X,F9.3),4X,F6.3)
  620 FORMAT(5X,'OUTPUT CORRESPONDENT TO ELAPSED TIME =',F10.2,/,5X,'SOL
     1UTION CONVERGED AFTER ',I4,' ITERATIONS'/)
  625 FORMAT(/,5X,'RADIUS',5X,'RAD. STRAIN',5X,'TAN. STRAIN',5X,'RAD. ST
     1RESS',5X,'TAN. STRESS',/,6X,'(M)',10X,'(M/M)',12X,'(M/M)',8X,'(KG/
     2CM**2)',5X,'(KG/CM**2)'/)
  630 FORMAT(4X,F7.3,3(2X,E12.5),3(4X,F9.3),4X,F6.3)
  635 FORMAT(//,'TIME FOR CREEP EXCEEDED - END OF EXECUTION ')
  640 FORMAT(//,'SOLUTION FOR TIME STEP ',I4,' DID NOT CONVERGE AFTER ',
     1I4,' ITERATIONS - END OF EXECUTION')
  700 FORMAT(5X,'*** TIME-DEPENDENT STRESS AND STRAIN DISTRIBUTION ***',
     1/,5X,'*** AXIALLY SIMMETRIC 2-D PLANE STRAIN                 ***')
  701 FORMAT(//,5X,'SOLUTION FOR LOAD APPLIED ALONG EXT. BOUNDARY',//)
  705 FORMAT(//,5X,'HOLLOW CYLINDER SIMULATING EXCAVATION',//)
  706 FORMAT(//,5X,'HOLLOW CYLINDER LOAD APPLIED EXTERNALLY',//)
  702 FORMAT(//,5X,'SOLUTION FOR CASE SIMULATING EXCAVATION',//)
  703 FORMAT(5X,'TUNNEL RADIUS=',F10.4,'(M)',/,5X,'EXTERNAL BOUNDARY=',F
     110.4,'(M)',/,5X,'EXTERNAL PRESSURE=',F10.4,'KG/CM**2')
  704 FORMAT(5X,'COHESION=',F10.4,'KG/CM**2',/,'ANGLE OFFRICTION=',F10.4
     1,'DEGREES',/,'CREEP PARAM. A=',E15.8,'(MIN-1)',/,'CREEP PARAM. ALP
     2HABAR=',F10.4,/,'CREEP PARAM. M=',F10.4,/,'YOUNGS MODULUS=',F10.4,
     3'KG/CM**2',/,'POISSON RATIO=',F5.2,/)
      END
C
C
C
```

Appendix C

Comparisons between measured and predicted results of multiple-stage creep tests

Next, the figures showing the comparisons between the measured and predicted results for the multiple-stage creep tests CT1, CT2, and CT3 are presented. The stress history associated with each test is indicated in Figure 4.10 and the parameters A and ' $\bar{\alpha}$ ' obtained from the analysis of these tests are indicated in Table 4.6.

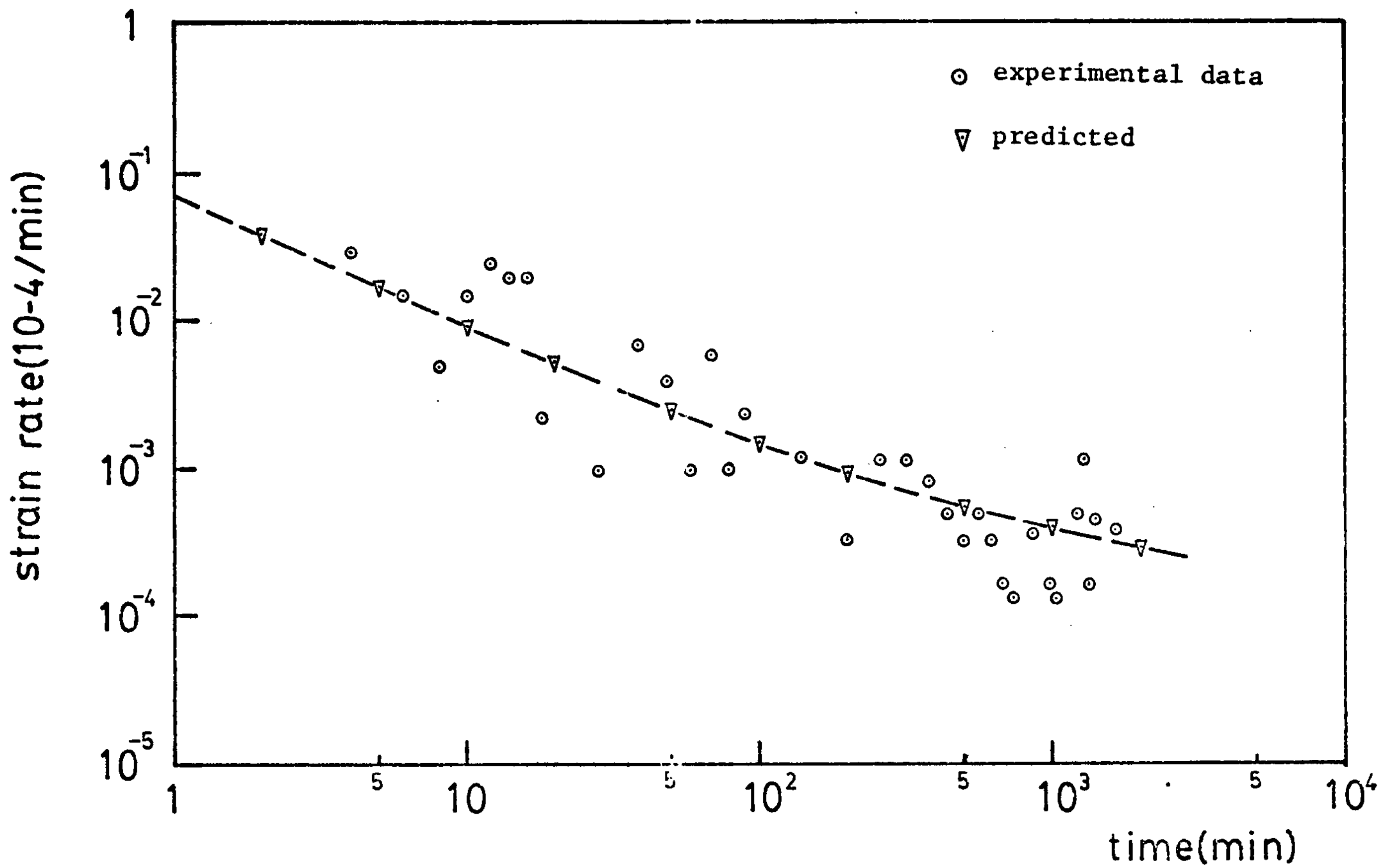

Figure C.1 - Test CT1 Stage No. 4

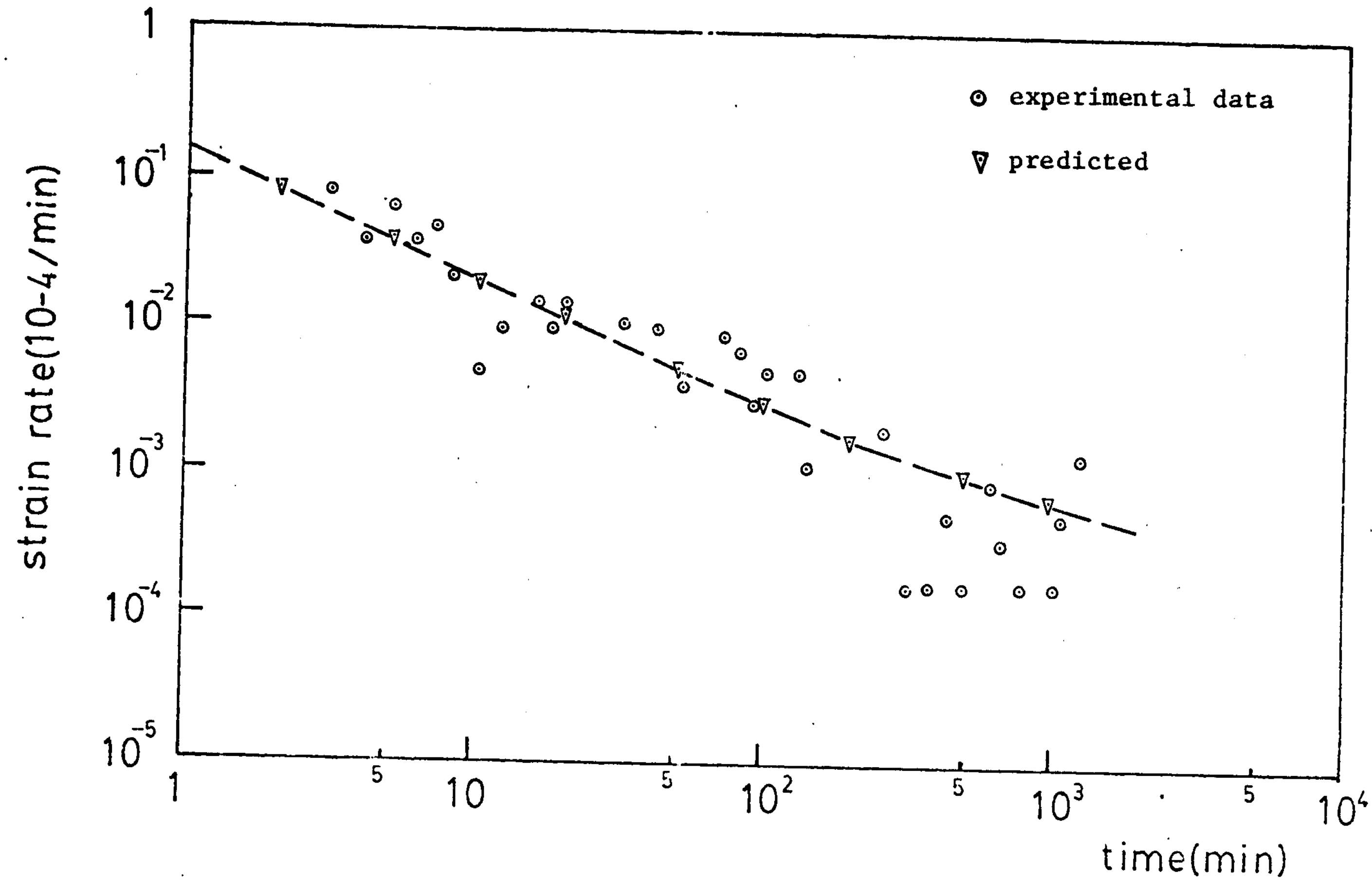

Figure C.3 - Test CT1 Stage No. 6

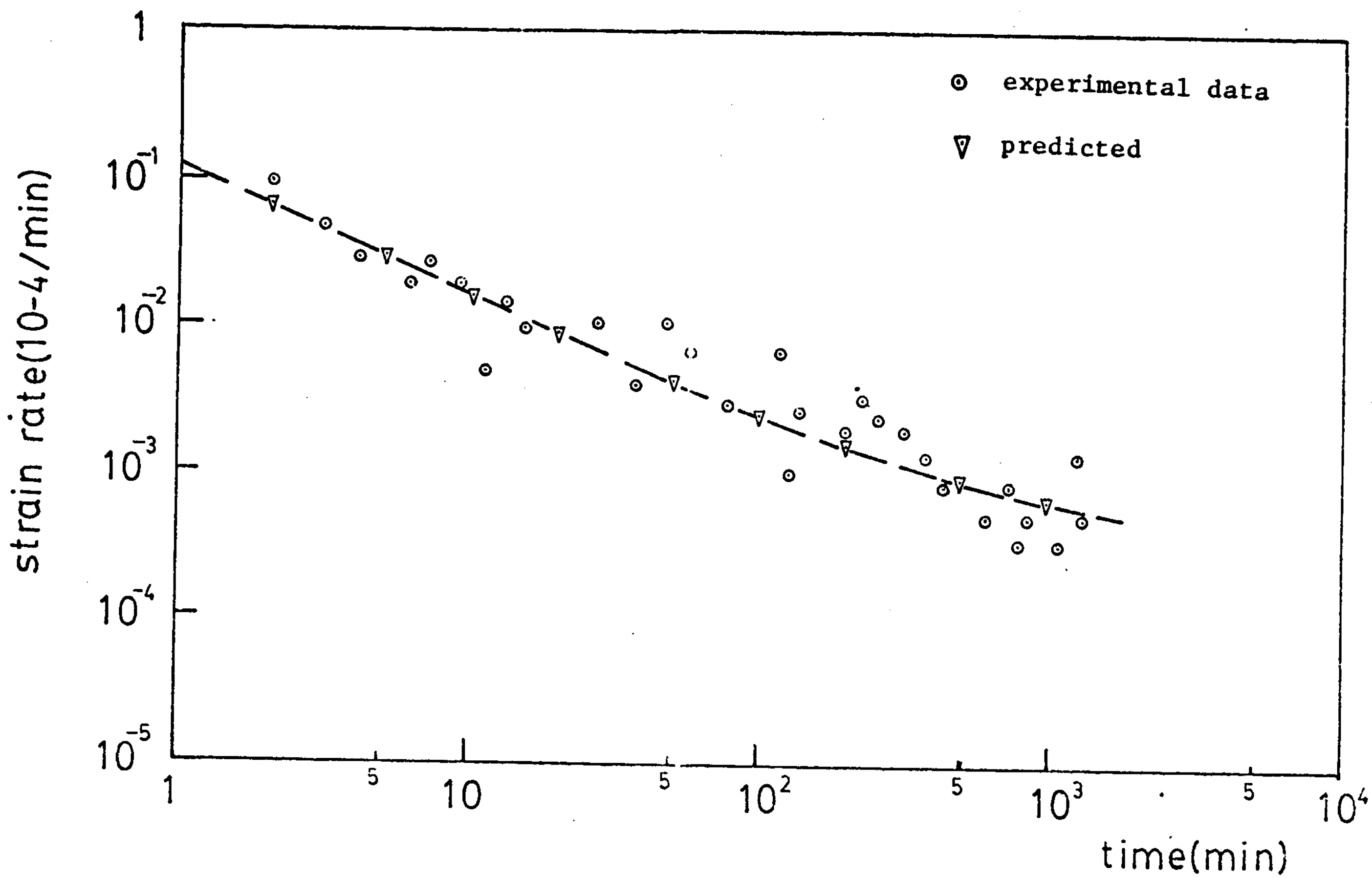

Figure C.4 - Test CT1 Stage No. 7

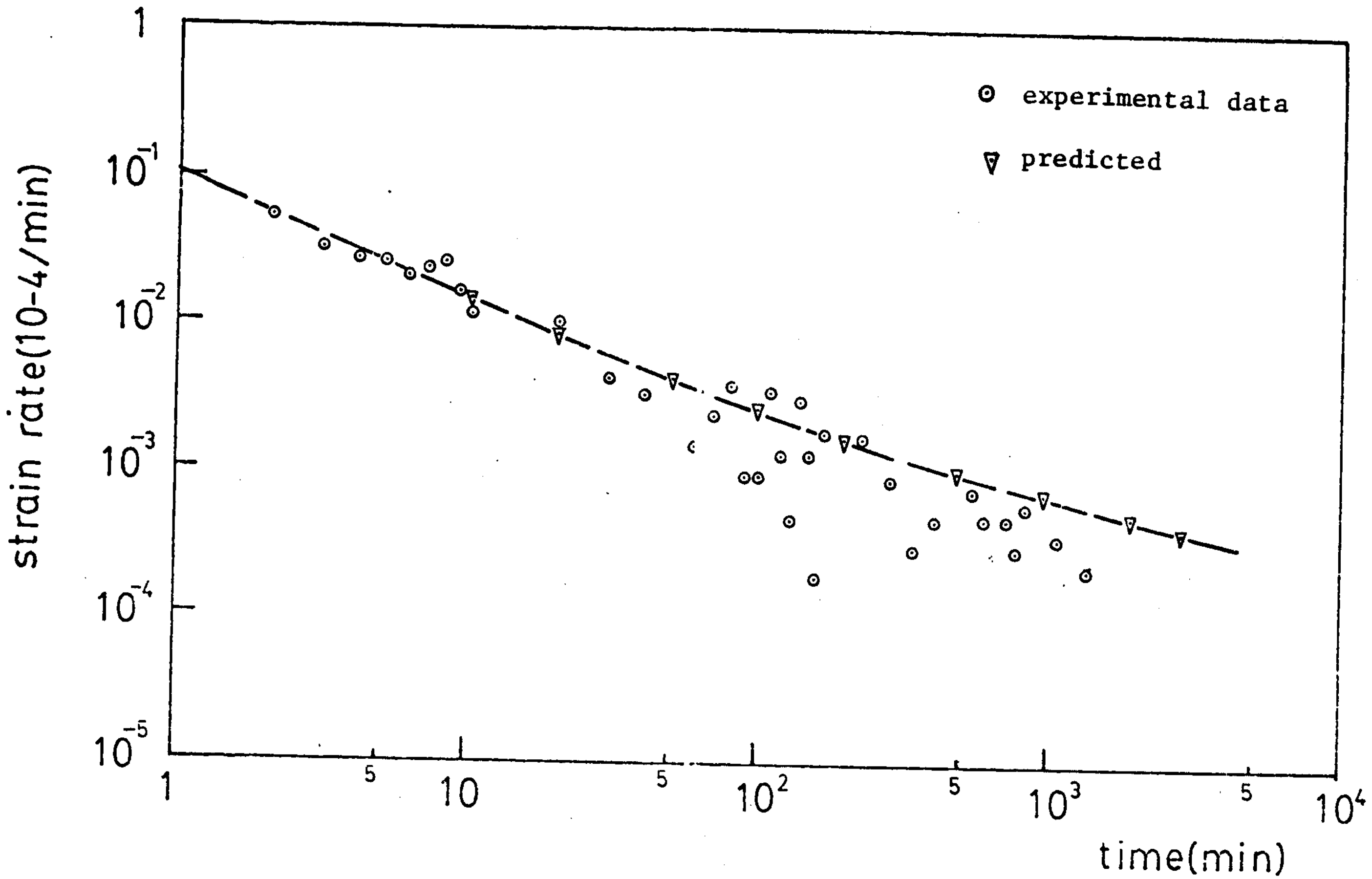

Figure C.5 - Test CT2 Stage No. 4

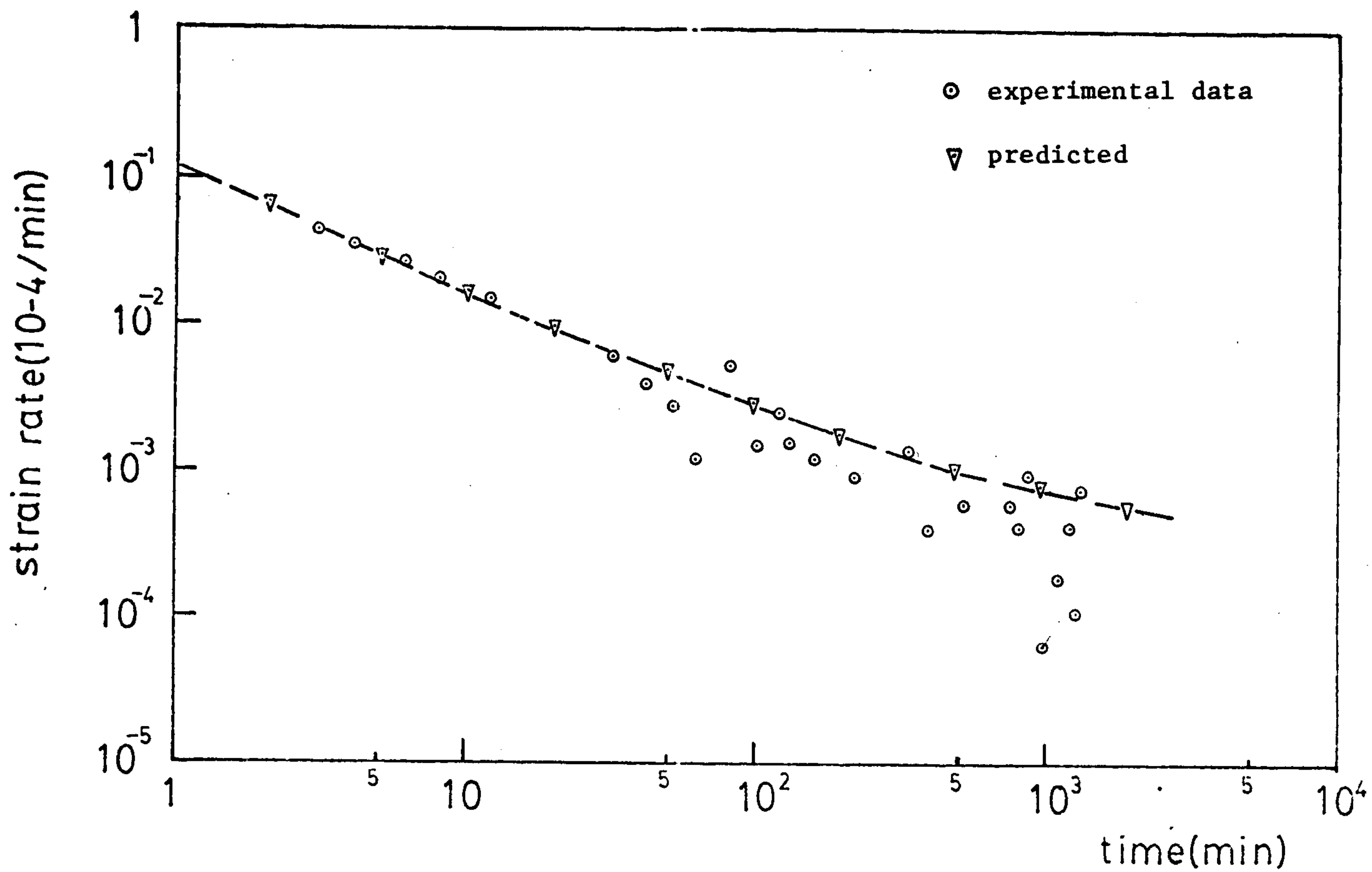

Figure C.6 - Test CT2 Stage No. 5

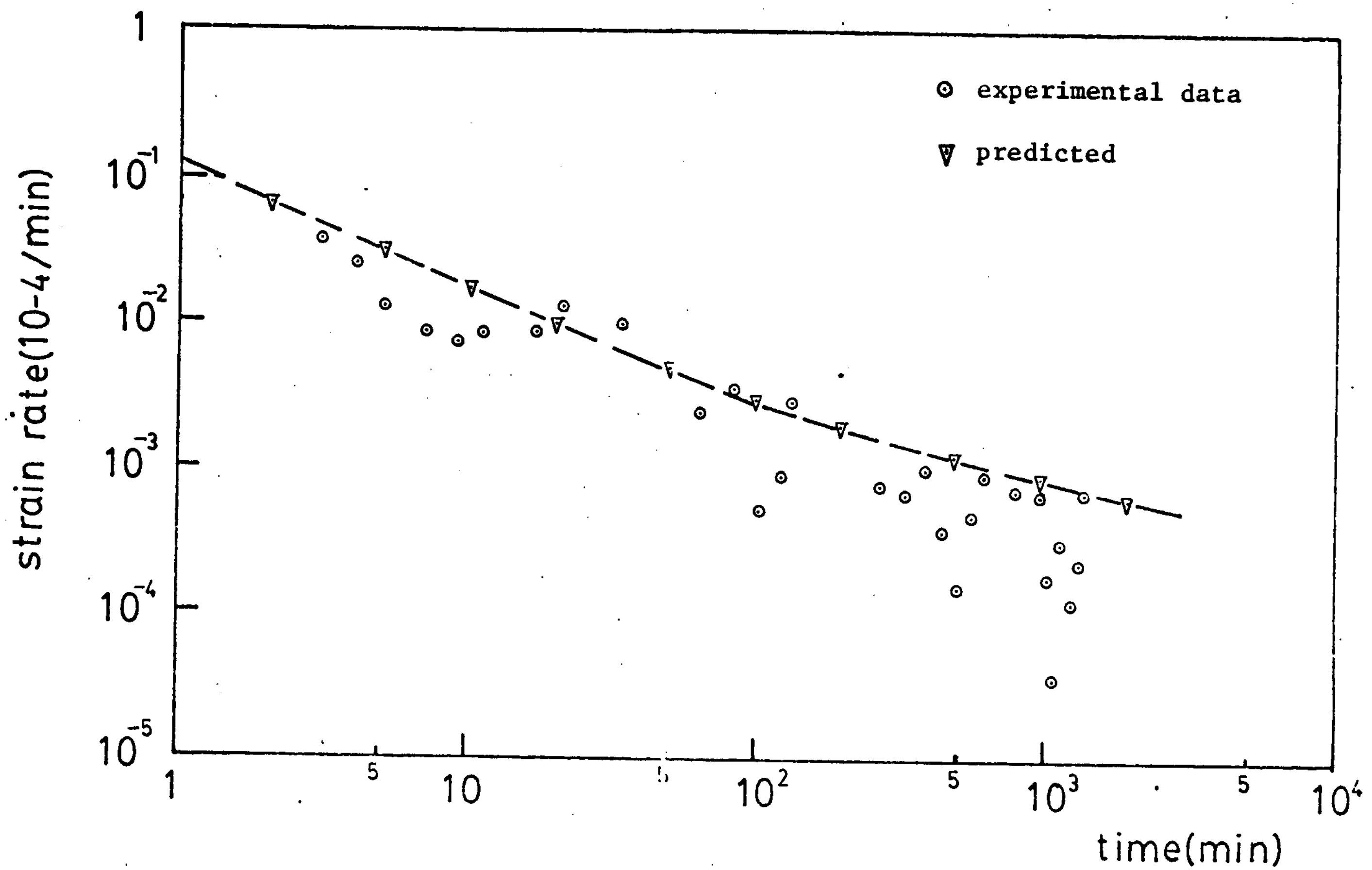

Figure C.7 - Test CT2 Stage No. 6

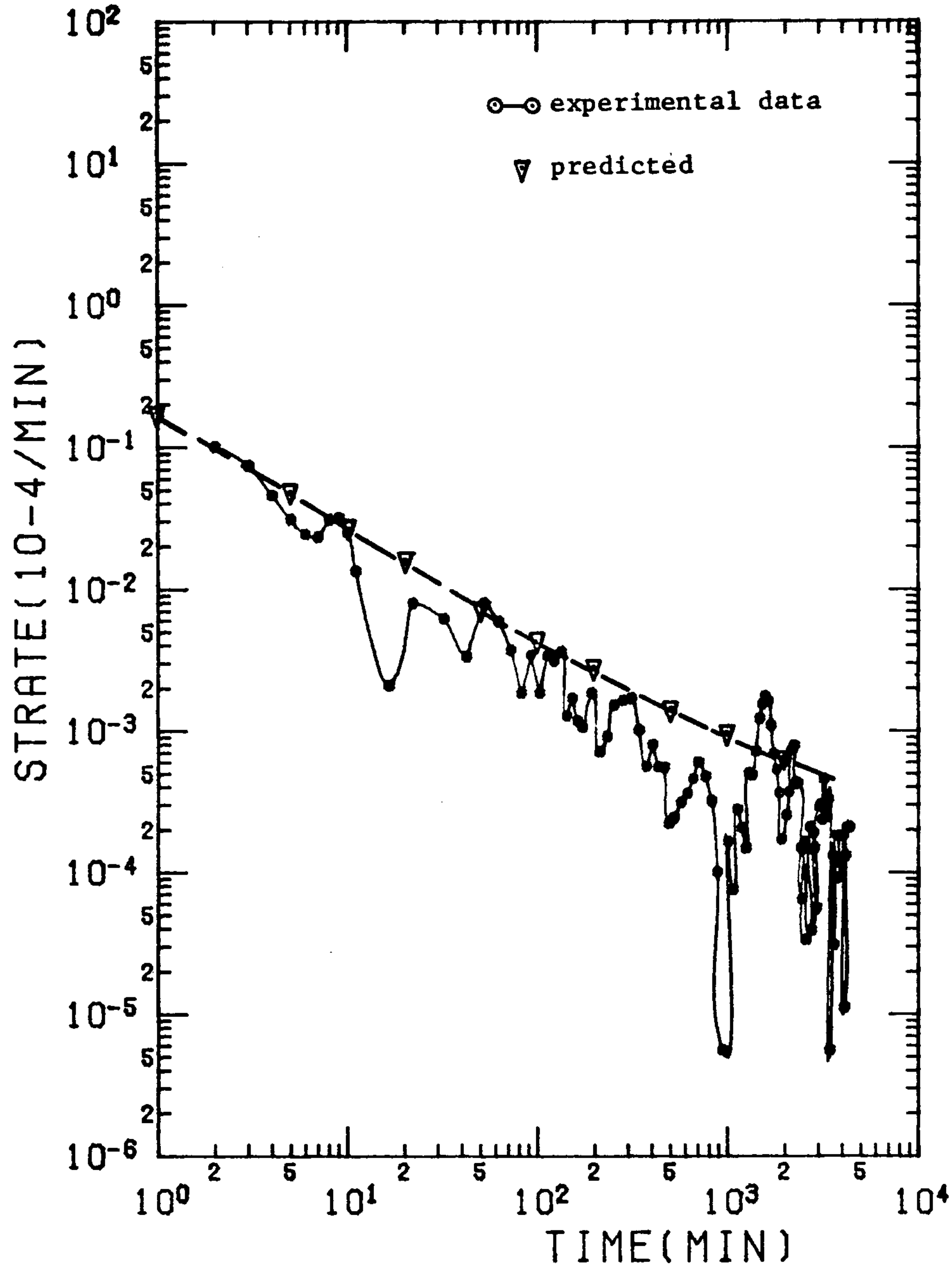

CREEP TEST CT-3 STAGE NO.=4 LOADING

Figure C.9 - Test CT3 Stage No.

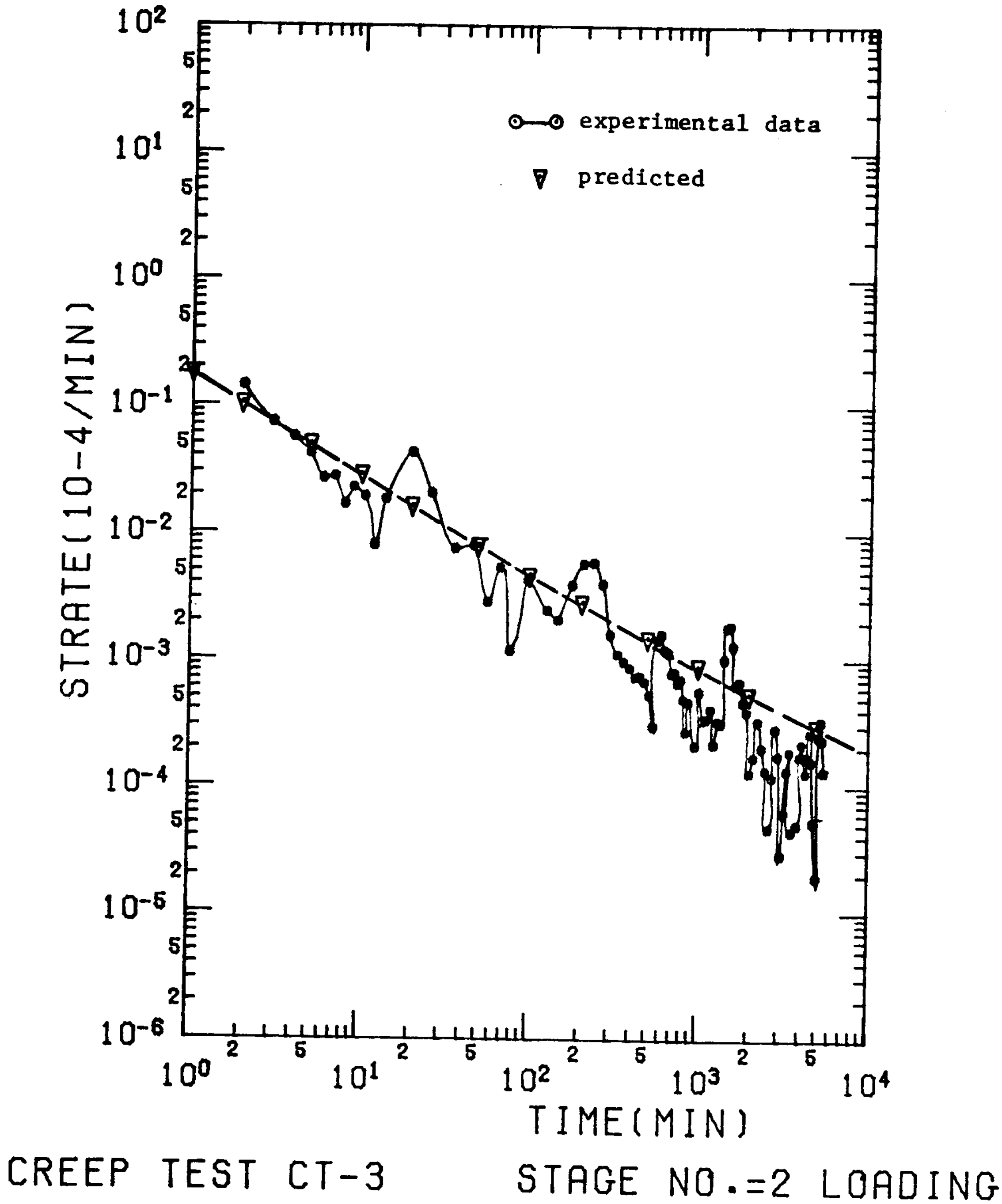

Figure C.10 - Test CT3 Stage No. 2

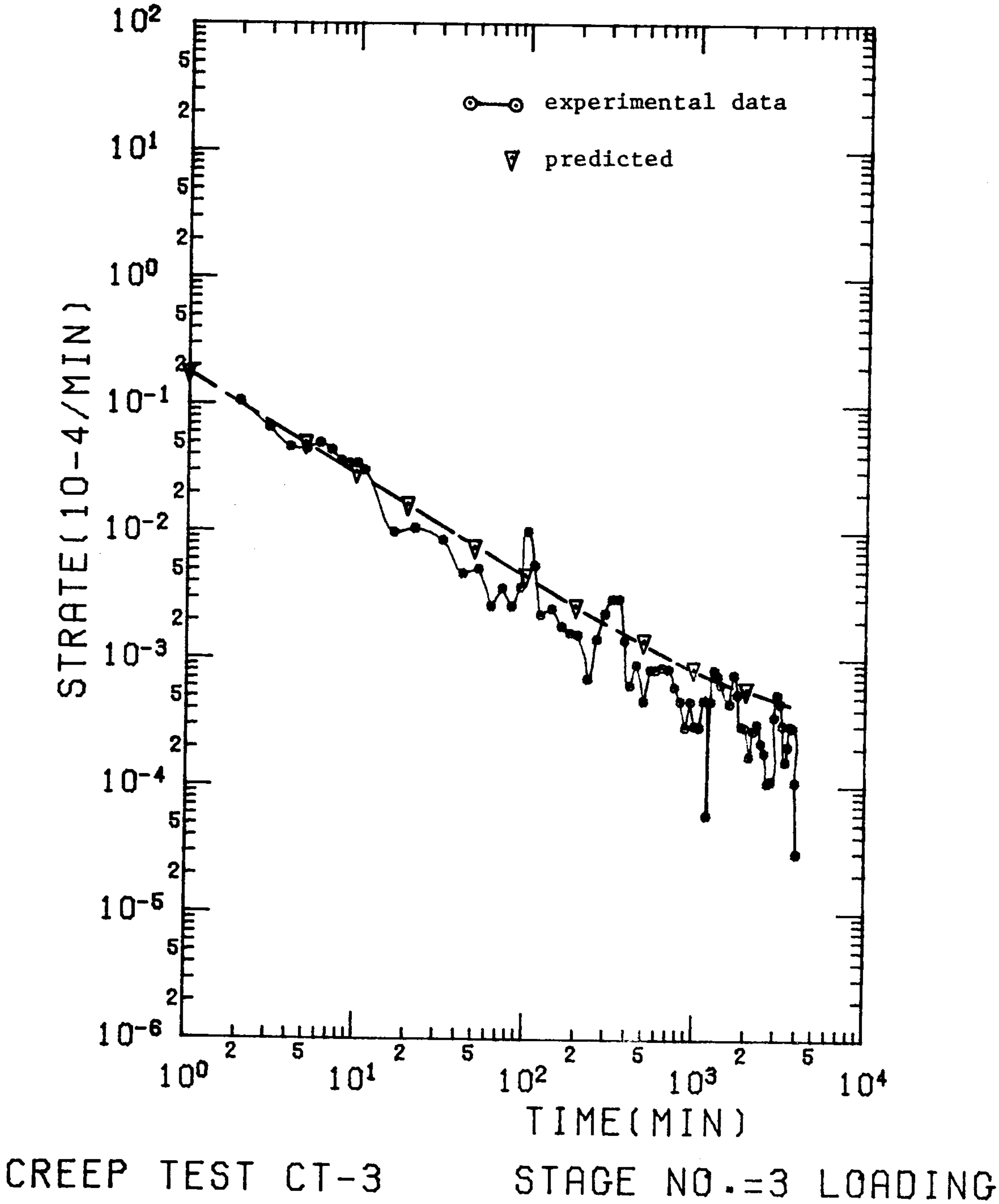

Figure C.11 - Test CT3 Stage No. 3